



Regulation of human CXCL12 expression by IKK α in bone cancer and cancer associated fibroblasts derived from clinical specimens obtained from breast cancer patients

By

Yousif Hendi Khalaf

A thesis submitted in the fulfilment of the requirements
for the degree of Doctor of Philosophy

October 2018

Strathclyde Institute of Pharmacy and Biomedical Sciences (SIPBS)

University of Strathclyde Glasgow, UK

Author's Declaration

This thesis is the result of the author's original research. It has been composed by the author and had not been previously submitted for examination which has led to the award of a degree.

The copyright of this thesis belongs to the author under the terms of the United Kingdom Copyright Acts as qualified by University of Strathclyde Regulation 3.50. Due acknowledgement must always be made of the use of any material contained in, or derived from, this thesis.

Signed:

Date:

Dedication

“To my late mother and father for whom I shall always be indebted to. You prepared me to face the challenges with faith and humility; always had confidence in me and offered me encouragement and support in all my endeavours. I know you would have been very proud to see this moment when I graduate with my doctorate degree. Mother, father, I miss you and love you both very dearly; I pray that one day we are reunited in the hereafter”

“I also dedicate this work to my dear wife, Fatimah and children. They are my constant source of love and inspiration. I started my research in the presence of my first beautiful daughter, Razan. Then Layan, our second daughter was born mid-way through my studies; and as I finalised my thesis for submission my wife gave birth to our third daughter, Seden. I feel very grateful and humbled to have such a great family support and join me throughout my journey”

Acknowledgements

First of all, I thank God, Allah for granting me the health, patience and wellbeing to embark on this long journey of knowledge, giving me strength and motivation to succeed.

I would like to express my sincere gratitude to my supervisor Prof. Robin Plevin for the opportunity to work within his research group and for his professional guidance and valuable support throughout my PhD. I have been extremely lucky to have such a great coach and mentor. I would also like to thank my second supervisor, Dr Andy Paul who always gave me great constructive feedback and advice in all my meetings with him.

A massive thank you to all the members of Plevin/Paul research group who have assisted me to develop my research skills: Dr Ho Ko, Dr Katy, Dr Anthony and Dr Musab. I would also like to thank everyone from the Plevin/Paul lab group especially Shilan. I am also extremely grateful to Dr. Rothwelle and Dr Margaret for their support. I also thank Dr Sara from the Beatson Institute for Cancer Research UK. She kindly provided the clinical samples of breast cancer which were valuable for my research.

My thanks of course also goes to the government of the republic of Iraq represented by the Ministry of Higher Education and Scientific Research, University Of Anbar and the Iraqi Cultural Attaché in London for providing me with this great opportunity to undertake this challenging and inspiring project, supporting me by funding my studies in the UK.

To my family, my brothers and sisters, thank you for your love and support. My brother Muhammed, I cannot thank you enough for supporting me spiritually throughout this experience. Finally, I offer my kind regards to all of my friends especially Abyd Adhami, Thaer, Yasir, Muhanned, Ahmad, Abdullah, and Baraa for every moment we have spent together in Glasgow and beyond.

Thank you to everyone who had helped me in any way during my research endeavours.

Abstract

Despite great progress in surgery, radio- and chemotherapy, the prognosis and treatment options for osteosarcoma and breast cancer remain extremely poor with a high inclination for metastatic spread to other organs. Compelling evidence has demonstrated that CXCL12/CXCR4 is implicated in human tumour pathogenesis. Therefore, targeting CXCL12 expression is a logical strategy for treating cancer patients. Moreover, studies have implicated inhibitory Kappa B kinase alpha (IKK α) as a key regulator in the non-canonical NF- κ B pathway and it has recently been demonstrated that IKK α can regulate CXCL12 expression. Therefore, the aim of the current study was to investigate the role of the IKK α -mediated non-canonical NF- κ B pathway in the regulation of CXCL12 expression in a human bone osteosarcoma cell line (U2OS) and cancer-associated fibroblasts (CAFs) derived from clinical specimens obtained from human breast cancer patients to determine the validity of this approach.

Initially, newly synthesised selective IKK α inhibitors (SU compounds) were characterised in LT $\alpha_1\beta_2$ -stimulated U2OS cells and were shown to be moderately potent and selective for the non-canonical NF- κ B pathway, whereas they exerted little effect on the classical NF- κ B pathway at high micromolar concentrations. In addition, it was unexpectedly found that both TNF α and IL-1 β were strong and early activators of the non-canonical NF- κ B pathway activated by IKK α , which was established using both siRNA and the selective inhibitors. Both TNF α and IL-1 β but not LT $\alpha_1\beta_2$, stimulated a strong increase in CXCL12 in reporter U2OS cells and when endogenously measured using RT-qPCR. CXCL12 expression was susceptible to both siRNA knock

down and IKK α inhibitors, suggesting that the early strong IKK α signal was significant for expression.

We further examined the role of IKK α in CXCL12 expression in CAFs derived from breast cancer patients. ELISA data revealed that CXCL12 protein secretion in CAFs was significantly higher than that of normal fibroblasts (NFs). However, our findings did not demonstrate a significant difference in the activation of the non-canonical NF- κ B pathway by LT α β β β . Moreover, the studies conducted using siRNA IKK α and SU compounds showed that CXCL12 expression was not altered in CAFs or NFs. Overall, these findings indicate that IKK α is not required for the regulation of CXCL12 expression in CAFs.

Taken together, these results highlight a novel early kinetically distinct mode of non-canonical NF- κ B signalling by IKK α , which is significant in the induction of CXCL12 in bone cells. Therefore, selective IKK α inhibition may be a target for cancer therapy but only for certain types of cancer and is not always linked to CXCL12 inhibition.

Poster and oral Presentation

Oral Presentation:

Khalaf Y, Paul, R. Plevin (2015). Regulation of human CXCL12 expression by IKK α in bone cancer. Postgraduate Research day. Strathclyde University, Glasgow, UK.

Poster Presentation:

Khalaf Y, Paul, R. Plevin (2016). TNF α drives rapid activation of IKK α -mediated non-canonical NF- κ B pathway in U2OS cells. Strathclyde University, Glasgow, UK.

Khalaf Y 1, McCluskey T, Sorensen A, Ho K, Breen D, Berretta G, Anthony N, Edwards J, Boyd M, Suckling C, MacKay S, Paul A, Plevin R. (2016). Finding New Drugs for Bone Cancer by Targeting Inhibitory Kappa B Kinase alpha (IKK α). Newcastle University, UK.

Khalaf Y 1, Al-Obaidi A, McCluskey T, Sorensen A, Ho K, Breen D, Berretta G, Anthony N, Edwards J, Boyd M, Suckling C, MacKay S, Paul A, Plevin R.(2017) Novel first-in-class selective IKK α inhibitors as anti-cancer drugs. Liverpool University, UK

Publications relating to this thesis;

Yousif Khalaf, Ka Ho Ho, Kathryn McIntosh, Ahlam Al-Obaidi, Louise Young, Nahoum Anthony, Stuart Lang, David Breen, Colin Suckling, Joanne Edwards, Marie Boyd, Andrew Paul, Simon Mackay and Robin Plevin (2018). A novel rapid activation of IKK α -dependent non-canonical NF- κ B signalling coupled to human CXCL12 expression in bone cancer cells (In preparation).

Abbreviations

ATP	Adenosine triphosphate
Adv	Adenovirus
AP2	Activator protein-2
ANOVA	Analysis of variance
AKT	Serine/threonine-protein kinase
APS	Ammonium persulphate
ATF-2	Activating transcription factor
BAFF	B cell activation factor
BLC	B lymphocyte chemoattractant
BSA	Bovine serum albumin
Bcl-2	B-cell lymphoma-2
CAFs	Cancer associated fibroblasts
CBP	CRE binding protein
CCL	C-C motif ligands
CETSA	Cellular thermal shift assay
CXCL-12	Chemokine (C-X-C motif) ligand
CXCR4	Chemokine (C-X-C) receptor 4
COX	Cyclooxygenase
DMEM	Dulbecco's Modified Eagle Medium
DN	Dominant negative
DTT	Dithiothreitol
ECL	Enhanced Chemiluminescence
ELISA	Enzyme-linked Immunosorbent Assay
ERK	Extracellular regulated kinase
FCS	Foetal calf serum
FGF	Fibroblast growth factor
GR	Glucocorticoid receptor
H ₂ O ₂	Hydrogen peroxide
HIF1 α	Hypoxia-inducible factor 1-alpha
HLH	Helix-loop-helix
HUVEC	Human umbilical vein endothelial cells
ICAM-1	Intracellular adhesion molecule-1
IL-1 β	Interleukin-1 beta
IL-1R	Interleukin-1 receptor
IL-8	Interleukin-8
I κ B α	Inhibitory kappa B alpha
IKK	Inhibitory kappa B kinase
kDa	kilo-Dalton

Luc	Luciferase
LT α β ₂	Lymphotoxin alpha 1 beta 2
MMP	Matrix metalloproteinase
MAPK	Mitogen activated protein kinase
MEF	Mouse Embryonic Fibroblast
NF κ B	Nuclear factor kappa B
NEMO	NF κ B essential modulator
NIK	NF κ B inducing kinase
NLS	Nuclear localisation sequence
NFs	Normal fibroblasts
PAGE	Polyacrylamide gel electrophoresis
PBS	Phosphate buffered saline
PI3K	Phosphoinositide-3 kinase
PKC	Protein kinase C
PCR	Polymerase chain reaction
RT-qPCR	Quantitative Real-Time Polymerase Chain Reaction
SCC	Squamous cell carcinomas
SLC	Secondary lymphoid tissue chemokine
SDS	Sodium dodecyl sulphate
Sp1	Specificity protein 1
SAR	Structure–Activity Relationship
siRNA	Small interfering RNA
shRNA	Short hairpin interfering RNA
RANK	Receptor activator of NF κ B
RANKL	Receptor activator of NF κ B ligand
TAB-2	TAK-1 binding protein 2
TAK-1	Transforming growth factor β –activated kinase 1
TEMED	N,N,N',N'-tetramethylethylenediamine
TGF β	Transforming growth factor β receptor
TLR	Toll like receptor
TNF α	Tumour necrosis factor alpha
TNFR	TNF-receptor
TRAF	TNF receptor-associated factor
VCAM-1	Vascular cell adhesion molecule 1
VEGF	Vascular endothelial growth factor
XIAP	X-linked inhibitor of apoptosis protein

Table of Contents

Acknowledgements.....	iv
Abstract.....	v
List of Figures	xvii
List of Tables.....	xxii
Chapter One	1
1.1 Bone and its development	2
1.2 Bone tumours	3
1.2.1 Primary bone tumours	4
1.2.1.1 Osteosarcoma.....	4
1.2.1.2 Chondrosarcoma.....	5
1.2.1.3 Ewing's sarcoma	6
1.2.1.4 Primary bone marrow tumours	6
1.3 Secondary bone tumours (Bone metastases).....	6
1.4 Signalling pathways in bone cancer.....	7
1.4.1 Wnt signalling pathway.....	8
1.4.2 TGF- β and BMP signalling pathway	9
1.4.3 PTH signalling pathway.....	11
1.4.4 The nuclear factor Kappa B (NF- κ B) signalling pathway	11
1.4.4.1 Members and structure of NF- κ B	12
1.4.4.2 I κ B structure	14
1.4.4.2.1 Regulation of I κ B α	15
1.4.4.2.2 Inhibitory NF- κ B2 (p100/p52).....	16
1.4.4.3 Inhibitory Kappa B kinases (IKKs) complex structure.....	17
1.4.4.4 Activation of NF- κ B via the canonical pathway.....	18
1.4.4.5 Activation of NF- κ B via the non-canonical pathway	22
1.4.4.6 Genes Regulated by NF- κ B pathway	25
1.5 Chemokines and their receptors.....	26
1.5.1 The formation and function of CXCL12	27
1.5.2 CXCL12/CXCR4 axis and human pathogenesis	28
1.5.3 Regulation of CXCL12 expression.....	30
1.6 The Role of NF- κ B pathway in cancer	31
1.6.1 The role of IKKs in cancer	32

1.6.2 The role of NF- κ B pathways in bone biology	34
1.7 The development of IKK α inhibitors	36
1.8 Research hypothesis and aims	38
Chapter Two	39
2.1 Materials	40
2.1.1 General Reagents	40
2.1.2 SU compounds (University of Strathclyde, Glasgow, UK)	41
2.2 Cell culture.....	42
2.2.1 Culturing human osteosarcoma (U2OS) cell line.....	42
2.2.2 Culture of human breast cancer cell lines.....	43
2.2.3 Clinical samples and patients	44
2.2.3.1 Culture of human mammary fibroblasts (CAFs and NFs).....	44
2.3 Treatment of cell lines and human mammary fibroblasts.....	45
2.3.1 SU compounds	45
2.3.2 siRNA-mediated silencing of IKK α or IKK β in cells.....	45
2.4 Preparation of nuclear extracts	47
2.4.1 Determination of protein concentration in the nuclear extract.....	47
2.5 Western Blot Analysis	48
2.5.1 Preparation of Whole Cell Extracts (Lysis of protein)	48
2.5.2 SDS-Polyacrylamide Gel Electrophoresis (SDS-PAGE).....	49
2.5.3 Electrophoretic Transfer of proteins to Nitrocellular Membrane....	50
2.5.4 Immunological detection of protein	50
2.5.5 Nitrocellulose membrane stripping and reprobing	53
2.5.6 Scanning densitometry and quantification of expression levels....	53
2.6 Cellular Thermal Shift Assay (CETSA)	53
2.7 Luciferase reporter activity assay	54
2.7.1 Construction of luciferase reporter plasmid	55
2.8 Polymerase chain reaction (PCR) amplification.....	55
2.8.1 Extraction of total cellular RNA.....	55
2.8.2 Measurement of RNA concentration.....	56
2.8.3 cDNA synthesis using Reverse Transcription (RT)	57
2.8.4 Quantitative real time PCR (RT-qPCR)	58
2.8.5 Quantification method.....	60
2.9 Enzyme-linked Immunosorbent Assay (ELISA)	60

2.9.1 Preparation and treatment of human mammary fibroblast.....	60
2.9.2 Measurement of CXCL12/SDF1-alpha.....	60
2.10 Data Analysis.....	62
Chapter Three.....	63
3.1 Introduction.....	64
3.2 Results.....	65
3.2.1 In vitro selectivity of SU compounds.....	65
3.2.2 Activation of the non-canonical NF- κ B signalling pathway in U2OS cells.....	66
3.2.2.1 The effect of LT $\alpha_1\beta_2$ on the non-canonical NF- κ B pathway in U2OS cells.....	67
3.2.2.2 The effect of SU compounds on LT $\alpha_1\beta_2$ -induced p100 phosphorylation and p52 formation in U2OS cells.....	69
3.2.2.3 IC ₅₀ values for p100 phosphorylation and p52 formation by SU compounds in U2OS cells.....	72
3.2.3. TNF α and IL-1 β stimulation of the canonical NF- κ B pathway in U2OS cells.....	73
3.2.3.1 The effect of SU compounds on TNF α -induced I κ B α degradation in U2OS cells.....	76
3.2.3.2 The effect of SU compounds on TNF α induced phosphorylation of p65 in U2OS cells.....	79
3.2.4 Developing more potent IKK α inhibitors and their effect on non-canonical signalling in breast cancer cells.....	82
3.2.4.1 The effect of SU compounds on LT $\alpha_1\beta_2$ -mediated p100 phosphorylation and p52 formation in MCF-7 cells.....	82
3.2.4.2 IC ₅₀ values of SU compounds for p100 phosphorylation and formation of p52 in LT $\alpha_1\beta_2$ stimulated MCF-7 cells.....	86
3.2.5 Thermal shift assay.....	87
3.2.5.2 The cellular thermal shift assay for evaluating drug target interactions in U2OS cells.....	87
3.2.5.1 The melting curves for ERK-MAPK and p38 α -MAPK within U2OS cells using the cellular thermal shift assay (CETSA).....	88
3.2.5.2 Comparisons of the target engagement for ERK, p38 α and IKK α in intact versus lysed cells.....	91
3.2.5.3 Effect of SB203580 on the melting curve for p38 MAP kinase in U2OS cells.....	92

3.2.5.4 Effect of SU1261 on the melting curve for IKK α kinase in U2OS cells.....	94
3.3 Discussion	96
Chapter Four.....	102
4.1 Introduction.....	103
4.2 Results.....	105
4.2.1 The role of IKK α in the regulation of the non-canonical NF- κ B pathway	105
4.2.1.1 LT α 1 β 2 slowly induces p52 and RelB nuclear translocation in U2OS cells	105
4.2.1.2 TNF α and IL-1 β induce rapid non-canonical NF- κ B signalling in U2OS cells.....	107
4.2.1.2.1 TNF α induces phosphorylation of p100 at early time in U2OS cells.....	107
4.2.1.2.2 TNF α induces p100 processing to p52 formation in whole cell extracts of U2OS cells.....	109
4.2.1.2.3 TNF α induces RelB expression in whole cell extracts of U2OS cells.....	109
4.2.1.2.4 TNF α rapidly induces p52 and RelB nuclear translocation in U2OS cells.....	112
4.2.1.2.5 IL-1 β induces phosphorylation of p100 at early time in U2OS cells.....	114
4.2.1.2.6 IL-1 β induces p100 processing to p52 formation in whole cell lysates of U2OS cells	115
4.2.1.2.7 IL-1 β induces RelB expression in whole cell lysates of U2OS cells.....	115
4.2.1.2.8 IL-1 β rapidly induces p52 and RelB nuclear translocation in U2OS cells.....	118
4.2.1.3 The activation of p100 phosphorylation in response to TNF α and IL-1 β in U2OS, MCF-7 and CAFs cells	120
4.2.1.4 Time course comparison of non-canonical NF- κ B activation by different agonists in U2OS cells	120
4.2.2 The effect of siRNA-mediated silencing of cellular IKK α expression on the non-canonical NF- κ B pathway in U2OS cells	122
4.2.2.1 Knockdown efficiency of siRNA-mediated silencing of IKK α and IKK β in U2OS cells.....	122
4.2.2.2 The effect of IKK α and IKK β siRNA silencing on LT α 1 β 2 induced p100 phosphorylation and p52 in U2OS cells.....	125

4.2.2.3 The effect of IKK α and IKK β siRNA silencing on TNF α -induced phosphorylation of p100 in U2OS cells	127
4.2.2.4 The effect of IKK α and IKK β siRNA silencing on IL-1 β -induced phosphorylation of p100 and p52 in U2OS cells	129
4.2.2.5 The effect of IKK α and β siRNA double knockdown upon TNF α -induced p100 phosphorylation in U2OS cells.....	131
4.2.2.6 The effect of IKK α siRNA silencing on TNF α -induced p52 and RelB nuclear translocation in U2OS cells.....	133
4.2.3 The effect of SU compounds on agonist-stimulated non-canonical NF- κ B pathway activation in U2OS cells	136
4.2.3.1 The effect of SU compounds on TNF α -induced phosphorylation of p100 in U2OS cells	136
4.2.3.2. The effect of SU compounds on IL-1 β -induced phosphorylation of p100 in U2OS cells	140
4.2.3.3 The effect of SU1261 on IL-1 β -mediated p52 and RelB nuclear translocation in U2OS cells	144
4.2.3.4 The effect of SU1266 on IL-1 β -mediated p52 and RelB nuclear translocation in U2OS cells	146
4.2.4 The effect of NIK inhibitor CW15407 upon TNF α -and IL-1 β -induced phosphorylation of p100 in U2OS cells	148
4.2.5 The effect of NIK inhibitor CW15407 upon LT α β β -induced phosphorylation of p100 in U2OS cells	151
4.2.6 The effect of selective IKK β inhibitor IKK2 X1 upon TNF α -and IL-1 β - induced phosphorylation of p100 in U2OS cells.....	153
4.2.7 The role of IKK α in the regulation of CXCL12 expression in U2OS-CXCL12 cells.....	157
4.2.7.1 LT α β β , TNF- α , and IL-1 β induced CXCL12 luciferase activity in U2OS- CXCL12 cells in concentration dependent manner	157
4.2.7.2 LT α β β , TNF α and IL-1 β induce CXCL12 luciferase activity in U2OS-CXCL12 cells	158
4.2.7.3 The effect of IKK α and IKK β siRNA silencing on LT α β β -induced CXCL12 luciferase activity in U2OS-CXCL12 cells	161
4.2.7.4 Characterisation of the role of IKK α and IKK β in the regulation of TNF α - induced CXCL12 luciferase activity in U2OS-CXCL12 cells	162
4.2.7.5 Characterisation of the role of IKK α and IKK β in the regulation of IL-1 β - induced CXCL12 luciferase activity in U2OS-CXCL12 cells	163

4.2.8 The effect of SU compounds on CXCL12 luciferase activity in U2OS-CXCL12 cells.....	164
4.2.8.1 The effect of SU compounds on LT $\alpha_1\beta_2$ induced CXCL12 luciferase activity in U2OS-CXCL12 cells	164
4.2.8.2 The effect of SU compounds on TNF α -induced CXCL12 luciferase activity in U2OS-CXCL12 cells	166
4.2.8.3 The effect of SU compounds on IL-1 β -induced CXCL12 luciferase activity in U2OS-CXCL12 cells	168
4.2.5.4 IC ₅₀ values for CXCL12 luciferase activity by SU compounds in U2OS-CXCL12 cells	170
4.2.9 The role of IKK α in the regulation of CXCL12 expression using RT-qPCR in U2OS cells	172
4.2.9.1 The effect of SU1261 and IKK α siRNA silencing on IL-1 β -induced CXCL12 mRNA expression in U2OS cells	174
4.3 Discussion	176
Chapter Five	182
5.1 Introduction.....	183
5.2 Results.....	184
5.2.1 Activation of the non-canonical NF- κ B pathway in NFs and CAFs	184
5.2.2 Activation of the non-canonical NF- κ B pathway in NFs.....	184
5.2.2.1 TRAF2 and TRAF3 degradation in NFs	186
5.2.2.2 NIK expression in NFs	187
5.2.3 Activation of the non-canonical NF- κ B pathway in CAFs.....	188
5.2.3.1 TRAF2 and TRAF3 degradation in CAFs	190
5.2.3.2 NIK expression in CAFs	191
5.2.4 The effect of silencing cellular IKK α expression on the non-canonical NF- κ B pathway in primary CAFs and NFs.....	191
5.2.4.1 siRNA silencing of IKK α in NFs	192
5.2.4.2 siRNA silencing of IKK α in CAFs.....	194
5.2.4.3 The effect of siRNA IKK α silencing on LT $\alpha_1\beta_2$ induced p100 processing in NFs	196
5.2.4.4 The effect of siRNA IKK α silencing on LT $\alpha_1\beta_2$ induced p100 processing in CAFs	197
5.2.5 The effect of SU compounds on non-canonical NF- κ B pathway in NFs and CAFs.....	198

5.2.5.1 The effect of SU compounds on LT $\alpha_1\beta_2$ induced p100 processing in NFs	198
5.2.5.2 The effect of SU compounds on LT $\alpha_1\beta_2$ induced phosphorylation of p100 and p52 in CAFs	200
5.2.6 The role of IKK α in CXCL12 expression in CAFs and NFs.....	203
5.2.7 Detection of CXCL12 protein expression in CAFs and NF cells using ELISA.....	204
5.2.7.1 The effect of SU1349 and IKK α siRNA silencing on CXCL12 protein expression in NFs and CAFs.....	204
5.3 Discussion	206
Chapter Six	210
6.1 General discussion and Future directions.....	211
6.2 Conclusion.....	218
References.....	219

List of Figures

Figure 1.1:	The structure of the various subunits of NF- κ B and I κ B members	14
Figure 1.2:	Schematic representation of the principal structural motifs of IKK α	18
Figure 1.3:	Schematic diagram of the NF- κ B pathways	21
Figure 1.4:	Regulation of the alternative NF- κ B pathway in resting vs receptor-stimulated cells	24
Figure 1.5:	The consequences of IKK α activation	34
Figure 3.1:	Time course of LT $\alpha_1\beta_2$ -mediated p100 phosphorylation and p100 processing in U2OS cells	68
Figure 3.2:	The effect of SU1261 upon LT $\alpha_1\beta_2$ -mediated p100 phosphorylation and p52 formation in U2OS cells	70
Figure 3.3:	The effect of SU1266 upon LT $\alpha_1\beta_2$ -mediated p100 phosphorylation and p52 formation in U2OS cells	71
Figure 3.4:	The IC ₅₀ values of SU1261 and SU1266 for inhibition p100 phosphorylation and p52 formation induced by LT $\alpha_1\beta_2$ in U2OS cells	72
Figure 3.5:	Time course for TNF α -mediated I κ B α degradation and p65 phosphorylation in U2OS cells	74
Figure 3.6:	Time course for IL-1 β -mediated I κ B α degradation and p65 phosphorylation in U2OS cells	75
Figure 3.7:	The effect of SU1261 upon TNF α -mediated I κ B α degradation in U2OS cells	77
Figure 3.8:	The effect of SU1266 upon TNF- α -mediated I κ B α degradation in U2OS cells.	78
Figure 3.9:	The effect of SU1261 upon TNF- α -mediated pp65 phosphorylation in U2OS	80
Figure 3.10:	The effect of SU1266 upon TNF- α -mediated p65 phosphorylation in U2OS cells	81
Figure 3.11:	The effect of SU1349 upon LT $\alpha_1\beta_2$ -mediated p100 phosphorylation and p52 formation in MCF-7 cells	84
Figure 3.12:	The effect of SU1433 upon LT $\alpha_1\beta_2$ -mediated p100 phosphorylation and p52 formation in MCF-7 cells	85
Figure 3.13:	The IC ₅₀ values of SU1349 and SU1433 for inhibition p100 phosphorylation and p52 formation induced by LT $\alpha_1\beta_2$ in MCF-7 cells	86
Figure 3.14:	The CETSA melting curves for (A) p38 α and (B) ERK in U2OS cells	89
Figure 3.15:	The CETSA melting curves for IKK α in U2OS cells	90

Figure 3.16:	The comparison of target engagement for p38 α , ERK and IKK α in the intact versus lysed U2OS cells	91
Figure 3.17:	SB203580 modulates the thermostability of p38 in U2OS cells	93
Figure 3.18:	SU1261 does not alter the thermostability of IKK α in U2OS cells	95
Figure 4.1:	LT $\alpha_1\beta_2$ induces p52 and RelB nuclear translocation in U2OS cells	106
Figure 4.2:	Time course of TNF α -mediated phosphorylation of p100 in U2OS	108
Figure 4.3:	Time course of TNF α -mediated p52 formation in U2OS cells	110
Figure 4.4:	Time course of TNF α -mediated RelB formation in U2OS cells	111
Figure 4.5:	TNF α induces p52 and RelB nuclear translocation U2OS cells	113
Figure 4.6:	Time course of IL-1 β -mediated phosphorylation of p100 in U2OS	114
Figure 4.7:	Time course of IL-1 β -mediated p52 in U2OS cells	116
Figure 4.8:	IL-1 β induces RelB formation in U2OS cells	117
Figure 4.9:	IL-1 β induces p52 and RelB nuclear translocation in U2OS cells	119
Figure 4.10:	Comparison of TNF α and IL-1 β -mediated phosphorylation of p100 in U2OS, MCF-7 and CAFs cells	120
Figure 4.11:	Comparison of kinetic profiles for p100, p52 and RelB for different agonists	121
Figure 4.12:	The effect of siRNA IKK α on IKK α expression in U2OS	123
Figure 4.13:	The effect of siRNA IKK β on IKK β expression in U2OS	124
Figure 4.14:	The effect of IKK α or β siRNA upon LT $\alpha_1\beta_2$ -mediated phosphorylation of p100 and p52 formation in U2OS cells	126
Figure 4.15:	The effect of IKK α or β siRNA upon TNF α -mediated phosphorylation of p100 in U2OS cells	128
Figure 4.16:	The effect of IKK α or β siRNA upon IL-1 β -mediated phosphorylation of p100 in U2OS cells	130
Figure 4.17:	The effect of double-knockdown of IKK α and IKK β siRNA upon TNF α -mediated p100 phosphorylation in U2OS cells	132

Figure 4.18:	The effect of IKK α siRNA upon TNF α -mediated p52 formation in U2OS cells	134
Figure 4.19:	The effect of IKK α siRNA upon TNF α -mediated RelB formation in U2OS cells	135
Figure 4.20:	The effect of SU1261 upon TNF α -mediated p100 phosphorylation in U2OS cells	137
Figure 4.21:	The effect of SU1266 upon TNF α -mediated p100 phosphorylation in U2OS cells	138
Figure 4.22:	The effect of SU1349 upon TNF α -mediated p100 phosphorylation in U2OS	139
Figure 4.23:	The effect of SU1261 upon IL-1 β -mediated p100 phosphorylation in U2OS cells	141
Figure 4.24:	The effect of SU1266 upon IL-1 β -mediated p100 phosphorylation in U2OS	142
Figure 4.25:	The effect of SU1349 upon IL-1 β -mediated p100 phosphorylation in U2OS cells	143
Figure 4.26:	The effect of SU1261 upon IL-1 β -mediated p52 and RelB nuclear formation in U2OS cells	145
Figure 4.27:	The effect of SU1266 upon IL-1 β -mediated p52 and RelB nuclear formation in U2OS cells	147
Figure 4.28:	The effect of CW15407 on TNF α induced phosphorylation of p100 in U2OS cells	149
Figure 4.29:	The effect of CW 15407 on IL-1 β induced phosphorylation of p100 in U2OS cells	150
Figure 4.30:	The effect CW15407 on LT $\alpha_1\beta_2$ induced phosphorylation of p100 in U2OS cells	152
Figure 4.31:	The effect IKK2 X1 on TNF α -mediated I κ B α degradation in U2OS cells	154
Figure 4.32:	The effect IKK2 X1 on TNF α induced phosphorylation of p100 in U2OS cells	155
Figure 4.33:	The effect IKK2 X1 on IL-1 β induced phosphorylation of p100 in U2OS cells	156
Figure 4.34:	Concentration dependency of LT $\alpha_1\beta_2$, TNF α and IL-1 β -induced CXCL12 luciferase activity in U2OS-CXCL12 cells	158
Figure 4.35:	Time course of LT $\alpha_1\beta_2$, TNF- α and IL-1 β -mediated CXCL12 luciferase activity in U2OS-CXCL12 cells	159
Figure 4.36:	The effect of TNF- α and IL-1 β on LT $\alpha_1\beta_2$ -induced CXCL12 luciferase activity in U2OS-CXCL12 cells	160
Figure 4.37:	The effect of IKK α and IKK β siRNA on LT $\alpha_1\beta_2$ induced CXCL12 luciferase activity in U2OS-CXCL12 cells	161

Figure 4.38:	The effect of IKK α and IKK β siRNA on TNF α induced CXCL12 luciferase activity in U2OS-CXCL12 cells	162
Figure 4.39:	The effect of IKK α and β siRNA on IL-1 β induced CXCL12 luciferase activity of CXCL12 in U2OS-CXCL12 cells	163
Figure 4.40:	The effect of SU1261 upon LT $\alpha_1\beta_2$ -mediated CXCL12 luciferase activity in U2OS-CXCL12 cells	165
Figure 4.41:	The effect of SU1266 upon LT $\alpha_1\beta_2$ -mediated CXCL12 luciferase activity in U2OS-CXCL12 cells	165
Figure 4.42:	The effect of SU1261 upon TNF α -mediated CXCL12 luciferase activity in U2OS-CXCL12 cells	167
Figure 4.43:	The effect of SU1266 upon TNF α -mediated CXCL12 luciferase activity in U2OS-CXCL12 cells	167
Figure 4.44:	The effect of SU1261 upon IL-1 β -mediated CXCL12 luciferase activity in U2OS-CXCL12 cells	169
Figure 4.45:	The effect of SU1266 upon IL-1 β -mediated CXCL12 luciferase activity in U2OS-CXCL12 cells	169
Figure 4.46:	IC ₅₀ values for SU1261 and SU1266 for inhibition of CXCL12 luciferase activity in U2OS-CXCL12 cells	171
Figure 4.47:	LT $\alpha_1\beta_2$ ligation induces non-canonical NF- κ B-dependent mRNA expression of CXCL12 in U2OS cells	173
Figure 4.48:	TNF α ligation induces non-canonical NF κ B-dependent mRNA expression of CXCL12 in U2OS cells	173
Figure 4.49:	IL-1 β ligation induces non-canonical NF κ B-dependent mRNA expression of CXCL12 in U2OS cells	174
Figure 4.50:	The effect of SU1261 and IKK α siRNA on IL-1 β induces non-canonical NF κ B-dependent mRNA expression of CXCL12 in U2OS cells	175
Figure 5.1:	Time course of LT $\alpha_1\beta_2$ -mediated p100 processing in NFs	185
Figure 5.2:	Time course of LT $\alpha_1\beta_2$ -mediated TRAF2 and TRAF3 degradation in NFs	186
Figure 5.3:	Time course of LT $\alpha_1\beta_2$ -mediated NIK expression in NFs	187
Figure 5.4:	Time course of LT $\alpha_1\beta_2$ -mediated p100 phosphorylation and p100 processing in CAFs	189
Figure 5.5:	Time course of LT $\alpha_1\beta_2$ -mediated TRAF2 and TRAF3 degradation in CAFs	190
Figure 5.6:	Time course of LT $\alpha_1\beta_2$ -mediated NIK expression in CAFs cells	191

Figure 5.7:	The effect of siRNA IKK α on IKK α expression in NFs	193
Figure 5.8:	The effect of siRNA IKK α on IKK α expression in CAFs	195
Figure 5.9:	The effect of IKK α siRNA upon LT $\alpha_1\beta_2$ -mediated p52 formation in NFs	196
Figure 5.10:	The effect of IKK α siRNA upon LT $\alpha_1\beta_2$ -mediated p52 formation in CAFs	197
Figure 5.11:	The effect of SU1349 upon LT $\alpha_1\beta_2$ -mediated p52 formation in NFs	199
Figure 5.12:	The effect of SU1349 upon LT $\alpha_1\beta_2$ -mediated p100 phosphorylation and p52 formation in CAFs	201
Figure 5.13:	The effect of SU1433 upon LT $\alpha_1\beta_2$ -mediated p100 phosphorylation and p52 formation in CAFs	202
Figure 5.14:	LT $\alpha_1\beta_2$ ligation induces non-canonical NF- κ B-dependent mRNA expression of CXCL12 in CAFs and NFs	203
Figure 5.15:	Expression level of CXCL12 protein in CAFs and NFs	204
Figure 5.16:	The effect of SU1261 and IKK α siRNA upon CXCL12 protein levels in NFs	205
Figure 5.17:	The effect of SU1261 and IKK α siRNA upon CXCL12 protein levels in CAFs	205
Figure 6.1:	A schematic diagram shows the effect of SU compounds to inhibit CXCL12 expression induced by LT $\alpha_1\beta_2$, TNF α - and IL-1 β via the non-canonical NF- κ B pathway in U2OS cells.	216

List of Tables

Table 2.1:	SiRNA transfection agents. Target gene, siRNA origin and target sequence	46
Table 2.2:	Antibodies used for Western blot and optimal conditions	52
Table 2.3:	Tetro cDNA synthesis Master Mix	58
Table 2.4:	TaqMan® Gene Expression Assays. The gene and assay ID are detailed	59
Table 2.5:	Applied Biosystems StepOne Plus thermal cycling program for TaqMan® RT-qPCR	59
Table 3.1:	The Ki values for SU compounds	66

Chapter One
General Introduction

1 Introduction

1.1 Bone and its development

Bone is the solid tissue that functions to move, support, and protect various organs of the body. It primarily consists of collagen and calcium phosphate. The biology of bone has been significantly described during the last few decades. The cells associated with bone biology consist of osteoblasts, osteoclasts and osteocytes, which are found only in the bone. Osteoblasts are the primary cells responsible for osteogenesis (bone formation) and mineralisation (Florencio-Silva et al., 2015). Osteoblasts are derived from the bone marrow and found on the surface of new bone, whereas osteoclasts are derived from the bone marrow, responsible for bone resorption, related to white blood cells and found on the surface of the bone mineral next to dissolving bone. Osteocytes are cells derived from osteoblasts that are located inside the bone. Moreover, osteocytes can sense cracks or pressure in the bone and help direct osteoclasts to where bone should be dissolved (Vaananen et al., 2000).

Physiological bone turnover has two temporal phases: 1) bone modelling, which occurs during the developmental phase; and 2) bone remodelling, which is a lifelong process involving tissue renewal (Soltanoff et al., 2009). Bone development can be divided into two processes: 1) intramembranous ossification takes place on the flat bones through the condensation of mesenchymal stem cells, then osteoprogenitors differentiate into osteoblasts that actively synthesise a new bone matrix. These cells later either change into osteocytes or undergo apoptosis. During this process, bone is formed in the absence of a cartilage model; and 2) endochondral ossification (Cartilage Model), which occurs in the long bone. During this process, a cartilage model is first formed and then subsequently replaced by bone tissue. To achieve this, osteoblasts enter following vascular invasion and replace the chondrocytes, and

osteoclasts create a bone marrow cavity (Berendsen and Olsen, 2015, Long and Ornitz, 2013).

The communication between bone cells is critical to bone health, which occurs constantly to maintain metabolic functions, structural integrity, and respond to external activators. While osteoclasts have an important role in modelling bone, osteoblasts and osteoclasts play a critical role in the bone remodelling process. Bone remodelling activity increases around menopause in women and is also associated with aging in men. Throughout life, osteoclasts remove bone and osteoblasts replace it, leading to a complete replacement of the skeleton every 10 years (Novack, 2011, Manolagas et al., 1995). The balance between osteoclastic bone resorption and osteoblastic bone formation is extremely important and most bone diseases are caused by a disturbance in this balance (e.g., multiple myeloma and osteoporosis). Thus, the study of the proliferation and differentiation of bone cells is critical to gain a deeper understanding of bone diseases and improve treatment.

1.2 Bone tumours

Cancer is a major public health problem in the United Kingdom and worldwide. In 2012, about 8.2 million cancer deaths were reported from a total 14.1 million people diagnosed with cancer (Torre et al., 2015). Despite advances in cancer therapy, cancer deaths are expected to continue to increase worldwide to reach 13 million in 2030 (Ferlay et al., 2010). According to the most recent statistics available from Cancer Research UK, around 580 new cases of bone sarcoma are diagnosed each year in the UK (CANCER_RESEARCH_UK, 2018), suggesting that there is an urgent need to develop novel anti-cancer therapies to reduce cancer mortality rates.

Bone tumours can be classified based on origin. Primary bone tumours involve cancer cells from the bone tissue or bone marrow itself. Secondary bone tumours (bone metastases) are metastasised to bone from a tumour that originated elsewhere in the body. In both types, despite surgery and chemotherapy, treatment of these tumours is extremely difficult, and the current therapies are not completely effective.

1.2.1 Primary bone tumours

Primary bone cancer is a relatively rare type of cancer that begins in the bone tissue or the bone marrow itself. It is the most common cancer in adolescents and elderly persons (Siegel et al., 2014). Osteosarcoma (OS), chondrosarcoma and Ewing's sarcoma are the three most common types of primary bone tumours.

1.2.1.1 Osteosarcoma

Osteosarcoma is the most common primary malignant bone tumour, which affects children, teenagers and elderly adults (Basu-Roy et al., 2013, Mirabello et al., 2009). Osteosarcoma occurs more frequently in the larger bones during the rapid growth period or in the final stages of life (Mutsaers and Walkley, 2014). Moreover, it is the sixth most common type of cancer in children (Niforou et al., 2008). Although the causes are unknown, rapid bone growth, irradiation and genetic influences are associated with its development. Osteosarcomas are commonly spread by metastases to other sites in the body, especially the lungs (Gill et al., 2013, Basu-Roy et al., 2013). Over 50 years ago, the human osteosarcoma U2OS cell line was derived from a sarcoma of the tibia of a 15-year-old girl (Bayani et al., 2003). The origin of these cells has not yet been definitively confirmed; however, there is evidence to suggest that their source was osteoblast precursors and mesenchymal stem cells

(MSCs), with mutations found mostly in the Retinoblastoma (RB) and p53 pathway (Mutsaers and Walkley, 2014). U2OS cells are widely used in biomedical research, including bone formation, arthritis, biochemistry, and molecular biology. Recently, several common molecular mechanisms have been described in sarcomagenesis, including mutations in genes that control cell cycle progression and constitutive activation of signal transduction pathways (Matushansky and Maki, 2005).

1.2.1.2 Chondrosarcoma

Chondrosarcoma is the second most common primary malignant bone tumour in adults over 40 years of age (Hemmati et al., 2011, Clark et al., 2010), which often grows slowly in bones that elongate due to endochondral ossification (van Oosterwijk et al., 2013). Due to poor vascularisation and its resistance to radio-chemotherapy, surgical resection remains an effective treatment for chondrosarcoma (Dai et al., 2011). Although metastasis is uncommon, the lung is the most frequent metastatic site in chondrosarcomas (Qureshi et al., 2010, Gelderblom et al., 2008). Preclinical studies have identified the upregulation of Hypoxia inducible factor 1-alpha (HIF1- α hypoxia pathway) and mutations in isocitrate dehydrogenases (IDH) as active pathways in chondrosarcoma (van Oosterwijk et al., 2013, Boeuf et al., 2010), as well as other pathways such as vascular endothelial growth factor (VEGF), mammalian target of rapamycin (mTOR), Protein kinase B (AKT) and the phosphoinositide-3 kinase signalling pathway (PI3K) (van Oosterwijk et al., 2013). Therefore, a combination of the targeted therapies may be the best approach to treat a tumour that exhibits low vascularity (Jamil et al., 2010).

1.2.1.3 Ewing's sarcoma

Ewing's sarcoma is most common in children and young adults, and primarily occurs in the pelvis and bones of the chest wall. It is currently believed that the origin of these cells is from MSCs. This type of sarcoma is characterised by aggressive behaviour with metastases, with the lungs and bone being the most common target organs (Hauer et al., 2013, Berghuis et al., 2012). A number of studies suggested that the *EWS-FLI-1* fusion gene, which is only expressed in tumour cells, acts as a transcription factor to regulate genes that mediate oncogenesis in Ewing's sarcoma (Lessnick and Ladanyi, 2012, Suva et al., 2009). NR0B1, NKX2.2, and IGF-binding protein 3 are the most downstream targets of EWS-FLI-1 (Kinsey et al., 2009, Smith et al., 2006, Prieur et al., 2004), which make it a promising molecular target for the treatment of Ewing's sarcoma.

1.2.1.4 Primary bone marrow tumours

These tumours can arise in cells that are produced in the bone marrow, including multiple myeloma, leukaemia and lymphoma.

1.3 Secondary bone tumours (Bone metastases)

Tumours that spread to the bones from other parts of the body are called secondary bone tumours, for which the breast, prostate, and lung are the most common types of cancer metastases to the bone. Moreover, this type is more common than primary bone tumours (Weilbaecher et al., 2011). The metastatic process is characterised by interactions between tumour cells and the bone microenvironment (Eil et al., 2013), which lead to the destruction of bone cells (Browne et al., 2014, Tagliaferri et al., 2012). Recent studies indicate that the receptor activator of NF- κ B ligand (RANKL)

with its receptor, RANK, promotes the metastasis of breast cancer cells into bone (Fata et al., 2000). Metastatic tumour cells move from vessels into bone through epithelial to mesenchymal transition (EMT), where the cells gain motility and become more invasive (Hehlmann et al., 2007). A number of cellular proteases have been implicated in the metastatic process in particular Matrix metalloproteinases (MMPs), which is also mediated through an increase in activated RANKL (Kreil et al., 2007). Insulin-like growth factors (IGFs) in bone resorption can also activate the NF- κ B signalling pathway to increase proliferation and decrease apoptosis (Hiraga et al., 2012). CXCL12 is highly expressed by bone marrow and osteoblasts, which interacts with MMP1, IL-11 and connective tissue growth factor (CTGF) to promote breast cancer cell migration to the bone (Cairolì et al., 2013).

1.4 Signalling pathways in bone cancer

Osteoblasts and osteoclasts reside in the bone marrow, maintaining the balance between bone formation and bone resorption, respectively. This balance is important because it affects bone maintenance as well as the general bone structure associated with pathological conditions (e.g., cancer metastasis and arthritis). Signalling pathways are critical for inducing different physiological responses in bone, which lead to either the formation or loss of bone. Therefore, a better understanding of the role of different signalling pathways in the development of bone cancer may allow improved disease targeting and lead to the development of new therapies. The following sections outline a number of signalling pathways associated with bone cancer.

1.4.1 Wnt signalling pathway

The Wnt signalling pathway plays an important role in the growth and differentiation of cells during development and is strongly associated with cancer. Wnt signalling pathway is divided into two major branches: 1) the canonical pathway (also called the Wnt/ β -catenin pathway); and 2) the non-canonical pathway (Logan and Nusse, 2004). The Wnt/ β -catenin pathway can be activated through the binding of ligands to the Wnt receptor on the cell membrane and activation of β -catenin. In cells at rest β -catenin is inactivated via binding to Glycogen synthase kinase 3 beta (GSK3- β). Phosphorylation of this complex triggers β -catenin release, accumulation within the cytosol and translocation into the nucleus where the subsequent expression of target genes occurs (Pasca di Magliano et al., 2007, Zeng et al., 2006). There are also two major Wnt non-canonical pathways: 1) the Wnt-Ca²⁺ pathway (Kohn and Moon, 2005) and 2); the Wnt-PCP pathway (Jenny, 2010).

Several studies have linked the activity of Wnt signalling pathways to bone development and bone diseases (Rawadi and Roman-Roman, 2005, Westendorf et al., 2004). Babij and colleagues found a high level of β -catenin in osteoblasts following activation of this pathway, resulting in the transcriptional activation of genes required for bone formation (Babij et al., 2003). Furthermore, in a preclinical study in rats, it was found that the activation of this pathway in osteoblasts caused increased translocation of β -catenin into the nucleus, inducing transcriptional co-activation of genes integral to bone formation (Little et al., 2002). On the other hand, It was found that the non-canonical pathway regulates vertebrate development (Veeman et al., 2003), limb morphogenesis (Wang et al., 2011), chondrogenesis (Randall et al., 2012, Witte et al., 2010), and osteoblastogenesis (Liu et al., 2007). The Wnt/ β -catenin pathway has been demonstrated to be associated with the initiation and progression of bone metastasis through regulation of gene expression, cell invasion, migration,

proliferation, and differentiation (Chu et al., 2014, Rabbani et al., 2013). Many studies reported that the aberrant activation of this pathway plays a critical role in the development and progression of osteosarcoma (Cai et al., 2014, Lin et al., 2013). In addition, it was demonstrated that blocking the Wnt/ β -catenin signalling resulted in decreased invasion, proliferation, migration, and induce apoptosis in human osteosarcoma cells (Leow et al., 2014, Liu et al., 2013).

1.4.2 TGF- β and BMP signalling pathway

The transforming growth factor-beta (TGF- β) superfamily consists of approximately 60 members (e.g., TGF- β s and Activin) (Guo and Wang, 2009, Feng and Derynck, 2005), as well as bone morphogenetic proteins (BMPs) which were discovered in 1965 (Urist, 1997). The TGF- β /BMP signalling pathway is fundamentally important in bone formation throughout life, including skeleton morphogenesis, growth plate development, osteoblast differentiation and mesenchyme condensation (Chen et al., 2012). This pathway can be activated through the activation of receptor serine/threonine kinases. Phosphorylation of TGF- β (I/II) or BMP receptors activates Smads as a downstream signalling intermediate of TGF- β /BMP signalling. Activated R-Smads form a complex with Smad and Smad4 and subsequently undergo nuclear translocation to direct transcriptional responses (Yi et al., 2010, Wagner et al., 2010).

As with Wnt, TGF- β /BMP signalling disorders have been linked to many bone diseases, including tumour metastasis, osteoporosis and osteoarthritis, autoimmune, cancer and cardiovascular diseases (Moustakas and Heldin, 2009, Papachroni et al., 2009, Miyazono et al., 2005, Siegel and Massague, 2003). In addition, TGF- β signalling pathway is a critical for the expansion and maintenance of progenitor stem cells for osteoblasts (Derynck and Akhurst, 2007). Furthermore, TGF- β promotes

osteoprogenitor proliferation, commitment to the osteoblastic lineage, and differentiation through the Smad2/3 and MAPKs pathways (Centrella et al., 1988). Recently, it was found that TGF- β indirectly associates with the TRAF6-TAB1-TAK1 complex through Smad2/3; this pathway is indispensable for RANKL-induced osteoclastogenesis (Yasui et al., 2011). Several studies have shown that the TGF- β pathway plays a role in different stages of carcinogenesis, TGF- β serves as a tumour suppressor through inhibiting cell proliferation (Sun, 2004, Massague et al., 2000). However, many studies have documented that primary tumour cells in the late stages of carcinogenesis could reprogram their response to TGF- β through mutational inactivation of various components of the TGF- β pathway, which leads to bone metastasis (Kominsky et al., 2007, Kang et al., 2005). Thus, inhibiting this pathway in advanced stages of cancer may lead to beneficial therapeutic responses via inhibiting metastatic progression (Bandyopadhyay et al., 2006).

In addition, it was found that BMP-2 is also required to induce bone formation (Noel et al., 2004), whereas BMP-7 induces calcium mineralisation and ATP activity (Shen et al., 2010, Gu et al., 2004). BMP plays a critical role in the formation of the skeleton and bone formation through the regulation of osteoblast lineage-specific differentiation (Beederman et al., 2013). Moreover, BMP-2 has been implicated in the tumour metastasis through facilitating bone metastasis in gastric cancer (Park et al., 2008). To date, commercial human-BMP2 and -BMP7 have been used clinically in over one million patients worldwide in a wide-range of therapeutic interventions, such as osteoporosis, acute fractures, spinal fusions and bone defects (Carreira et al., 2014).

1.4.3 PTH signalling pathway

Parathyroid hormone (PTH) is an 84-amino-acid polypeptide hormone secreted from the parathyroid glands, that can activate its receptor (PTH1R), which is expressed on osteoblasts (Juppner et al., 1991). This pathway has an important role as an essential mediator of bone remodelling and a major regulator of calcium and phosphate homeostasis (Swarthout et al., 2002). The interaction between the PTH and the receptor leads to elevated calcium levels in the blood due to the phosphorylation of the receptor. This has a negative feedback effect on the parathyroid gland, which results in reducing the release of the PTH (Tawfeek et al., 2002, Chauvin et al., 2002). Several studies have demonstrated that the PTH pathway is useful to prevent fractures in osteoporosis via calcium reabsorption through the activation of protein-kinase A (PKA) and/or cAMP (Lindsay et al., 2007, Cosman and Lindsay, 2004). Initially, studies noted that PTH could increase the bone mass of rats (Bauer et al., 1929); however, it is now well-established that the injection of PTH leads to increased bone mass in patients with osteoporosis (Sone et al., 1995). This increased bone mass is largely due to enhanced proliferation and differentiation of osteoblasts as a result of an increased number of these cells (Datta et al., 2007, Lindsay et al., 2007), and decreased osteoblast apoptosis (Manolagas, 2000).

1.4.4 The nuclear factor Kappa B (NF- κ B) signalling pathway

The transcription factor NF- κ B was first identified in 1986 by Sen and Baltimore as the nuclear factor that regulated immunoglobulin kappa (κ) light chain gene expression in B cells (Sen and Baltimore, 1986). Today, NF- κ B is regarded as a ubiquitous signalling pathway which plays an important role in a number of both physiological and pathophysiological processes including; cancer, inflammation and atherosclerosis, immunity, foetal development, cellular proliferation and apoptosis

(Hoesel and Schmid, 2013, Oeckinghaus and Ghosh, 2009, Bonizzi et al., 2004, Brand et al., 1996). There are two main NF- κ B pathways: 1) the canonical (classical) NF- κ B pathway; and 2) the non-canonical (alternative) NF- κ B pathway. Both pathways can be regulated by the inhibitory κ B kinases IKKs (IKK α/β), as upstream regulators of these NF- κ B pathways, leading to the formation of NF- κ B subunits, subsequent nuclear localisation and regulation of a large number of genes that control various biological processes (Xiao and Ghosh, 2005). Although variations exist within each pathway, the molecular structures of each of the components share similar features, which are outlined below (Gamble et al., 2012).

1.4.4.1 Members and structure of NF- κ B

Since the discovery of NF- κ B in 1986, five members of the NF- κ B transcription factors have been identified, including NF- κ B1 (p50/p105), NF- κ B2 (p52/p100), RelA (p65), RelB and c-Rel genes, which function as homodimers and heterodimers (Hayden and Ghosh, 2008). All NF- κ B members have a conserved N- terminal region called the Rel homology domain (RHD), which is responsible for DNA binding, dimerisation, the nuclear localisation sequence (NLS) and I κ B binding (Hayden and Ghosh, 2008, Chen and Ghosh, 1999, Blank et al., 1992).

These proteins are structurally linked as a homodimer or heterodimer by their N-terminal amino acid Rel homology domains (RHD) and translocate into the nucleus where they bind with specific DNA sequences as κ B sites (Siebenlist et al., 1994). Several studies have demonstrated that NF- κ B dimers are present in the cytoplasm in an inactive form by binding to inhibitory proteins (i.e., I κ Bs) which block specific NLS domains. I κ Bs subunits include I κ B α , I κ B β , I κ B γ , I κ B ϵ , and Bcl-3 (Ferreiro and

Komives, 2010), I κ Bzeta (Muta, 2006), I κ BNS (Kuwata et al., 2006), and the precursor proteins p100 (NF- κ B2) and p105 (NF- κ B1) (Hayden and Ghosh, 2012). (Figure 1.1).

I κ Bs contain ankyrin repeats; interestingly, p100 and p105, the precursors of p52 and p50 respectively, also have this region in their C-terminus. In contrast, RelA, RelB and c-Rel all contain a transactivation domain (Marienfeld et al., 2003). However, when p52 or p50 bind to RelB and RelA respectively, they comprise a transcriptional activator and one I κ B subunit (Bcl-3), which contains the transactivation domains and can link to the p52 and p50 dimers and perform complex transcriptional activities (Bours et al., 1993, Nolan et al., 1993).

The NF- κ B family of proteins is further divided into subfamilies. Class one NF- κ B proteins consist of p105/p50 and p100/p52. Since these proteins do not have C-terminal transactivation domains, they have a number of ankyrin repeats that functions as a transrepression region when binding with κ B proteins (Guan et al., 2005, Brown et al., 1994, Plaksin et al., 1993). In contrast, the second class subfamily of NF- κ B proteins includes RelA, RelB and c-Rel. These NF- κ B proteins have a transactivation region in their C-terminal RHD which contains acidic, serine and hydrophobic amino acids. A mutation in any of these amino acids will lead to decreased transcription activity and the transcription of NF- κ B itself, which is dependent on these genes (Dobrzanski et al., 1993). In addition, this class of subunits contains an N-terminal leucine zipper region (LZ) which allows the NF- κ B proteins to physically relate to each other. Complete activation of most NF- κ B subunits occurs as a result of the activation of the C-terminal; interestingly, the complete activation of RelB requires the presence of both C- and N-terminals (Dobrzanski et al., 1993). Figure 1.1 illustrates the structure of the various subunits of NF- κ B and I κ B members.

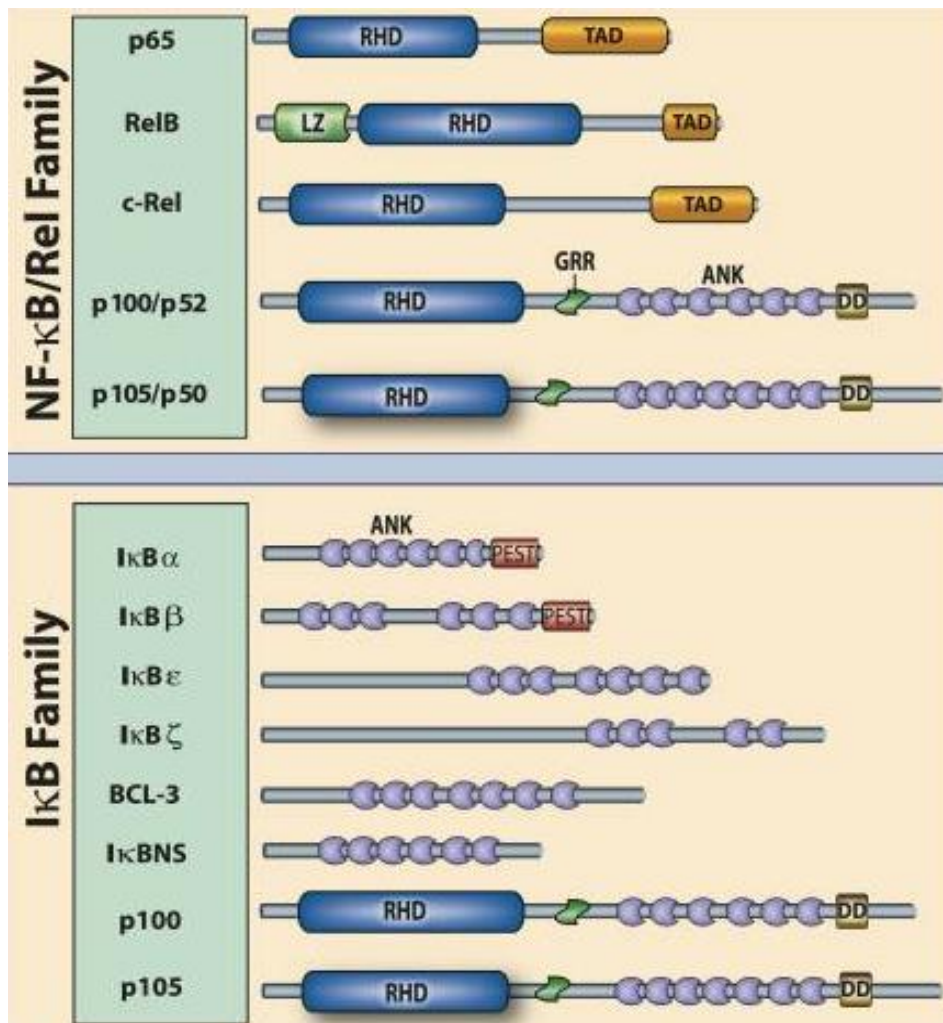


Figure 1.1: The structure of the various subunits of NF-κB and IκB members. The number of amino acids is shown next to each NF-κB and IκB member. LZ: leucine zipper; TD: transactivation domain; RDH: homology domain; PEST region: polypeptide sequence enriched in proline (P); glutamic acid (E); serine (S); and threonine (T) region; GRR: glycine-rich region; DD: death domain. [Adapted from (Hayden and Ghosh, 2012)].

1.4.4.2 IκB structure

In 1988, Baeuerle and Baltimore discovered inhibitory kappa B proteins (IκBs) as NF-κB inhibitor proteins, which control NF-κB signalling by binding to NF-κB in the cytoplasm (Baeuerle and Baltimore, 1988). Mammalian IκB subunits have a number of structures that have been cloned by cDNA, including IκBα (Davis et al., 1991), IκBβ

(Thompson et al., 1995), I κ B γ (Inoue et al., 1992), I κ B ϵ (Li and Nabel, 1997), Bcl-3 (Ray et al., 1995).

I κ B subunits can be classified into NF- κ B precursors (p105 and p100), classical I κ Bs (I κ B α , I κ B β and I κ B ϵ), and nuclear I κ Bs (Bcl-3 and I κ B- γ) (Huxford and Ghosh, 2009). All I κ B family members have an ankyrin repeat domain (Figure 1.1) which binds to the RHD regions within the Rel/ NF- κ B dimer (Cervantes et al., 2009). This binding between the I κ B subunits and the NF- κ B family results in the NLS being masked by the I κ B protein. Consequently, NF- κ B is retained in the cytoplasm and prevents the nuclear translocation of Rel/ NF- κ B proteins (Beg et al., 1992). Furthermore, mutations within the ankyrin repeats of I κ Bs can lead to loss of binding between NF- κ B and I κ B, resulting in NF- κ B translocation into the nucleus and DNA binding (Inoue et al., 1992). A number of studies have demonstrated that each subunit of the I κ B family is associated a preferred partner of the NF- κ B family. For instance, while non-classical I κ Bs are able to link with all NF- κ B members, the classical I κ Bs preferentially bind to either p65 or c-Rel (Huxford and Ghosh, 2009, Michel et al., 2001).

1.4.4.2.1 Regulation of I κ B α

In 1990, Zabel and co-workers discovered two major I κ B isoforms associated with NF- κ B. These proteins were I κ B α and I κ B β (Zabel and Baeuerle, 1990). I κ B α has been found to play a key role in the canonical NF- κ B pathway as a specific inhibitor to prevent p65 NF- κ B (RelA) translocation into the nucleus when cells are at rest (Jaffray et al., 1995). Another study demonstrated that I κ B α can bind to p50/p65 heterodimers at a much higher affinity compared to p65 homodimers with a moderate affinity and p50 homodimers with low affinity (Malek et al., 1998).

Following cellular stimulation by agonists such as $\text{TNF}\alpha$, $\text{I}\kappa\text{B}\alpha$ is phosphorylated at serine residues 32 and 36 within the N-terminus (Karin and Ben-Neriah, 2000, Brockman et al., 1995). $\text{I}\kappa\text{B}\alpha$ phosphorylation functions to initiate ubiquitination and targets the protein for degradation by the 26S proteasome, which leads to the release of the NF- κB subunits. Lysine residues 22 and 21 have been identified as the primary site for signal-induced ubiquitination of $\text{I}\kappa\text{B}\alpha$, which is a critical step prior to degradation. Any mutation that occurs in these sites leads to an inhibition of ubiquitination and degradation processes, the NF- κB units remain in the cytoplasm because they cannot be separated from $\text{I}\kappa\text{B}\alpha$ (Chen et al., 1996, Scherer et al., 1995)

1.4.4.2.2 Inhibitory NF- κB 2 (p100/p52)

The activation of p52/RelB heterodimer is largely distinct from other NF- κB subunits and the role of p100 as an $\text{I}\kappa\text{B}$ member is unique. p100/p52 is also called NF- κB 2 but was originally named as p98 when characterised as a 98 kDa protein (Mercurio et al., 1993). NF- κB 1 and NF- κB 2 are synthesised as large precursors called p105 and p100, which undergo ubiquitin mediated-proteasomal degradation to generate p50 and p52 NF- κB subunits (Senftleben et al., 2001, Karin and Ben-Neriah, 2000). Similar to $\text{I}\kappa\text{B}\alpha$, both p100 and p105 subunits also contain ankyrin repeats within the C-terminal region, and the C-terminal domains of both p100 and p105 are required to retain NF- κB in the cytoplasm (Mercurio et al., 1993, Rice et al., 1992). Both the p52 and p50 NF- κB subunits do not have transactivation domains in their C terminal unlike RelA, RelB and c-Rel. Nevertheless, they can participate in targeting gene transactivation through the formation of heterodimers with RelB, RelA or c-Rel (Li and Verma, 2002). In addition, the p52 and p50 homodimers can function as transcriptional activators through binding to the nuclear protein, Bcl-3 (Fujita et al.,

1993). Further details will be discussed in relation to signalling through the non-canonical NF- κ B pathway in Section 1.4.4.5.

1.4.4.3 Inhibitory Kappa B kinases (IKKs) complex structure

The upstream regulators of I κ B α function were not identified for some years. In 1996, the I κ B kinases (IKKs) were identified by Chen and colleagues as a series of enzymes that regulate I κ B α phosphorylation at Ser 32 and Ser 36 (Chen et al., 1996). IKKs complex (700-900 kDa) are composed of three subunits: IKK α (IKK1), IKK β (IKK2) and IKK γ (NEMO) (Figure 1.2), which are the major regulatory kinases within the NF- κ B pathway (Ghosh et al., 1998). Investigations into the functional role of the IKK complex was first carried out by DiDonato and colleagues in 1997, who demonstrated that TNF α has the ability to activate IKK complexes and then induce I κ B α phosphorylation and degradation in HT-29 cells (DiDonato et al., 1997).

In fact, both IKK α and IKK β are highly homologous proteins, sharing around 52% of their protein sequence identity, including the leucine-zipper (LZ) region which facilitates the dimerization of the kinases, the terminal helix-loop-helix (HLH) domain which modulates the kinase activity, the C-terminal NEMO binding domain (NBD) and the N terminal kinase domain (Figure 1.2). Moreover, IKK β , but not IKK α , has a ubiquitin-like domain (ULD) between the kinase domain and LZ, which appears to be essential for its activation. In contrast to IKK β , IKK α has a predicted NLS, which also implies a nuclear function. While the activity of IKK α kinase crucially depends on the phosphorylation of Ser 176 and 180, IKK β kinase depends on the phosphorylation of Ser 177 and 181 found within the activation loop (Hinz and Scheidereit, 2014, DiDonato et al., 1997, Mercurio et al., 1997).

The third component in the IKK complex is IKK γ , also known as NF- κ B essential modulator (NEMO) or IKK-associated protein 1 (IKKAP1), which is a non-catalytic 48 kDa protein. It is an α -helical rich protein with two coiled coil zones (CC1 and CC2), LZ and zinc finger domain (Z) (Figure 1.2). The kinase-binding domain is located in the amino acid sequence 44–111. Despite the lack of kinase activity, NEMO serves as a regulatory subunit in the canonical NF- κ B pathway (Solt et al., 2009, Rothwarf et al., 1998, Yamaoka et al., 1998). NEMO also has an N-terminal region that interacts with the carboxyl terminus of the IKK α and IKK β subunits (Rushe et al., 2008, May et al., 2002, Miller and Zandi, 2001). Significantly, IKKs can activate two main NF- κ B signalling pathways: 1) the canonical (or classical) pathway; and 2) the non-canonical (or alternative) pathway.

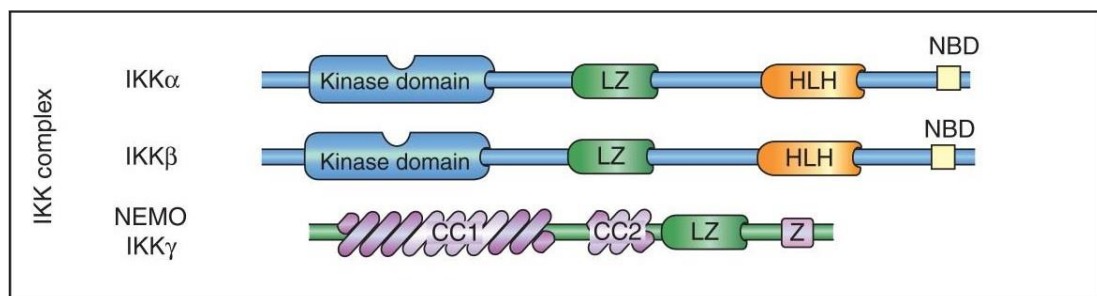


Figure 1.2: Schematic representation of the principal structural motifs of IKK α , IKK β and IKK γ (NEMO). Abbreviations: CC: coiled coil region; LZ: leucine zipper motif; HLH: helix-loop-helix domain; NBD: NEMO-binding domain. [Adapted from (Oeckinghaus and Ghosh, 2009)].

1.4.4.4 Activation of NF- κ B via the canonical pathway

It has become apparent that the canonical pathway predominates within the NF- κ B cascade. This pathway is triggered by multiple activators, such as pro-inflammatory cytokines (e.g., TNF α and IL-1 β), LPS, as well as the interleukin-1 receptor/Toll-like receptor (IL-1R/TLR) superfamily (Plotnikov et al., 2011, Bianchi and Meier, 2009,

Hayden and Ghosh, 2008). In response to stimulation, the IKK complex is linked to TNFR1 through TNF receptor-associated factor 2 (TRAF2), leading to the activation of the pathway (Plotnikov et al., 2011, Devin et al., 2001). This view is supported by Rothe and co-workers, who found that the overexpression of TRAF2 leads to increased p65-DNA binding (Rothe et al., 1995). Following cellular stimulation, the IKK complex is activated by the transforming growth factor β -activated kinase 1 (TAK-1), which is a member of the mitogen-activated protein/ERK kinase 3 family (MAP3K) (Takaesu et al., 2003, Sakurai et al., 1998). In contrast, IL-1 β activates the classical NF- κ B pathway through engagement of TRAF6, where TAB2 functions as an adaptor protein, linking TAK-1 and TRAF6 in the cytosol (Takaesu et al., 2000). It was shown by Kishida and co-workers that TAK-1 facilitates the ubiquitination of TRAF6 during stimulation of cells with IL-1 (Kishida et al., 2005). Both TAB2 and TAB3 have a functional role in binding to TRAF6 through the zinc finger (ZnF) region, and any mutations in this region abolishes this binding and results in failure of TAK1 activation of the IKK complex (Kanayama et al., 2004).

A critical role of IKK β has been established within in the canonical NF- κ B pathway. Studies using IKK β knockout (KO) mice show a substantial reduction in NF- κ B1 (p50/p105) and RelA (p65) subunit activity following stimulation with either IL-1 α or TNF α (Li et al., 1999a). As shown in Figure 1.3, the IKK complex (i.e., IKK β) phosphorylates I κ B α at Ser 32 and Ser 36 then, as described previously, it is ubiquitinated at lysines 21 and 22 by the E3 ubiquitin ligase and subsequently degraded by the 26S proteasome. p65/p50 dimers are then liberated and translocate into the nucleus to regulate the transcription of various genes, which leads to a variety of cellular responses including, growth, cell proliferation, differentiation and adhesion (Oeckinghaus and Ghosh, 2009, Malek et al., 1998).

Unlike IKK β , IKK α appears to play a minor role in the canonical NF- κ B pathway (Xiao et al., 2006, Karin and Greten, 2005). Cells from mice that lack IKK α exhibit normal activation of the IKK complex by pro-inflammatory stimuli (e.g., TNF α and IL-1 β), and phosphorylation and degradation of I κ B α (Hu et al., 1999), suggesting that IKK α is not necessary for activation of the canonical NF- κ B pathway. However, other studies have reported that IKK α can indirectly regulate the expression of some p65-dependent genes, including endothelial adhesion molecules (e.g., *E-selectin* and vascular cell adhesion molecule-1 (*VCAM-1*) and chemokines (e.g., interleukin-8 (*IL-8*)) (Gloire et al., 2007, Huang et al., 2007, Denk et al., 2001).

NEMO or IKK γ is a non-catalytic enzyme characterised by the absence of kinase activity. It plays a regulatory function for both IKK β and IKK α kinase activity. NEMO modulates the IKK complex through interaction with IKK α and IKK β through the NEMO-Binding Domain (NBD) (May et al., 2002). A number of studies have demonstrated that mutations in the C-terminal region or NBD domains of IKK γ abolish the IKK complex and consequently inhibit NF- κ B activity, reflecting the importance of the IKK γ in the recruitment of upstream activators (Solt et al., 2009, Rothwarf et al., 1998).

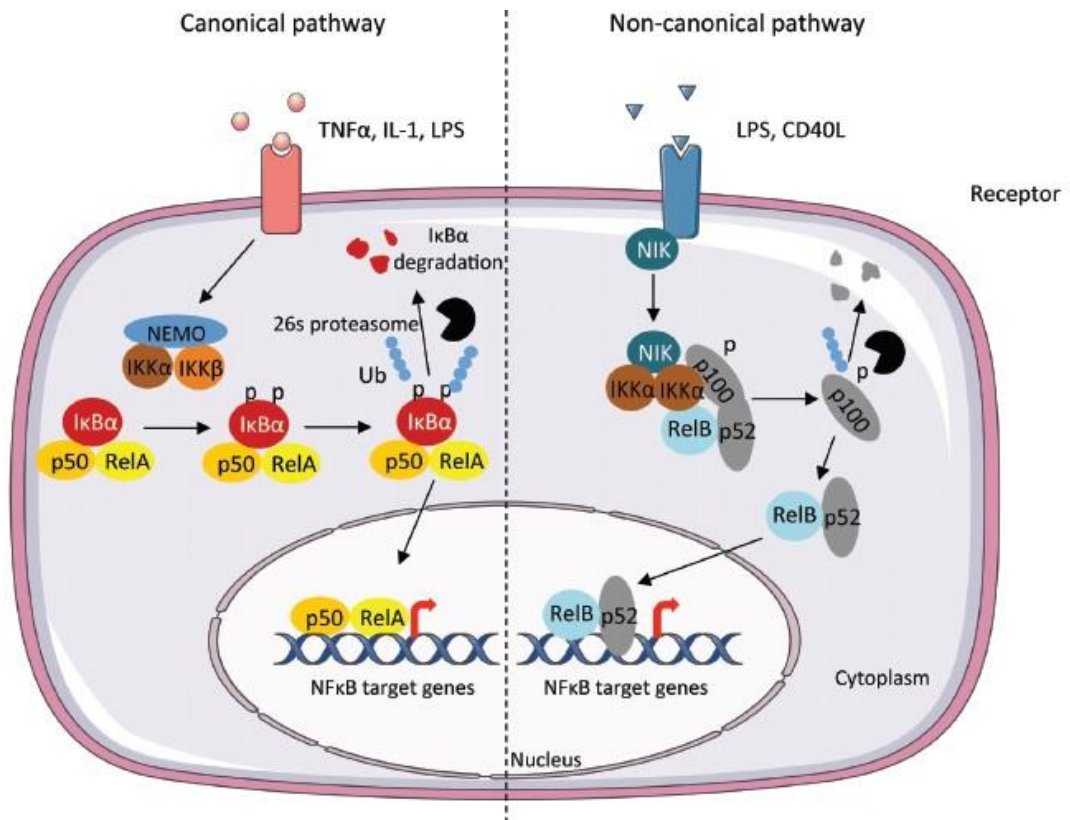


Figure 1.3: Schematic diagram of the NF- κ B pathways. There are two NF- κ B pathways: the canonical and non-canonical pathways. The canonical NF- κ B pathway is triggered by different stimuli, such as TNF α , leading to phosphorylation of the IKK complex, which subsequently activates I κ B α and induces the translocation of p65-containing heterodimers into the nucleus and promoting expression of target genes. The non-canonical NF- κ B pathway is triggered by various ligands, such as lymphotoxin β (LT β), which phosphorylates the IKK α subunit, leading to the processing of p100 to p52 and generation of active p52-RelB heterodimers. These heterodimers then translocate into the nucleus to promote the transcription of target genes. [Adapted from (Viennois et al., 2013)].

1.4.4.5 Activation of NF- κ B via the non-canonical pathway

The non-canonical, or alternative NF- κ B pathway, is one of the atypical pathways prevalent in a restricted number of cell types and is characterised by p100/p52 processing. After the discovery of this pathway, it became evident that it differs from the canonical pathway. While canonical NF- κ B activation was found to be rapid, the activation of the non-canonical NF- κ B is slow and dependent on protein synthesis (Liao et al., 2004). Furthermore, the alternative NF- κ B pathway is primarily IKK α -dependent, the participation of IKK β or IKK γ /NEMO is excluded, suggesting a lack of a requirement for the classical IKK complex (Liang et al., 2006, Dejardin et al., 2002, Claudio et al., 2002). The non-canonical NF- κ B pathway is triggered by TNFR superfamily members, including lymphotoxin β receptor (LT β R) (Dejardin et al., 2002), B cell-activating factor receptor (BAFFR) (Claudio et al., 2002, Kayagaki et al., 2002), CD40 (Coope et al., 2002), and RANK (Novack et al., 2003). This pathway can also be activated by receptor activator of nuclear factor kappa-B ligand (RANKL) to regulate osteoclast differentiation during bone formation (Novack et al., 2003, Teitelbaum, 2000).

Currently, it is clear that ligation of the LT β R directly promotes tumour cell apoptosis and inflammation-related gene expression (Daller et al., 2011, Haybaeck et al., 2009, Yang et al., 2007, Lukashev et al., 2006). However, several studies suggest that targeting LT β R can suppress tumour development in human cancer therapy (Lukashev et al., 2006). The ligand LT $\alpha_1\beta_2$ is the common agonist used to activate the non-canonical NF- κ B pathway. Previous studies have shown that LT $\alpha_1\beta_2$ can activate the non-canonical NF- κ B pathway and, as a consequence, activate the transcription process for a number of genes relevant to cancer such as CXCL12 (Madge and May, 2010, Madge et al., 2008, Dejardin et al., 2002). This ligand is therefore appropriate to use for studies that focus on activation of the non-canonical pathway.

Over the past decade, NF- κ B-inducing kinase (NIK) a member of the mitogen-activating protein 3 kinases (MAP3K), has been identified as a key upstream component of the non-canonical NF- κ B pathway (Razani et al., 2010, Qing et al., 2005). Normally, NIK levels are absent or very low due to its degradation via a TRAF3-dependent mechanism. Increasing evidence suggests that TRAF3 functions by forming a complex comprised of NIK, TRAF2, c-IAP1 and c-IAP2 to maintain the NIK levels below the threshold required for its activation (Vallabhapurapu et al., 2008, Zarnegar et al., 2008). Knockdown or inhibition of these proteins leads to the accumulation of basal levels of NIK in the absence of its ligand (Gardam et al., 2011, Varfolomeev et al., 2007, Vince et al., 2007). Following the stimulation of the non-canonical NF- κ B pathway, TRAF3 and TRAF2 undergo degradation by the proteasome, which leads to NIK accumulation and subsequent activation via autophosphorylation; this process is also known as NIK stabilisation (Figure 1.4). NIK activates the IKK α homodimers through the phosphorylation of Ser 176 and Ser 180 (Xiao et al., 2001, Senftleben et al., 2001). Subsequently, the activation of IKK α kinase leads to the phosphorylation of p100 on Ser 866 and Ser 870, which is crucial for p100 processing (Liang et al., 2006, Xiao et al., 2004). The phosphorylation of p100 induces its ubiquitination by E3 ubiquitin ligase and degradation by the proteasome to liberate p52. Subsequently, active NF- κ B p52/RelB heterodimers translocate into the nucleus to induce gene expression (Figure 1.3) (Xiao and Fu, 2011, Solan et al., 2002).

It is important to note that downstream intermediates can function to regulate upstream components of the non-canonical NF- κ B pathway. For instance, IKK α functions to phosphorylate and destabilise NIK, which prevents the over-activation of non-canonical NF- κ B signalling (Razani et al., 2010). According to Xiao and co-workers, NIK is more effective than IKK α at inducing p100 processing (Xiao et al.,

2004). Although the mechanisms that regulate non-canonical NF- κ B activation are not yet fully understood, both of IKK α and NIK could be potential targets for the inhibition of this pathway.

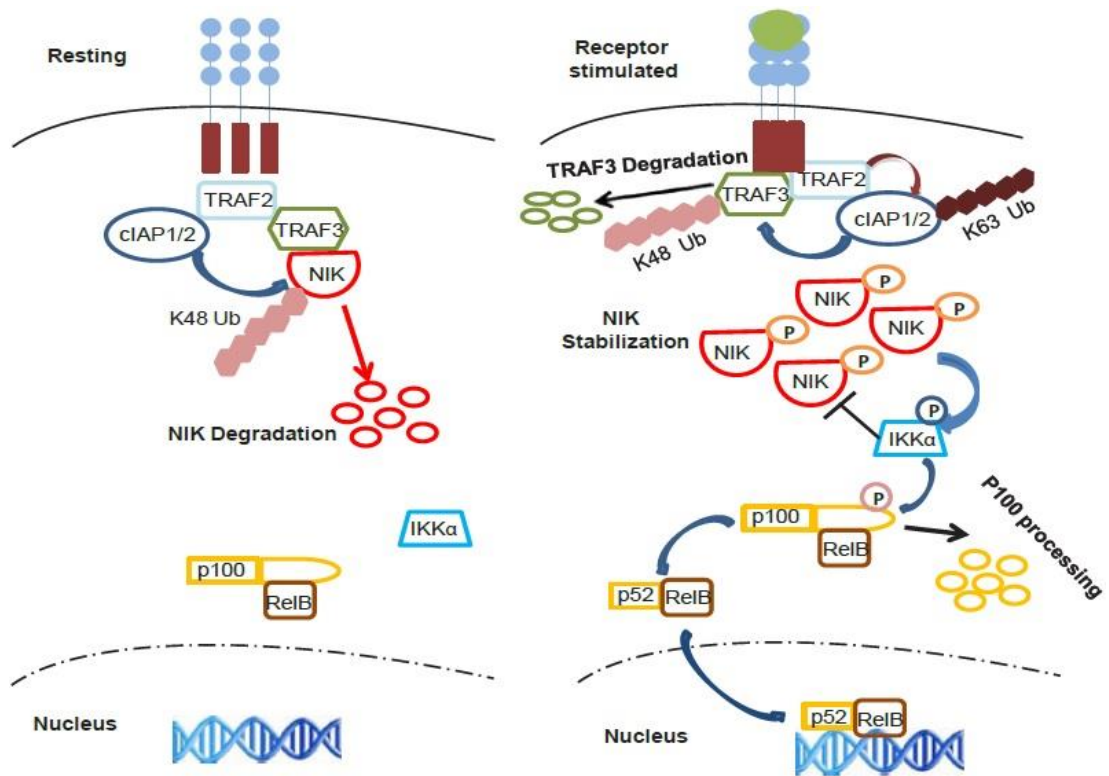


Figure 1.4: Regulation of the alternative NF- κ B pathway in resting vs receptor-stimulated cells. In resting cells, the kinase, NIK, is constitutively targeted for degradation by a ubiquitination complex containing cIAP1, cIAP2, TRAF2 and TRAF3, making NIK levels invisible. Upon receptor activation, NIK is stabilised and activated, where it escapes the ubiquitination by the cIAP-TRAF2-TRAF3 complex due to the rapid degradation of TRAF3, leading to IKK α activation, which in turn phosphorylates p100 and results in p100 processing into p52. RelB-p52 dimers then translocate to the nucleus and activate transcription. [Adapted from (Vallabhapurapu et al., 2013)].

1.4.4.6 Genes Regulated by NF- κ B pathway

NF- κ B plays a key role in many cellular functions including survival, growth, apoptosis, development and differentiation, which occurs by transcriptional regulation of a specific subset of NF- κ B dependent genes following binding of homo or heterodimer to specific DNA binding motifs. For p65/p50, the core sequence for specific DNA binding has been identified as 5-GGGRNYYYCC-3, (where R=A or G; Y=C or T; W=T or A; V=A, C or G) (Chen and Ghosh, 1999, Chen et al., 1998). The p65/p50 heterodimer is responsible for regulating the expression of several genes for instance, *COX-2*, *VCAM-1*, and *ICAM-1* (Denk et al., 2001). In addition, p65 (RelA) is responsible for the regulation of cellular survival and proliferation through expression of pro-survival factors (e.g., Bcl-2) and anti-apoptotic genes (e.g., cellular inhibitor of apoptosis protein [c-IAP] and X-related inhibitor of apoptosis protein [XIAP]) (Fulda, 2014, Catz and Johnson, 2001, Stehlik et al., 1998).

In contrast to RelA, RelB is responsible for the regulation of developmental phenotypes, including adaptive immunity, cellular activation, immune cell trafficking, lymphoid development and angiogenesis. The sequence that RelB binds to within DNA has also been identified as 5'-GGGRVWTTY-3. Several studies clearly show that the gene regulation by the non-canonical NF- κ B pathway differs from that of the canonical NF- κ B pathway (Britanova et al., 2008, Dejardin, 2006). Bonizzi and colleagues demonstrated that the promoter regions of IKK α -dependent genes are specific for RelB/p52 heterodimers (Bonizzi et al., 2004). Moreover, studies have shown that IKK α -mediated activation of the non-canonical NF- κ B pathway regulates expression of a number of chemokines (e.g., chemokine C-C motif ligands [CCL19 and CCL21], C-X-C motif ligands [CXCL12 and CXCL13], B lymphocyte chemoattractant [BLC], secondary lymphoid tissue chemokine [SLC] and cytokine B cell activation factor [BAFF]) which regulates the process of lymphoid organogenesis

(Dejardin et al., 2002). Additional evidence has shown that IKK α regulates other inflammatory genes such as *CXCL3*, *ICAM-1*, *IL-8* (Hirata et al., 2006), *IL-6* and *CCL2* (Yang et al., 2008). Furthermore a number of *in vivo* studies confirms an important role in B-lymphocyte function and lymphoid organogenesis (Lawrence and Bebien, 2007, Bonizzi and Karin, 2004, Senftleben et al., 2001).

It is clear that a number of these genes are related to the development of solid tumours and lymphoid malignancies (Allen et al., 2012, Wharry et al., 2009). Several are also related to angiogenesis, such as *CXCL12*, *IL-8*, *MMP-2*, *MMP-9* and *VEGF* (Birbrair et al., 2015, Liekens et al., 2010, Agarwal et al., 2005). IKK α itself is also implicated in the regulation of a number of cell cycle genes, including cyclin D1 and Aurora-A (Song et al., 2010, Prajapati et al., 2006, Kwak et al., 2005). Together, these results suggest a potential role for the non-canonical NF- κ B pathway in the development of cancer as highlighted later in the chapter.

1.5 Chemokines and their receptors

Chemokines are a superfamily of chemoattractant cytokines, 8–10 kDa in size. Most chemokines are expressed in response to a stimulus; however, some are constitutively expressed by stromal cells, including endothelial cells and fibroblasts (Teicher and Fricker, 2010, Dewan et al., 2006). The primary function of chemokines is to regulate the directional migration of leukocytes to sites of infection and inflammation (Lieberman et al., 2012). Chemokines control leucocyte circulation, homing, recirculation between the blood vessels, lymphatic vessels and lymphoid organs and tissues (Hippe et al., 2010).

Recently, there has been increasing evidence demonstrating that chemokines are associated in the regulation of tumour development and metastasis (Balkwill, 2004). To date, more than 50 chemokines have been identified, and they are divided into

four groups (CXC, CX3C, CC and C) based on the position and number of conserved cysteine residues. C denotes the number of cysteine residues and X represents the number of intervening amino acids between the conserved cysteines (Sun et al., 2010, Wang et al., 2006). According to a new classification, chemokines have been renamed as chemokine ligands (L) and receptors (R) (Zlotnik and Yoshie, 2000).

Chemokine receptors are comprised of seven-transmembrane cell surface receptors and currently over 20 chemokine receptors have been identified (Sun et al., 2010), divided into four groups (CXCR, CX3CR, CCR and XCR) based on their specific chemokine preference (Burger and Kipps, 2006). These receptors were initially identified on leukocytes, where they play an important role in inflammation (Loetscher et al., 2000). The binding of chemokines to their receptors results in the activation of several downstream signalling pathways which regulate a number of events, including proliferation, migration, tumour progression and metastasis (Wang et al., 2006).

1.5.1 The formation and function of CXCL12

CXCL12 (stromal derived factor 1 [SDF1]) is a member of the CXC subfamily of chemokines. It was first cloned from bone marrow stromal cells and was later described as a pre-B-cell growth stimulating factor (Nagasawa et al., 1996). CXCL12 appears to be expressed in two main isoforms; SDF-1 α which consists of 68 amino acids (8 kDa) and is the predominant isoform SDF-1 β , which differs by an additional four amino acids. Functional and biological differences between these isoforms have not yet been described (Yu et al., 2006). CXCL12 is widely expressed in various organs, including the bone marrow, heart, brain, liver, lungs, kidney, skin, and skeletal muscle. The major cellular sources for CXCL12 in these organs are vascular endothelial cells, stromal fibroblasts and osteoblasts (Teicher and Fricker, 2010, Jung

et al., 2006, Gomperts et al., 2006, Katayama et al., 2006). The primary role of CXCL12 is to facilitate the homing of hematopoietic stem cells to the bone marrow (Aiuti et al., 1997). CXCL12 secretion is increased after tissue damage, such as excessive bleeding (Ratajczak et al., 2004), hypoxia (Santiago et al., 2011) cardiac and limb ischemia (Peled et al., 1999), toxic liver damage (Kollet et al., 2003), tissue damage related to irradiation and chemotherapy (Ponomaryov et al., 2000), arthritis (Nanki et al., 2000), and malignancies (Santiago et al., 2011). Studies have shown that CXCL12 was necessary for organ regeneration and injured tissue repair (Kucia et al., 2005, Kucia et al., 2004). In 2001, CXCL12 was first reported in human ovarian cancer (Zou et al., 2001). Subsequent studies have also reported high levels of CXCL12 expression in various types of human cancers (Dewan et al., 2006).

1.5.2 CXCL12/CXCR4 axis and human pathogenesis

Chemokines are a group of key molecules functioning within the immune, nervous and cardiovascular systems. CXCL12 is recognised as an important member of this family (Yu et al., 2006). The effects of CXCL12 are mediated primarily via the interaction with the G-protein coupled receptor, CXCR4 (Lagerstrom and Schioth, 2008, Murdoch, 2000). However, it has been recently demonstrated that CXCL12 can interact with another receptor, CXCR7, at a much higher affinity than CXCR4 (Levoye et al., 2009, Balabanian et al., 2005). A large body of evidence now supports a major role for the CXCL12/CXCR4 axis in a number of physiological functions and pathophysiological conditions. CXCL12 is essential in development, guiding various progenitor cells to different locations (Lewellis and Knaut, 2012). Moreover, CXCL12 plays a key role in haematopoietic stem-cell functionality, retention in the bone marrow, proliferative status and repopulating activity (Greenbaum et al., 2013, Tzeng et al., 2011, Bonig et al., 2004, Nagasawa et al., 1996). These events are relevant to

cancer as high levels of CXCL12 expressed by cancer cells promote the migration of CXCR4-positive cells, including CD45+ myeloid cells and endothelial cell progenitor, into the tumour mass, often from distant sites (Du et al., 2008). Through the activation of CXCR4, CXCL12 also has a direct effect upon cancer cell proliferation within the tumour, which is mediated via the PI3 and MAP kinase pathways.

An emerging and important aspect of CXCL12 biology is within the tumour microenvironment, stromal (myo) fibroblasts were recently identified as a major source of CXCL12 in breast cancer, which promotes tumour growth and angiogenesis (Kojima et al., 2010, Orimo et al., 2005); the latter is promoted via the regulation of endothelial cell function (Kryczek et al., 2005). Therefore, cancer cells, the tumour stroma and CAFs, as the main components of the tumour microenvironment, can all produce CXCL12. Studies have reported a correlation between CXCL12 expression and bone marrow and lymph node metastasis of breast (Muller et al., 2001) and prostate cancer (Taichman et al., 2002). Today, CXCL12 expression has been observed in more than 20 types of human non-hematological tumours (Kryczek et al., 2007). These multiple functions make CXCL12 important in cancer metastases (Hinton et al., 2010, Matsusue et al., 2009) and a target for novel therapies.

The role of CXCL12 is not limited to cancer pathology. Both CXCL12 and CXCR4 are strongly expressed in the synovium of RA patients and are associated with the migration and accumulation of CD4+ memory T-cells within the joint (Nanki et al., 2000). In another study, neutralisation of CXCL12 was found to reduce eosinophilia and bronchial hyper-reactivity in a model of allergic airway disease (Gonzalo et al., 2000). Within the brain, CXCL12 is associated with neurogenesis, controlling axonal guidance and neurite outgrowth but is also thought to play a role in neuroinflammation (Guyon, 2014). In the cardiovascular system, genome-wide association studies of coronary heart disease have identified a locus linked to CXCL12 (Farouk et al., 2010).

This correlates with a number of *in vivo* studies in which a reduction in vascular remodelling following injury was achieved following the neutralisation of CXCL12 or blockade of CXCR4 (Zernecke et al., 2005, Schober et al., 2003).

Taken together, these data implicate the potential of the CXCL12/CXCR4 axis to regulate several disease conditions. Moreover, several clinical trials have examined the efficacy of CXCR4 inhibitors in renal impairment, immune deficiency and several cancers (i.e., related to circumventing resistance to chemotherapy) (Domanska et al., 2013). The CXCR4 inhibitor, AMD3100, has been approved for autologous transplantation for the treatment of Non-Hodgkin's lymphoma and multiple myeloma (DiPersio et al., 2009). However, not all trials have been successful and it is now recognised that CXCR7, previously thought to function as a decoy receptor, may mediate some biological effects of CXCL12 (Puchert and Engele, 2014), limiting the effectiveness of drugs targeting only CXCR4. Thus, targeting of CXCL12 production at the level of transcription may be important to improving treatment success.

1.5.3 Regulation of CXCL12 expression

To date, work assessing the regulation of CXCL12 expression is restricted to relatively few papers, despite its central importance in a number of diseases (Garcia-Moruja et al., 2005). Studies have indicated that there are a number of factors that affect the expression of CXCL12. It has been reported that CXCL12 expression can be regulated by DNA-damage caused by irradiation and chemotherapy (e.g., 5-fluorouracil and cyclophosphamide) in mouse bone marrow and cultured cells (Ponomyrov et al., 2000). Furthermore, recent studies have revealed that hypoxia-inducible factor-1 α (HIF-1 α) triggers the expression of CXCL12 in hypoxic or damaged tissues by hematopoietic stem cells (HSC), endothelial cells (Ceradini et al.,

2004), primary human ovarian tumour cells (Kryczek et al., 2005), and synovial fibroblasts (Hitchon et al., 2002). Moreover, it was found that oestradiol activates oestrogen receptors and induces CXCL12 production in ovarian and breast cancer cells (Hall and Korach, 2003).

A number of studies indicate that IKK α , the major regulator of the non-canonical NF- κ B pathway, can play a role in the regulation of CXCL12 expression. Moreover, several ligands which activate this pathway also induce CXCL12. Madge and May have demonstrated that siRNA knock-down of IKK α inhibits CXCL12 mRNA in endothelial cells, whereas IKK β deletion enhances CXCL12 production (Madge and May, 2010, Madge et al., 2008). These data suggest that CXCL12 expression can be regulated by hypoxia and the non-canonical NF- κ B signalling pathway.

1.6 The Role of NF- κ B pathway in cancer

It is well recognised that NF- κ B plays a major role in the regulation of cellular immunity and inflammatory responses. However, researchers have recently shown an interest in its role in the progression of malignant cancers (Senegas et al., 2015). Several studies have highlighted cellular processes that link NF- κ B activity and tumour development, including enhanced cell proliferation, inhibition of apoptosis, and the stimulation of angiogenesis and metastasis (Liu et al., 2015, Hoesel and Schmid, 2013, DiDonato et al., 2012, Lee and Hung, 2008). Constitutive NF- κ B activation in cancer cells has been shown to increase resistance to genotoxic anticancer therapy and ionizing radiation (Ahmed and Li, 2008, Montagut et al., 2006), which may be due to the ability of NF- κ B to reduce the apoptotic responses to these therapies. This hypothesis was supported by studies which show that the inhibition of NF- κ B activity results in an increase in their sensitivity to chemo- or radiotherapies (Shostak and Chariot, 2015, Karin et al., 2002).

Several chemokines are produced via NF- κ B pathways which promote metastatic spread. For instance, Interleukin-8 (IL-8) has been found to stimulate angiogenesis, which is important for the proliferation and metastasis of tumour cells (Koch et al., 1992). NF- κ B activation not only leads to overexpression of IL-8 but also vascular endothelial growth factors (VEGF) (Huang et al., 2000), which promotes migration and angiogenesis. In addition, NF- κ B activation promotes the ability of cancer cells to invade surrounding tissues through enhancing the production of several matrix metalloproteinases (MMPs) (Takeshita et al., 1999). Recent studies have found that high NF- κ B activity is correlated with the clinical outcomes of several types of cancer, including prostate, pancreatic, colorectal, lung, and breast cancers (Senegas et al., 2015, Lu and Stark, 2004, Cogswell et al., 2000). In addition, high levels of NF- κ B have also been noted in melanoma, leukaemia and lymphoma (Karin, 2006).

1.6.1 The role of IKKs in cancer

More recently, studies have sought to examine the role of the IKKs in cancer development (Lee and Hung, 2008). Constitutive activation of IKKs has been reported in several types of cancers, such as breast, colorectal, and prostate cancer (Fusella et al., 2017, Charalambous et al., 2003, Gasparian et al., 2002, Romieu-Mourez et al., 2001). To date, mutations in genes for intermediates of the non-canonical NF- κ B pathway (e.g., TRAF2, TRAF3, cIAP1, cIAP2, NIK and p52/p100) have been observed in only few cell types, for instance in multiple myeloma (Annunziata et al., 2007, Keats et al., 2007) making targeted inhibition challenging.

The role of IKK β has been the most intensely studied IKK in cancer and more advanced in terms of therapeutic targeting with limited examples identified here. For example pre-treatment with PS1145, an IKK β inhibitor inhibits canonical NF- κ B activity and results in the death of multiple myeloma cancer cells (Castro et al., 2003,

Hideshima et al., 2002). Another study demonstrated that IKK β knockdown prevents the development of melanoma tumours in mice through the inhibition of G2/M transition and induction of apoptosis (Yang et al., 2010). In fibroblasts co-cultured with breast cancer cells, phosphorylation of IKK β induced by IL-13 leads to fibrosis, inflammation and tumour development (Li et al., 2016). In addition, over-activation of the canonical NF- κ B pathway by IKK β overexpression is associated with tumour progression and increased angiogenesis in breast cancer (Lee et al., 2007).

IKK α has also been reported to influence tumour progression in a number of cancers, including breast, pancreatic, colorectal, gastric and prostate (Fernandez-Majada et al., 2007, Luo et al., 2007, Hirata et al., 2006, Shiah et al., 2006, Park et al., 2005). For instance, knockdown of IKK α by shRNA led to the deactivation of silencing mediator for retinoic acid and thyroid hormone receptor (SMRT) which results in growth inhibition and apoptosis in human colorectal cancer cells *in vitro* and in mice-null *in vivo* (Margalef et al., 2012). In addition, IKK α -mediated activation of the non-canonical NF- κ B pathway prevents the expression of Maspin, a tumour suppressor gene in a prostate cancer mouse metastatic model (Koch and Radtke, 2007).

The role of IKK α is however, not restricted to activation of the non-canonical NF- κ B pathway (Figure 1.5); there is evidence showing that IKK α can promote cell proliferation and consequently tumorigenesis in various cancer types through NF- κ B independent pathways. Several studies demonstrate that IKK α can regulate the expression of a number of transcription factors such as estrogen receptor- α (ER α), steroid receptor coactivator-3 (SRC3), and β -catenin in breast cancer which consequently induces cyclin D1 expression, a protein involved in the regulation of the cell cycle (Perkins, 2007, Carayol and Wang, 2006, Park et al., 2005). In addition, it was found that activation of IKK α induces its nuclear translocation to independently regulate other factors that lead to gene expression (Chariot, 2009). For instance, IKK α

regulates gene transcription by phosphorylation of a number of nuclear targets including histone H3 and CBP (Huang et al., 2007, Yamamoto et al., 2003). IKK α is also implicated in toll-like receptors 7 and 9 mediated interferon- α (IFN α) induction through phosphorylation of interferon regulatory factor-7 (IRF7). Both TLRs have roles in microbial recognition and dendritic cell activation (Hoshino et al., 2006). Thus, IKK α may link immune responses to tumour development.

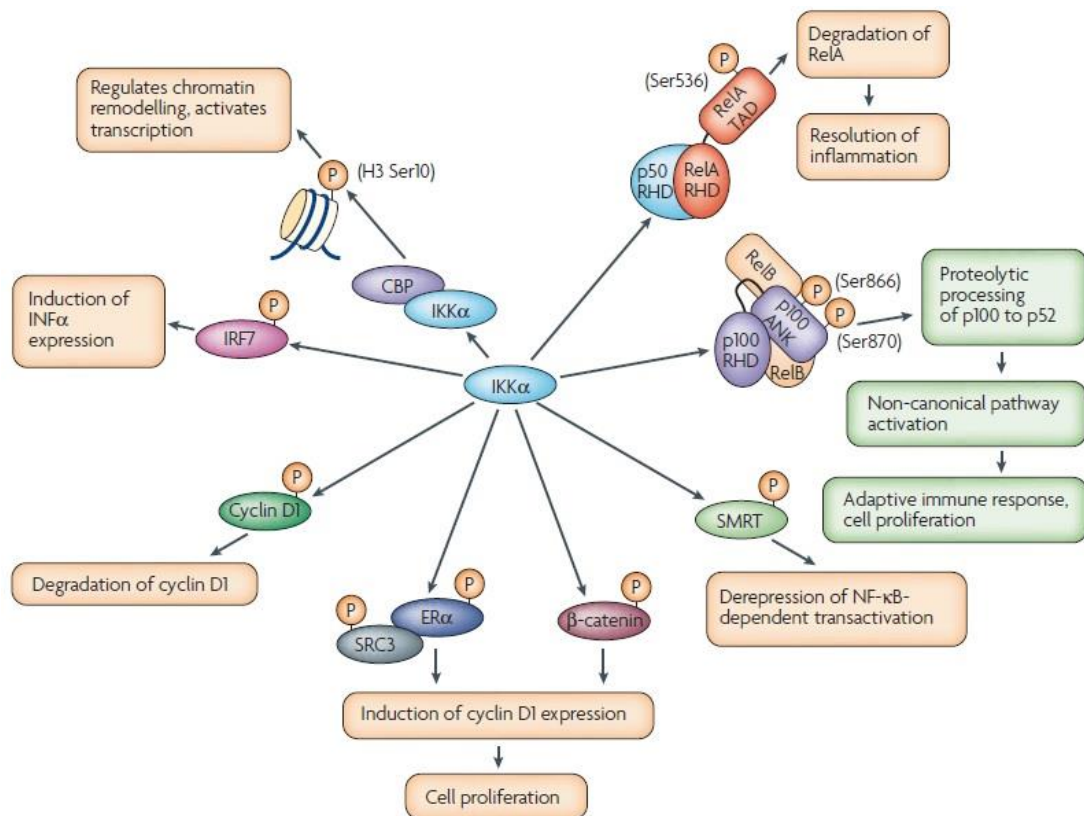


Figure 1.5: The consequences of IKK α activation. In addition to activation of the non-canonical signalling pathway through phosphorylation of the p100 NF- κ B subunit, IKK α is now thought to phosphorylate a number of other substrates. [Adapted from (Perkins, 2007)].

1.6.2 The role of NF- κ B pathways in bone biology

There have been a growing number of studies investigating the role of the NF- κ B pathway in bone from both a clinical perspective and experimental work conducted using cell lines. The NF- κ B pathway is considered to be a major cause of the

pathogenesis of osteolysis in inflammatory diseases (e.g., Paget's disease, rheumatoid arthritis and periodontitis) and also mediates the action of several cytokines involved in osteoporosis in post-menopausal women. The NF- κ B pathways have been implicated in bone abnormalities and pathologies. Furthermore, it was shown that inhibition of this pathway was an effective approach to inhibit osteoclast formation and bone resorption activity (Abu-Amer, 2013). The role of NF- κ B in bone homeostasis was first investigated following the combined deletion of the p50 and p52 subunits in mice, which resulted in osteopetrosis due to the complete lack of osteoclasts (Iotsova et al., 1997, Franzoso et al., 1997).

RANKL produced by osteoblasts is one of the few known activators of the non-canonical pathway that plays an important role in the regulation and activation of osteoclast differentiation through the RANK/RANKL/OPG signalling pathway. It was shown by Novack and colleagues that a NIK deficiency inhibits the nuclear translocation of p52 and RelA in response to RANKL stimulation; the lack of p100 proteolysis as a result of NIK loss prevents the formation of osteoclasts (Novack et al., 2003). Furthermore, Vaira and colleagues observed that RelB, but not RelA, salvages the differentiation defect of the osteoclast precursors, suggesting that NIK stimulation of the proteolytic processing of p100 is necessary for the osteoclastogenesis (Vaira et al., 2008). Furthermore, the role of the non-canonical NF- κ B pathway has been studied in an inflammatory arthritis model. It has been well-established that osteoclasts are responsible for the degradation of bone in arthritis, and several studies have reported that inhibition of this pathway induced by RANKL improves bone erosion in certain arthritis models (Pettit et al., 2001, Kong et al., 1999). For instance, several studies have demonstrated that Bisphosphonates and Denosumab inhibit RANKL, which results in reduced bone resorption and osteoclast apoptosis (Zaheer et al., 2015, Russell, 2011).

After further analysis, the critical role of IKK α in the bone was established using gene deletion studies. *In vivo* studies have demonstrated that IKK α -null mice exhibit skeletal abnormalities and ossification of limbs, sternum, vertebrae and cranial bones (Chaisson et al., 2004, Mercurio et al., 1997). In contrast, other studies have demonstrated that bone development and osteoclastogenesis were not affected by the absence of IKK α . It was shown by Ruocco and colleagues that IKK β -null mice resulted in normal skeletal development and osteopetrosis (Ruocco et al., 2005). In addition, IKK β inhibitors (e.g., NBD) have been reported to inhibit a number of inflammatory responses (e.g., inflammatory osteolysis) (Clohisy et al., 2006, Jimi et al., 2004), suggesting that NF- κ B is required for osteoclast formation and activity.

In contrast to osteoclastogenesis, the role of NF- κ B pathway in bone cancer was studied. Vaira and co-workers demonstrated an inhibition of tumour-induced bone loss in NIK $^{-/-}$ and RelB $^{-/-}$ mice injected with B16 melanoma cells (Vaira et al., 2008). This suggests that the non-canonical NF- κ B pathway may be a potential therapeutic target in metastatic bone cancers. Furthermore, NF- κ B has also been reported to block osteoblast differentiation in Saos2 osteosarcoma cells (Eliseev et al., 2006). Recently, NF- κ B has also been demonstrated to play a pro-survival role in osteoblastic cells following radiation injury (Xiao et al., 2009). Therefore, identifying novel approaches for targeting the non-canonical NF- κ B pathway are important for improving the treatment success for bone cancer and other diseases.

1.7 The development of IKK α inhibitors

As described above, it is clear that the NF- κ B pathway plays a critical role in the development and progression of various human cancers, as well as a vital function in the regulation of cellular immunity and inflammatory responses. Thus, the inhibition of the NF- κ B pathway has become an important therapeutic target in the development

of anticancer drugs. Several NF- κ B pathway inhibitors have been developed for experimental and clinical use, including MG132 (Dimmeler et al., 1999) and disulfiram (Wang et al., 2003). However, these agents exhibit a wide-range of actions within the pathway.

Since IKKs have been identified as key regulators in the NF- κ B signalling pathways, their inhibition has become a primary strategy used to prevent the over-activation of NF- κ B pathway. As a result, several small molecule IKK inhibitors have been developed. These inhibitors commonly function as ATP-competitive molecules or alternatively possess allosteric actions to limit IKK activities (Gamble et al., 2012). Several IKK β inhibitors have been reported over the past 15 years, such as BMS-345541 and TPCA-1 (Podolin et al., 2005, Burke et al., 2003). In addition, the proteasome inhibitor, Bortezomib, which can block NF- κ B signalling pathway in tumour cells, is a clinically effective treatment for MM (Raab et al., 2009).

Recent evidence suggests that IKK α is strongly involved in the regulation of a number of genes that control cellular processes associated with cancer development (e.g., proliferation, metastasis, invasion and resistance to chemotherapy) (Doppler et al., 2013, Kaileh and Sen, 2012, Ammirante et al., 2010, Fernandez-Majada et al., 2007, Hirata et al., 2006, Park et al., 2005). To date, no completely selective IKK α inhibitors have been developed. Importantly, the targeting of NF- κ B activity by IKK inhibitors is associated with a number of issues which preclude clinical effectiveness. For instance, chronic inflammation, immunosuppression and increased susceptibility to infection, hepatotoxicity and toxicity in non-cancer cells (Chariot, 2009, Pasparakis, 2009, Li et al., 1999b).

Considering all of the evidence presented in this chapter, it appears that IKK α is a distinctive regulatory kinase in the NF- κ B pathway. Therefore, the development of

selective IKK α inhibitors may be indispensable in terms of therapeutic targeting for human cancers and other diseases.

1.8 Research hypothesis and aims

It is now becoming clear that the non-canonical NF- κ B signalling pathway has a potential role in cancer development. How this is mediated is not completely clear, the role of the pathway in tumour development has not been well defined. Evidence suggests that CXCL12 expression can be regulated by IKK α through non-canonical NF- κ B signalling therefore inhibiting CXCL12 production may be a strategy to treat some cancers. This possibility is appropriate for investigation as CXCR4 inhibitors have not been as clinically successful as predicted. Furthermore, more recently, it has been demonstrated that CXCL12 is able to interact with another receptor CXCR7 at much higher affinity than CXCR4. Therefore this project aims to inhibit CXCL12 production at the level of transcription by targeting IKK α . Thus, targeting this kinase might be a promising approach for the development of a novel treatment for bone and breast cancer. In order to test this hypothesis, the main objectives in this thesis are to:

1- Evaluate the pharmacological effects of novel, selective IKK α inhibitors at the cellular level in terms of their selectivity and the potency against outputs of the canonical and non-canonical NF- κ B pathways in bone and breast cancer.

2- Characterise the role of IKK α in the regulation of non-canonical NF- κ B pathway in U2OS cells and CAFs via a knockdown of IKK α using siRNA and a pharmacological approach with SU compounds.

3- Examine the function of IKK α in the regulation of CXCL12 expression in U2OS cells and CAFs using reporter cells, RT-qPCR and ELISA.

Chapter Two
MATERIALS AND METHODS

2.1 Materials

2.1.1 General Reagents

All the materials used were supplied by Sigma Aldrich Chemical Company Ltd. (Poole, Dorset UK) or other reputable companies unless otherwise stated, which were of highest commercial purity available.

Thermo Fisher Scientific UK Ltd (Leicestershire, UK)

Bovine Serum Albumin (BSA, Fraction V)

L – Glutamine

Gibco™ Penicillin-Streptomycin

Gibco™ Fetal Bovine Serum

Dulbecco's Modified Eagle Medium (DMEM)

Cell culture plates and dishes

Amersham™ Protran™ – ECL nitrocellulose membrane

Insight Biotechnology Limited (Wembley, UK)

Recombinant Human Tumour Necrosis Factor-alpha (TNF- α)

Bio-Rad Laboratories (Hertfordshire, UK)

Bio-Rad AG® 1-X8 Resin

Pre-stained SDS-page molecular weight markers

Boehringer Mannheim (East Sussex, UK)

Bovine Serum Albumin (BSA, Fraction V)

Carl Roth GmbH + CO. KG (Karlsruhe, Germany)

Rotiphorese® Gel 30 (37.5:1) acrylamide

Corning B.V (Buckinghamshire, UK)

All tissue culture dishes, plates, flasks, and graduated pipettes

GE Healthcare (Buckinghamshire, UK)

Amersham Hybond ECL Nitrocellulose Membrane

GIBCO BRL (Paisley, UK)

Fetal Calf Serum (FCS), L-glutamine, Minimal Essential Medium (x10), Non-essential amino acids, Penicillin/Streptomycin, Sodium Bicarbonate.

Whatmann (Kent, UK)

Nitrocellulose Membrane, 3MM blotting paper

Roche Diagnostics Ltd (Burgess Hill, UK)

Dithiothreitol (DTT)

Sarstedt AG & Co LTD (Leicester, UK)

Serological pipette 5ml

Serological pipette 10ml

Thermo Fisher Scientific Inc. (Surrey, UK)

Multidish 6 wells

Multidish 12 wells

2.1.2 SU compounds (University of Strathclyde, Glasgow, UK)

SU1261, SU1266, SU1349, and SU1433

NIK inhibitors

CW15407 (synthesized in-house)

IKK β inhibitors (Calbiochem)

IKK2 X1

2.1.3 Antibodies

Cell signaling Technology Inc. (Hertfordshire, UK)

Anti-IkBa (Rabbit monoclonal, 92424L)

Anti-p-NF kappa B2 p65 (Rabbit polyclonal, 3031L)

Anti-p- NF-kappa B2 p100 (Rabbit monoclonal, 4810L)

Anti-RelB (Rabbit monoclonal, 10544)

Anti-TRAF2 (Rabbit polyclonal, 4724s)

Anti-TRAF3 (Rabbit polyclonal, 4729s)

Anti-GAPDH (Rabbit monoclonal, 14C10)

Anti-Nucleolin (Rabbit monoclonal, 14574s)

Abcam (Cambridge, UK)

Anti-IKKβ (Rabbit polyclonal, ab32135)

Santa Cruz Biotechnology Inc. (California, USA)

Anti-NFκB p65 (Rabbit polyclonal, C-20)

Anti-p38α (Rabbit monoclonal, N-20)

Anti-tERK (Rabbit monoclonal, N-20)

Millipore (U.K.) Limited (Watford, UK)

Anti-NFκB p100/p52 (Mouse, 32534)

Anti-IKKα (Mouse monoclonal, 14A231)

Liquid Nitrogen (provide from any local)

2.2 Cell culture

Cell culture work was done in cell culture hood under aseptic conditions. All the cells were grown in flasks 25 cm² and 75 cm².

2.2.1 Culturing human osteosarcoma (U2OS) cell line

Human osteosarcoma U2OS cells were routinely cultured in McCoy's 5A medium containing 10% (v/v) bovine calf serum, 1% (v/v) penicillin/streptomycin and 1% (v/v) L-glutamine. Cells were grown in T-75 cm² flasks and maintained in 5% CO₂ and 95%

air at 37°C, with media changed at least twice per week. Cells were sub-cultured upon reaching approximately 90% confluency. To passage cells, the media was removed and the cells washed once with 2 ml of a sterile solution of trypsin (0.5%) to remove traces of serum. The solution was then removed and 3 ml of trypsin was reintroduced into the flask and left in an incubator at 37 °C until cells detached (2-3 min). The flask was then gently tapped to completely detach the cells from the surface and then McCoy's 5A medium was added to the flask. Cells were gently pipetted on the side of the flask to break any clusters. Cells were then seeded into various sizes of sterile dishes and plates for experimentation. Cells were maintained in 5% CO₂ and 95% air at 37 °C and medium was replaced every two-three days to maintain healthy cells.

2.2.2 Culture of human breast cancer cell lines

MCF7 (ER positive) and MDA-MB-231 (ER negative) human breast cancer cells were routinely cultured in Dulbecco's Modified Eagle Medium (DMEM) supplemented with 10% (v/v) bovine calf serum, 1% (v/v) penicillin/streptomycin and 1% (v/v) L-glutamine. Cells were grown in T-75 cm² flasks and maintained in 5% CO₂ and 95% air at 37 °C, with media changed at least twice per week and cells passaged once a confluency of around 90% was reached. To passage cells, the media was removed and the cells washed once with 1.5 ml of a sterile solution of trypsin (0.5%) to remove traces of serum. The solution was then removed and 2-3 ml trypsin was added and then incubated at 37 °C until cells detached. The flask was then gently tapped to completely detach the cells from the surface and then the DMEM was added to the flask. Cells were gently pipetted on the side of the flask to break any clusters. Cells were then seeded into various sizes of sterile dishes and plates for experimentation. Cells were maintained in 5% CO₂ and 95% air at 37 °C and medium was replaced every two-three days to maintain healthy cells.

2.2.3 Clinical samples and patients

Breast cancer specimens were kindly provided by Dr. Sara Zanivan from the Beatson Institute for Cancer Research UK. Cancer-associated fibroblasts (CAFs) and normal fibroblasts (NFs) were isolated from primary tumors and adjacent normal tissues of breast cancer patients (Women aged 40 to 45 years). The purity of cells have been verified by immunostaining. They were prepared with minimal contamination by epithelial, endothelial, or hematopoietic cells, such as leukocytes and erythrocytes. Fibroblasts in cancer tissues are similar in morphology to myofibroblasts, which are large spindle-shaped cells. Differential trypsinisation was used during sub-culturing for the growth of fibroblasts. CAFs and NFs were always cultured simultaneously, in the same conditions and at similar passages (3–10).

2.2.3.1 Culture of human mammary fibroblasts (CAFs and NFs)

Human mammary fibroblasts were maintained in DMEM supplemented with 10% (v/v) bovine calf serum, 1% (v/v) penicillin/streptomycin and 1% (v/v) L-glutamine. Cells were grown in T-75 cm² flasks and maintained in 5% CO₂ and 95% air at 37 °C, the media being changed three times per week. CAFs and NFs were passaged upon reaching approximately 80-90% confluency. The media was removed and the mammary fibroblasts washed once with 2 ml of trypsin (0.5%). The solution was then removed and 3 ml of trypsin was reintroduced into the flask and left in an incubator at 37°C for 2-5 min until cells began to round up, indicating that they had begun to detach the cells from the flask. The medium was then added to the flask, and gently pipetted on the side of the flask to break any clusters. Human fibroblasts were then cultured into various sizes of sterile dishes and plates for experimentation, and they incubated in 5% CO₂ and 95% air at 37 °C and media was replaced every two days to maintain healthy fibroblasts.

2.3 Treatment of cell lines and human mammary fibroblasts

2.3.1 SU compounds

SU compounds: SU1261, SU1266, SU1349 and SU1433 were developed at the University of Strathclyde, Glasgow, UK. Based on the weight and the molecular weight (M.W) of these compounds, a 20 mM stock solution was prepared by dissolving the chemical in a calculated volume of DMSO. The prepared solutions were stored at -20°C. U2OS cells were treated with a concentration range of 0.3-30 µM for pharmacological study, whereas 0.1-10 µM was used for breast cancer cells (MCF7 & MDA-MB321) and human mammary fibroblast (CAFs & NFs).

2.3.2 siRNA-mediated silencing of IKK α or IKK β in cells

Small interfering RNA (siRNA) is a molecular biology method that is used to study the functions and role of different proteins in cellular processes in cells. It belongs to a class of double stranded RNA (20 - 25 base pairs) which inhibits the expression of targeted genes with complementary nucleotide sequences causing mRNA to be shut down, leading to halted translation and synthesis for a particular protein (Elbashir et al., 2001). In order to observe the effect the loss of the IKKs on the cells and human mammary fibroblasts, cells were transfected with siRNA against IKK α and IKK β in comparison to non-target siRNA (NT) supplied from Thermo Fisher Scientific® (Thermo Fisher Scientific, Surrey, UK). Target sequences are shown in Table 2.1. Newly purchased siRNA was re-suspended in RNase-free 1x siRNA buffer (Dharmacon, Buckinghamshire, UK). To prepare a 20µM stock, 500ul of 1X siRNA buffer were added to 10nmol of siRNA then mixed by pipetting. The diluted solution was then placed on an orbital mixer for 30 minutes at room-temperature, before being aliquoted and stored at -20°C.

U2OS cells and fibroblasts were seeded into 6 wells plates and cultured until they reached approximately 50-60% confluence on the day of transfection. For each well, two labelled Ependorfs were prepared, tube 1 containing the siRNA mixture and tube 2 containing the Lipofectamine® mixture. Tube 1 was made up to 100µl with Opti-MEM® medium (Life Technologies, Paisley, UK) as follows: 25 nM (1.25 µl siRNA + 98.75 µl Opti-MEM®), 50 nM (2.5 µl siRNA + 97.5 µl Opti-MEM®), 75 nM (3.75 µl siRNA + 96.25 µl Opti-MEM®) and 100 nM (5 µl siRNA + 95 µl Opti-MEM®). These were used to establish the optimal concentration. In the second tube, 5 µl Lipofectamine RNAiMAX® (Invitrogen®, Paisley, UK) was diluted into 100µl Opti-MEM®. Lipofectamine RNAiMAX® was used as the transfection reagent to deliver the siRNA to the cells. Both tubes then mixed together at a 1:1 ratio and left to incubate at room temperature for 20 min to allow the formation of complexes. Full media were then replaced with 800 ul Opti-MEM®. After 20 min, the transfection mixture (Final volume 200 µl) was added to the appropriate wells dropwise. Plates were incubated for 16-18h in 5% CO₂ and 95% air at 37°C. After this period, the transfection mixture was aspirated off and replaced with full media. The cells were then incubated for 96 h (U2OS cells) or 72 h (CAFs and NFs) at 37°C and 5% CO₂. Whole sample extracts were then collected and stored in -20°C for IKK expression levels by Western blot analysis (Section 2.5).

Table 2.1: siRNA transfection agents. Target gene, siRNA origin and target sequence.

Target Gene	On-Target plus siRNA	Target Sequence
IKK α (CHUK)	Human CHUK Cat. NO: J-003473-09	GCGUGAAACUGGAAUAAU
IKK β (IKBKB)	Human IKBKB (3551) Cat-No: J-003503-13	GAGCUGUACAGGAGAUAA
Non-target (NT)	Non-target Cat No: D-001810-01-20	UGGUUUACAUGUCGACUAA

2.4 Preparation of nuclear extracts

Cells were grown on 6-well plates until 90% confluency and then exposed to appropriate agonists for indicated time period. The reaction was terminated by washing on ice with 0.75 ml of cold PBS, cells were scraped into 0.5 ml PBS and transferred to Eppendorf tubes. Cells were then centrifuged at 14000 rpm for 2 min at 4°C. The pellet was re-suspended in 400µl of buffer 1 (10 mM Hepes pH 7.9, containing 1mM DTT, 0.5 mM PMSF, 0.1 mM EDTA, 0.1 mM EGTA, 10 mM KCl, 10 µg/ml pepstatin, 10 µg/ml leupeptin and 10 µg/ml aprotinin) and it was left on ice for 15 min. Next, 25 µl of 10% (w/v) NP-40 was added, and the samples vortexed at full speed for 10 sec. The centrifugation was employed at 20,817 g for 60 sec in order to separate the nuclear fraction. The supernatants were removed and the pellets were resuspended in 50 µl of buffer 2 (20mM Hepes, (pH 7.9), 25% (v/v) glycerol, 0.4 mM NaCl, 1 mM EGTA, 1 mM DTT, 0.5 mM PMSF, 10 µg/ml aprotinin, 10 µg/ml leupeptin and 10 µg/ml pepstatin) and agitated at 4°C for 15 min. The samples were sonicated in ice bath twice for 30 sec. Nuclear proteins were then recovered by centrifugation at 20,817 g for 15 min, and the soluble nuclear extract (supernatant) was collected and stored at -80°C until use.

2.4.1 Determination of protein concentration in the nuclear extract

Quantification of protein concentration in nuclear extracts was determined by using the Bio-Rad DC™ protein assay dye reagent by the Bradford assay method. A standard curve was performed using various concentrations (2-20 µg) of BSA. The dilutions of the standards and the nuclear extracts samples were made up in sterile dH₂O (790-795µl) and mixed with 200µl of dye agent. The samples then were transferred into a cuvette and the colour development quantified at 595 nm on an

Ultrospec®2000 UV/visible spectrophotometer. The protein concentration of each sample was calculated from the standard curve.

2.5 Western Blot Analysis

The Western blot (protein immunoblot) is an analytical technique used to measure specific proteins in a tissue homogenate or cell extract.

2.5.1 Preparation of Whole Cell Extracts (Lysis of protein)

U2OS cells and human mammary fibroblast were exposed to appropriate agonists or siRNA for the relevant period of time and they were then placed on ice to stop the reaction and prevent protein degradation or dephosphorylation. Cells were immediately washed twice with 500µl ice cold PBS before adding 150-200µl of pre-heated laemmli's sample buffer (63mM Tris-HCl (pH 6.8), 2mM Na₄P₂O₇, 5mM EDTA, 10% (v/v) glycerol, 2% (w/v) SDS, 50mM DTT, 0.007% (w/v) bromophenol blue) . The cells were then scraped and the chromosomal DNA sheared by repeatedly pushing through a 21 gauge needle. The cells were then transferred to Eppendorf tubes and boiled for 5min to denature the proteins in the samples, before keeping at -20°C or -80°C until use.

2.5.2 SDS-Polyacrylamide Gel Electrophoresis (SDS-PAGE)

The principle is based on the migration of negatively charged proteins due to presence of SDS towards the positive anode via the polyacrylamide gel. By this process, the smaller proteins move faster than the large ones through the pores produced by the acrylamide thus proteins are separated by the polyacrylamide gel according to their molecular weight.

To begin this process, firstly, gel kit apparatus was cleaned in 70% ethanol before assembly, then distilled water was added to check the glass plates were flush and not leaking. Resolving gels were prepared, depending on the size of the protein of interest containing an appropriate amount (15 (w/v) %, 10 (w/v) %, 8.5 (w/v) % 7.5 (w/v) %) acrylamide (Rotiphorese® Gel 30 (37.5:1), 0.375M Tris base (pH8.8), 0.1% (w/v), SDS and 10% (w/v) Ammonium persulfate (APS). The appropriate amount of 30% acrylamide/bisacrylamide stock depending on the size of the protein of interest. Polymerization process was started by the addition of 0.05% (v/v) N, N, N', N' tetramethylethylenediamine (TEMED). Glass plates were set up on a Mini-PROTEAN casting chamber and the solution was poured between the two glass plates with 200 µl of 0.1% SDS added on top to make the upper end of the gel in line shape. Following gel polymerisation the SDS solution was removed and a stacking gel containing 0.125 M Tris base (pH6.8), 10% acrylamide, 0.1% SDS, 10% APS, and 0.05% TEMED was poured on top of the resolving gel, and a teflon comb was immediately inserted into the stacking gel solution. After the polymerization process was completed, the comb was carefully removed and gels were assembled in a Bio-Rad Mini-PROTEAN electrophoresis tank filled with electrophoresis buffer (0.1% SDS, 25 mM Tris, 129 mM glycine). By using a Hamilton microsyringe, aliquots of samples (20-30 µg/ml) were then loaded into the wells. A prestained marker of known molecular weights was run on the same gel in order to identify the protein of interest by size and ensure

transfer to membrane was successful. Samples were electrophoresed at a constant voltage of 130 V, until the bromophenol dye had reached the bottom of the gel.

2.5.3 Electrophoretic transfer of proteins to nitrocellular membrane

The proteins separated on the gel by SDS-PAGE were transferred to nitrocellulose membranes by electrophoretic blotting using a standard protocol (Towbin et al., 1979). In wet conditions, the gel was placed and pressed firmly against a nitrocellulose membrane and assembled in a transfer cassette sandwiched between two whatmann 3 MM filter papers porous pads and two sponge pads. The cassette was then immersed in transblotting buffer (25 M Tris, 19 mM glycine, 20% methanol) in a Bio-Rad Mini- PROTEAN electrophoresis tank and was run for 105 min at constant current of 300 mA with an ice pack included to cool the tank. The presence of SDS gives the protein a negative charge, the cassette therefore was oriented with the membrane towards the anode meaning protein would move towards this positive electrode and bind to the membrane.

2.5.4 Immunological detection of protein

Following transfer of the proteins from the gel to the nitrocellulose membrane, the membrane was trimmed to the size of the gel and non-specific binding blocked by incubation in a solution of 2% (w/v) BSA/ in NaTT buffer (150 mM NaCl, 20 mM Tris (pH 7.4), 0.2% (v/v) Tween -20) for two hours with gentle agitation on a platform shaker. Then blocking buffer was removed and nitrocellulose membranes incubated overnight, either at room temperature or 4°C, with primary antibody specific to the target protein diluted to optimal concentration in NaTT buffer containing 0.2% BSA. Optimised for each antibody are listed in Table 2.2. On the following day, the membranes were washed in NaTT every 15 min for 90 min with gentle agitation. The

membranes were further incubated with gentle agitation for a 90 min at room temperature with secondary (either rabbit or mouse, depending on primary antibody used) horseradish peroxidase-conjugated IgG directed against the first immunoglobulin diluted to approximately 1:10000 in NaTT buffer containing 0.2% (w/v) BSA. Again the membranes were washed six times in NaTT every 15 min before being incubated in enhanced chemiluminescence (ECL) reagent (1:1 mixture of solution 1 [1M Tris pH8.5, 250 mM luminol, 250 mM coumaric acid and water] and solution 2 [1M Tris pH8.5, 0.19% H₂O₂ and water]) for two minutes with agitation to detect immunoreactive protein bands. Membranes were then placed into a cassette, covered with cling film and in the dark room exposed to X-ray film (B Plus – Full Blue) for the required time and developed using either an X-OMAT machine (KODAK M35-M X-OMAT processor) or X-Ray Film Processor JP-33.

Table 2.2: Antibodies used for Western blot and optimal conditions.

Protein of interest	Antibody source	Blocking conditions	Species	Antibody conditions
I κ B α	Cell Signaling 92424	2% BSA in NaTT	Rabbit	1/3000 (4°C)
p-p65 (S536)	Cell Signaling 3031	2% BSA in NaTT	Rabbit	1/3000 (4°C)
p65	Santa Cruz C-20	2% BSA in NaTT	Rabbit	1/15000 (RT)
p-p100	Cell Signaling 4810	3% BSA in NaTT	Rabbit	1/3000 (4°C)
p100/52	Millipore 32534	2% BSA in NaTT	Mouse	1/5000 (4°C)
RelB	Cell Signaling 10544	2% BSA in NaTT	Rabbit	1/3000 (4°C)
I κ K α	Calbiochem 14A231	3% BSA in NaTT	Mouse	1/3000 (4°C)
I κ K β	Abcam ab32135	3% BSA in NaTT	Rabbit	1/3000 (4°C)
NIK	Santa Cruz H-248	3% BSA in NaTT	Rabbit	1/3000 (4°C)
TRAF2	Cell Signaling 4724	2% BSA in NaTT	Rabbit	1/3000 (4°C)
TRAF3	Cell Signaling 4729	2% BSA in NaTT	Rabbit	1/3000 (4°C)
Nucleolin	Cell Signaling 14574	2% BSA in NaTT	Rabbit	1/15000 (RT)
GAPDH	Cell Signaling 14C10	2% BSA in NaTT	Rabbit	1/15000 (RT)

2.5.5 Nitrocellulose membrane stripping and reprobing

Nitrocellulose membranes processed by Western blotting were reprobed for the subsequent detection of other cellulose proteins or to confirm equal loading of total proteins. The first step in this process was stripping the membrane of any previous antibody using a stripping buffer (2% SDS and 0.05 M Tris-HCl). The membrane was incubated at 60°C in 15 ml of stripping buffer with 0.1 M (105 µl) β-mercaptoethanol for 60 min on a shaker. The stripping buffer was then removed in a fume hood sink and the membrane was washed in NaTT three times for 10 min to remove residual stripping buffer. Membranes were then ready for reprobing, following the protocol previously described (Section 2.5).

2.5.6 Scanning densitometry and quantification of expression levels

Western blot films were scanned on an HP Scanjet G2710 Scanner using Adobe Photoshop 5.0.2 software. The captured images were then normalised to a control and quantified using Scion Image (Scion Corp., Maryland, USA). Fold increase in protein levels compared to control or agonist stimulated control were calculated using one-or-two way analysis of variance (ANOVA) using GraphPad Prism software, version 5.0, (GraphPad Software Inc, CA, USA).

2.6 Cellular thermal shift assay (CETSA)

The cellular thermal shift assay is a new analytical technique used to monitor drug binding to its target protein inside cells and tissue samples (Martinez Molina et al., 2013). Cells at approximately 90% confluency were washed once with 5 ml PBS. The cells were then scraped before being pelleted by centrifugation 106 g for 3 min at room temperature, the pellet was then resuspended in either 2 ml PBS (with proteasome inhibitor) or 2 ml Lysis buffer (with proteasome inhibitor). Cells were then

aliquoted into 100 μ l volumes in 10 PCR tubes (0.5 ml). The samples were then incubated with temperature gradient covering 40-70 $^{\circ}$ C for 3 min. The samples were then freeze-thawed twice for 3 min using liquid nitrogen and a re-heating block by incubating the samples for 3 min at 25 $^{\circ}$ C. Briefly vortex between each thaw process was made. The samples were then centrifuged at 20,817 g for 20 min at 4 $^{\circ}$ C to pellet the cellular debris. The samples were kept on ice without disturbing the pellet. Following this, 90 μ l of supernatant samples were then transferred to a new eppendorf tubes before 90 μ l of reducing load buffer was added. The samples were then homogenised, and heated at 70 $^{\circ}$ C for 10 min or boiled for 3 min. At this stage, the samples were ready for Western blot analysis (Section 2.5).

2.7 Luciferase reporter activity assay

A U2OS-CXCL12 reporter cell line was developed in our laboratory by Liam Ireland using a CXCL12 promoter construct donated by Garcia-Moruja group (Garcia-Moruja et al., 2005). Cells were grown to confluency in 96 well plates, the cells were then starved for 24 h by removing media and adding 100 μ l serum free media. Cells were exposed to a various agonists at the indicated time points before performing the reporter assay or pre-treated with selective IKK α inhibitors (SU compounds) for one hour prior stimulation. Lysis buffer was prepared as follows: (25mM Tris-Phos 1% Triton X-100, 15% Glycerol, 1 mM DTT, and Vol up to 500 mL with distilled water. 10 ml of the lysis buffer was added to a beaker along with 0.1 g BSA. At the same time, 0.0015 g luciferin, 0.0055 g ATP, and 0.003g DTT were weighted and stored in fridge. The media was aspirated from the wells. Cells were washed with 100 μ l PBS and then removed it. Immediately, luciferin, ATP and DTT were added to the lysis buffer. Cells were incubated with 100 μ l of luciferase buffer (lysis buffer containing 1 mM ATP, 1% (v/v) BSA and 0.2 mM luciferin substrate) for 5 min in room temperature. Finally, the

relative light units were measured using microplate reader (PerkinElmer/Wallac 1450-021 Trilux MicroBeta Liquid Scintillation and Luminescence Counter).

2.7.1 Construction of luciferase reporter plasmid

Construction of luciferase reporter plasmid was conducted by Garcia-Moruja and colleagues (Garcia-Moruja et al., 2005) as follows: pCMVLUC plasmid containing the CMV promoter upstream of the luciferase gene was created by subcloning the HindIII–XhoI fragment from pGEMLUC (Promega) in pCDNA3.1 (Invitrogen). This plasmid was used as a luciferase positive control in all experiments. A negative control plasmid was created by deleting the SpeI–BamHI fragment that contains the CMV promoter sequence. This plasmid was named pDPROMLUC. A 1.1 kb fragment of SDF1 50 flanking region and first exon was PCR-amplified using the primer set SDF-INTER (TGAGGATCCAGGCACGACCACGACCTTGGCGTTCAT3), SDF-1100 (TGAAACTAGTCACCGCCGAGGGACGGCTCCGTGG) from human genomic DNA using Pfu DNA polymerase (lower mutation rate). A SpeI site was added to the 50 end of SDF-1100 and a BamHI site was added to the 50 end of SDF-INTER, the plasmid pPSDF1100LUC was created by subcloning this fragment in pDPROMLUC.

2.8 Polymerase chain reaction (PCR) amplification

The polymerase chain reaction (PCR) is a technique which allows the exponential amplification of a specific region of DNA via repeating a three-step process: denaturation, annealing, and extension (synthesis).

2.8.1 Extraction of total cellular RNA

RNA was extracted by using Isolate II RNA Mini Kit (Bioline, London, UK). Cells were exposed to appropriate agonists or treatment. U2OS cells and patient samples were

grown to 80% confluency in 6-well cell culture plates. The cell culture media was removed and 350 μ l of a mixture of Isolate II RLY buffer with 3.5 μ l of 2-mercaptoethanol added to lyse the cells in the wells. The suspension was transferred to 1.5 ml microcentrifuge. An equal volume of 70% ethanol was added and then vortexed for 5 sec. The solution was transferred to an Isolate II RNA Mini spin column in a 2 ml collection tube, and then centrifuged at 12,851 g for 30 sec to bind the RNA to the purification column. Next the column membrane was washed using 350 μ l of Membrane desalting buffer (MDM). After centrifugation, 95 μ l of DNase digestion buffer (90 μ l of RDN plus 10 μ l DNase) was added directly to the center of membrane and incubated for 15 min at room temperature to degrade any cell line genomic DNA which might be co-purified by the spin-column. The membranes (Containing RNA) were washed with RW1 buffer followed by two washes with RW2 buffer to help remove genomic DNA and protein contaminants. Next, the membranes were placed into a sterile RNase-free 1.5 ml microfuge tube and 40 μ l of Diethyl-pyrocabonate (DEPC)-treated water (RNase-free water) was added directly onto center of membrane, and then centrifuged at 11,000 rpm for 1 min to elute and collect the RNA from the spin column. The purified RNA was stored at -80 °C until required for further analysis.

2.8.2 Measurement of RNA concentration

RNA concentrations of prepared samples were measured using NanoDrop® ND-2000C Spectrophotometer (R&D Systems, Minneapolis, MN, USA). This instrument also allows for determination of quality and purity of RNA through UV absorption curve. Firstly the probe of the spectrophotometer was cleaned by a tissue wetted with distilled water. 2 μ l of distilled water was pipetted onto the probe to blank the spectrophotometer. The probe was once again cleaned before 2 μ l of purified RNA was

pipetted onto the probe. The software displays the sample absorption curve as well as the calculated RNA concentration and ratios ($A_{260\text{nm}}/A_{280\text{nm}}$; $A_{260\text{nm}}/A_{230\text{nm}}$). The ratio at $A_{260\text{nm}}/A_{230\text{nm}}$ around 2.0 indicates low salt contamination and the ratio at $A_{260\text{nm}}/A_{280\text{nm}}$ provides an evaluation of the purity of RNA and protein contamination. Pure RNA should have an $A_{260\text{nm}}/A_{280\text{nm}}$ ratio of 2. All extracted RNA samples used for PCR in this study had acceptable purity ratios of around 2 for $A_{260\text{nm}}/A_{280\text{nm}}$ and $A_{260\text{nm}}/A_{230\text{nm}}$.

2.8.3 cDNA synthesis using reverse transcription (RT)

To quantify the mRNA transcripts of the genes under investigation, mRNA in the total RNA extracted from samples was reverse transcribed to complementary DNA (cDNA) using Tetro cDNA synthesis kit (Bioline, London, UK). The kit can transcribe a maximum of 5 μg of total RNA per reaction. For the purposes of this study, 1 μg of purified total RNA from each of the samples was used in all of the cDNA reactions and the cDNA synthesis was carried out as described in the manufacturer's manual. All reactions were prepared on ice. The volume which contained 1 μg total RNA from each sample was added to a sterile RNase-free PCR tube and the volume was adjusted to 12 μl by adding RNase-free water. Subsequently, the cDNA synthesis master mix with Oligo dT as the first-strand synthesis primer was prepared as shown in Table 2.3, and then 8 μl of the Tetro cDNA synthesis master mix was added for each 12 μl RNA mixture to give a final volume of 20 μl . The samples were gently mixed by pipette, and then incubated for 30 min at 45 $^{\circ}\text{C}$. The reaction was terminated at 85 $^{\circ}\text{C}$ for 5 min and then quick chilled on ice. These samples were labelled "RT+". To check for the presence of persisting contaminating genomic DNA, an additional reaction tube, labelled "RT-" was set up in parallel for each RNA sample. This reaction contained all of the cDNA synthesis components and total RNA with the exception of

Tetro reverse transcriptase. These “RT-“samples were processed under the same conditions of “RT+” samples. PCR carried out using an aliquot of an “RT-“control sample should not generate an amplicon. The cDNA samples were stored at -20 °C until required. The resulting cDNAs were then used as the DNA template for quantitative real-time PCR (Section 2.8.4) for gene expression analysis.

Table 2.3: Tetro cDNA synthesis Master Mix

Component	Volume (µl)
Primer: Oligo (dT) ₁₈	1
10mM dNTP mix	1
5x RT buffer	4
RiboSafe RNase Inhibitor	1
Tetro Reverse Transcriptase (200u/µl)	1

2.8.4 Quantitative real time PCR (RT-qPCR)

Reverse-transcribed real-time quantitative PCR allows for the detection and measurement of products generated during each cycle of the PCR process. Quantitation of CXCL12 cDNA was performed using probe-based TaqMan® real time quantitative PCR assay. All reactions were conducted in triplicate on a MicroAmp® Optical 96-well reaction plate (Applied Biosystems, UK). Each RT-qPCR reaction mixture was made up to a total of 20 µl, which contained; 2 µl of the cDNA template, 7 µl RNase-free water, 1 µl of Gene Expression Assay (The Gene Assay IDs for the target genes can be found in Table 2.4), and 10 µl TaqMan® Universal PCR Master Mix (Applied Biosystems, UK). Negative no-template control blank wells with reaction mix without cDNA were included to ensure amplification derived from the samples' cDNA and not from contaminants. In addition, “RT-“ samples were employed as another negative control, where no reverse transcriptase was added to the RNA

samples during the cDNA synthesis step. Any amplification present in these reactions would suggest genomic DNA carryover in the RNA samples. Plates were then sealed and centrifuged for 2 min at 106 g. The thermal cycling and amplicon detection was conducted on a StepOne Plus real-time PCR system (The cycling conditions are detailed in Table 2.5). Crossing threshold (Ct) values were obtained from the real time quantitation of CXCL12 mRNA in U2OS cells and patient samples. The negative controls such as water blank and “RT-“ gave undetermined Ct values as expected.

Table 2.4: TaqMan® Gene Expression Assays. The gene and assay ID are detailed.

Gene	Gene Assay ID	Amplicon length
CXCL12	Hs00171022_m1	77bp
ACTB	Hs01060665_g1	63bp

Table 2.5: Applied Biosystems StepOne Plus thermal cycling program for TaqMan® RT-qPCR.

Times and Temperature			
Initial Steps		40 Cycles	
		Melt	Anneal/Extend
Hold	Hold	Cycle	
2 min* 50 °C	10 min** 95 °C	15 sec 95 °C	1 min 60 °C

* The 2 min hold at 50 °C is required for optimal uracil N-glycosylase (UNG) activity.

** The 10 min hold at 95 °C is required for DNA polymerase activation.

2.8.5 Quantification method

Relative quantitation ($\Delta\Delta C_t$), also known as the comparative threshold method, was used to quantify real-time RT- qPCR results (Livak and Schmittgen, 2001). Levels of CXCL12 gene expression were normalised to the levels of an endogenous housekeeping gene (β -actin). The comparative threshold method was used to quantify relative gene expression compared to control using the formula:

$$\text{Fold Change} = 2^{-\Delta(\Delta C_t)}$$

, where ΔC_t Control = (Ct, target gene - Ct, reference gene); ΔC_t Stimulated = (Ct target gene - Ct reference gene); and $\Delta(\Delta C_t) = \Delta C_t$, stimulated - ΔC_t , control.

2.9 Enzyme-linked Immunosorbent Assay (ELISA)

2.9.1 Preparation and treatment of human mammary fibroblast

CAFs and NFs were cultured on six-well plates with 2 ml of DMEM complete media. After 12 h of incubation, the media was changed to 1 ml of DMEM 2 % calf serum, followed by incubation with $LT\alpha_1\beta_2$ for 24 and 48 h or the cells were transfected with 100nM of siRNA IKK α and pre-treated with SU1349 (1 and 10 μ M). The media conditioned by fibroblasts were collected by centrifugation for 3 minutes at 106 g and processed for ELISA protein expression analysis immediately or stored at -20 °C until use.

2.9.2 Measurement of CXCL12/SDF1-alpha

CXCL12 levels in the DMEM supernatant were measured using the Quantikine human CXCL12/SDF-1 immunoassay (R&D Systems, Minneapolis, MN 55413, USA) in accordance with the manufacturer's instructions as follows:

ELISA solutions and buffers

Solutions and buffers were prepared in room temperature as follows:

Wash Buffer: 20 ml of wash buffer concentrate was added to distilled water to prepare 500 ml of wash buffer.

Substrate Solution: colour reagents A and B should be mixed together in equal volumes within 15 min of use.

Human CXCL12/SDF-1 α standard: The human CXCL12/SDF-1 α standard was reconstituted in distilled water to produce a stock solution of 100,000 pg/mL. This the standard solution was then mixed well to ensure complete reconstitution and allowed to sit for a minimum of 30 minutes prior to making dilutions or stored in at -20°C until use.

Use polypropylene tubes (CXCL12 standards): 100 μ L of CXCL12 stock solution (100,000 pg/mL) was added into 900 μ L of Calibrator Diluent RD6Q in polypropylene tube to prepare a final concentration of 10,000 pg/mL. Then, a serial dilution was carried out in order to prepare different concentrations of CXCL12 and Calibrator Diluent RD6Q serves as the zero standard (0 pg/mL).

Assay procedure:

A monoclonal antibody specific for human CXCL12 has been pre-coated onto a 96-well microplate. 100 μ L of Assay Diluent RD1-55 and 100 μ L of standard, control, or samples were added to each well. The adhesive strip provided was used to cover the plate, and it was then incubated for 2 h at room temperature on a horizontal orbital microplate shaker set up at 300 rpm. Then, the plate was washed for four times to remove excess capture antibody using washing buffer (400 μ L) and was dried well by

invert the plate and hitting on clean tissues. Next, 200 μ L of Human SDF-1 α Conjugate was added as secondary antibody to each well. Again, the plate was covered with a new adhesive strip and incubated later for 2 h at room temperature on the shaker (300 rpm) before the final wash four times. After drying, 200 μ L of Substrate Solution (Colour reagents A and B) was added to each well. The plate was then wrapped with tin foil and incubated for 30 min at room temperature. The reaction was finally stopped with 50 μ L of Stop Solution (The colour in the wells should change from blue to yellow. If the color in the wells is green or the colour change does not appear uniform, the plate gently tapped to ensure thorough mixing). The optical density was measured at 450 nm within 30 min using SPECTRAmax 190 microtiter plate spectrophotometer and Softmax PRO 3.0 software (Molecular Devices, CA, USA).

2.10 Data analysis

All data shown were expressed as mean \pm s.e.m and were representative of at least three separate experiments. Most statistics were calculated using GraphPad Prism version 5.01. The statistical significance of differences between mean values from control and treated groups were determined by one-or-two way analysis of variance (ANOVA) with Dunnett's post-test. For the IC₅₀ values, GraphPad Prism software version 7.0 (GraphPad Software California) was used, p values <0.05 were considered significant.

Chapter Three

**Characterisation of the inhibitory effect of selective
IKK α inhibitors (SU compounds) on canonical and non-
canonical NF- κ B pathways in U2OS and MCF7 cells**

3.1 Introduction

As outlined earlier (Chapter 1), it is clear that IKKs play a central role in the regulation of NF- κ B pathways (Oeckinghaus and Ghosh, 2009, Lee and Hung, 2008). The non-canonical NF- κ B pathway can be activated by different stimuli, such as lymphotoxin β (LT β), which leads to phosphorylation of p100 by IKK α subunits followed by the processing of p100 to generate p52. p52-RelB heterodimers then translocate into the nucleus to promote specific gene transcription (Oeckinghaus and Ghosh, 2009). Evidence indicates that IKK α signalling is up regulated in U2OS osteosarcoma cell line derived from bone cancer patients (Leopizzi et al., 2017). Moreover, it is one of the first cell lines used in biomedical research, including bone formation (Niforou et al., 2008). Therefore, U2OS cell line was selected as the system to demonstrate IKK α mediated NF- κ B activity.

Furthermore, IKK α has been implicated in the progression, invasion, metastasis and the development of various types of cancer such as, breast, pancreatic, gastric, colorectal, and prostate cancer (Ben-Neriah and Karin, 2011, Hao et al., 2010, Nadiminty et al., 2010, Luo et al., 2007, Fernandez-Majada et al., 2007, Shiah et al., 2006, Hirata et al., 2006). However, in spite of IKK α having been implicated in different aspects of cancer, development of selective inhibitors for IKK α have not, as yet, been developed as a therapeutic approach. Therefore, novel first-in-class selective IKK α Inhibitors (SU compounds) were generated in-house of the University of Strathclyde, using enzyme isoform specific *in vitro* kinase assays. Early compound scaffolds have been generated and have potential as selective inhibitors of the non-canonical NF- κ B pathway (Anthony et al., 2017) but issues of potency still remained. Thus, a more advanced set of SU compounds were utilised such as SU1261, SU1266, SU1349, and SU1433.

Thus, the aim of the work in this chapter is to evaluate SU compounds at the cellular level in terms of their selectivity and the potency against outputs of the canonical and non-canonical NF- κ B pathways in human osteosarcoma (U2OS) and breast cancer cell lines (MCF7-ER-positive and MDA-MB-231-ER-negative). In other words, to assess whether effective target engagement with selectivity against IKK α could be achieved. In addition to measurement of standard outputs, a thermostability assay was used in an attempt to assess a direct interaction between IKK α and SU compounds.

3.2 Results

3.2.1 In vitro selectivity of SU compounds

A large number of SU compounds were generated and screened in-house however, for the purpose of the thesis only four compounds were utilised. The inhibitory activity of the SU compounds; SU1261, SU1266, SU1349 and SU1433, on IKK α or β kinase activities were tested using an *in vitro* kinase assay, performed at the University of Strathclyde by Mrs. Louise C. Young, using a kinase assay kit (Cell Signalling Technology, Inc., Danvers, MA, USA). Using either purified IKK α or IKK β , kinase activity was assessed using a biotinylated peptide substrate containing serine 32 of I κ B α . The extent of phosphorylation was assessed by dissociation-enhanced lanthanide fluorescent immunoassay (DELFI) and the time-resolved fluorescence (TRF). Results from at least three individual experiments were used to determine the IC₅₀ curves.

Table 3.1 shows the Ki values or the dissociation constant values (the concentration of the compound in which 50% of the kinase activity is inhibited) of SU compounds for IKK α and IKK β . The Ki value for SU1261 for IKK α was 10 nM, whereas the Ki value of IKK β was 70-fold higher than that of IKK α (Ki value = 680 nM). Similarly, the

Ki value for SU1349 on IKK α was 21 nM, while the Ki value for IKK β was 120-fold higher than IKK α (Ki value = 2445 nM). SU1433 was also more selective against IKK α (Ki value = 11 nM) than IKK β which was 220-fold (Ki value = 2295 nM). These data suggest that these compounds are highly selective for IKK α . However, the Ki values for SU1266 were much lower for both IKK α (Ki value = 2 nM) and IKK β (Ki value = 77 nM), although the selectivity ratio was the lowest at approximately 1:40 for this compound.

Table 3.1: The Ki values for SU compounds.

Ki value (nM)	SU1261	SU1433	SU1349	SU1266
IKK α	10	11	21	2
IKK β	680	2295	2445	77

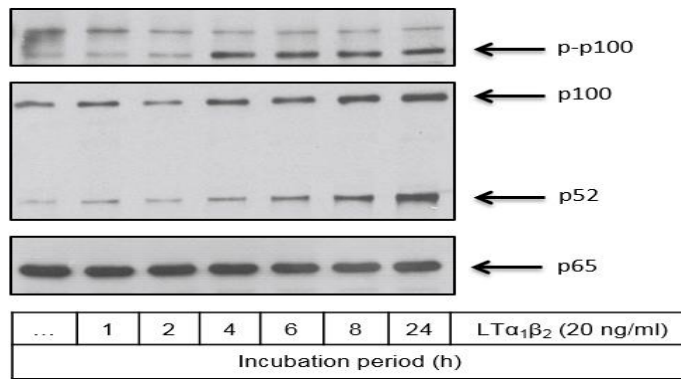
3.2.2 Activation of the non-canonical NF- κ B signalling pathway in U2OS cells

Within the non-canonical NF- κ B pathway, p100 processing is a key up-stream marker which leads to p52 formation and nuclear translocation of RelB/p52. Evidence suggests that IKK α is responsible for p100 processing through phosphorylation on residues S866, S870 and S872 (Liang et al., 2006, Xiao et al., 2004). The aim of the initial stage of the study was to define the optimal time for activation of the non-canonical NF- κ B signalling pathway and then define the role of IKK α by evaluating the impact of novel first-in-class SU compounds (IKK α Inhibitors).

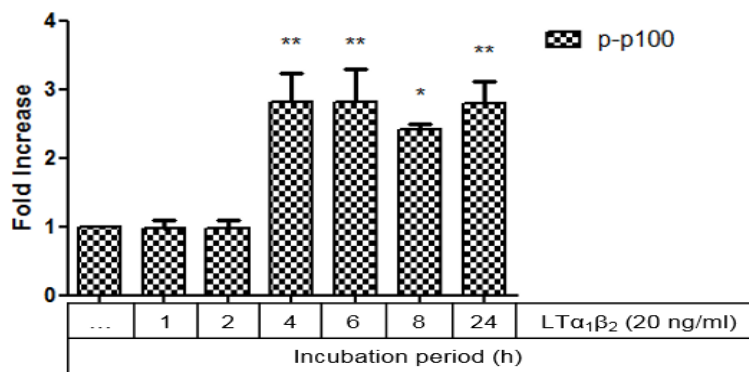
3.2.2.1 The effect of $LT\alpha_1\beta_2$ on the non-canonical NF- κ B pathway in U2OS cells

Figure 3.1 shows a time course over 24 h for $LT\alpha_1\beta_2$ induced p100 phosphorylation and p100 processing in U2OS cells. After a substantial delay, $LT\alpha_1\beta_2$ stimulated the phosphorylation of p100 at 4 h which remained elevated for up to 24 h. A maximum response was achieved at 6 h (Fold stim = 2.82 ± 0.49 , $p < 0.01$). $LT\alpha_1\beta_2$ also induced p100 processing, the formation of p52 was also found to be delayed following $LT\alpha_1\beta_2$ stimulation, with no stimulatory effect on p52 formation until 6 h, reaching a maximum response at 24 h, the longest time point studied (Fold stim = 4.88 ± 1.33 , $p < 0.05$). Interestingly, p100 expression followed a similar pattern as observed for p52 formation, again with a maximal expression at 24 h following $LT\alpha_1\beta_2$ stimulation (Fold stim = 2.67 ± 0.34). This suggests that $LT\alpha_1\beta_2$ can mediate the processing of p100 to p52 and the subsequent translocation of p52-RelB heterodimers to the nucleus.

A



B



C

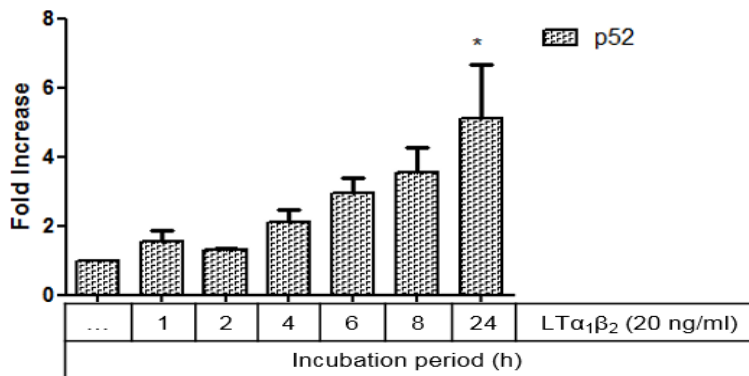


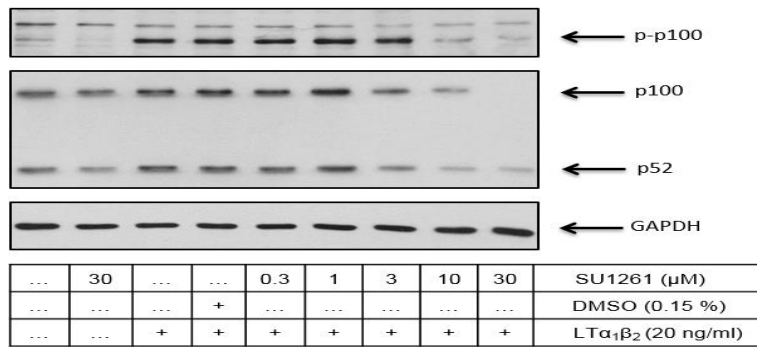
Figure 3.1: Time course of LT $\alpha_1\beta_2$ -mediated p100 phosphorylation and p100 processing in U2OS cells. Cells were stimulated with LT $\alpha_1\beta_2$ (20 ng/ml) for a maximum 24 h. Whole cell extracts were assessed for A) p100 phosphorylation (100 kDa), p52 formation (52 kDa), and total p65 (65kDa) which was used as a loading control, as outlined in Section 2.5. Blots were semi-quantified by scanning densitometry and results expressed as fold increase relative to control for B) p-p100 and C) p52. Each value represents the mean \pm SEM of three independent experiments. Data was analysed using a one-way ANOVA test, * $p < 0.05$, ** $p < 0.01$ vs control.

3.2.2.2 The effect of SU compounds on LT $\alpha_1\beta_2$ -induced p100 phosphorylation and p52 formation in U2OS cells

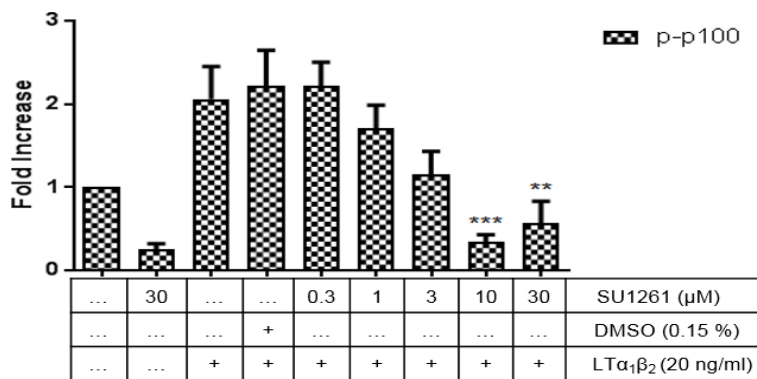
The effect of both SU1261 and SU1266 on LT $\alpha_1\beta_2$ -induced phosphorylation of p100 and p100 processing in U2OS cells was assessed (Figures 3.2 and 3.3 respectively). As shown in Figure 3.2, stimulation by LT $\alpha_1\beta_2$ alone induced an approximate two-fold increase in p100 phosphorylation (Fold stim = 2.06 ± 0.38 , $p < 0.05$) and a slight increase in p52 formation compared with non-stimulated cells. In the absence of stimulation, SU1261 alone reduced the low basal phosphorylation of p100 by about 75% (Fold increase = 0.25 ± 0.06 , $p < 0.05$) while, about 50% of p52 formation was inhibited by SU1261 alone (Fold increase = 0.52 ± 0.12 , $p < 0.05$). However, following LT $\alpha_1\beta_2$ stimulation, SU1261 mediated a concentration-dependent inhibition of both p100 phosphorylation and p52 formation with statistical significance at 10 and 30 μM (p-p100: SU1261 30 μM : Fold increase = 0.56 ± 0.26 , $p < 0.01$, p52: SU1261 30 μM : Fold increase = 0.37 ± 0.14 , $p < 0.001$). Levels of p100 expression were not changed significantly over a concentration range from 0.3 to 30 μM of SU1261 compared with untreated control cells.

In Figure 3.3, when U2OS cells were pre-treated with SU1266, p100 phosphorylation stimulated by LT $\alpha_1\beta_2$ was substantially decreased in the low micromolar range (3-30 μM) of SU1266 (p-p100: SU1266 3 μM : Fold increase = 1.18 ± 0.34 , SU1266 10 μM : Fold increase = 0.45 ± 0.22 , $p < 0.001$). Similarly, p52 formation was substantially reduced following pre-treatment with 10 and 30 μM of SU1266 (p52: SU1266 10 μM : Fold increase = 0.69 ± 0.05 , $p < 0.05$, SU1266 30 μM : Fold increase = 0.41 ± 0.05 , $p < 0.01$). However, the p100 protein levels remained unchanged in all concentrations (0.3 to 30 μM) of SU1266 compared with untreated control cells.

A



B



C

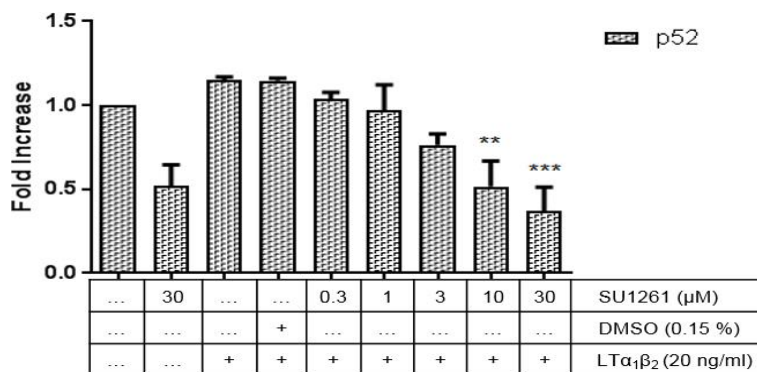


Figure 3.2: The effect of SU1261 upon LT $\alpha_1\beta_2$ -mediated p100 phosphorylation and p52 formation in U2OS cells. Cells were pre-treated with SU1261 for 1h prior to stimulation with LT $\alpha_1\beta_2$ (20 ng/ml) for 6 h. Whole cell extracts were assessed for A) phosphorylation of p100 (100 kDa), p52 formation (52 kDa), and GAPDH (37 kDa) which was used as a loading control, as outlined in Section 2.5. Blots were semi-quantified by scanning densitometry and results expressed as fold increase relative to control for B) p-p100. C) p52 formation. Each value represents the mean \pm SEM of three independent experiments. Data was analysed using a one-way ANOVA test, **p < 0.01, ***p < 0.001 vs LT $\alpha_1\beta_2$ and DMSO as an agonist stimulated control.

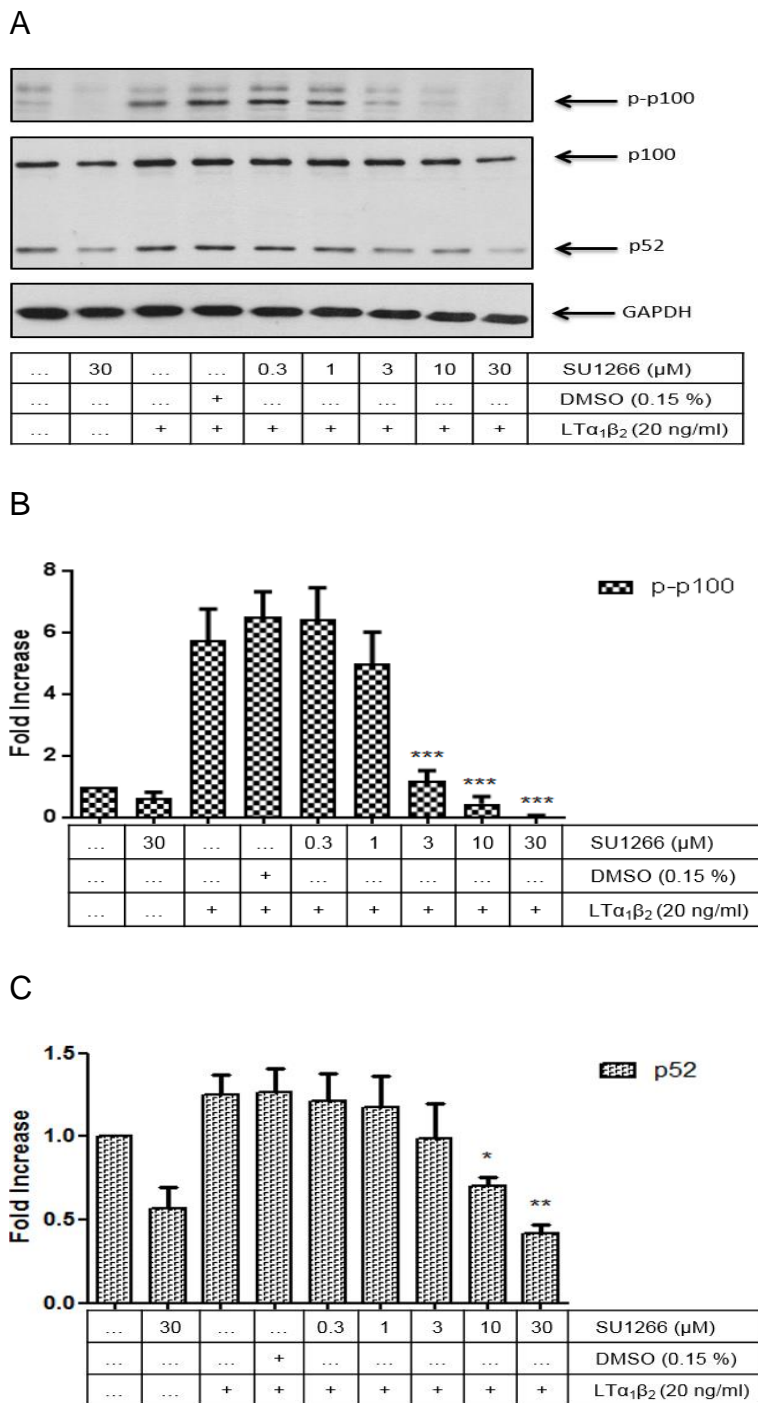


Figure 3.3: The effect of SU1266 upon LT $\alpha_1\beta_2$ -mediated p100 phosphorylation and p52 formation in U2OS cells. Cells were pre-treated with SU1266 for 1h prior to stimulation with LT $\alpha_1\beta_2$ (20 ng/ml) for 6 h. Whole cell extracts were assessed for A) phosphorylation of p100 (100 kDa), p52 formation (52 kDa), and GAPDH (37 kDa) which was used as a loading control, as outlined in section 2.5. Blots were semi-quantified by scanning densitometry and results expressed as fold increase relative to control for B) p-p100. C) p52 formation. Each value represents the mean \pm SEM of three independent experiments. Data was analysed using a one-way ANOVA test, * $p < 0.05$, ** $p < 0.01$, *** $p < 0.001$ vs LT $\alpha_1\beta_2$ and DMSO as an agonist stimulated control.

3.2.2.3 IC₅₀ values for p100 phosphorylation and p52 formation by SU compounds in U2OS cells

Next, based on the results obtained from the Western blotting of SU compounds (Figures 3.2 and 3.3), the data were fitted in a sigmoidal concentration-response curve and the IC₅₀ values of SU1261 and SU1266 calculated using GraphPad Prism software, version 7.0 (Figure 3.4, A-D). Interestingly, the IC₅₀ of SU1261 for the phosphorylation of p100 was 1.93 μM ± 0.56 μM (Panel A), while the IC₅₀ value for this agent for p52 formation was 5.20 ± 1.65 μM (Panel B). For SU1266 the IC₅₀ was 1.59 μM ± 0.17 μM for the phosphorylation of p100 (Panel C), with a higher IC₅₀ value for p52 formation (10.56 μM ± 3.33 μM) (Panel D).

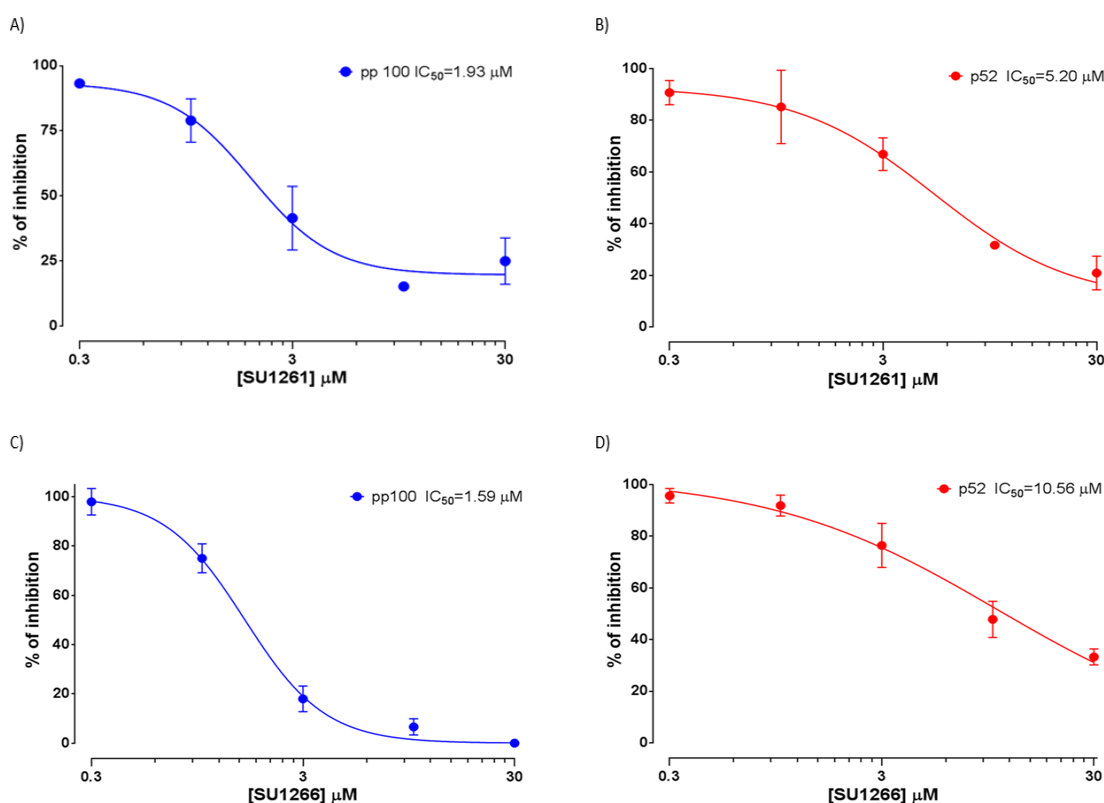


Figure 3.4: The IC₅₀ values of SU1261 and SU1266 for inhibition p100 phosphorylation and p52 formation induced by LTα₁β₂ in U2OS cells. Using GraphPad Prism software, version 7.0, the data obtained by Western blot analysis of SU1261 and SU1266 were fitted in a sigmoidal concentration-response curve for A) SU1261 for p-p100, B) SU1261 for p52 formation, C) SU1266 for p-p100, and D) SU1266 for p52 formation.

3.2.3. TNF α and IL-1 β stimulation of the canonical NF- κ B pathway in U2OS cells

Several studies have documented that TNF α and IL-1 β can induce activation of the IKK complex and subsequently the canonical NF- κ B pathway, IKK β but not IKK α plays a key role in the degradation of I κ B α and phosphorylation of p65 (Discussed in Section 1.4.4.4). As shown in Figure 3.5. Following TNF α stimulation, I κ B α degradation was observed early with a significant loss in cellular levels between 5 and 60 min ($p < 0.001$). I κ B α degradation was maximal at 30 min (% basal I κ B α expression = 5.67%). Thence, the expression of I κ B α gradually recovered, reverting towards basal values by 120 min. TNF α also induced an increase in the phosphorylation of p65 NF- κ B after 15 min and levels were maximal at this time (Fold stim = 5.94 ± 1.53 , $p < 0.05$) before returning gradually to basal levels by 120 min.

Figure 3.6 shows a short time course of I κ B α loss and p65 phosphorylation induced by IL-1 β in U2OS cells. Following IL-1 β (5 ng/ml) stimulation, levels of I κ B α declined rapidly between 5 min and 120 min ($p < 0.001$), degradation reached a minimum value at 30 min (% basal I κ B α expression = $0.92\% \pm 0.43$, $p < 0.001$). I κ B α expression then returned to near basal levels by 240 min. Overall IL-1 β stimulation was more pronounced relative to TNF α .

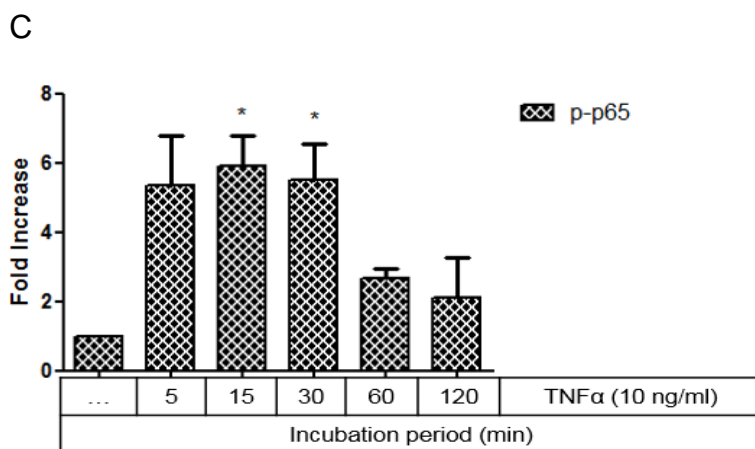
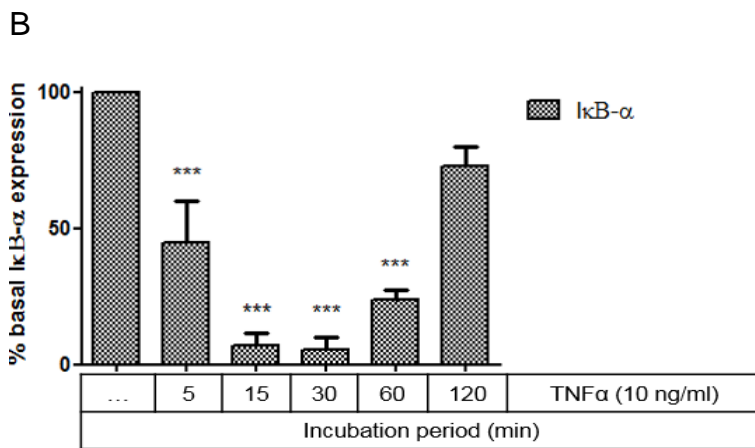
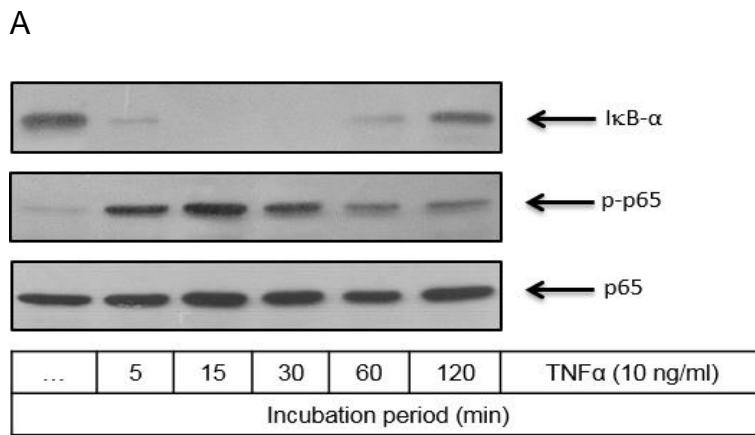


Figure 3.5: Time course for TNF α -mediated I κ B α degradation and phosphorylation of p65 in U2OS cells. Cells were exposed to TNF α (10 ng/ml) for the indicated time points. Whole cell extracts were assessed for A) I κ B α (37 kDa), p65 (65 kDa) phosphorylation and total p65 (65 kDa) which was used as a loading control, as outlined in Section 2.5. Blots were semi-quantified by scanning densitometry and results expressed as fold increase relative to control for B) % basal I κ B α expression and C) p-p65. Each value represents the mean \pm SEM of three independent experiments. Data was analysed using a one-way ANOVA test, * $p < 0.05$, *** $p < 0.001$ vs control.

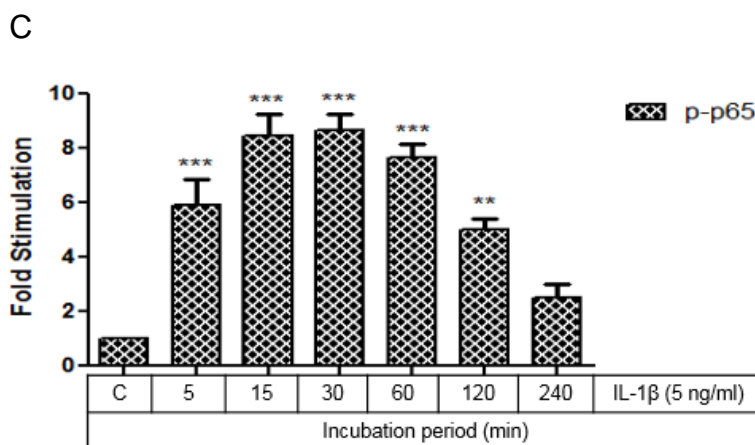
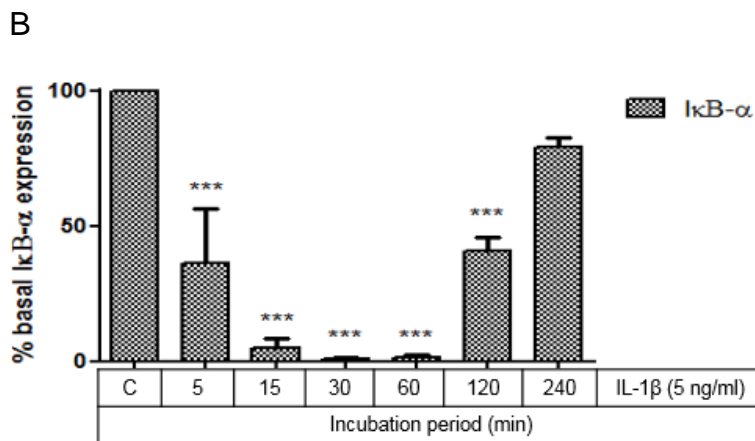
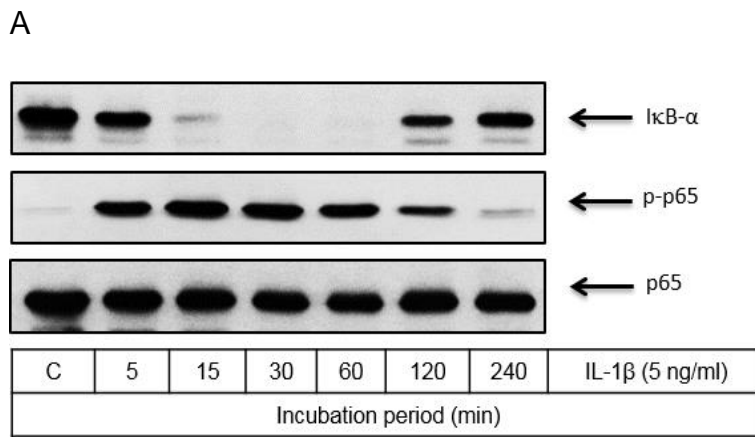
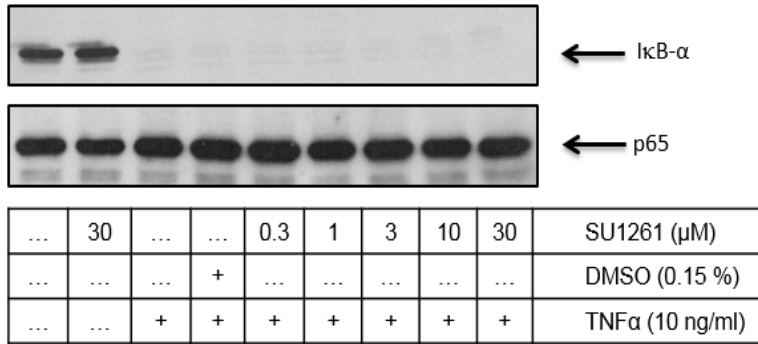


Figure 3.6: Time course for IL-1 β -mediated IkB α degradation and p65 phosphorylation in U2OS cells. Cells exposed to IL-1 β (5 ng/ml) for the indicated time points. Whole cell extracts were assessed for A) IkB α (37 kDa), p65 (65 kDa) phosphorylation and total p65 (65 kDa) which was used as a loading control, as outlined in Section 2.5. Blots were semi-quantified by scanning densitometry and results expressed as fold increase relative to control for B) % basal IkB α expression and C) p-p65. Each value represents the mean \pm SEM of three independent experiments. Data was analysed using a one-way ANOVA test, ** p <0.01, *** p <0.001 vs control.

3.2.3.1 The effect of SU compounds on TNF α -induced I κ B α degradation in U2OS cells

The effect of both SU compounds were then tested on the two markers of the canonical NF- κ B pathway signalling, cellular I κ B α degradation and phosphorylation of p65. As shown in Figure 3.7, TNF α (10 ng/ml) induced significant I κ B α degradation by 98% (% basal I κ B α expression = 2.10 ± 1.34 , $p < 0.001$) compared with non-stimulated cells. However, pre-treatment with increasing concentrations of SU1261 (0.3-30 μ M) did not prevent the loss in cellular I κ B α in cells exposed to TNF α . In contrast, as shown in Figure 3.8, I κ B α loss in response to TNF α was substantially reversed with increasing concentrations (3-30 μ M) of SU1266. These results suggest that only SU1266 had an effect on IKK β within the canonical NF- κ B pathway in U2OS cells.

A



B

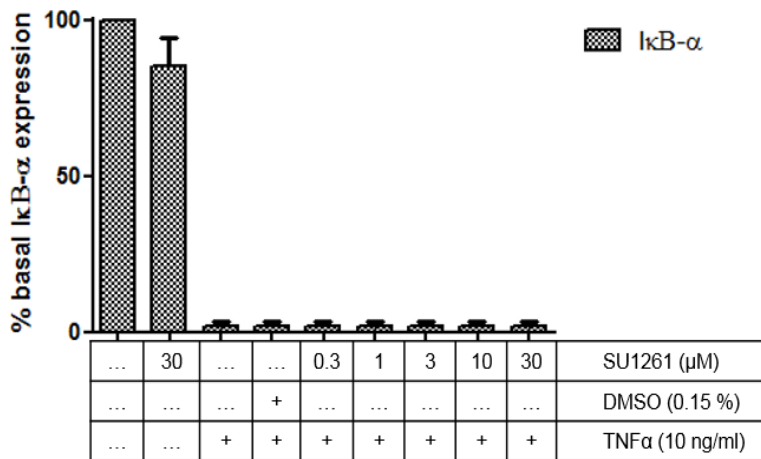
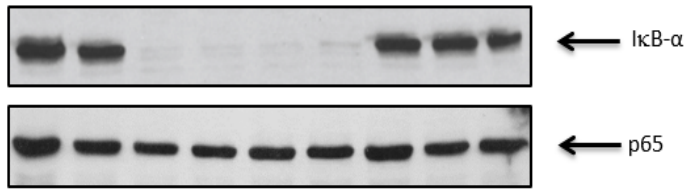


Figure 3.7: The effect of SU1261 upon TNF α -mediated I κ B α degradation in U2OS cells. Cells were pre-treated with SU1261 for 1 h prior to stimulation with TNF α (10 ng/ml) for 30 min. Whole cell extracts were assessed for A) I κ B α (37 kDa) and total p65 (65kDa) which was used as a loading control, as outlined in Section 2.5. Blots were semi-quantified by scanning densitometry and results expressed as fold increase relative to control for B) % basal I κ B α expression. Each value represents the mean \pm SEM of three independent experiments. Data was analysed using a one-way ANOVA test.

A



...	30	0.3	1	3	10	30	SU1266 (μM)
...	+	DMSO (0.15 %)
...	...	+	+	+	+	+	+	+	TNFα (10 ng/ml)

B

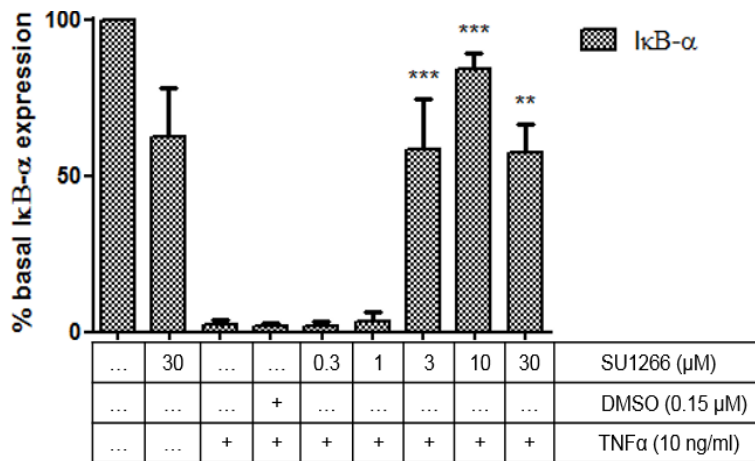
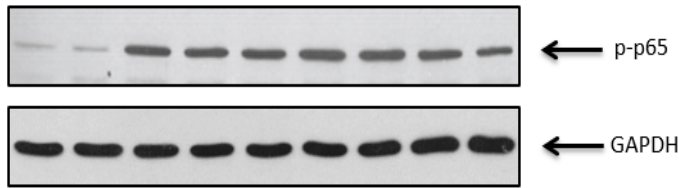


Figure 3.8: The effect of SU1266 upon TNFα-mediated IκBα degradation in U2OS cells. Cells were pre-treated with SU1266 for 1 h prior to stimulation with TNFα (10ng/ml) for 30 min. Whole cell extracts were assessed for A) IκBα (37kDa) and total p65 (65kDa) which was used as a loading control, as outlined in Section 2.5. Blots were semi-quantified by scanning densitometry and results expressed as fold increase relative to control for B) % basal IκBα expression. Each value represents the mean ± SEM of three independent experiments. Data was analysed using a one-way ANOVA test, **p<0.01, ***p<0.001 vs TNFα and DMSO as an agonist stimulated control.

3.2.3.2 The effect of SU compounds on TNF α induced phosphorylation of p65 in U2OS cells

Figure 3.9 shows that pre-treatment of U2OS with increasing concentrations of SU1261 did not change the phosphorylation of p65 induced by TNF α stimulation. However, this response was decreased at the highest concentration of SU1261 but this inhibition was not statistically significant relative to the TNF α response. In Figure 3.10, TNF α (10 ng/ml) stimulated the phosphorylation of p65 significantly by more than six-fold compared with unstimulated cells (Fold stim = 6.48 ± 1.27 , $p < 0.05$). However, the response of p65 phosphorylation was reversed in the presence of SU1266 at the low micromolar 3-30 μM ($p < 0.01$). Furthermore, both SU1261 and SU1266 showed a small inhibitory effect upon p65 phosphorylation in the absence of TNF α .

A



...	30	0.3	1	3	10	30	SU1261 (μM)
...	+	DMSO (0.15 %)
...	...	+	+	+	+	+	+	+	TNF α (10 ng/ml)

B

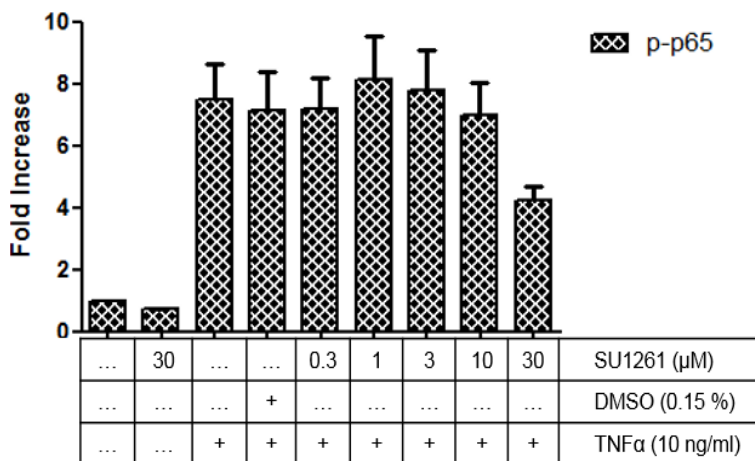


Figure 3.9: The effect of SU1261 upon TNF α -mediated p-p65 phosphorylation in U2OS cells. Cells were pre-treated with SU1261 for 1 h prior to stimulation with TNF α (10 ng/ml) for 30 min. Whole cell extracts were assessed for A) p-p65 (65 kDa) and GAPDH (37 kDa) which was used as a loading control, as outlined in Section 2.5. Blots were semi-quantified by scanning densitometry and results expressed as fold increase relative to control for B) p-p65 expression. Each value represents the mean \pm SEM of three independent experiments. Data was analysed using a one-way ANOVA test.

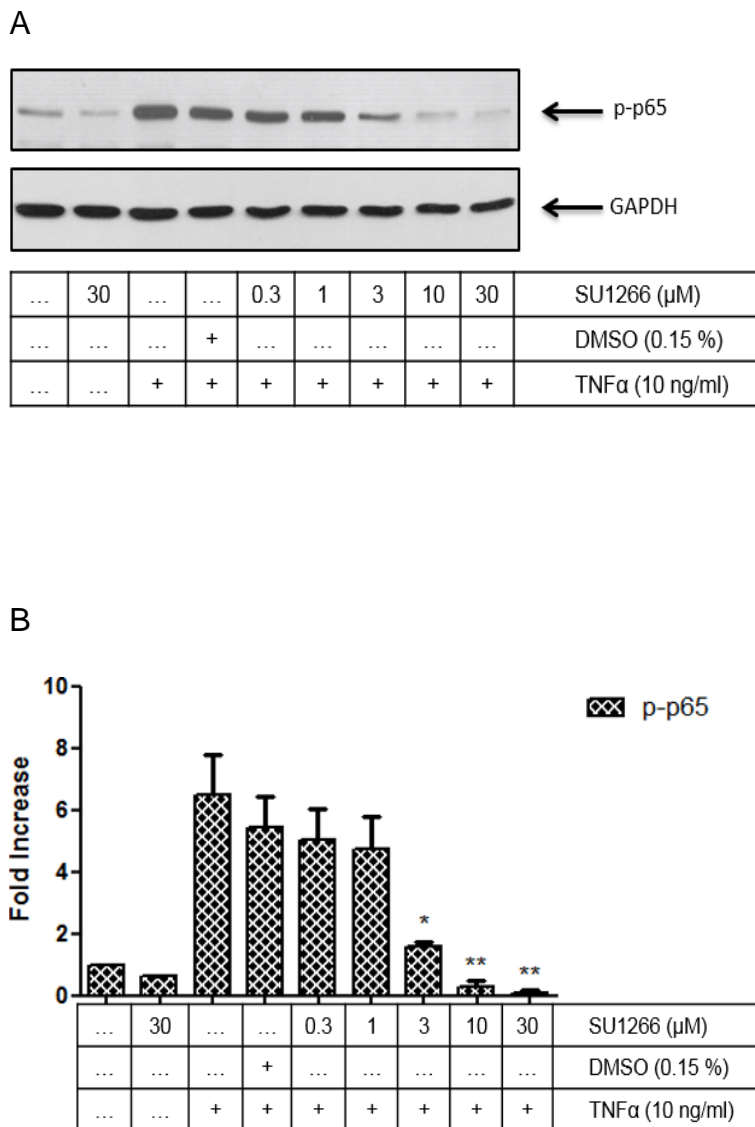


Figure 3.10: The effect of SU1266 upon TNF α -mediated p65 phosphorylation in U2OS cells. Cells were pre-treated with SU1266 for 1 h prior to stimulation with TNF α (10ng/ml) for 30 min. Whole cell extracts were assessed for A) p-p65 (65 kDa) and GAPDH (37 kDa) which was used as a loading control, as outlined in Section 2.5. Blots were semi-quantified by scanning densitometry and results expressed as fold increase relative to control for B) p-p65 expression. Each value represents the mean \pm SEM of three independent experiments. Data was analysed using a one-way ANOVA test, * $p < 0.05$, ** $p < 0.01$ vs TNF α and DMSO as an agonist stimulated control.

3.2.4 Developing more potent IKK α inhibitors and their effect on non-canonical signalling in breast cancer cells

The first part of the chapter demonstrated the effect of SU compounds (SU1261 and SU1266) to inhibit LT $\alpha_1\beta_2$ -stimulated activation of the non-canonical NF κ B pathway in U2OS cells. More potent IKK α -inhibitors SU1349 and SU1433 were developed in-house with improved activity and selectivity as demonstrated by *in vitro* kinase assay (Table 3.1). However, breast cancer (MCF-7 cells) rather than U2OS cells were used to evaluate the potential for this class of compounds to be effective in multiple forms of cancer.

3.2.4.1 The effect of SU compounds on LT $\alpha_1\beta_2$ -mediated p100 phosphorylation and p52 formation in MCF-7 cells

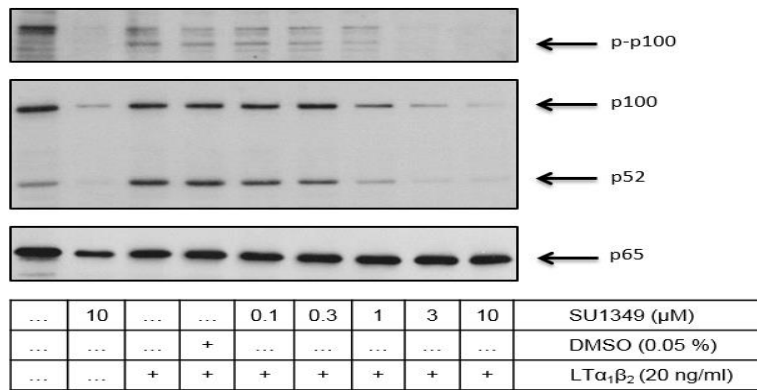
Figure 3.11 demonstrates the effect of SU1349 on LT $\alpha_1\beta_2$ -induced p100 phosphorylation and p52 formation in MCF-7 cells. As with U2OS cells LT $\alpha_1\beta_2$ significantly induced phosphorylation of p100 and p52 formation in MCF7 cells at 8 h (p-p100: Fold stim = 2.74 ± 0.1 , $p > 0.001$, p52: Fold stim = 1.93 ± 0.12 , $p > 0.001$). Alone, SU1349 (10 μ M) caused a substantial inhibitory effect upon basal p100 phosphorylation and p52 formation, the inhibition of both was more than 90% compared with untreated control cells (p-p100: SU1349 10 μ M: Fold stim = 0.08 ± 0.01 , p52: SU1349 10 μ M: Fold stim = 0.07 ± 0.01 , $p > 0.001$). Significantly, pre-treatment with this inhibitor also significantly reduced LT $\alpha_1\beta_2$ -stimulated p100 phosphorylation in a concentration-dependent manner over the low micromolar range (SU1349, 3 μ M: Fold increase = 0.11 ± 0.01 , 10 μ M: Fold increase = 0.1 ± 0.01 , $p > 0.001$). In addition, p52 formation was found to be significantly inhibited after stimulation with LT $\alpha_1\beta_2$ over the low micromolar range (SU1349 10 μ M: Fold = 0.09 ± 0.04 , $p > 0.001$). Interestingly, a statistically significant decrease in p100 protein level

was recorded at the same concentration range of SU1349 (SU1349 3 μ M: Fold increase = 0.24 ± 0.07 , $p > 0.01$, 10 μ M: Fold increase = 0.07 ± 0.01 , $p > 0.001$). Surprisingly, SU1349 (1-10 μ M) was found to have statistically significant inhibitory effect upon basal expression of all three parameters in addition to its effect upon LT $\alpha_1\beta_2$ stimulation.

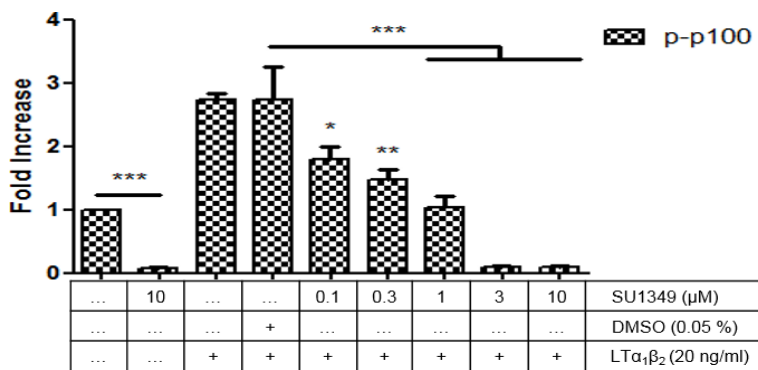
The effect of SU1433 upon LT $\alpha_1\beta_2$ induced phosphorylation of p100 and p52 formation is illustrated in Figure 3.12. LT $\alpha_1\beta_2$ alone significantly stimulated the phosphorylation of p100 and p52 formation compared with unstimulated control cells (p-p100: Fold stim = 2.26 ± 0.16 , $p > 0.001$, p52: Fold stim = 2.28 ± 0.27 , $p > 0.01$). Pre-treatment of MCF-7 cells with 10 μ M of SU1433 alone significantly reduced the phosphorylation of p100 and formation of p52 compared with control (p-p100: SU1433 10 μ M: Fold stim = 0.12 ± 0.05 , p52: SU1433 10 μ M: Fold stim = 0.05 ± 0.01 , $p > 0.05$). Furthermore, pre-treatment with increasing concentrations of SU1433 prior to addition of LT $\alpha_1\beta_2$ significantly inhibited the phosphorylation of p100 compared to the stimulated group (SU1433 10 μ M: Fold increase = 0.11 ± 0.04 , $p > 0.001$). Furthermore, formation of p52 was found to be inhibited at both 3 and 10 μ M compared with the stimulated group (SU1433 3 μ M: Fold increase = 1.13 ± 0.15 , $p > 0.01$, 10 μ M: Fold increase = 0.24 ± 0.1 , $p > 0.001$). However, p100 expression was decreased modestly with 10 μ M of SU1433 alone, whereas it was not altered significantly when the cells were treated with SU1433 (0.1-10 μ M) followed by LT $\alpha_1\beta_2$ -stimulation.

These findings suggested that SU1349 and SU1433 could inhibit the agonist stimulated non-canonical NF κ B pathway in MCF7 cells in a concentration-dependent manner. Moreover, at maximal concentrations, these agents abolished LT $\alpha_1\beta_2$ -stimulated and basal constitutive p100 phosphorylation and p52 formation by more than 95% compared to the control basal level or when compared to the LT $\alpha_1\beta_2$ /DMSO control.

A



B



C

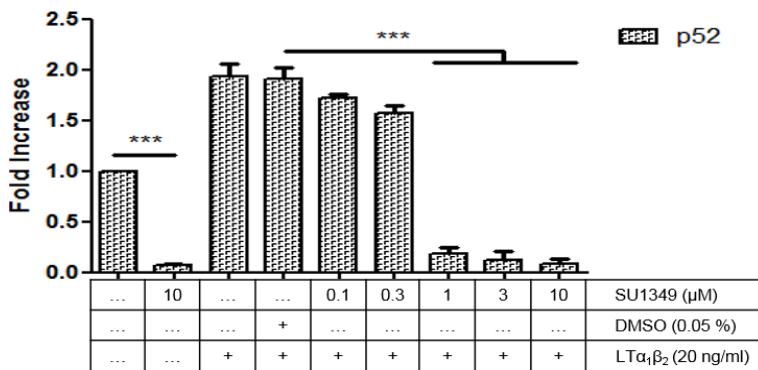


Figure 3.11: The effect of SU1349 upon LT $\alpha_1\beta_2$ -mediated p100 phosphorylation and p52 formation in MCF-7 cells. Cells were pre-treated with SU1349 for 1 h prior to stimulation with LT $\alpha_1\beta_2$ (20 ng/ml) for 8 h. Whole cell extracts were assessed for A) phosphorylation of p100 (100 kDa), p52 formation (52 kDa), and total p65 (65 kDa) which was used as a loading control, as outlined in Section 2.5. Blots were semi-quantified by scanning densitometry and results expressed as fold increase relative to control for B) p-p100. C) p52 formation. Each value represents the mean \pm SEM of three independent experiments. Data was analysed using a one-way ANOVA test, * $p < 0.05$, ** $p < 0.01$, *** $p < 0.001$ vs LT $\alpha_1\beta_2$ and DMSO as an agonist stimulated control.

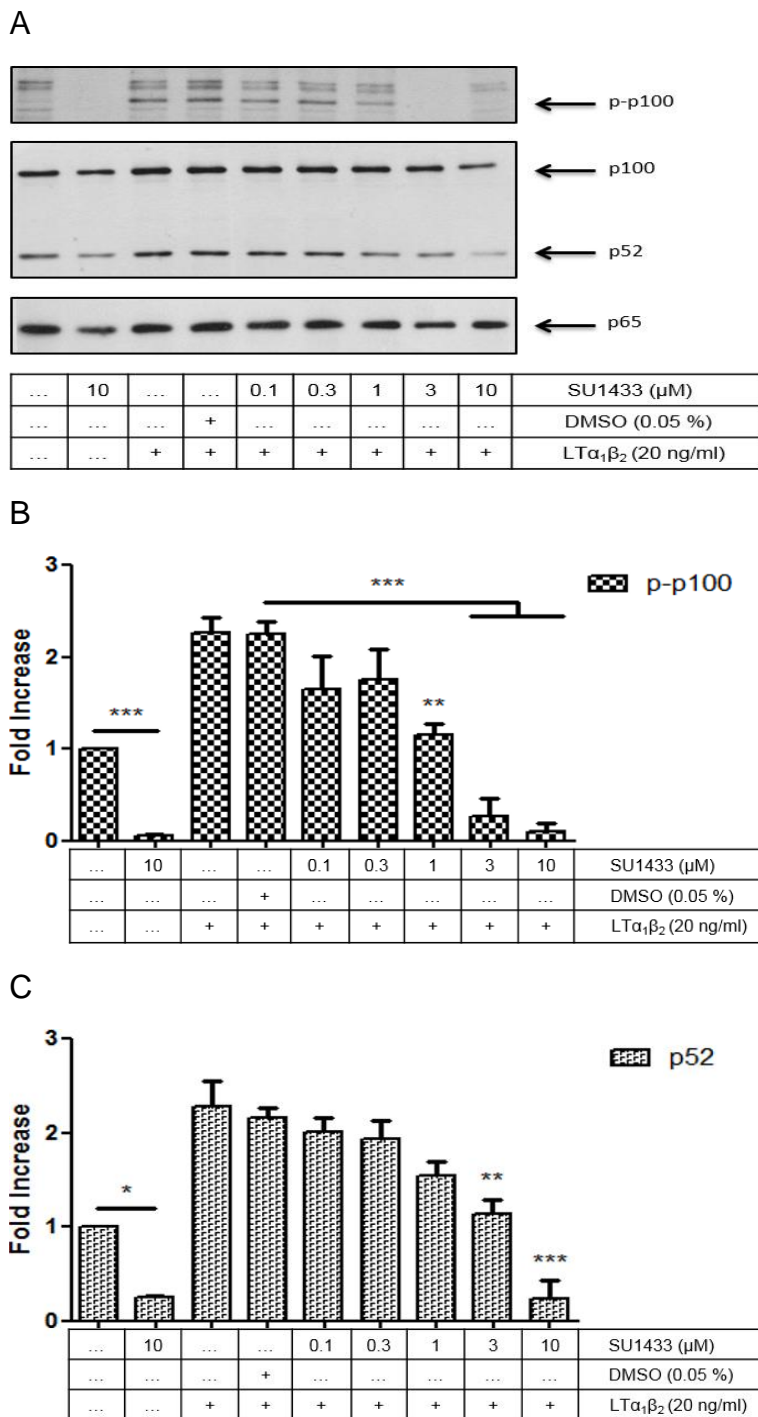


Figure 3.12: The effect of SU1433 upon LT $\alpha_1\beta_2$ -mediated p100 phosphorylation and p52 formation in MCF-7 cells. Cells were pre-treated with SU1433 for 1 h prior to stimulation with LT $\alpha_1\beta_2$ (20 ng/ml) for 8 h. Whole cell extracts were assessed for A) phosphorylation of p100 (100 kDa), p52 formation (52 kDa), and total p65 (65 kDa) which was used as a loading control, as outlined in Section 2.5. Blots were semi-quantified by scanning densitometry and results expressed as fold increase relative to control for B) p-p100. C) p52 formation. Each value represents the mean \pm SEM of three independent experiments. Data was analysed using a one-way ANOVA test, ** $p < 0.01$, *** $p < 0.001$ vs LT $\alpha_1\beta_2$ and DMSO as an agonist stimulated control.

3.2.4.2 IC₅₀ values of SU compounds for p100 phosphorylation and formation of p52 in LT $\alpha_1\beta_2$ stimulated MCF-7 cells

As with SU1261 and SU1266, IC₅₀ values of SU1349 and SU1433 were calculated from the Western blotting results. Interestingly, the IC₅₀ of SU1349 for the phosphorylation of p100 was 1.0 $\mu\text{M} \pm 0.33\mu\text{M}$ (Figure 3.13, panel A), while the IC₅₀ for p52 formation was only 0.51 $\pm 0.09 \mu\text{M}$ (Figure 3.13, panel B). However, the IC₅₀ value of the SU1433 was recorded as 1.32 $\mu\text{M} \pm 0.44 \mu\text{M}$ for the phosphorylation of p100 (Figure 3.13, panel C), whereas it was 3.10 $\mu\text{M} \pm 0.55\mu\text{M}$ for p52 formation (Figure 3.13, panel D).

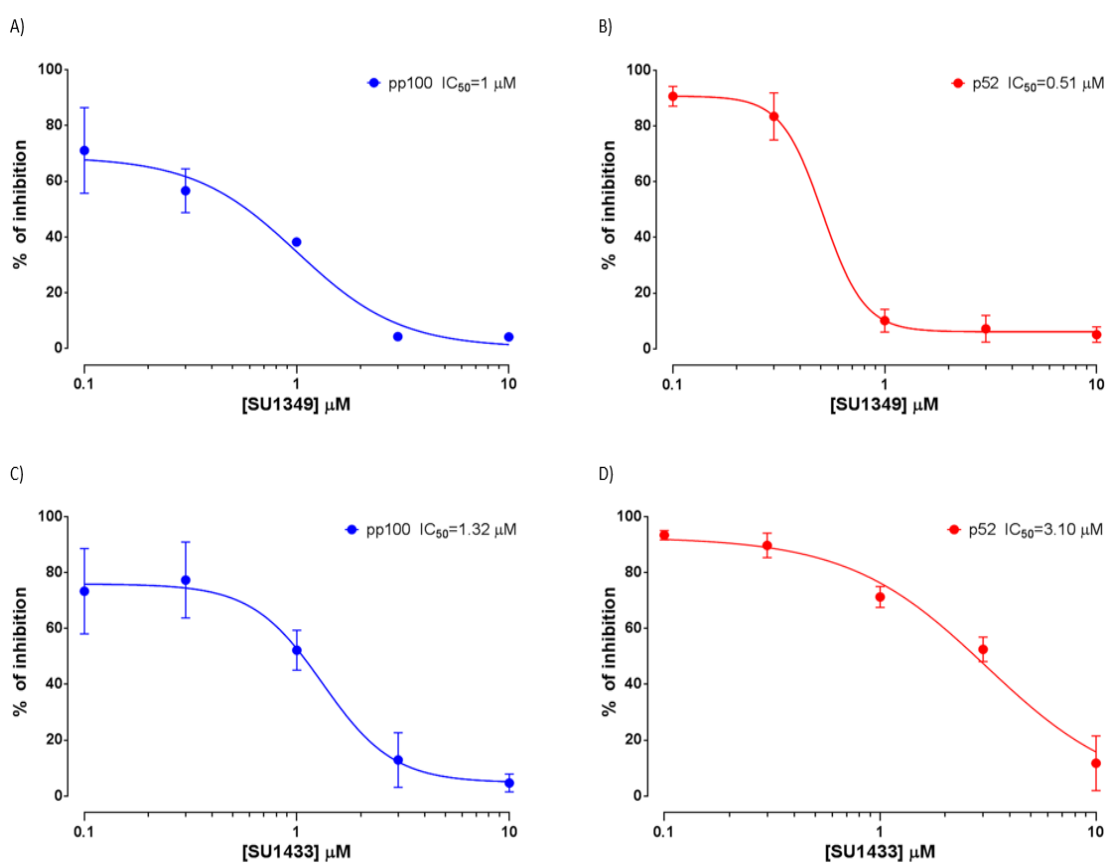


Figure 3.13: The IC₅₀ values of SU1349 and SU1433 for inhibition p100 phosphorylation and p52 formation induced by LT $\alpha_1\beta_2$ in MCF-7 cells. Using GraphPad Prism software, version 7.0, the data obtained by Western blot analysis of SU1349 and SU1433 were fitted in a sigmoidal concentration-response curve for A) SU1349 for p-p100, B) SU1349 for p52 formation, C) SU433 for p-p100, and D) SU1433 for p52 formation.

3.2.5 Thermal shift assay

Whilst studies in this chapter have thus far strongly indicated inhibition of IKK α activity in cells which correlates with effects in biochemical assays, a direct interaction between the drug and IKK α has yet to be established. Recently, Martinez and co-workers have developed a method to monitor drug binding to its target protein in the cellular format by using the cellular thermal shift assay CETSA (Martinez Molina et al., 2013), based on the thermal stabilisation resulting from a direct interaction between the drug and its target protein. The cellular thermal shift assay has been used extensively but not in relation to inhibitors of the non-canonical NF- κ B pathway.

There are two main parts in the CETSA experiments; first, melting curve experiments for the target protein in control and treated cells in order to determine the extent of stabilisation in the presence of compounds. Secondly, concentration-response experiments at a constant temperature (isothermal dose-response fingerprints or ITDRF_{CETSA}) (Jafari et al., 2014), which are similar to the melting curve experiments, but the compound is at different concentrations at a constant temperature during the heating step. Moreover, the melting curve experiments must be followed by concentration-response experiments in the same cells.

3.2.5.2 The cellular thermal shift assay for evaluating drug target interactions in U2OS cells

Before running the thermal shift assay with IKK α , as a new target protein, initial experiments were conducted to assess ERK and p38 α MAPK comparing to the data reported by Jafari and colleagues in HL-60 cells (Jafari et al., 2014). Firstly melting curves (40 to 70 °C) were established for these proteins alone, without any drugs, then the aggregation temperatures compared with and without drugs.

3.2.5.1 The melting curves for ERK-MAPK and p38 α -MAPK within U2OS cells using the cellular thermal shift assay (CETSA)

Figure 3.14 (A and B) shows results from the melting curves for p38 α and ERK in U2OS cells in the absence of any drug. Both ERK and p38 α were identified at the lower test temperatures and then destabilised readily with increasing temperatures in intact cells. Both target proteins were destabilised at the higher temperatures in lysed cells. The destabilisation values of ERK and p38 α in U2OS cells for both lysed and intact cells were as follows: ERK = 55.97 ± 0.6 °C in lysed cells and 49.80 ± 0.8 °C in intact cells, p38 α = 57.74 ± 0.9 °C in lysed cells and 53.45 ± 0.7 °C in intact cells.

From these data, it was concluded that both ERK and p38 α could be destabilised as the temperature increased, and it was apparent that intact cells were more sensitive than lysed samples, which were more resistant to high temperature.

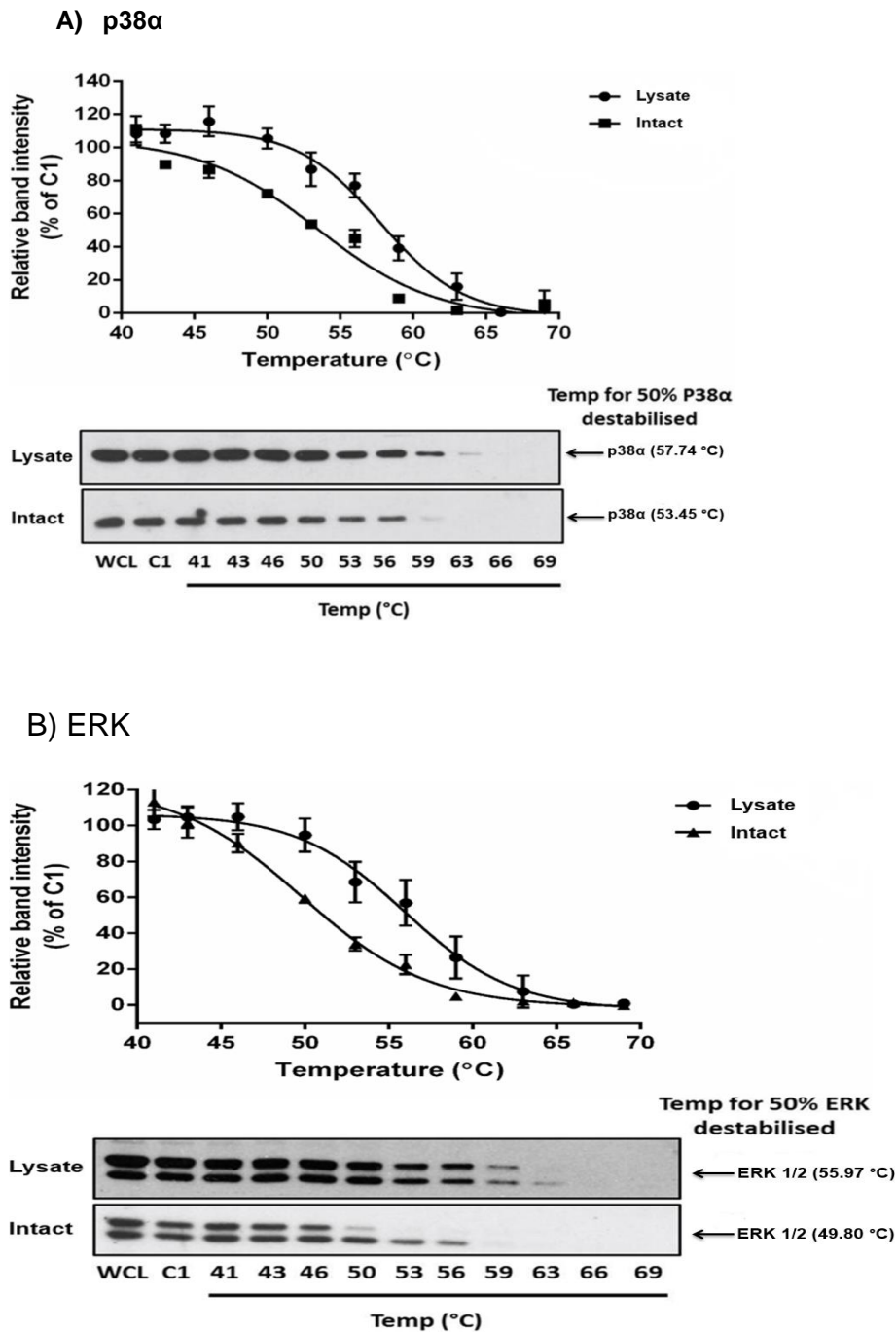


Figure 3.14: CETSA melting curves for p38 α (A) and ERK (B) in U2OS cells. Cells were heated at gradient temperature from 41 °C to 69 °C for 3 min then freeze-thawed 2 times. p38 α and ERK were detected by Western blotting. Blots were quantified by scanning densitometry for each protein in lysate and intact cells and expressed as a percentage of the control C1 which was not subjected to any change in temperature. All experiments were performed on 3 independent occasions, and data presented as the average \pm S.E.M. From these experiments. The solid lines represent the best fits of the data to the Boltzmann sigmoid within the GraphPad Prism software. Data was analysed using a two-way ANOVA test. All data were obtained as outlined in Section 2.6.

3.2.5.1 The melting curve for IKK α within U2OS cells using the cellular thermal shift assay (CETSA)

Figure 3.15 illustrates the melting curve for IKK α in U2OS cells. Western blots demonstrated that IKK α was stabilised at lower temperatures and then destabilised markedly with increasing temperatures in intact cells. In lysed cells, IKK α was more resistant to destabilisation which was more marked at higher temperatures. The destabilisation value for IKK α in lysed U2OS cells was 59.03 ± 0.8 °C, whereas, it was 42.46 ± 0.7 °C in intact cells.

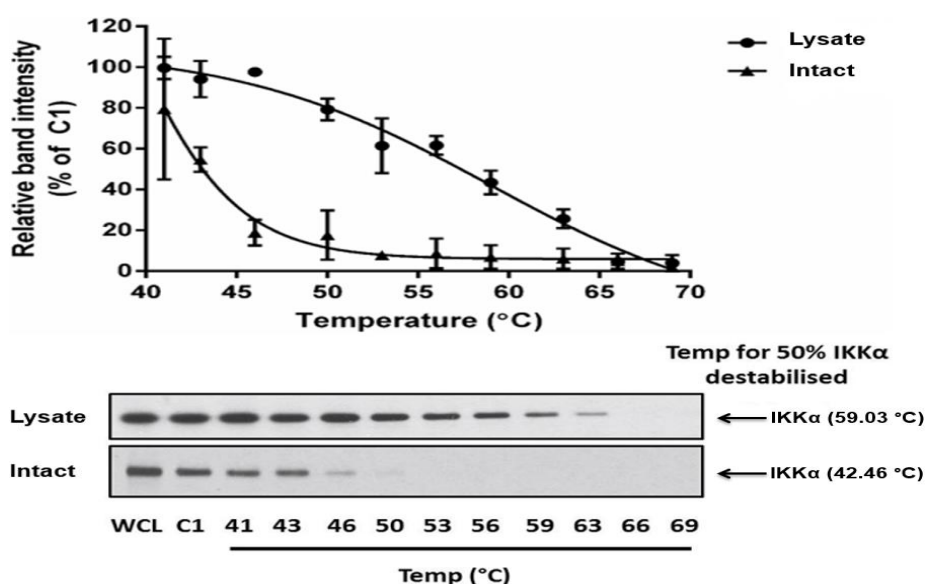


Figure 3.15: The CETSA melting curves for IKK α in U2OS cells. Cells were heated at gradient temperature from 41 °C to 69 °C for 3 min then freeze-thawed 2 times. IKK α was detected by Western blotting. Blots were quantified by scanning densitometry in lysate and intact cells and expressed as a percentage of the control C1 which was not subjected to any change in temperature. All experiments were performed at 3 independent occasions, and data are given as the average \pm S.E.M. From these experiments. The solid lines represent the best fits of the data to the Boltzmann sigmoid within the GraphPad Prism software. Data was analysed using a two-way ANOVA test. All data were obtained as outlined in Section 2.6.

3.2.5.2 Comparisons of the target engagement for ERK, p38 α and IKK α in intact versus lysed cells

Figure 3.16 (A and B), shows the comparison of the target engagement for ERK, p38 α and IKK α in intact versus lysed U2OS cells. It is clear that IKK α was far more labile in intact cells in comparison to lysed cells and there was difference in lability between IKK α and ERK and p38 α in intact cells (IKK α > ERK > p38 α).

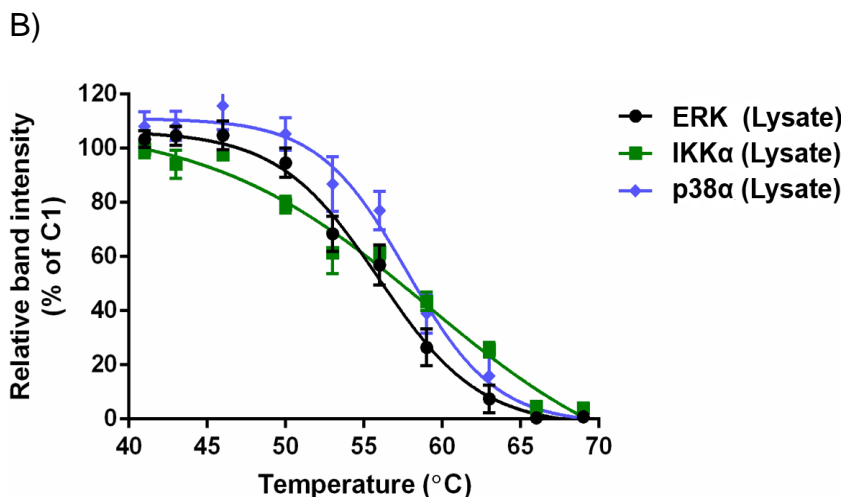
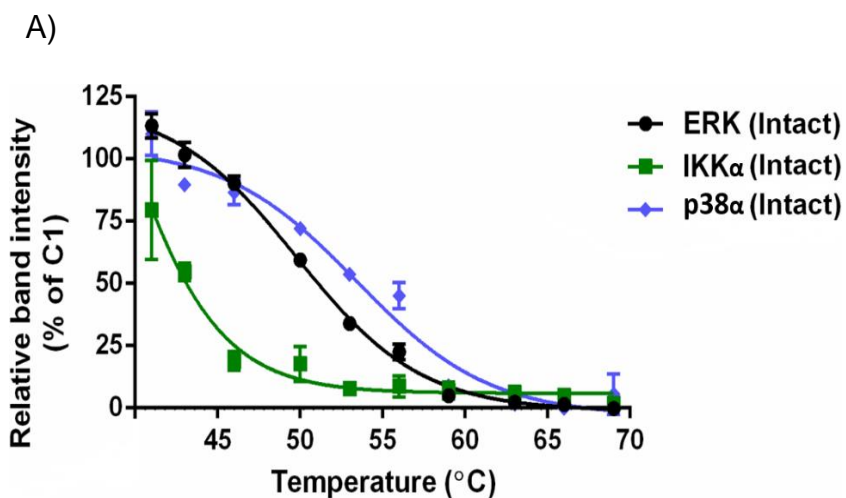
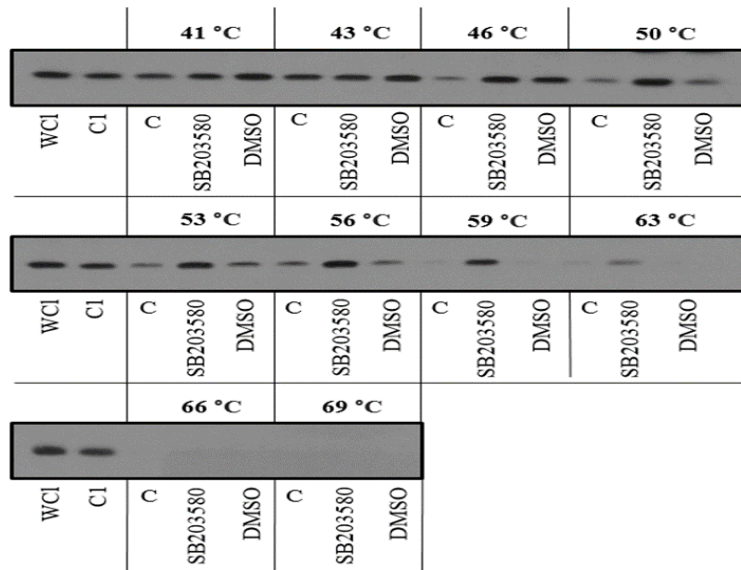


Figure 3.16 (A and B) shows the comparison for target engagement for p38 α , ERK and IKK α in intact versus lysed U2OS cells. Data was analysed using a two-way ANOVA test.

3.2.5.3 Effect of SB203580 on the melting curve for p38 MAP kinase in U2OS cells

Figure 3.17 (A and B) illustrates results from the melting curve for protein kinase p38 α MAPK in intact U2OS cells following pre-treatment with SB203580, as a recognised inhibitor of p38 α kinase activity (Cuenda et al., 1995). Western blots again showed that p38 α was stabilised at lower temperatures and degraded quickly as the temperature increased. However whilst DMSO was without effect, SB203580 pre-treatment significantly increased the stabilisation of p38 α with a shift in the aggregation temperature to 63 ± 0.3 °C.

A)



B)

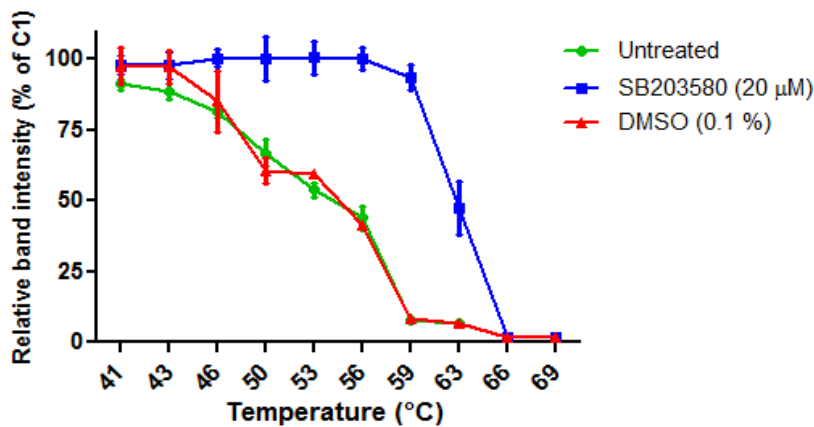
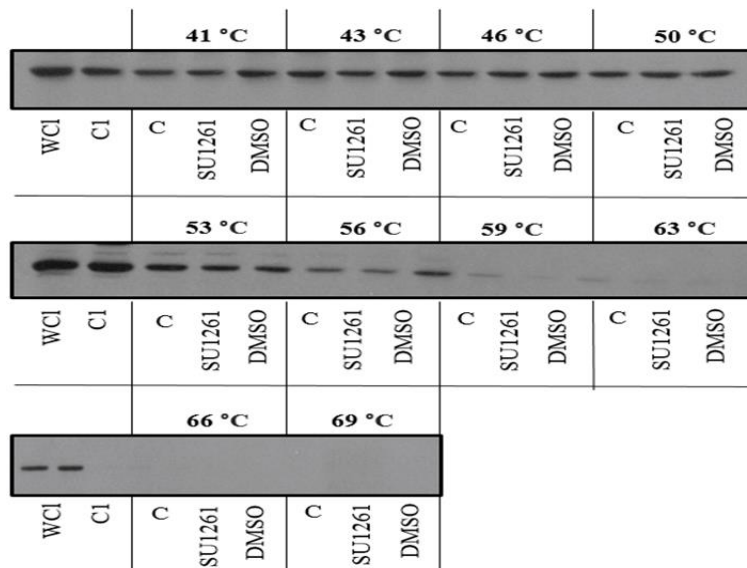


Figure 3.17: SB203580 modulates the thermostability of p38 in U2OS cells. (A) Cells were treated with DMSO (0.1%) or 20 μ M of SB203580 for 1 h. The treated and control cells were heated at gradient temperature from 41 °C to 69 °C for 3 min then freeze-thawed 2 times. Levels of p38 α were detected by Western blotting. (B) Blots were quantified by scanning densitometry in the intact cells and expressed as a percentage of the control C1 which was not subjected to any change in temperature. Data were obtained in the untreated cells (green circle) and in the presence of DMSO (red triangle) as a negative control and the established p38 α inhibitor SB203580 (blue square) as positive control. All experiments were performed at 3 independent occasions, and data are given as the average \pm s.e.m. From these experiments, the solid lines represent the best fits of the data to the Boltzmann sigmoid within the GraphPad Prism software. Data was analysed using a two-way ANOVA test. All data were obtained as outlined in Section 2.6.

3.2.5.4 Effect of SU1261 on the melting curve for IKK α kinase in U2OS cells

Figure 3.18 (A and B) shows results for the melting curve associated with IKK α in intact U2OS cells following pre-treatment with SU1261. Again IKK α was found to be strongly temperature sensitive, however, addition of SU1261 to cells did not cause the thermal stabilisation of IKK α . When the relative difference in the intensities of the bands for IKK α were quantified, it did not show any difference in the apparent melting curves using this approach. This data suggest that the stability of IKK α was not affected by SU1261 and disappointingly direct target engagement with IKK α could not be demonstrated.

A)



B)

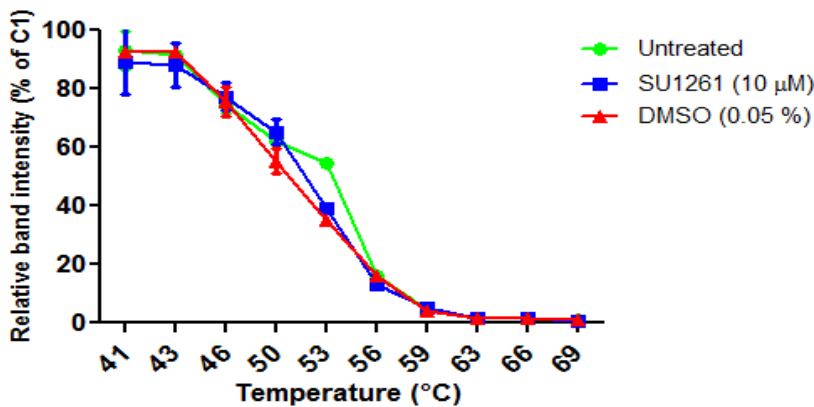


Figure 3.18: SU1261 does not alter the thermostability of IKK α in U2OS cells. (A) Cells were treated with DMSO (0.05%) or 10 μ M of SU1261 for 1 h. The treated and control cells were heated at gradient temperature from 41 °C to 69 °C for 3 min then freeze-thawed 2 times. IKK α levels were detected by Western blotting. (B) Blots were quantified by scanning densitometry in the intact cells and expressed as a percentage of the control C1 which was not subjected to any change in temperature. Data were obtained in the untreated cells (green circle) and in the presence of DMSO (red triangle) as a negative control and the established IKK α inhibitor SU1261 (blue square) as positive control. All experiments were performed at 3 independent occasions, and data are given as the average \pm s.e.m. From these experiments. The solid lines represent the best fits of the data to the Boltzmann sigmoid within the GraphPad Prism software. Data was analysed using a two-way ANOVA test. All data were obtained as outlined in Section 2.6.

3.3 Discussion

As explained earlier in Chapter 1, the non-canonical NF- κ B signalling pathway is now recognised to be involved in the pathogenesis of many chronic human diseases, including cancer, arthritis and cardiovascular disease (Karin, 2006, Xiao and Ghosh, 2005). Therefore, inhibition of this pathway has become an attractive strategy for the treatment of various diseases. This has only been moderately successful as the development of truly selective kinase inhibitors is challenging (Cohen, 1999).

To date, the most successful approach employed to prevent the over-activation of NF- κ B signalling pathway involves proteasomal inhibition. It is based on the inhibition of I κ B α loss and prevention of nuclear translocation of p65 NF- κ B. One such agent, Bortezomib, has been utilised for the treatment of multiple myeloma and leukaemia (Zheng et al., 2012, Picot et al., 2011, Raab et al., 2009).

Since the initial identification of I κ B kinases (IKKs) by Chen and co-workers in 1996, overwhelming evidence has accumulated to demonstrate a central role in the regulation of NF- κ B signalling pathways (Karin, 2006, Xiao and Ghosh, 2005). Therefore, targeting these kinases has become the logical therapeutic approach. Significantly, a number of IKK β inhibitors have been developed such as CHS828 (Hjarnaa et al., 1999), SPC-839 (Palanki et al., 2002), BMS-345541 (Burke et al., 2003), ML120B and the β -carboline natural product PS-1145 (Wen et al., 2006, Castro et al., 2003). Both PS-1145 and ML120B were demonstrated to be effective against different cancers including diffuse large B-cell lymphoma, multiple myeloma and chronic myelogenous leukemia (Yemelyanov et al., 2006, Cilloni et al., 2006, Lam et al., 2005). Moreover, apigenin (4', 5, 7-trihydroxyflavone) has been shown to inhibit proliferation and invasiveness in human prostate cancer (Shukla et al., 2015).

However, none of the previous IKK β inhibitors have been used clinically due to a number of associated serious complications such as immunosuppression, chronic

inflammatory disorders, fatal hepatotoxicity and infectious disease (Chariot, 2009, Li et al., 1999b). Therefore, an alternative if belated strategy has been to develop selective pharmacological inhibitors of IKK α . Interestingly, recent publications have reported that IKK α has an important role in a number of cancers (Ben-Neriah and Karin, 2011, Ammirante et al., 2010, Cogswell et al., 2000). In spite of IKK α having been implicated in these events, selective IKK α inhibitors have not been forthcoming.

In this project, three different selective IKK α inhibitors were used, SU1261, SU1349 and SU1433, as they became available during the drug development programme. In the absence of a crystal structure for IKK α , compounds were developed using standard Structure–Activity Relationship (SAR) approaches using *in vitro* kinases assays. For these and a series of other compounds, K_i values for IKK α were in the mid-nanomolar range with selectivity ratios (IKK α vs IKK β) in the region of 50 to 200 fold. The exception was SU1266 which had a relatively low K_i value for IKK α (2 nM) but had the lowest selectivity ratio. These small molecule inhibitors (SU compounds) specifically bind to the ATP binding domain of the IKK α amino-terminal kinase domain to inhibit activity.

Initial experiments demonstrated good inhibition of cellular non-canonical NF- κ B signalling confirming results from kinases assays *in vitro*. However there were a number of interesting aspects to the pharmacological effects in U2OS cells. First of all for both SU1261 and SU1266, inhibition of agonist-stimulated p100 phosphorylation was some 30-100 fold less effective than observed in the biochemical assays. This is a common aspect of drug development for example, SP-600125, a small-molecule ATP-competitive inhibitor of JNK, showed poor potency and selectivity in cells compared to biochemical assay (Bain et al., 2003, Bennett et al., 2001). In the same vein, AS601245 and other potent JNK inhibitors, only inhibit c-Jun phosphorylation at relatively high concentrations (Gaillard et al., 2005). These

contradictions are likely due to a combination of ATP concentration, differences between cellular environment and biochemical sensitivities to inhibitors, and limited cellular penetration (Zhang et al., 2012). In addition, there may have been compound degradation in cells routinely incubated with cells for up to 5 hours but there was not sufficient opportunity to study this possibility in detail.

Also it was evident that there were differences in the IC_{50} values when measuring inhibition of different components of the non-canonical NF- κ B pathway. The observed decrease in IC_{50} values in cell-based assay compared to dissociation constants *in vitro* is most likely a reflection of high ATP concentrations present in the cells (Bennett et al., 2001). However, IC_{50} values were consistently lower for inhibition of agonist-stimulated p100 phosphorylation than for downstream p52 formation, an output reflecting p100 degradation subsequent to the phosphorylation process itself (Xiao et al., 2004, Amir et al., 2004, Senftleben et al., 2001, Xiao et al., 2001). In fact, full inhibition of p52 formation was not always achieved at the maximum concentration of compound (Figures 3.2 and 3.3). This may suggest that both processes are not completely linked. Moreover, high concentrations of SU compounds may have off-target effects which may indirectly mediate the effects on p52 formation. Indeed p100 expression itself increased over a similar time course and therefore there may be a different mechanism by which p52 is formed following prolonged stimulation times. Studies do show p100 expression to be regulated by the non-canonical NF- κ B pathway (Xiao et al., 2004, Xiao et al., 2001, Senftleben et al., 2001). This aspect of $LT\alpha_1\beta_2$ induced non-canonical NF- κ B signalling will be further examined in Chapter 4. Nevertheless, despite these caveats, the study demonstrates that SU1261 is a selective inhibitor of the non-canonical NF- κ B signalling with little effect on agonist-stimulated IKK β -mediated phosphorylation of p65. This exemplifies for the first time a successful strategy to develop a selective IKK α inhibitors for use in defining the role

of this kinase in the cellular biology of U2OS cells and elsewhere. In contrast, it was found that SU1266 despite a selectivity ratio of 40 did not retain such a selectivity in cellular systems. This suggests a minimum selectivity ratio in biochemical assays required to manifest selectivity in cells. Also one additional aspect may be the relatively low K_i of SU1261 for IKK α , the absolute potencies may also be a factor requiring K_i values for IKK β above 1-3 μ M for selectivity.

Furthermore, these findings compared very favourably with other work using compounds synthesised as selective IKK α inhibitors such as noraristeromycin (Asamitsu et al., 2008) and the glucosamine derivative, 2-(N-Acetyl)-L-phenylalanylamido-2-deoxy-beta-D-glucose (Scotto d'Abusco et al., 2010). Asamitsu and co-workers demonstrated that noraristeromycin (NAM) inhibited the kinase activity of IKK α more than IKK β . However, it was found that I κ B α degradation and p65 phosphorylation were also inhibited by noraristeromycin, suggesting that canonical NF- κ B pathway inhibition predominates. Also, they found this agent had no effect upon p100 phosphorylation or p52 formation. Similarly, Scotto d'Abusco and colleagues found that the glucosamine derivative, 2-(N-Acetyl)-L-phenylalanylamido-2-deoxy-beta-D-glucose (NAPA) inhibited IKK α nuclear translocation in human chondrocytes, but this inhibition took place only at very high concentrations (250-500 μ M). Taken together these studies exemplify the challenges in developing such a class of compounds.

These findings were initially established for U2OS cells and suggest a potential application for these novel inhibitors in bone cancer. However, recent evidence also indicates a role for IKK α in breast cancer (Hao et al., 2010, Cao et al., 2007), pancreatic cancer (Liou et al., 2013, Storz, 2013, Doppler et al., 2013), and prostate cancer (Ammirante et al., 2010, Luo et al., 2007). Indeed, testing the later compounds, SU1349 and SU1433, in MCF 7 cells showed their utility in different breast cancers.

For example, published work from Bennett and co-worker demonstrated high expression of the cellular kinase IKK α as well as high levels of the androgen receptor (AR) in triple negative breast cancer patients (Negative for ER/PR/HER2) compared to AR-negative alone (Bennett et al., 2017). Others studies showed that IKK α -mediated non-canonical p100 NF- κ B2 signalling has a critical role in cancer development in a number of tumour settings (Gamble et al., 2012, Perkins, 2007). IKK α -related readouts identified that p100 phosphorylation and p52 formation were inhibited by SU1349 and SU1433 in MCF7 cells (Figures 3.11 and 3.12) but less potently in MDA-MB-231 cells, which display a much higher basal level of p100 phosphorylation (data not shown).

In an independent study, it was shown by Qing and colleagues that p100 processing induced by BAFF was inhibited by geldanamycin (GA), however, GA had no effect on p100 expression (Qing et al., 2007). Interestingly, in contrast to Qing, our results showed that SU1349 can inhibit the levels of p100 in MCF-7 cells (Figure 3.11), which could be explained by the fact that IKK α can also regulate the expression of p100 (Senftleben et al., 2001). Collectively, these data suggest that inhibitors of IKK α would be of benefit in ER-positive breast cancer patients who develop endocrine resistance.

Finally, experiments were conducted to confirm a direct interaction between IKK α and SU1261 in U2OS cells using the cellular thermostability assay (CETSA). Based on Western blot analysis, distinct melting curves for p38 α , ERK and IKK α were established in the absence of any compound. Inhibition of extracts with SB203580 induced an obvious shift in the melting curve of p38 α due to the direct interaction between them which led to a substantial stabilisation of this protein. On the other hand, IKK α was found to be strongly temperature sensitive in intact cells compared with lysates. However, the stability of IKK α was not affected by SU1261. Indeed, most kinase inhibitors bind to both active and inactive conformation of kinase (Frantz et al.,

1998), whereas other inhibitors selectively target the inactive conformation of kinase (Wan et al., 2004, Pargellis et al., 2002). Therefore, SU1261 may act by shifting the equilibrium between active and inactive conformation of IKK α in a way that prevents kinase activation rather than by inhibiting its activity directly. This view is supported by Jafari et al., (2014) who reported that the absence of this stabilisation may be the consequence of antibody recognition of a non-functional form of the protein, for instance the form lacking activating phosphorylation. Moreover, it is important that any negative result after performing CETSA be followed by appropriate troubleshooting experiments. In this regard, Jafari and co-workers identified a number of the most common issues in CETSA with appropriate solutions. Time did not allow further investigating the direction interaction between the SU compounds and IKK α using the thermostability assay.

CETSA has been used successfully in other instances. It was shown by Qin and colleagues that the compound JapA inhibited breast tumour growth and metastasis through direct targeting of the MDM2 oncogene, surprisingly, the binding of JapA to MDM2 induced a very large shift melting curve in MDM2 (>15 °C) in MCF-7 and MDA-MB-231 cells (Qin et al., 2015). In another study, Bai and co-worker investigated the binding of the novel inhibitor BM-1197 to the antiapoptotic Bcl-2 family proteins Bcl-2 and Bcl-xL in the Mcl-1 knockout mouse embryonic fibroblast (MEF) cells. BM-1197 showed strong thermo-stabilisation of Bcl-xL and, to a lesser extent, thermo-stabilisation of Bcl-2 (Bai et al., 2014). Moreover, Martinez Molina et al., (2013) showed engagement of Olaparib and Iniparib, classical PARP-1 inhibitors, with Poly [ADP-ribose] polymerase 1 (PARP-1), revealing a large thermal shift for PARP-1 in cells treated with Olaparib, while Iniparib failed to induce a real thermal shift. More studies with a series of SU compounds may reveal the potential for this assay system to assist in identifying active compounds.

Chapter Four

A novel rapid activation of IKK α -dependent non-canonical NF- κ B signalling coupled to human CXCL12 expression in bone cancer cells

4.1 Introduction

The activation of both NF- κ B pathways in response to cellular activation leads to increased expression of at least 500 genes, including chemokines (Birbach et al., 2002) which play a key role in normal physiology and disease (Karin, 2006, Xiao and Ghosh, 2005). CXCL12 is secreted by vascular endothelial cells, stromal fibroblasts and osteoblasts, and is widely expressed in a number of organs, including bone marrow (Teicher and Fricker, 2010), and it is essential in the homing of hematopoietic stem cells to bone marrow (Aiuti et al., 1997). The majority of studies have demonstrated a role of the CXCL12-CXCR4 axis in the metastasis and tumour progression for various types of cancer, including bone sarcoma (Dewan et al., 2006, Perissinotto et al., 2005). Huang and co-workers reported that the activation of the MEK-ERK-IKK α/β -NF- κ B pathway played a role in the CXCL12-induced migration of human OS cells, which was inhibited by AMD3100, a CXCR4 inhibitor, and siRNA against CXCR4 (Huang et al., 2009). Moreover, CTCE-9908, a CXCR4 inhibitor, has been shown to reduce the metastatic process in OS K7M2 cells *in vivo* and *in vitro* by disruption of the CXCL12-CXCR4 interaction. However, to date, there are few studies that have investigated the role of CXCL12-CXCR4 axis in tumour growth and progression. Miura and colleagues pointed out that the formation of tumours *in vivo* is positively associated with the levels of CXCR4 expression in human HOS OS cells (Miura et al., 2005).

IKK α solely controls the non-canonical NF- κ B pathway via activation of p100 phosphorylation which in turn releases NF- κ B p52/RelB heterodimers and initiates transcription of a specific subset of genes relevant to cancer (Oeckinghaus and Ghosh, 2009, Hacker and Karin, 2006). This includes CXCL12, CXCL13, CCL19, and CCL21 (Wharry et al., 2009, Bonizzi and Karin, 2004, Dejardin et al., 2002). Furthermore, Madge and May have demonstrated that siRNA knockdown of IKK α

inhibits CXCL12 mRNA in endothelial cells, whereas IKK β deletion enhances CXCL12 production (Madge and May, 2010, Madge et al., 2008). This suggests that IKK α -mediation of the non-canonical NF- κ B pathway is implicated in the regulation of CXCL12 expression. Furthermore, publications have reported that IKK α was found to regulate certain genes implicated in cancer cell transformation and angiogenesis (Birbrair et al., 2015, Luo et al., 2007, Huang et al., 2007).

However, despite the importance of CXCL12, very few studies have investigated the role of IKK α in the regulation of CXCL12 expression. Moreover, no previous study has investigated the ability of the non-canonical NF- κ B pathway to regulate CXCL12 expression in a bone cancer setting, or to explore its inhibition by blocking this pathway. In this chapter, the aim is to identify a key intermediate of the non-canonical NF- κ B pathway, inhibitory kappa B kinase alpha (IKK α) in the regulation of CXCL12 expression. Our results in chapter three indicated that our lead SU compounds, demonstrated selectivity against IKK α . Therefore the novel compounds, as a classical pharmacological inhibition strategy, and siRNA-mediated silencing of IKK α , as a non-pharmacological inhibition strategy, were employed to target IKK α and thus target CXCL12 production at the level of transcription.

4.2 Results

4.2.1 The role of IKK α in the regulation of the non-canonical NF- κ B pathway

4.2.1.1 LT $\alpha_1\beta_2$ slowly induces p52 and RelB nuclear translocation in U2OS cells

As demonstrated in the previous chapter (Figure 3.1), LT $\alpha_1\beta_2$ slowly increased the phosphorylation of p100 and p52 formation which were apparent at 4 h and sustained for up to 24 h. To confirm such a profile, the nuclear accumulation of both p52 and RelB in response to LT $\alpha_1\beta_2$ was assessed in nuclear extracts from U2OS cells. As illustrated in Figure 4.1, p52 nuclear translocation increased slowly and was apparent between 4-24 h, however levels did not reach statistical significance until 24 h after stimulation (Fold increase = 2.72 ± 0.73 , $p < 0.05$). On the other hand, RelB nuclear translocation increased more than three-fold following LT $\alpha_1\beta_2$ -stimulation, this response was apparent from 4 h, maximal by 8 h (Fold increase = 3.43 ± 0.35 , $p < 0.01$) and sustained up to 24 h.

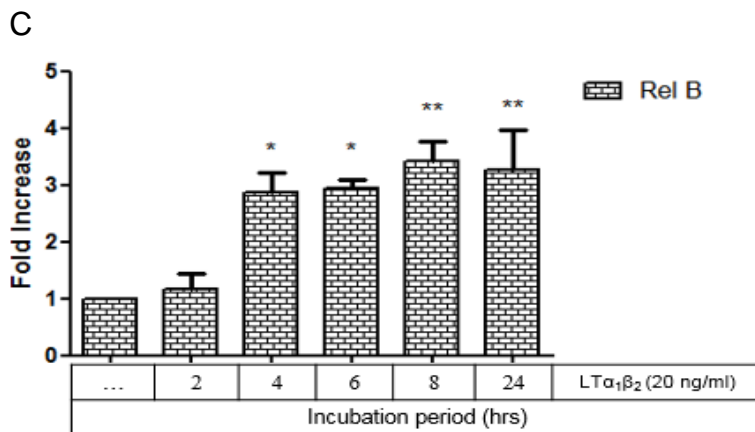
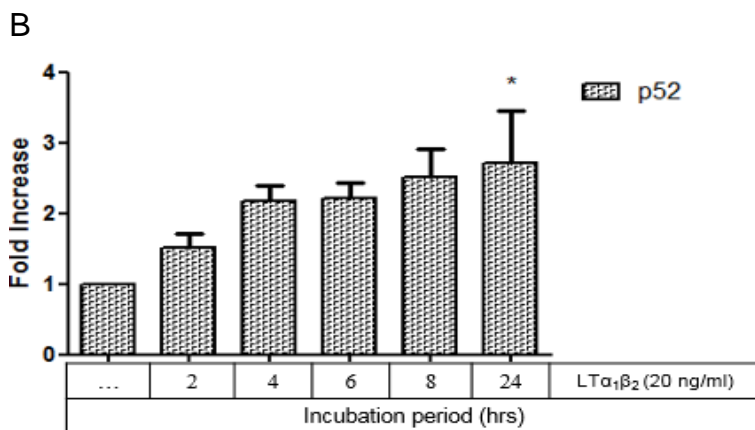
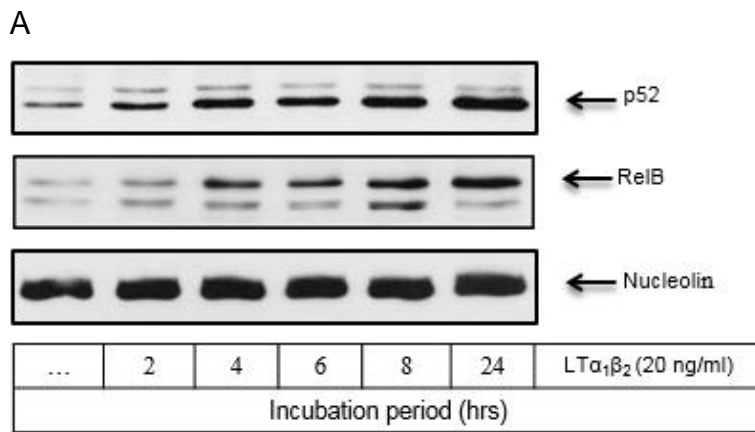


Figure 4.1: LTα₁β₂ induces p52 and RelB nuclear translocation in U2OS cells. Cells were exposed to LTα₁β₂ (20 ng/ml) for the indicated time points, then nuclear extracts were blotted for A) p52 (52 kDa), RelB (68 kDa) and Nucleolin (106 kDa) which was used as a loading control, as outlined in Section 2.5. Blots were semi-quantified by scanning densitometry and results expressed as fold increase relative to control for B) p52 and C) RelB. Each value represents the mean ± SEM of three independent experiments. Data was analysed using a one-way ANOVA test, *p<0.05, **p<0.01 vs control.

4.2.1.2 TNF α and IL-1 β induce rapid non-canonical NF- κ B signalling in U2OS cells

In further experiments TNF α and IL-1 β were utilised to determine if these agents, which have the potential to stimulate CXCL12 production, can also activate the non-canonical NF- κ B pathway. TNF α has been shown to stimulate the delayed formation of p52 formation in endothelial cells in the absence of p100 phosphorylation (Ko Ha Ho personal communication), so this concept was further examined here.

4.2.1.2.1 TNF α induces phosphorylation of p100 at early time in U2OS cells

Figure 4.2 shows a time course for TNF α induced phosphorylation of p100 in U2OS cells. Unexpectedly, phosphorylation of p100 was observed to be very rapid with a significant increase between 5-60 min. A maximum response was obtained by 15 min (Fold stim = 12.53 ± 0.66 , $p < 0.001$) after which the p-p100 levels returned towards basal values. By comparison LT $\alpha_1\beta_2$ gave the expected delayed response (Figure 3.1), which shown here was weaker at the maximum time point, 4 h, than that maximally induced by TNF α .

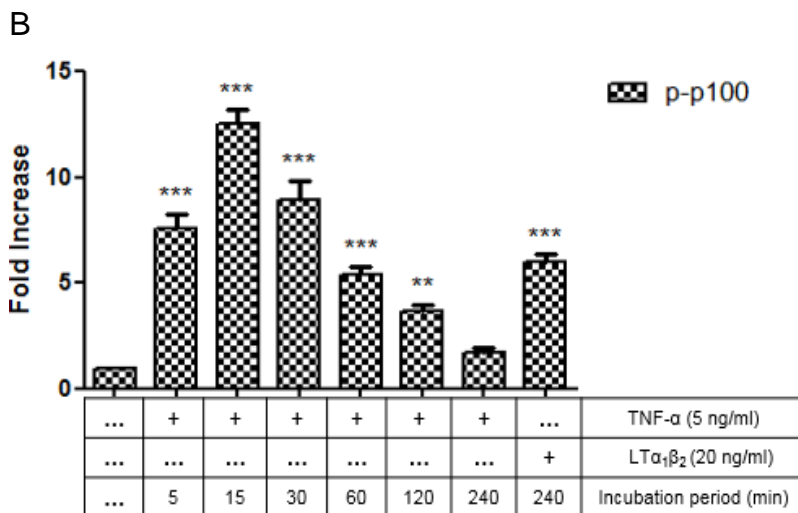
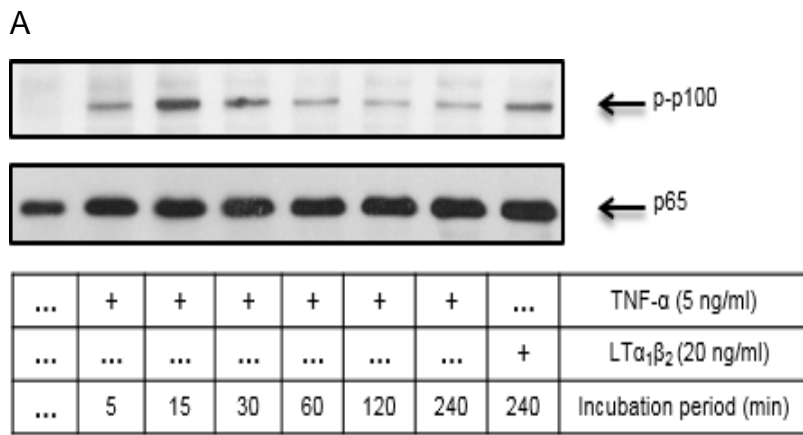


Figure 4.2: Time course of TNF- α -mediated phosphorylation of p100 in U2OS cells. Cells were stimulated with TNF α (5 ng/ml) for the times indicated. LT $\alpha_1\beta_2$ was used as a positive control. Whole cell extracts were assessed for A) p-p100 (100 kDa) and total p65 (65 kDa) which was used as a loading control, as outlined in Section 2.5. Blots were semi-quantified by scanning densitometry and results expressed as fold increase relative to control for B) p-p100. Each value represents the mean \pm SEM of three independent experiments. Data was analysed using a one-way ANOVA test, ** $p < 0.01$, *** $p < 0.001$ vs control.

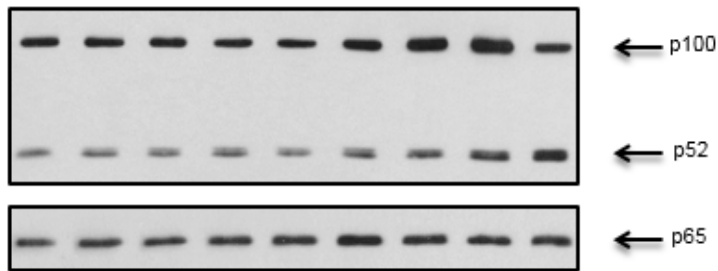
4.2.1.2.2 TNF α induces p100 processing to p52 formation in whole cell extracts of U2OS cells

Figure 4.3 shows a time course of p100 processing following stimulation by TNF α in U2OS cells. Interestingly, p52 formation significantly increased between 4 and 8 h (8 h Fold stim = 2.64 ± 0.2 , $p < 0.05$). The expression of p100 also increased in response to TNF α with similar kinetics to that observed for p52 formation.

4.2.1.2.3 TNF α induces RelB expression in whole cell extracts of U2OS cells

Figure 4.4 shows a time course for RelB expression induced by TNF α . As with p52, the expression of RelB was found to be delayed before an increase was observed at 4h with significance reached by 6 h (Fold increase = 2.09 ± 0.25 , $p < 0.05$) and with a further increase by 8 h (Fold increase = 2.48 ± 0.28 , $p < 0.01$). In contrast, LT $\alpha_1\beta_2$ (20 ng/ml) at the 8 h time point gave a modest increase of RelB expression compared with TNF α .

A



...	+	+	+	+	+	+	+	...	TNF- α (5 ng/ml)
...	+	LT $\alpha_1\beta_2$ (20 ng/ml)
...	15	30	1	2	4	6	8	8	Incubation period

B

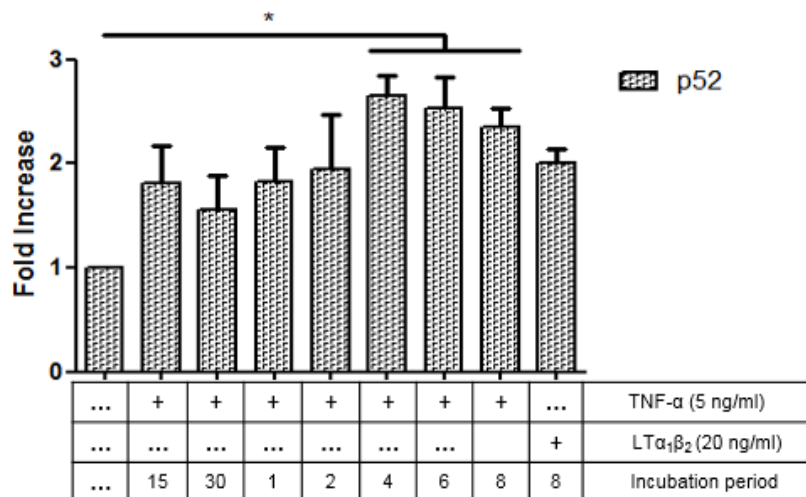


Figure 4.3: Time course of TNF α -mediated p52 formation in U2OS cells. Cells were stimulated with 5 ng/ml of TNF α for a maximum 8 h time period. LT $\alpha_1\beta_2$ (20 ng/ml) was used as a positive control. Whole cell extracts were assessed for A) p52 (52 kDa) formation and total p65 (65 kDa) which was used as a loading control, as outlined in Section 2.5. Blots were semi-quantified by scanning densitometry and results expressed as fold increase relative to control for B) p52 formation. Each value represents the mean \pm SEM of three independent experiments. Data was analysed using a one-way ANOVA test, * $p < 0.05$ vs control.

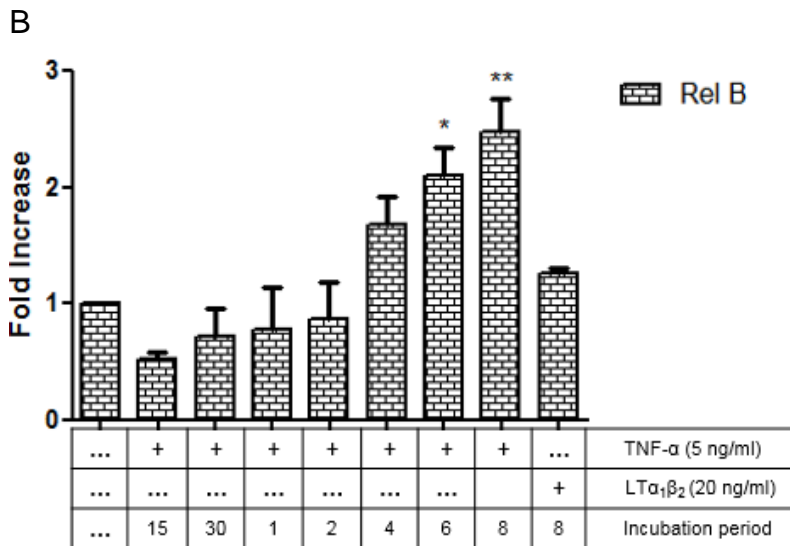
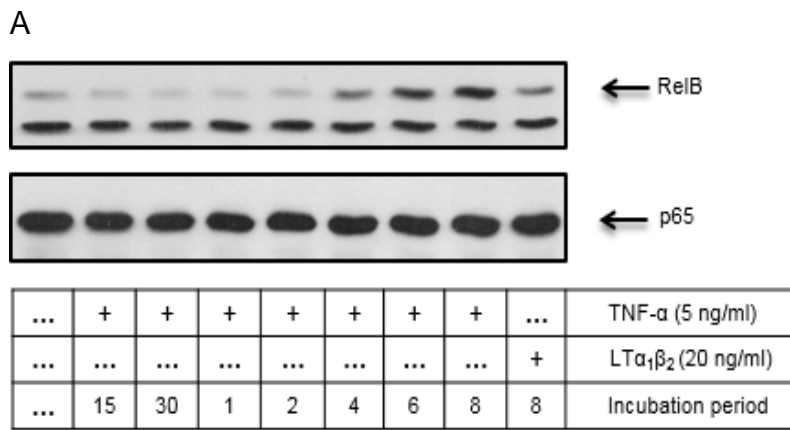


Figure 4.4: Time course of TNF α -mediated RelB formation in U2OS cells. The cells were exposed with TNF α (5 ng/ml) for the times indicated. LT $\alpha_1\beta_2$ (20 ng/ml) was used as a positive control. Whole cell extracts were blotted for A) RelB (68 kDa) and total p65 (65 kDa) which was used as a loading control, as outlined in Section 2.5. Blots were semi-quantified by scanning densitometry and results expressed as fold increase relative to control for B) RelB expression. Each value represents the mean \pm SEM of three independent experiments. Data was analysed using a one-way ANOVA test, * p <0.05, ** p <0.01 vs control.

4.2.1.2.4 TNF α rapidly induces p52 and RelB nuclear translocation in U2OS cells

Whilst the rapid phosphorylation of p100 did not correspond to a noted increase in p52 and RelB, these markers in nuclear extracts were examined as a further indicator of pathway activation. In contrast to results obtained in whole cells, Figure 4.5 shows that TNF α induced a rapid increase in nuclear translocation of p52 starting from as early as 15 min with a significant response reached between 60 and 240 min (Fold increase at 60 min = 11.65 ± 1.52 , $p < 0.001$). Similarly, the formation of RelB increased gradually from 30 min reaching a peak between 60 and 240 min of stimulation (Fold increase at 240 min = 14.94 ± 0.58 , $p < 0.001$).

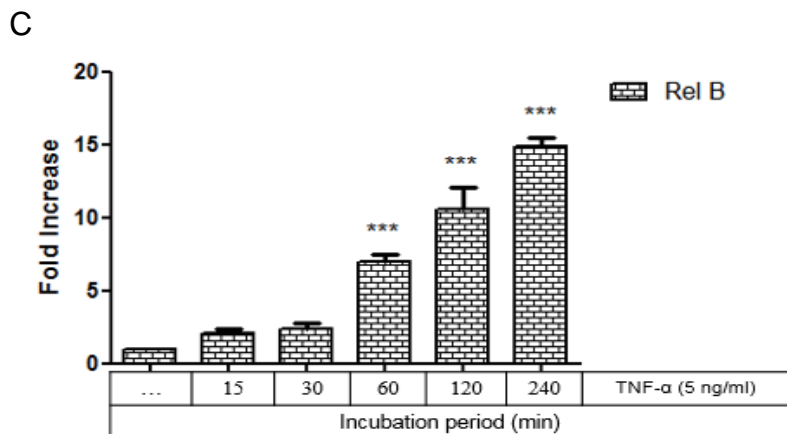
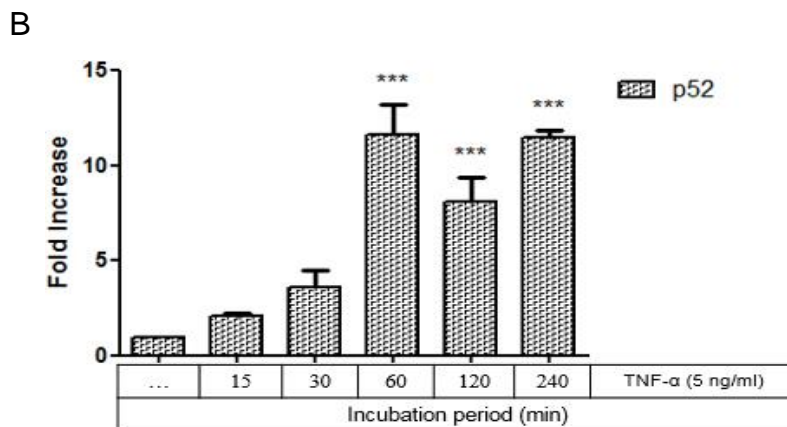
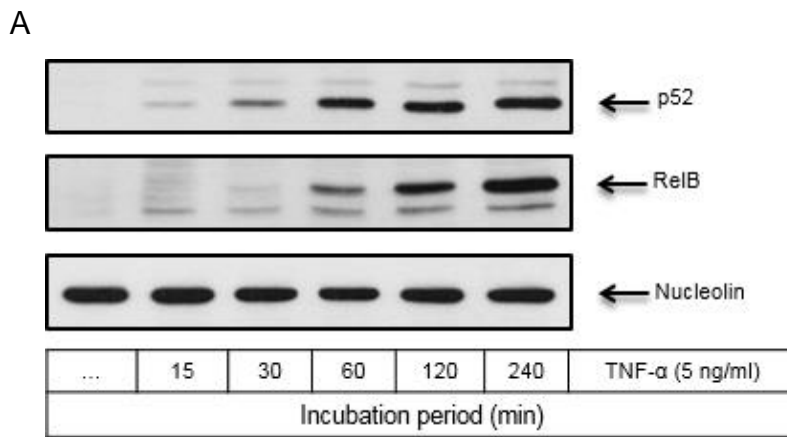


Figure 4.5: TNF α induces p52 and RelB nuclear translocation in U2OS cells. Cells were exposed to TNF α (5 ng/ml) for the times indicated. Nuclear extracts were blotted for A) p52 (52 kDa), RelB (68 kDa) and Nucleolin (106 kDa) which was used as a loading control, as outlined in Section 2.5. Blots were semi-quantified by scanning densitometry and results expressed as fold increase relative to control for B) p52 and C) RelB. Each value represents the mean \pm SEM of three independent experiments. Data was analysed using a one-way ANOVA test, *** p <0.001 vs control.

4.2.1.2.5 IL-1 β induces phosphorylation of p100 at early time in U2OS cells

The experiments outlined above were then repeated with IL-1 β . Figure 4.6 shows that as with TNF α , IL-1 β increased p100 phosphorylation rapidly and strongly with a significant response between 15 and 60 min ($p < 0.001$), the highest response being achieved at 30 min (Fold stim = 35.90 ± 0.93 , $p < 0.001$).

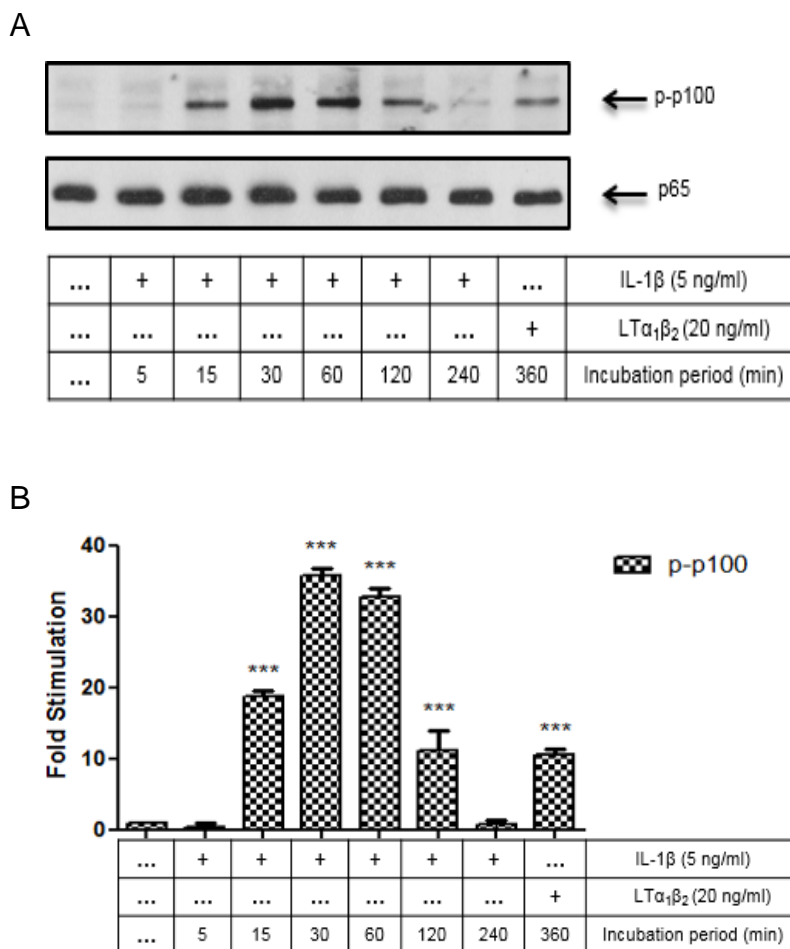


Figure 4.6: Time course of IL-1 β -mediated phosphorylation of p100 in U2OS cells. Cells were exposed to IL-1 β (5 ng/ml) for the times indicated. LT $\alpha_1\beta_2$ (20 ng/ml) was used as a positive control. Whole cell extracts were assessed for A) p100 phosphorylation (100 kDa) and total p65 (65 kDa) which was used as a loading control, as outlined in Section 2.5. Blots were semi-quantified by scanning densitometry and results expressed as fold increase relative to control for B) p100 phosphorylation. Each value represents the mean \pm SEM of three independent experiments. Data was analysed using a one-way ANOVA test, *** $p < 0.001$ vs control.

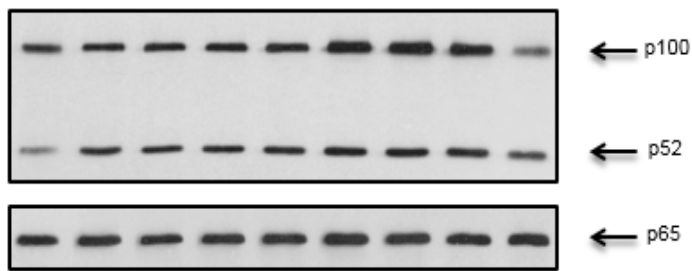
4.2.1.2.6 IL-1 β induces p100 processing to p52 formation in whole cell lysates of U2OS cells

In a similar fashion to TNF α , Figure 4.7 shows a time course of p100 processing in response to IL-1 β . Following stimulation by IL-1 β (5 ng/ml), p52 formation significantly increased between 4 and 8 h, a maximal response was achieved at 6 h (Fold stim = 3.60 ± 0.65 , $p < 0.05$). The expression of p100 also increased in response to IL-1 β .

4.2.1.2.7 IL-1 β induces RelB expression in whole cell lysates of U2OS cells

Figure 4.8 shows that as with TNF α , the lag period before an increase in cellular RelB expression by IL-1 β was similar. IL-1 β significantly induced RelB expression starting from 6 h with a maximum response achieved by 8 h (Fold increase = 2.80 ± 0.26 , $p < 0.01$).

A



...	+	+	+	+	+	+	+	...	IL-1 β (5 ng/ml)
...		+	LT $\alpha_1\beta_2$ (20 ng/ml)
...	15	30	1	2	4	6	8	8	Incubation period

B

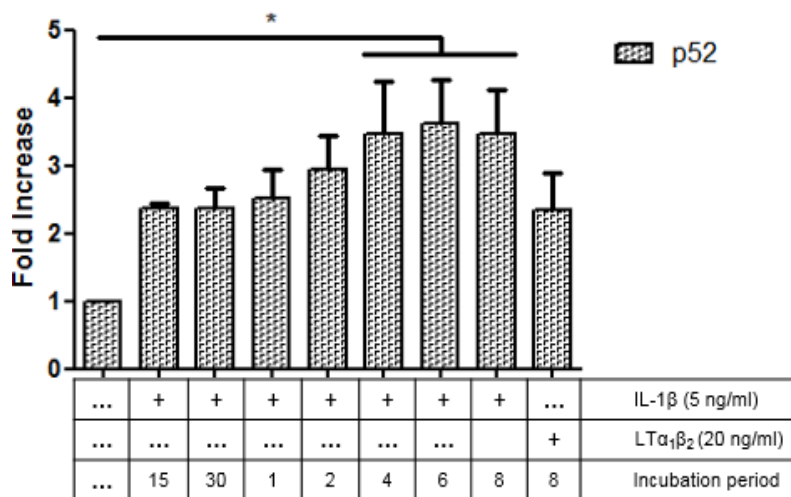


Figure 4.7: Time course of IL-1 β -mediated p52 formation in U2OS cells. Cells were stimulated with 5 ng/ml of IL-1 β for indicated time points. LT $\alpha_1\beta_2$ (20 ng/ml) was used as a positive control. Whole cell extracts were assessed for A) p52 (52 kDa) formation and total p65 (65 kDa) which was used as a loading control, as outlined in Section 2.5. Blots were semi-quantified by scanning densitometry and results expressed as fold increase relative to control for B) p52 formation. Each value represents the mean \pm SEM of three independent experiments. Data was analysed using a one-way ANOVA test, *p<0.05 vs control.

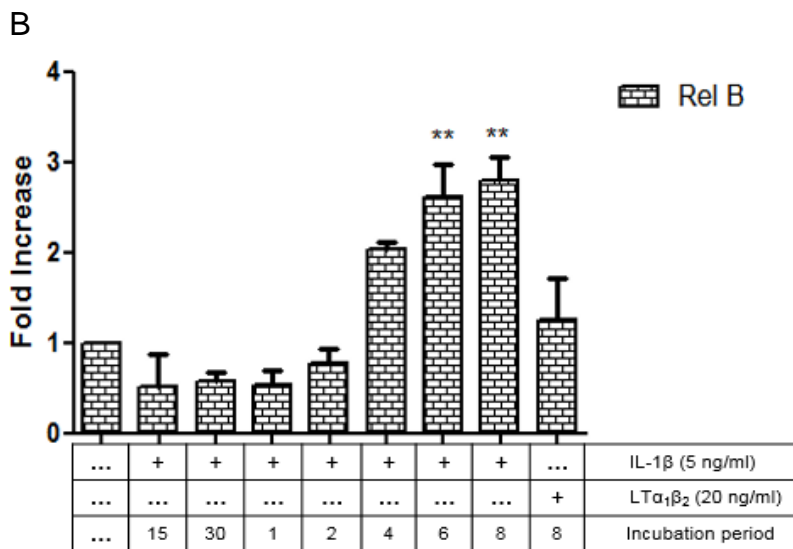
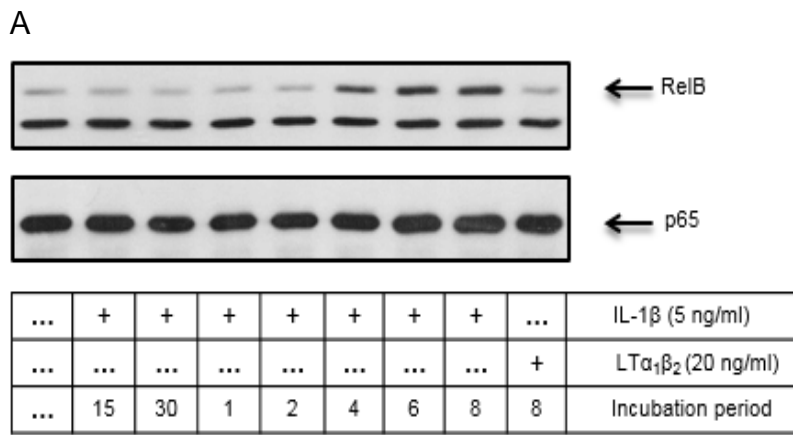


Figure 4.8: IL-1 β induces RelB expression in U2OS cells. Cells were exposed for IL-1 β (5 ng/ml) for the indicated time points. LT $\alpha_1\beta_2$ (20ng/ml) was used as a positive control. Whole cell lysates were blotted for A) RelB (68 kDa) and total p65 (65 kDa) which was used as a loading control, as outlined in Section 2.5. Blots were semi-quantified by scanning densitometry and results expressed as fold increase relative to control for B) RelB formation. Each value represents the mean \pm SEM of three independent experiments. Data was analysed using a one-way ANOVA test, ** $p < 0.01$ vs control.

4.2.1.2.8 IL-1 β rapidly induces p52 and RelB nuclear translocation in U2OS cells

Figure 4.9 shows that as with TNF α , IL-1 β rapidly stimulated an increase in nuclear p52 formation with a significant response between 60 and 240 min compared with non-stimulated cells. The maximum response was obtained at 60 min (Fold increase = 6.26 ± 0.77 , $p < 0.001$). Similar to p52 formation, IL-1 β also significantly increased nuclear RelB expression starting from 60 min up to 240 min, the maximum response was obtained at 240 min (Fold increase = 13.30 ± 2.48 , $p < 0.001$).

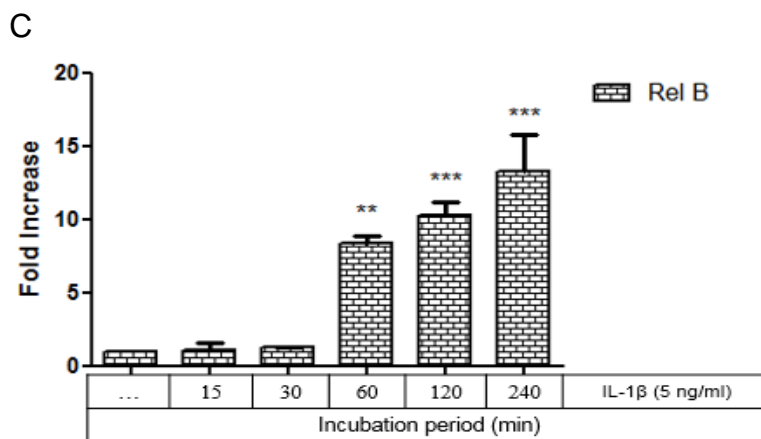
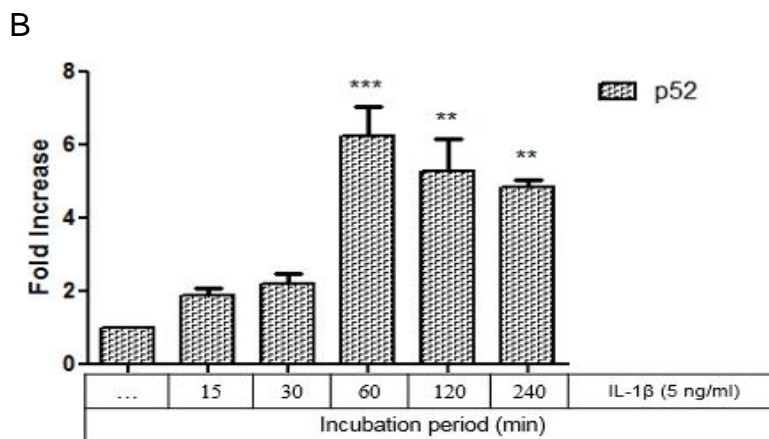
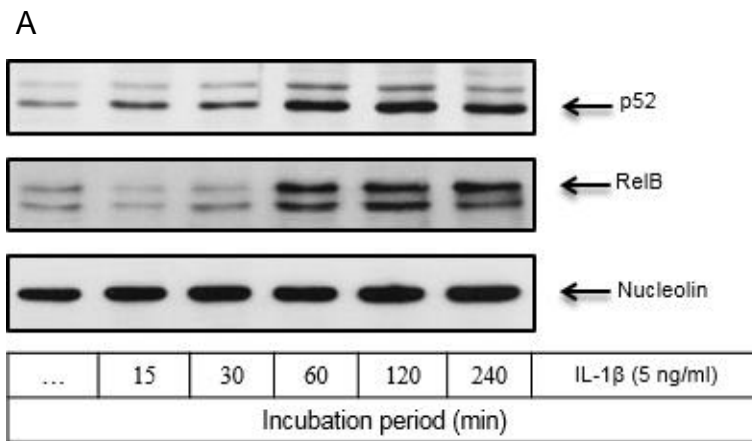


Figure 4.9: IL-1 β induces p52 and RelB nuclear translocation in U2OS cells. Cells were exposed to IL-1 β (5 ng/ml) for the indicated time points. Nuclear extracts were blotted for A) p52 (52 kDa), RelB (68 kDa) and Nucleolin (106 kDa) which was used as a loading control, as outlined in Section 2.5. Blots were semi-quantified by scanning densitometry and results expressed as fold increase relative to control for B) p52 and C) RelB. Each value represents the mean \pm SEM of three independent experiments. Data was analysed using a one-way ANOVA test, ** p <0.01, *** p <0.001 vs control.

4.2.1.3 The activation of p100 phosphorylation in response to TNF α and IL-1 β in U2OS, MCF-7 and CAFs cells

Other cells types were tested to determine if the responses observed in U2OS cells were cell type specific (Figure 4.10). In both MCF-7 cells and CAFs no equivalent stimulation of p100 phosphorylation at early time points was observed.

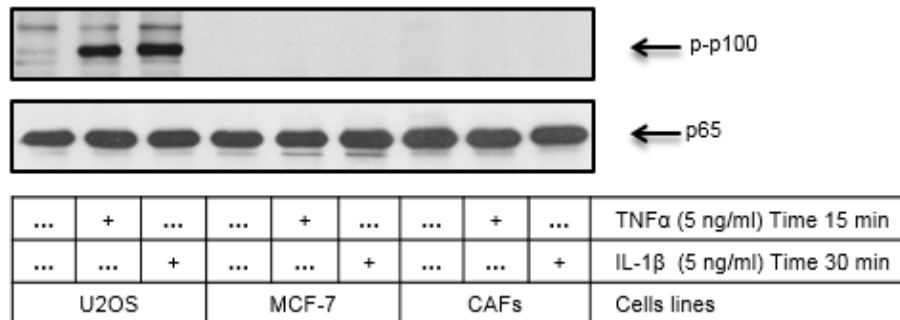


Figure 4.10: Comparison of TNF α and IL-1 β -mediated phosphorylation of p100 in U2OS, MCF-7 and CAFs cells. Cells were stimulated with TNF α (5 ng/ml) for 15 min or IL-1 β (5 ng/ml) for 30 min. Whole cell extracts were assessed for p100 phosphorylation (100 kDa) and total p65 (65 kDa) which was used as a loading control, as outlined in Section 2.5. The results are representative of three independent experiments.

4.2.1.4 Time course comparison of non-canonical NF- κ B activation by different agonists in U2OS cells

Bringing the results obtained in Chapter 3 for LT $\alpha_1\beta_2$ together with results here allows for a direct comparison between the agonists (Figure 4.11 panels A, B and C). On the basis of our collective findings, a novel early activation in the non-canonical NF- κ B pathway was observed in U2OS cells in response to TNF α and IL-1 β in contrast to the usual delayed response to LT $\alpha_1\beta_2$.

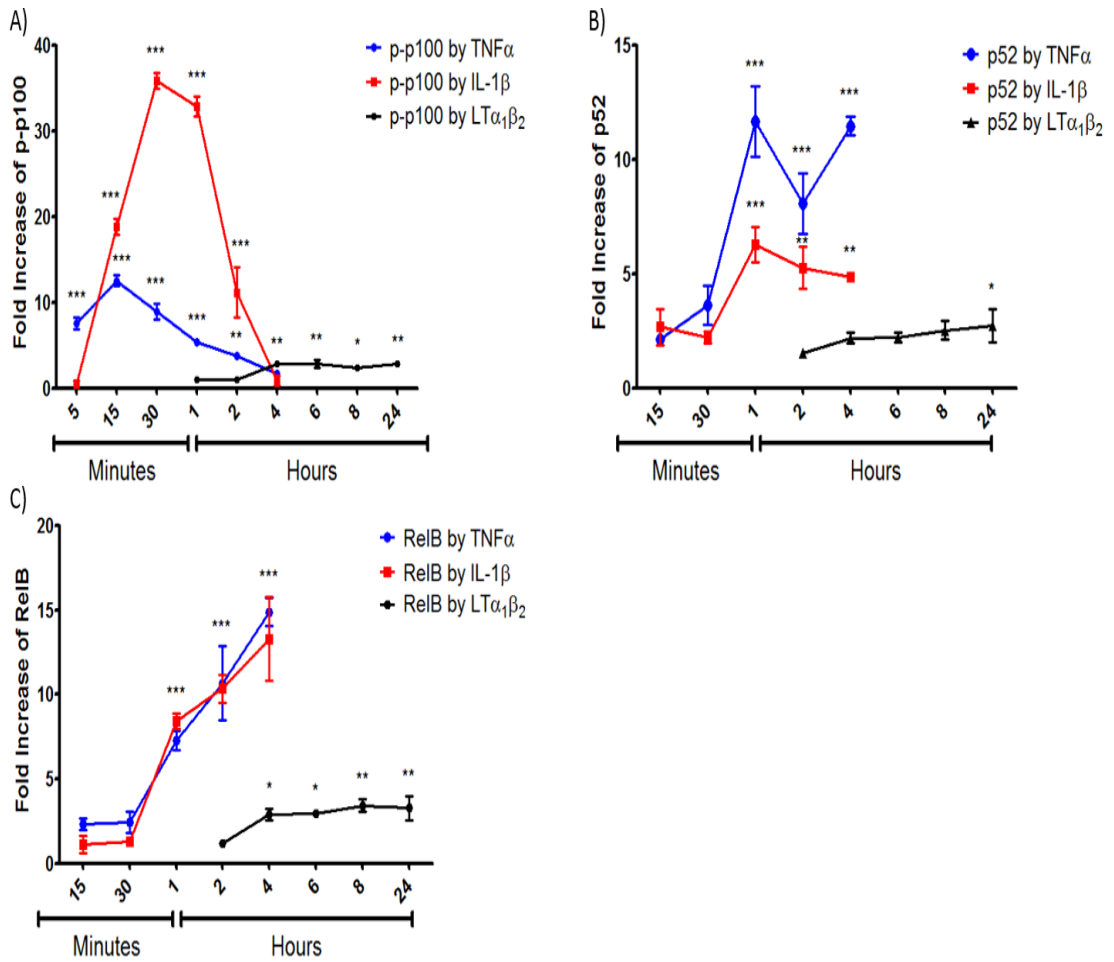


Figure 4.11: Comparison of kinetic profiles for p100 phosphorylation, p52 and RelB for different agonists in U2OS cells. Cells were stimulated with either LT $\alpha_1\beta_2$ (20 ng/ml) for 0-24 h or TNF α (5 ng/ml) and IL-1 β (5 ng/ml) for 0-240 min. Protein levels were analysed by Western blotting and then semi-quantified by scanning densitometry and results expressed as fold increase relative to control for (A) p100 phosphorylation (B) p52 nuclear translocation (C) RelB nuclear translocation, each value represents the mean \pm S.E.M. The results are representative of three independent experiments. Data was analysed using a two-way ANOVA test, * $p < 0.05$, ** $p < 0.01$, *** $p < 0.001$ vs non-stimulated cells.

4.2.2 The effect of siRNA-mediated silencing of cellular IKK α expression on the non-canonical NF- κ B pathway in U2OS cells

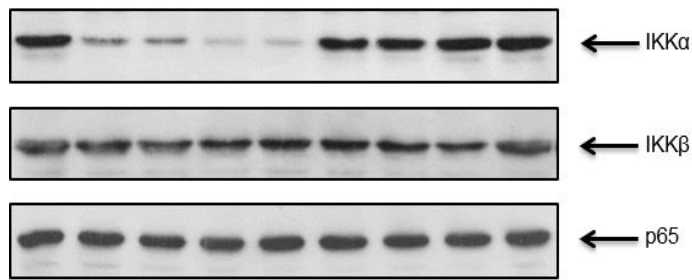
Having identified the rapid activation of non-canonical NF- κ B signalling in response to TNF α and IL1 β , the role of IKK α was examined using both molecular and pharmacological approaches.

4.2.2.1 Knockdown efficiency of siRNA-mediated silencing of IKK α and IKK β in U2OS cells

Initial experiments sought to optimise the knockdown of IKKs using siRNA; increasing concentrations of IKK α and IKK β siRNA were transfected into U2OS cells for 96 h which was found to be the optimal period for silencing. The same concentrations of non-targeting (NT) siRNA were also used to exclude any effect which may occur as a result of the transfection process (Figure 4.12). Whilst the NT construct was without effect, increasing concentrations (25-50nM) of siRNA effectively reduced endogenous IKK α expression by as much as 70% whilst at higher concentrations, 75-100 nM, the loss was approximately 95% (75 nM: % basal IKK α expression = 5.27 ± 1.97 ; 100 nM: % basal IKK α expression = 5.25 ± 1.39 , $p < 0.001$). Furthermore, IKK α siRNA did not exhibit any non-selective targeting of IKK β .

In the same fashion, Figure 4.13 demonstrates the knockdown efficiency siRNA IKK β in U2OS cells. Following transfection siRNA IKK β (25-100 nM) into U2OS cells for 96 h, IKK β knockdown was successfully achieved by more than 95% ($p < 0.001$) at all four concentrations tested. Non-targeting (NT) siRNA (25-100 nM) was again without effect. Moreover, treatment of cells with siRNA IKK β show no off-target effect on IKK α expression.

A



...	25	50	75	100	siRNA IKKα (nM)
...	25	50	75	100	siRNA NT (nM)

B

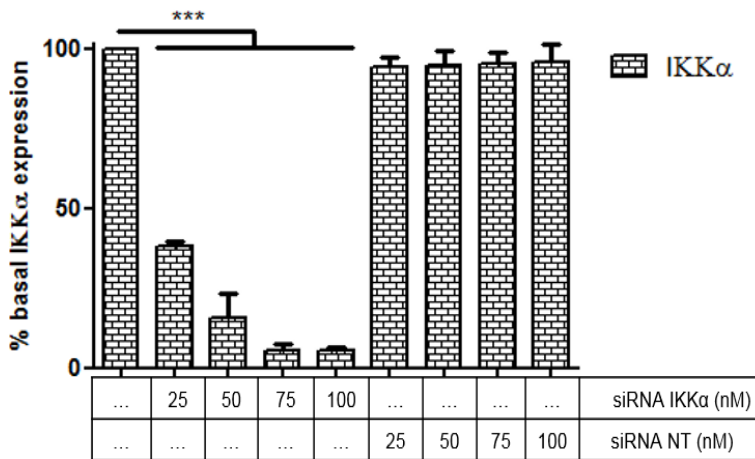


Figure 4.12: The effect of siRNA IKKα on IKKα expression in U2OS cells. Cells were transfected with siRNA IKKα or non-targeting (NT) up to a concentration of 100nM for 96 h. Whole cell extracts were assessed for A) IKKα (84kDa), IKKβ and total p65 (65 kDa) which was used as a loading control, as outlined in Section 2.5. Blots were semi-quantified for percentage of basal IKKα expression by scanning densitometry and results expressed as a relative to untreated control for B) IKKα. Each value represents the mean percentage knockdown ± S.E.M. of three independent experiments. Data was analysed using a one-way ANOVA test, ***p<0.001 vs control.

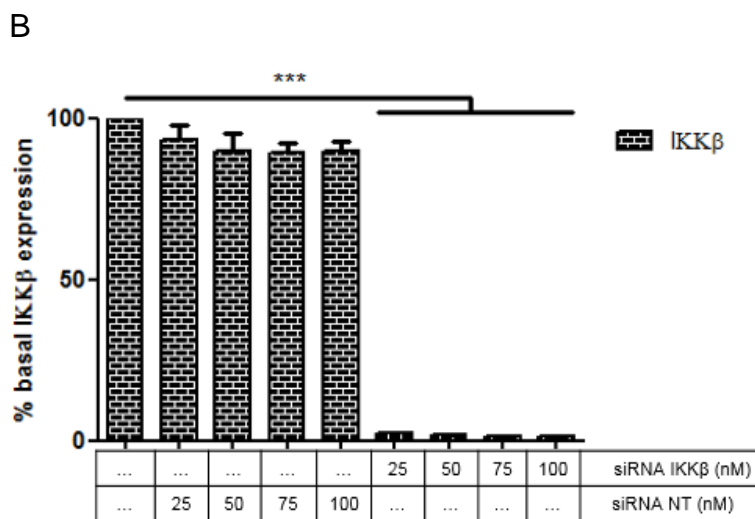
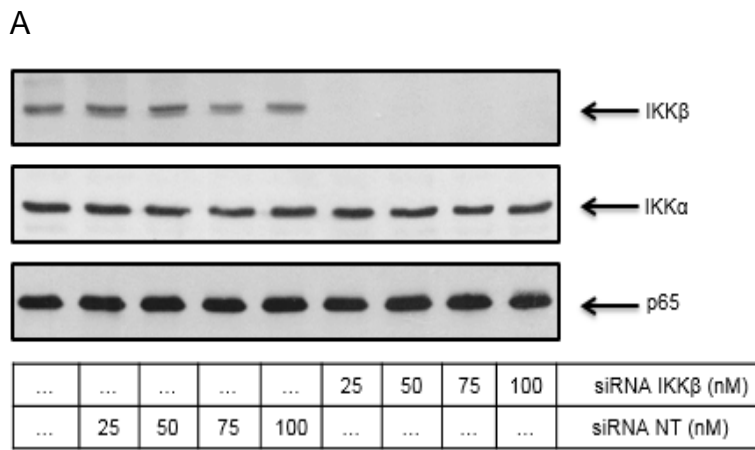


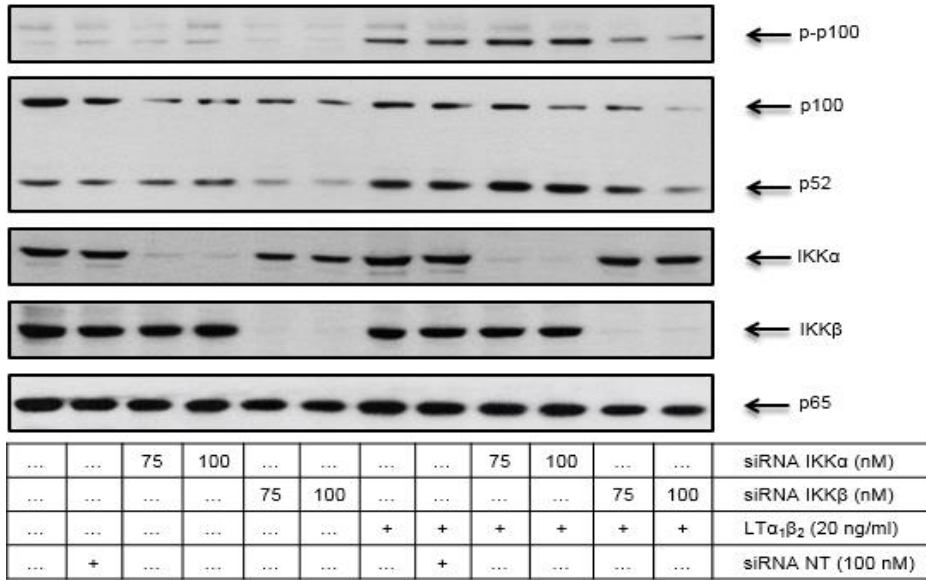
Figure 4.13: The effect of siRNA IKKβ on IKKβ expression in U2OS cells. Cells were transfected with siRNA IKKβ or non-targeting (NT) up to a concentration of 100nM for 96 h. Whole cell extracts were assessed for A) IKKβ (86 kDa), IKKα and total p65 (65 kDa) which was used as a loading control, as outlined in Section 2.5. Blots were semi-quantified for percentage of basal IKKβ expression by scanning densitometry and results expressed as a relative to untreated control for B) IKKβ. Each value represents the mean percentage knockdown \pm S.E.M. of three independent experiments. Data was analysed using a one-way ANOVA test, *** $p < 0.001$ vs control.

4.2.2.2 The effect of IKK α and IKK β siRNA silencing on LT $\alpha_1\beta_2$ induced p100 phosphorylation and p52 in U2OS cells

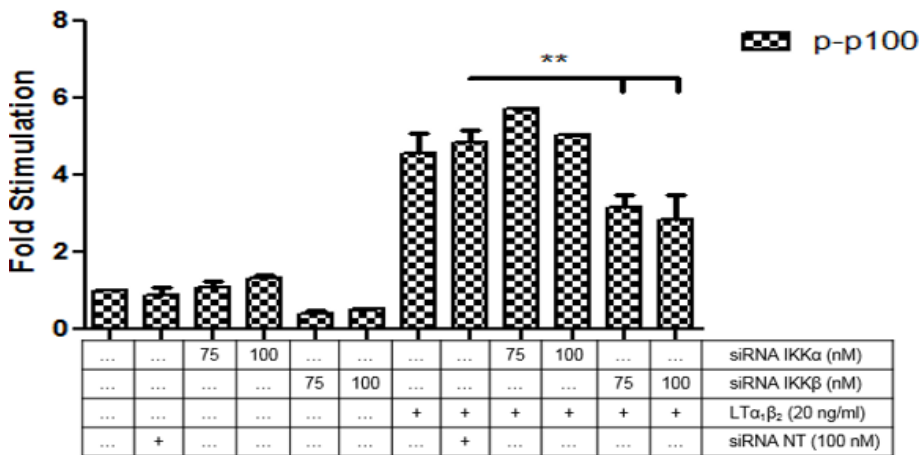
Having optimised knockdown conditions, the effect of siRNA IKK α or siRNA IKK β on LT $\alpha_1\beta_2$ induced p100 phosphorylation and p100 processing in U2OS cells were examined (Figure 4.14). LT $\alpha_1\beta_2$ alone induced a significant increase in p100 phosphorylation at 6 h (Fold increase = 4.57 ± 0.50 , $p < 0.001$). Surprisingly, the phosphorylation of p100 was significantly reduced following IKK β siRNA (IKK β siRNA 75nM: Fold increase = 3.17 ± 0.32 , IKK β siRNA 100nM: Fold increase = 2.83 ± 0.63 , $p < 0.01$), while there was no significant effect for IKK α siRNA.

In a similar fashion, LT $\alpha_1\beta_2$ (20 ng/ml) modestly induced p52 formation (Fold increase = 1.50 ± 0.19). Again, as with p-p100, LT $\alpha_1\beta_2$ -stimulated p52 formation was modestly reduced following IKK β siRNA but this reduction was not statistically significant. This response was not affected by IKK α siRNA. In addition, IKK α or IKK β siRNA alone knocked down p100 expression compared to non-stimulated cells. Moreover, the non-targeting (NT) construct as a negative control, did not target p-p100 or p52 formation.

A



B



C

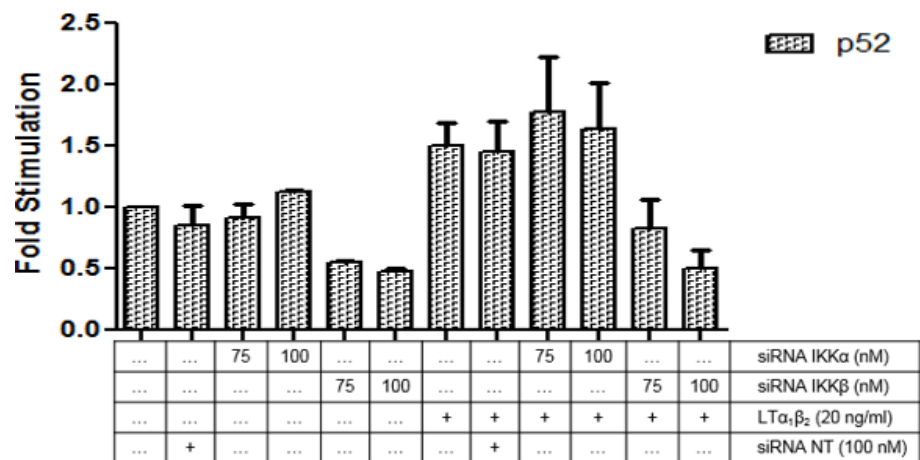
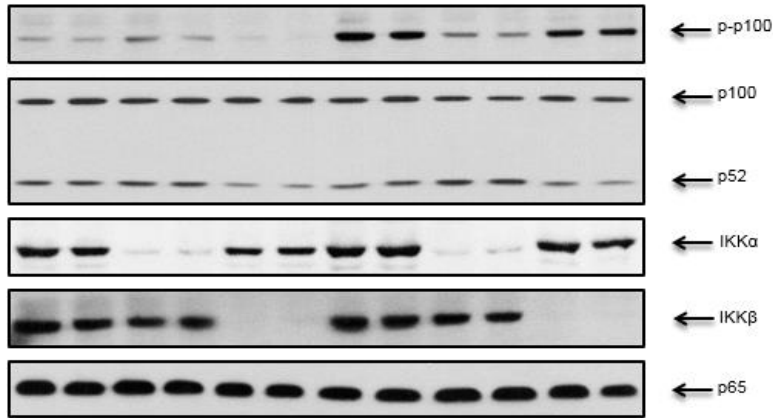


Figure 4.14: The effect of IKK α or β siRNA upon LT $\alpha_1\beta_2$ -mediated phosphorylation of p100 and p100 processing in U2OS cells. Cells were transfected with non-targeting siRNA (NT) 100nM, IKK α and IKK β siRNA (75 and 100nM) for 96 h prior stimulation with LT $\alpha_1\beta_2$ (20 ng/ml) for 8 h. Whole cell extracts were assessed for A) p-p100 (100 kDa), p52 (52kDa), IKK α (84 kDa), IKK β (86 kDa) and total p65 (65 kDa) which was used as a loading control, as outlined in Section 2.5. Blots were semi-quantified by scanning densitometry and results expressed as fold increase relative to control for B) p100 phosphorylation and C) p52 formation. Each value represents the mean \pm SEM of three independent experiments. Data was analysed using a one-way ANOVA test, ** $p < 0.01$ vs an agonist-stimulated control.

4.2.2.3 The effect of IKK α and IKK β siRNA silencing on TNF α -induced phosphorylation of p100 in U2OS cells

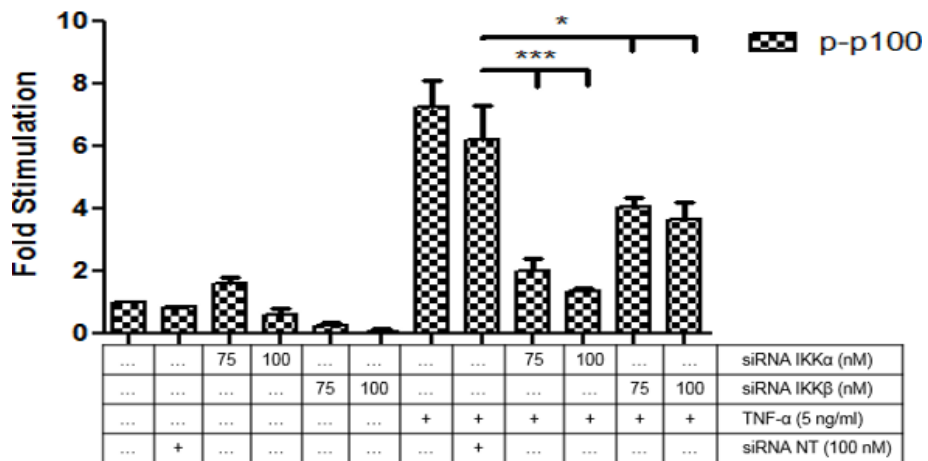
The effect of siRNA IKK α or siRNA IKK β on TNF α induced p-p100 and p100 processing in U2OS cells were then examined (Figure 4.15). TNF α alone caused a marked stimulation of p100 phosphorylation at 15 min (Fold increase = 7.25 ± 0.84 , $p < 0.001$). Interestingly, IKK α siRNA at both 75 and 100nM concentrations significantly reduced TNF α induced p100 phosphorylation by approximately 80% compared to the non-target (NT) control (IKK α siRNA 75nM; Fold increase = 1.98 ± 0.40 ; 100nM: Fold increase = 1.34 ± 0.11 , $p < 0.001$). In contrast, IKK β siRNA reduced the signal marginally but the effect was not significant. It was also observed that p52 formation in both TNF α -stimulated and control cells was significantly reduced in the presence of 100 nM IKK β siRNA (See also Figure 4.15). Furthermore, transfection of cells with IKK α or IKK β siRNA did not cause any changes in p100 levels compared to TNF α alone or when compared to the control.

A



...	...	75	100	75	100	siRNA IKKα (nM)
...	75	100	75	100	...	siRNA IKKβ (nM)
...	+	+	+	+	+	+	TNF-α (5 ng/ml)
...	+	+	siRNA NT (100 nM)

B



C

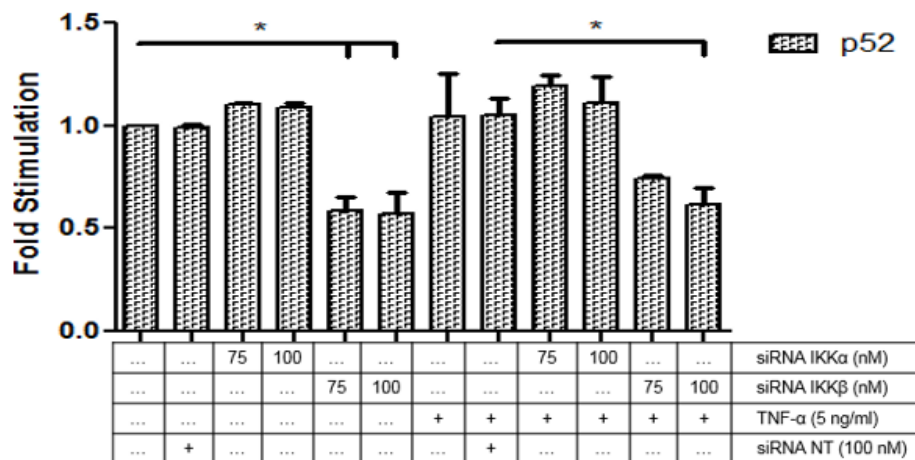
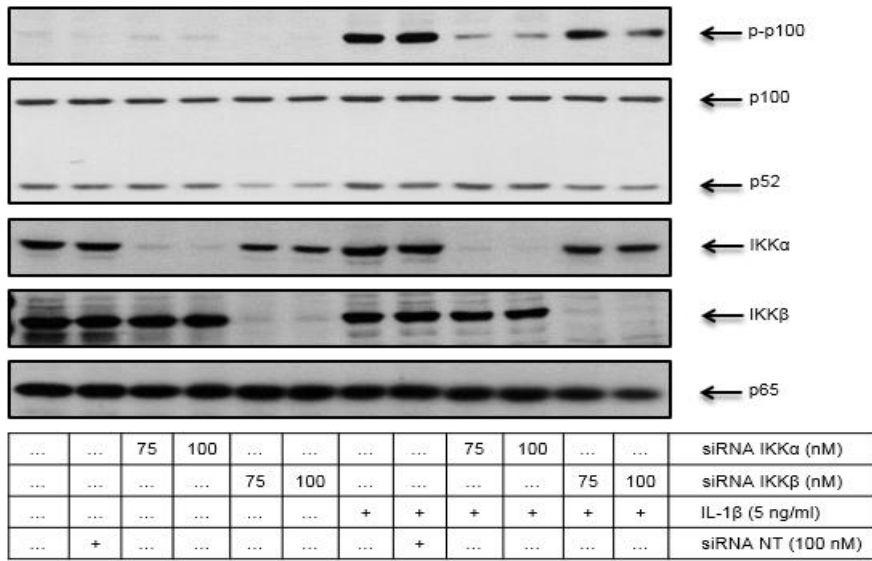


Figure 4.15: The effect of IKK α or β siRNA upon TNF α -mediated phosphorylation of p100 and p100 processing in U2OS cells. Cells were transfected with non-targeting (NT) siRNA 100nM, IKK α and IKK β siRNA (75, 100 nM) for 96 h prior stimulation with TNF α (5 ng/ml) for 15 min. Whole cell extracts were assessed for A) p-p100 (100 kDa), IKK α (84 kDa), IKK β (86 kDa) and total p65 (65 kDa) which was used as a loading control, as outlined in Section 2.5. Blots were semi-quantified by scanning densitometry and results expressed as fold increase relative to control for B) p100 phosphorylation and C) p52 formation. Each value represents the mean \pm SEM of three independent experiments. Data was analysed using a one-way ANOVA test, * $p < 0.05$, *** $p < 0.001$ vs an agonist-stimulated control.

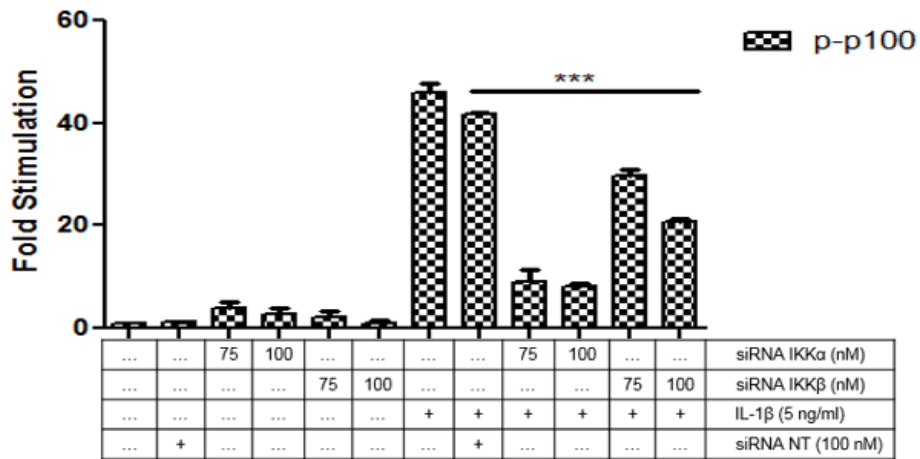
4.2.2.4 The effect of IKK α and IKK β siRNA silencing on IL-1 β -induced phosphorylation of p100 and p52 in U2OS cells

Similar to previous results with TNF α , Figure 4.16 illustrates the effect of IKK α and β siRNA on IL-1 β induced phosphorylation of p100 and p100 processing in U2OS cells. Stimulation with IL-1 β alone induced a 46-fold increase in the phosphorylation of p100 (Fold increase = 46.09 ± 1.65 , $p < 0.001$). Interestingly, following transfection of the cells with siRNA IKK α , the phosphorylation of p100 induced by IL-1 β was markedly reduced by approximately 80% at both 75 and 100 nM concentrations tested compared to the non-target (NT) control (IKK α siRNA 75nM: Fold increase = 9.18 ± 2.17 , IKK α siRNA 100nM: Fold increase = 8.10 ± 0.56). In contrast IKK β siRNA slightly reduced the response but this effect was not significant. Similarly, p52 formation in both IL-1 β -stimulated and control cells was significantly reduced in the presence of 100 nM of IKK β siRNA (Figure 4.16).

A



B



C

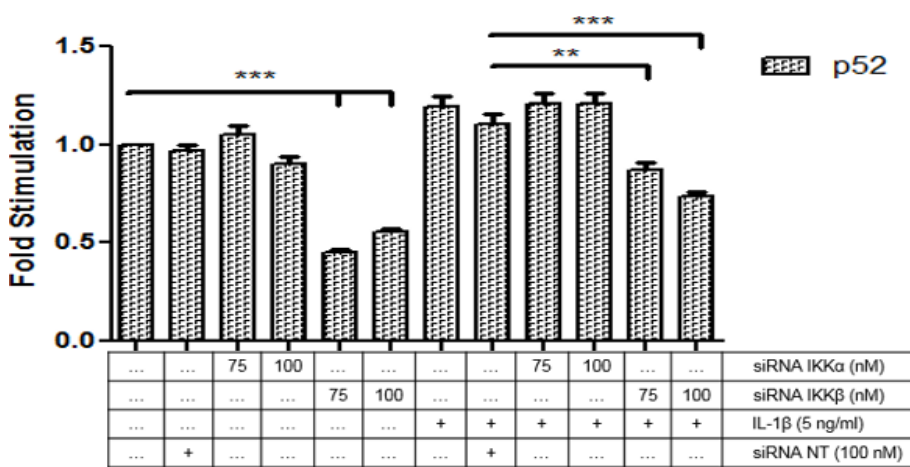
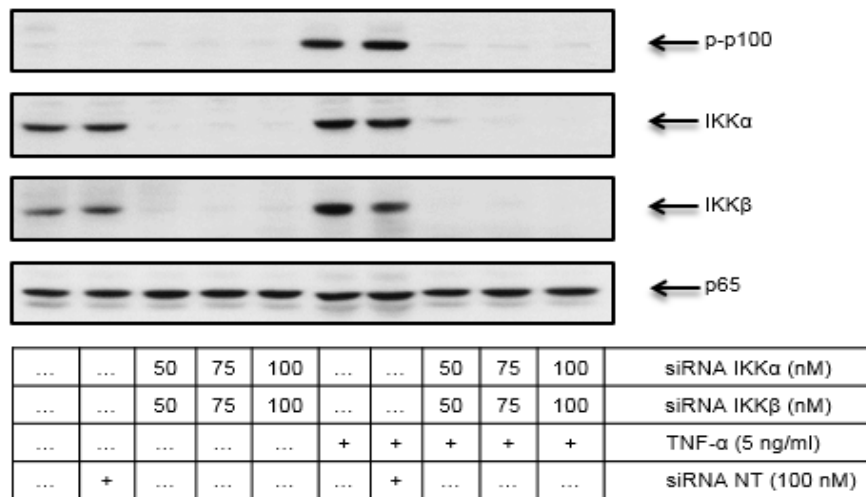


Figure 4.16: The effect of IKK α or β siRNA upon IL-1 β -mediated phosphorylation of p100 and p100 processing in U2OS cells. Cells were transfected with non-targeting (NT) siRNA 100nM, IKK α and IKK β siRNA for 96 h prior stimulation with IL-1 β for 30 min. Whole cell extracts were assessed for A) p-p100 (100 kDa), p52 (52 kDa), IKK α (84 kDa), IKK β (86 kDa) and total p65 (65 kDa) which was used as a loading control, as outlined in Section 2.5. Blots were semi-quantified by scanning densitometry and results expressed as fold increase relative to control for B) p100 phosphorylation and C) p52 formation. Each value represents the mean \pm SEM of three independent experiments. Data was analysed using a one-way ANOVA test, ** $p < 0.01$, *** $p < 0.001$ vs agonist-stimulated control.

4.2.2.5 The effect of IKK α and β siRNA double knockdown upon TNF α -induced p100 phosphorylation in U2OS cells

Since single knockdown of either IKK α or β siRNA had the potential to reduce TNF α -induced p100 phosphorylation, the effect of both together was assessed (Figure 4.17). Following stimulation, TNF α (5 ng/ml) alone significantly induced a 15-20 fold increase in p100 phosphorylation (17.13 ± 0.38 , $p < 0.001$) compared to non-stimulated cells. Interestingly, when the cells were transfected to double-knockdown of IKK α and IKK β siRNA (50–100 nM), the phosphorylation of p100 induced by TNF α was totally inhibited at all the concentrations tested compared to the non-target (NT) control (IKK α & β siRNA 50nM: Fold increase = 1.13 ± 0.03 , IKK α & β siRNA 75nM: Fold increase = 0.89 ± 0.09 , $p < 0.001$). This suggested the potential of both isoforms to work in conjunction to regulate p100 phosphorylation.

A



B

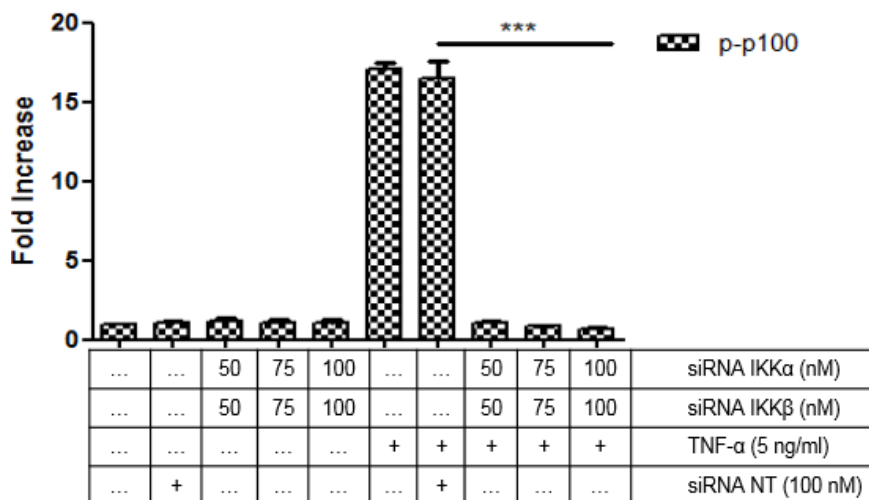


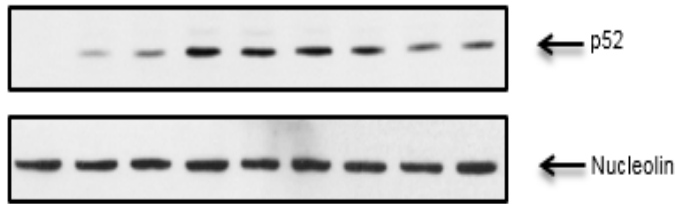
Figure 4.17: The effect of double-knockdown of IKKα and IKKβ siRNA upon TNFα-mediated p100 phosphorylation in U2OS cells. Cells were transfected with non-targeting (NT) siRNA 100 nM, IKKα and IKKβ siRNA (50-100 nM) for 96 h prior stimulation with TNFα (5 ng/ml) for 15 min. Whole cell extracts were assessed for A) p-p100 (100 kDa), IKKα (84 kDa), IKKβ (86 kDa) and total p65 (65 kDa) which was used as a loading control, as outlined in Section 2.5. Blots were semi-quantified by scanning densitometry and results expressed as fold increase relative to the control for B) p100 phosphorylation. Each value represents the mean ± SEM of three independent experiments. Data was analysed using a one-way ANOVA test, ***p<0.001 vs an agonist-stimulated control.

4.2.2.6 The effect of IKK α siRNA silencing on TNF α -induced p52 and RelB nuclear translocation in U2OS cells

The effect of siRNA silencing was then examined at the level of p52 and RelB. Figure 4.18 shows that TNF α alone caused a significant stimulation of p52 nuclear translocation (Fold increase = 2.84 ± 0.42 , $p < 0.001$). When the cells were treated with increasing concentrations of siRNA IKK α a decrease in TNF α -induced p52 translocation was observed which was significant at higher concentrations (Fold increase = 1.44 ± 0.16 , $p < 0.05$). Non-targeted siRNA (NT) showed a minimal non-significant effect on p52 translocation in these experiments.

Using the same scenario, Figure 4.19 shows nuclear RelB induced by TNF α following transfection of the cells with increasing concentrations of siRNA IKK α (50-150 nM). Alone TNF α produced an 8.67 fold increase (± 1.12 , $p < 0.001$) in RelB nuclear translocation in comparison to unstimulated cells. Interestingly, all four concentrations of IKK α siRNA significantly diminished RelB nuclear translocation, and as Figure 4.19 demonstrates, higher concentrations of IKK α siRNA completely inhibited the nuclear translocation of RelB compared to the non-target (NT) control (Fold increase = 0.37 ± 0.38 , $p < 0.001$).

A



...	...	150	50	75	100	150	siRNA IKK α (nM)
...	+	+	siRNA NT(150 nM)
...	+	+	+	+	+	+	TNF- α (5 ng/ml)

B

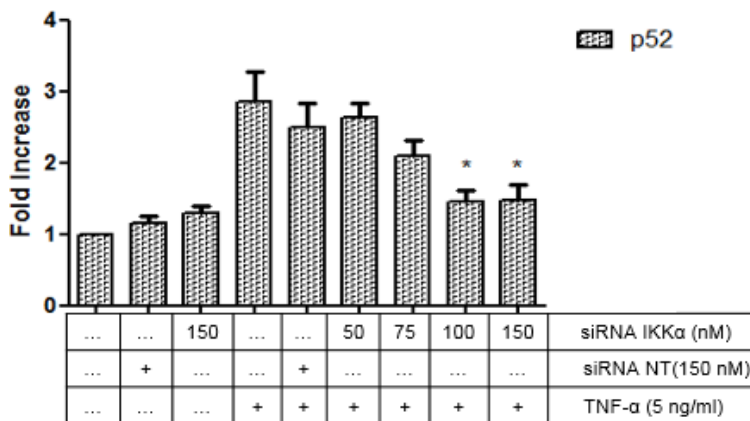
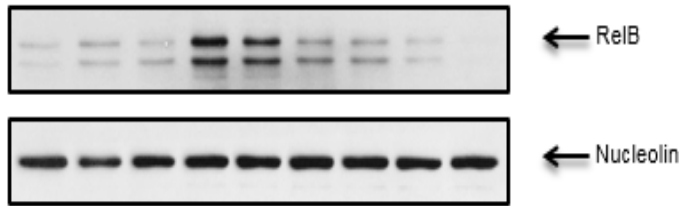


Figure 4.18: The effect of IKK α siRNA upon TNF α -mediated p52 nuclear localisation in U2OS cells. Cells were transfected with non-targeting (NT) siRNA 150nM, IKK α siRNA (50-150 nM) for 96 h prior stimulation with TNF α (5 ng/ml) for 60 min. Nuclear extracts were assessed for p52 (52 kDa) and Nucleolin (106 kDa) which was used as a loading control, as outlined in Section 2.5. Blots were semi-quantified by scanning densitometry and results expressed as fold increase relative to control for B) p52. Each value represents the mean \pm SEM of three independent experiments. Data was analysed using a one-way ANOVA test, * $p < 0.05$ vs an agonist-stimulated control.

A



...	...	150	50	75	100	150	siRNA IKK α (nM)
...	+	+	siRNA NT(150 nM)
...	+	+	+	+	+	+	TNF- α (5 ng/ml)

B

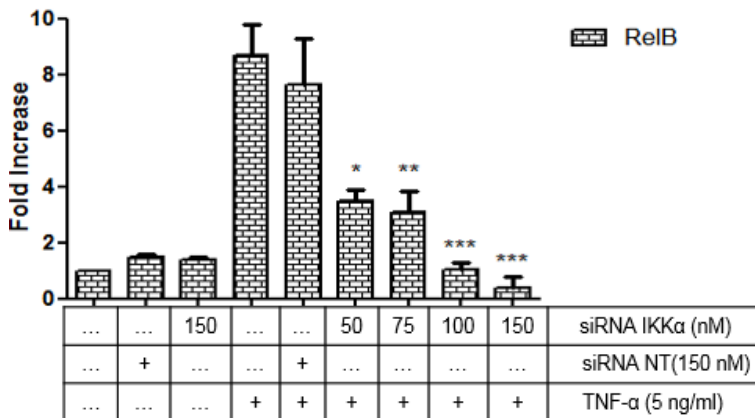


Figure 4.19: The effect of IKK α siRNA upon TNF α -mediated RelB nuclear localisation in U2OS cells. Cells were transfected with non-targeting (NT) siRNA 150nM, IKK α siRNA (50-100nM) for 96 hr prior stimulation with TNF α (5 ng/ml) for 60 min. Nuclear extracts were assessed for RelB (66 kDa) and Nucleolin (106 kDa) which was used as a loading control, as outlined in Section 2.5. Blots were semi-quantified by scanning densitometry and results expressed as fold increase relative to control for B) RelB. Each value represents the mean \pm SEM of two independent experiments. Data was analysed using a one-way ANOVA test, * p <0.05, ** p <0.01, *** p <0.001 vs an agonist-stimulated control.

4.2.3 The effect of SU compounds on agonist-stimulated non-canonical NF- κ B pathway activation in U2OS cells

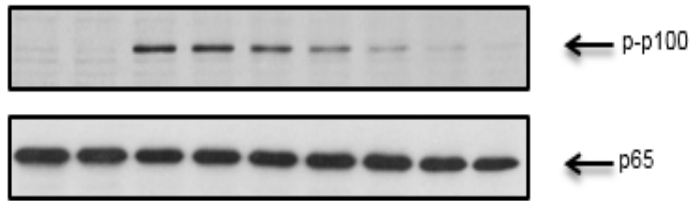
4.2.3.1 The effect of SU compounds on TNF α -induced phosphorylation of p100 in U2OS cells

Having utilised siRNA to reveal a novel regulation of early p100 phosphorylation by either TNF α or IL-1 β , the three SU compounds characterised in Chapter 3 were utilised. Figure 4.20 shows the effect of SU1261 compound on TNF α -induced phosphorylation of p100 in U2OS cells. As expected, TNF α alone induced a marked increase in p100 phosphorylation (Fold stim = 11.63 \pm 0.66, $p < 0.001$) and whilst the DMSO vehicle was without effect, incubation with increasing concentrations of SU1261 over the low to mid micromolar range significantly reduced the response. An approximate IC₅₀ of SU1261 was obtained, 1.31 μ M.

Similar to the effect of SU1261, pre-treatment with SU1266 also reduced TNF α (5 ng/ml) stimulated phosphorylation of p100 (Figure 4.21). The response was significantly reduced at all concentrations tested giving an IC₅₀ value 0.32 μ M, which was more potent than that observed with SU1261.

The final SU compound tested in this section was SU1349. As shown in Figure 4.22, treatment of U2OS cells with this compound reduced p100 phosphorylation at higher concentrations. These inhibitory profiles were consistent with those observed for LT $\alpha_1\beta_2$ stimulated responses and support a role of IKK α in rapid phosphorylation of p100.

A



...	30	0.3	1	3	10	30	SU1261 (μM)
...	+	DMSO (0.15 %)
...	...	+	+	+	+	+	+	+	TNF α (5 ng/ml)

B

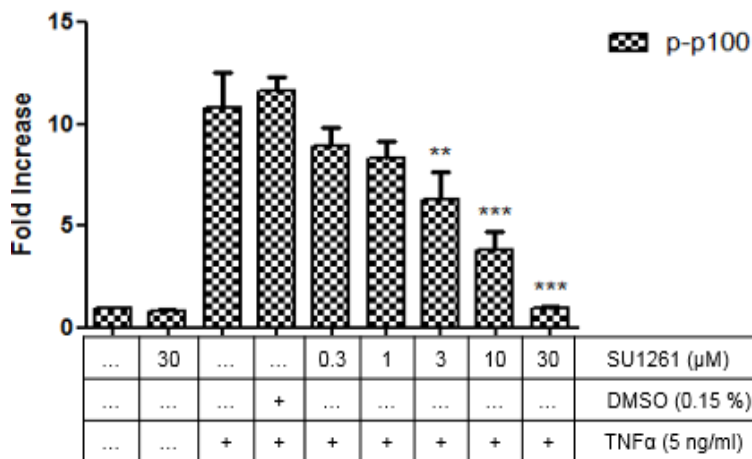
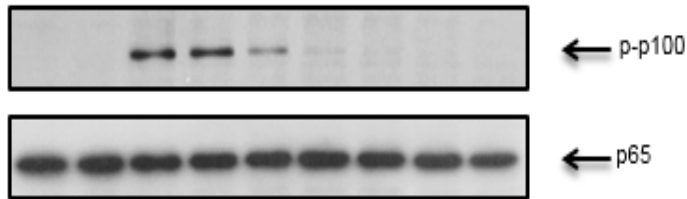


Figure 4.20: The effect of SU1261 upon TNF α -mediated p100 phosphorylation in U2OS cells. Cells were pre-treated with SU1261 for 1 h prior to stimulation with TNF α (5 ng/ml) for 15 min. Whole cell extracts were assessed for A) phosphorylation of p100 (100 kDa) and total p65 (65 kDa) which was used as a loading control, as outlined in Section 2.5. Blots were semi-quantified by scanning densitometry and results expressed as fold increase relative to control for B) p-p100. Each value represents the mean \pm SEM of three independent experiments. Data was analysed using a one-way ANOVA test, ** $p < 0.01$, *** $p < 0.001$ vs TNF α and DMSO as an agonist stimulated control.

A



...	30	0.3	1	3	10	30	SU1266 (μM)
...	+	DMSO (0.15 %)
...	...	+	+	+	+	+	+	+	TNF α (5 ng/ml)

B

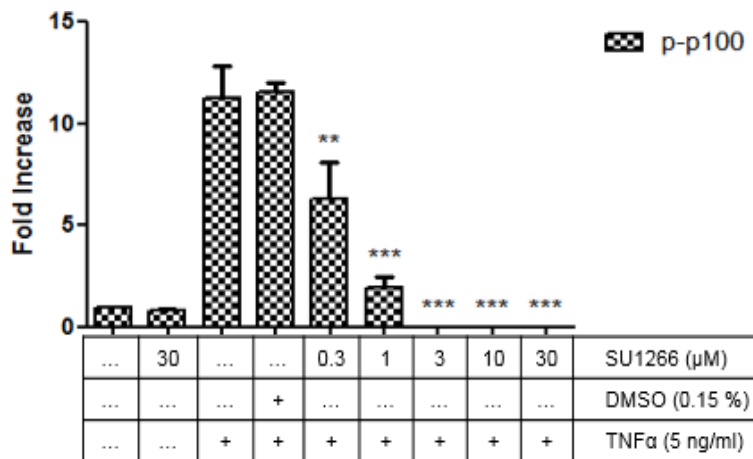
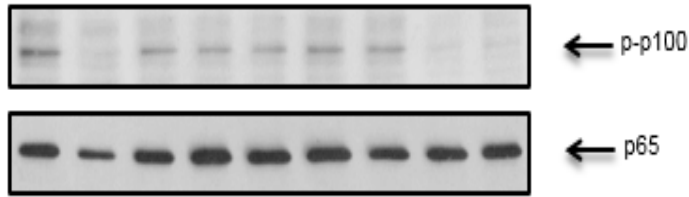


Figure 4.21: The effect of SU1266 upon TNF α -mediated p100 phosphorylation in U2OS cells. Cells were pre-treated with SU1266 for 1 h prior to stimulation with TNF α (5 ng/ml) for 15 min. Whole cell extracts were assessed for A) phosphorylation of p100 (100 kDa) and total p65 (65 kDa) which was used as a loading control, as outlined in Section 2.5. Blots were semi-quantified by scanning densitometry and results expressed as fold increase relative to control for B) p-p100. Each value represents the mean \pm SEM of three independent experiments. Data was analysed using a one-way ANOVA test, ** $p < 0.01$, *** $p < 0.001$ vs TNF α and DMSO as an agonist stimulated control.

A



...	30	0.3	1	3	10	30	SU1349 (μM)
...	+	DMSO (0.15 %)
...	...	+	+	+	+	+	+	+	TNF α (5 ng/ml)

B

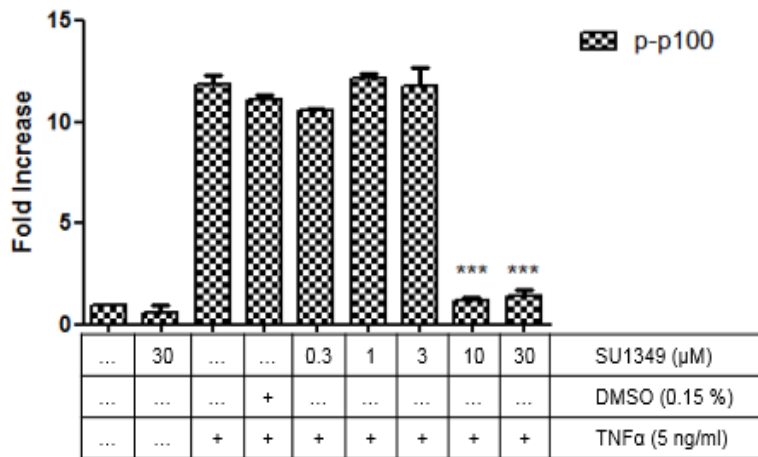
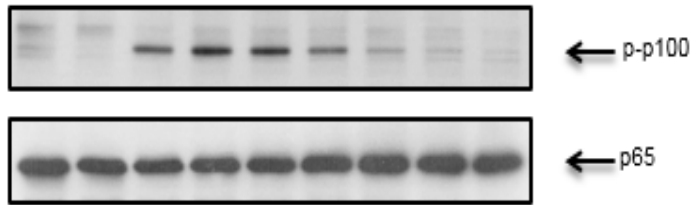


Figure 4.22: The effect of SU1349 upon TNF α -mediated p100 phosphorylation in U2OS cells. Cells were pre-treated with SU1349 for 1 h prior to stimulation with TNF α (5 ng/ml) for 15 min. Whole cell extracts were assessed for A) phosphorylation of p100 (100 kDa) and p65 (65 kDa) which was used as a loading control, as outlined in Section 2.5. Blots were semi-quantified by scanning densitometry and results expressed as fold increase relative to control for B) p-p100. Each value represents the mean \pm SEM of three independent experiments. Data was analysed using a one-way ANOVA test, *** p <0.001 vs TNF α and DMSO as an agonist stimulated control.

4.2.3.2. The effect of SU compounds on IL-1 β -induced phosphorylation of p100 in U2OS cells

As with TNF α , the effect of SU1261, SU1266 and SU1349 were tested against IL-1 β -induced phosphorylation of p100 in U2OS cells. As indicated in Figure 4.23, increasing concentrations of SU1261 between 1 and 30 μ M, significantly decreased p100 phosphorylation. At 30 μ M, the highest concentration used, there was complete inhibition. Figure 4.24 shows the effect of SU1266 against-IL-1 β induced phosphorylation of p100 in U2OS cells. Similar to SU1261, increasing concentrations of SU1266, inhibited IL-1 β -induced phosphorylation of p100. Again, at concentrations of 3-30 μ M, SU1266 totally abolished p100 phosphorylation. The effect of SU1349 on p100 phosphorylation is also illustrated in Figure 4.25. Pre-treatment with SU1349 (0.3-3 μ M) gradually decreased IL-1 β -stimulated phosphorylation of p100, but this decrease was not statistically significant until higher concentrations of the compound were employed.

A



...	30	0.3	1	3	10	30	SU1261 (μM)
...	+	DMSO (0.15 %)
...	...	+	+	+	+	+	+	+	IL-1 β (5 ng/ml)

B

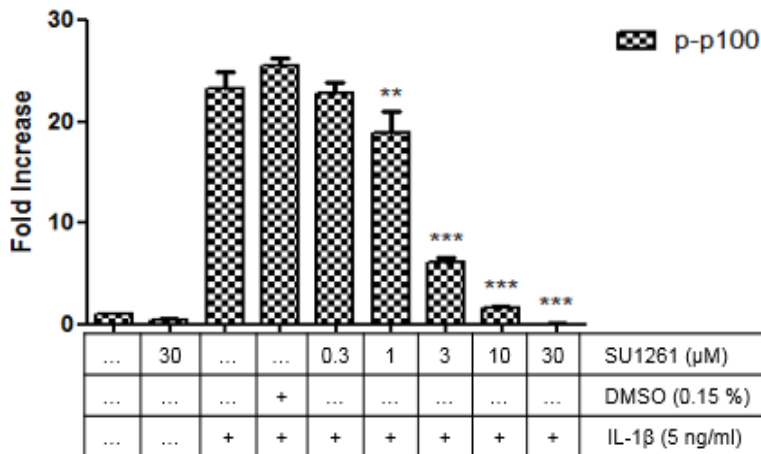
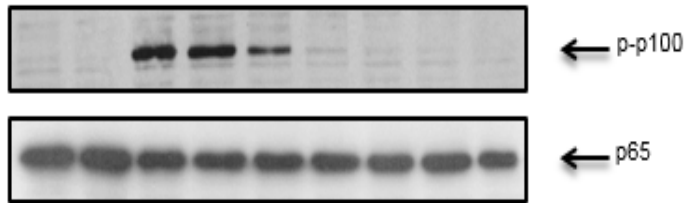


Figure 4.23: The effect of SU1261 upon IL-1 β -mediated p100 phosphorylation in U2OS cells. Cells were pre-treated with SU1261 for 1 h prior to stimulation with IL-1 β (5 ng/ml) for 30 min. Whole cell extracts were assessed for A) phosphorylation of p100 (100 kDa) and total p65 (65 kDa) which was used as a loading control, as outlined in Section 2.5. Blots were semi-quantified by scanning densitometry and results expressed as fold increase relative to control for B) p-p100, each value represents the mean \pm SEM of three independent experiments. Data was analysed using a one-way ANOVA test, ** $p < 0.01$, *** $p < 0.001$ vs IL-1 β and DMSO as an agonist stimulated control.

A



...	30	0.3	1	3	10	30	SU1266 (μM)
...	+	DMSO (0.15 %)
...	...	+	+	+	+	+	+	+	IL-1 β (5 ng/ml)

B

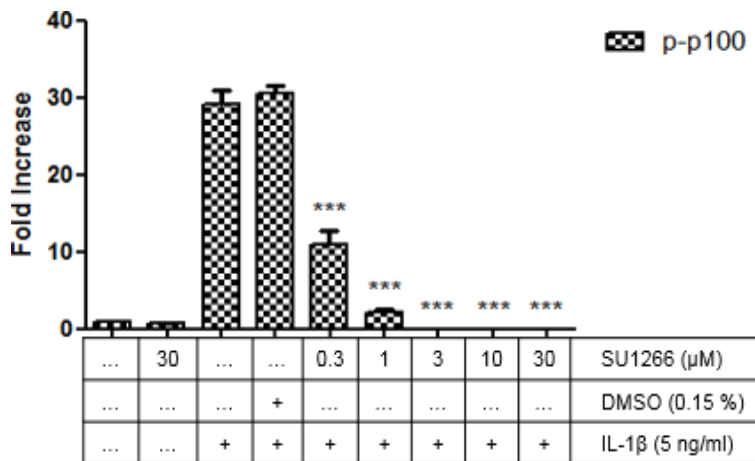
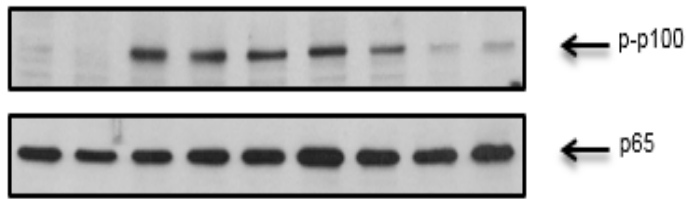


Figure 4.24: The effect of SU1266 upon IL-1 β -mediated p100 phosphorylation in U2OS cells. Cells were pre-treated with SU1261 for 1 h prior to stimulation with IL-1 β (5 ng/ml) for 30 min. Whole cell extracts assessed for A) phosphorylation of p100 (100 kDa) and total p65 (65 kDa) which was used as a loading control, as outlined in Section 2.5. Blots were semi-quantified by scanning densitometry and results expressed as fold increase relative to control for B) p-p100. Each value represents the mean \pm SEM of three independent experiments. Data was analysed using a one-way ANOVA test, *** p <0.001 vs IL-1 β and DMSO as an agonist stimulated control.

A



...	30	0.3	1	3	10	30	SU1349 (μM)
...	+	DMSO (0.15 %)
...	...	+	+	+	+	+	+	+	IL-1 β (5 ng/ml)

B

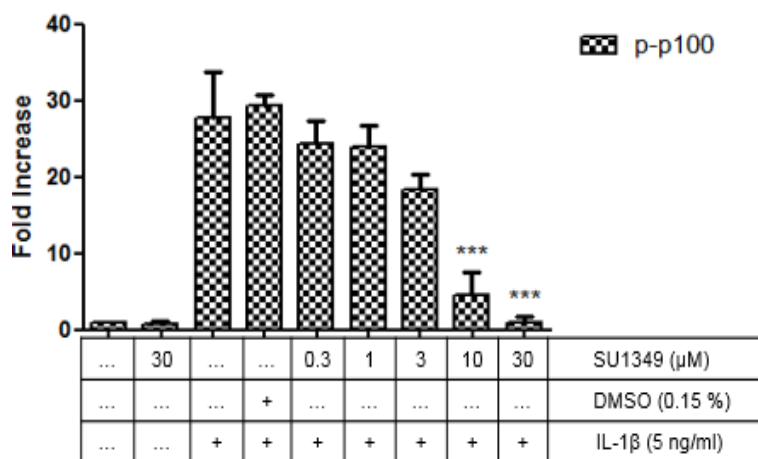


Figure 4.25: The effect of SU1349 upon IL-1 β -mediated p100 phosphorylation in U2OS cells. Cells were pre-treated with SU1261 for 1 h prior to stimulation with IL-1 β (5 ng/ml) for 30 min. Whole cell lysates were assessed for A) phosphorylation of p100 (100 kDa) and total p65 (65 kDa) which was used as a loading control, as outlined in Section 2.5. Blots were semi-quantified by scanning densitometry and results expressed as fold increase relative to control for B) p-p100. Each value represents the mean \pm SEM of three independent experiments. Data was analysed using a one-way ANOVA test, *** p <0.001 vs IL-1 β and DMSO as an agonist stimulated control.

4.2.3.3 The effect of SU1261 on IL-1 β -mediated p52 and RelB nuclear translocation in U2OS cells

Figure 4.26 illustrates the effect of SU1261 (0.3-30 μ M) on nuclear translocation of both p52 and RelB in U2OS cells. IL-1 β alone significantly induced both p52 and RelB nuclear translocation (p52: Fold increase = 2.33 ± 0.05 , RelB: Fold increase = 3.48 ± 0.03 , $p < 0.001$) compared with the control group. Pre-treatment of cells with increasing concentrations of SU1261 (0.3-30 μ M) inhibited the IL-1 β response with a significant effect observed at the maximal concentrations of SU1261.

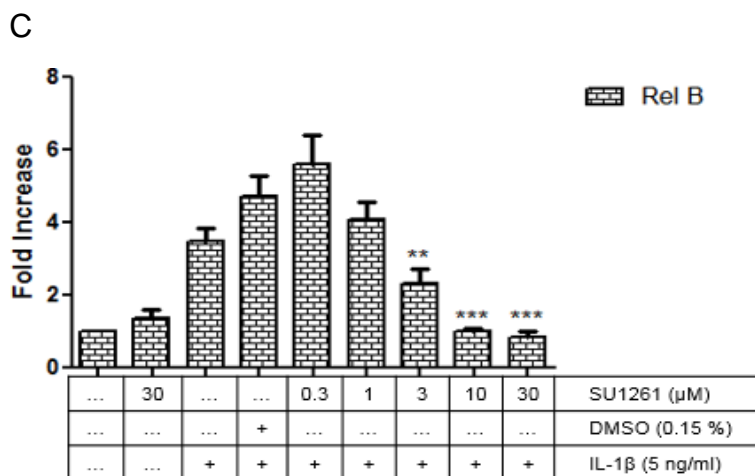
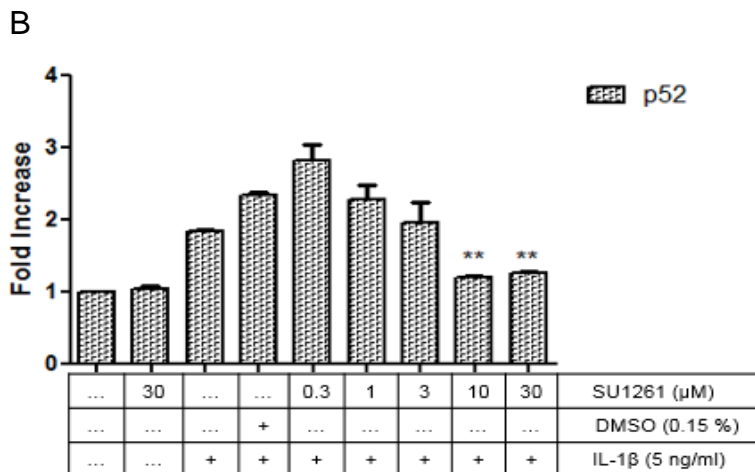
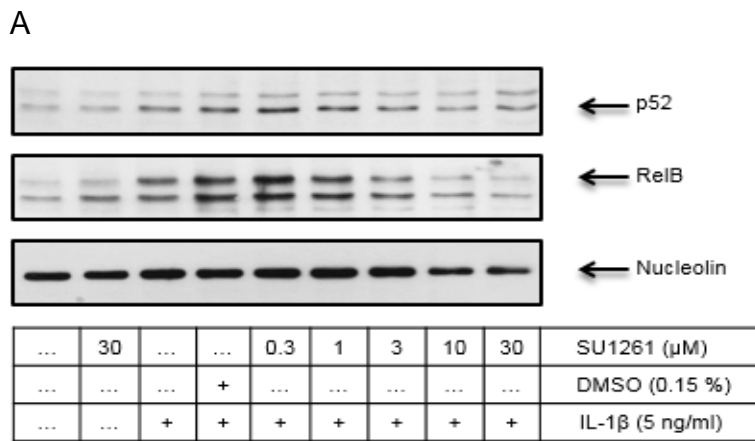


Figure 4.26: The effect of SU1261 upon IL-1 β -mediated p52 and RelB nuclear localisation in U2OS cells. Cells were pre-treated with SU1261 for 1 h prior to the stimulation with IL-1 β (5ng/ml) for 1 h. Nuclear extracts were assessed for A) p52 (52 kDa), RelB (68 kDa) and nucleolin (106 kDa) which was used as a loading control, as outlined in Section 2.5. Blots were semi-quantified by scanning densitometry and results expressed as fold increase relative to control for B) p52 and C) RelB. Each value represents the mean \pm SEM of three independent experiments. Data was analysed using a one-way ANOVA test, ** p <0.01 and *** p <0.001 vs IL-1 β and DMSO as an agonist stimulated control.

4.2.3.4 The effect of SU1266 on IL-1 β -mediated p52 and RelB nuclear translocation in U2OS cells

As with SU1261, the effect of SU1266 on nuclear translocation of both p52 and RelB is illustrated in Figure 4.27. IL-1 β significantly increased both p52 and RelB nuclear translocation (p52: Fold increase = 1.82 ± 0.03 , RelB: Fold increase = 2.38 ± 0.18 , $p < 0.001$) However, with increasing concentrations of SU1266, nuclear levels both p52 and RelB were significantly decreased compared to IL-1 β treated cells.

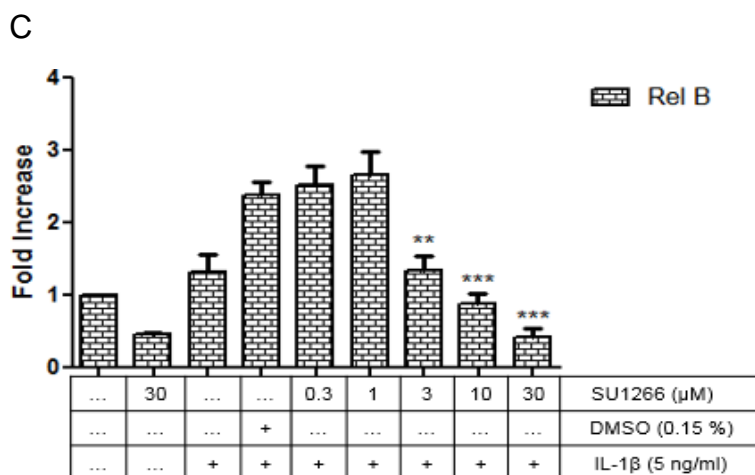
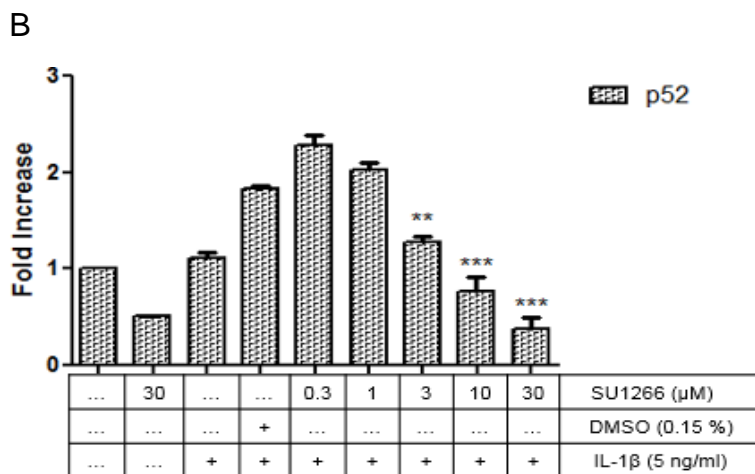
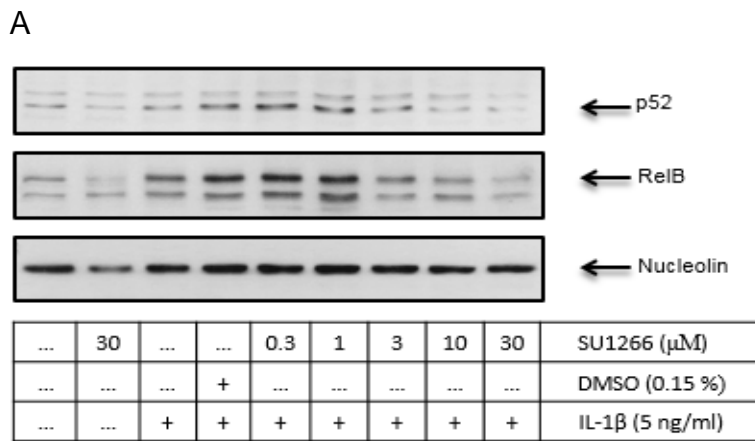
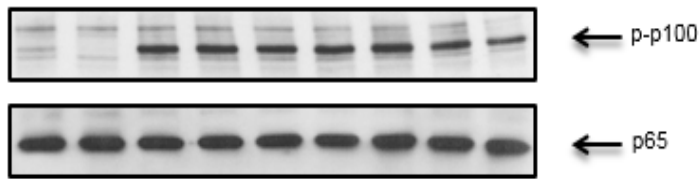


Figure 4.27: The effect of SU1266 upon IL-1 β -mediated p52 and RelB nuclear localisation in U2OS cells. Cells were pre-treated with SU1266 for 1 h prior to the stimulation with IL-1 β (5ng/ml) for 1 h. Nuclear extracts were assessed for A) p52 (52 kDa), RelB (68 kDa) and nucleolin (106 kDa) which was used as a loading control, as outlined in section 2.5. Blots were semi-quantified by scanning densitometry and results expressed as fold increase relative to control for B) p52 formation and C) RelB formation. Each value represents the mean \pm SEM of three independent experiments. Data was analysed using a one-way ANOVA test, ** p <0.01 and *** p <0.001 vs IL-1 β and DMSO as an agonist stimulated control.

4.2.4 The effect of NIK inhibitor CW15407 upon TNF α -and IL-1 β -induced phosphorylation of p100 in U2OS cells

As mentioned in Chapter 1, NF- κ B-inducing kinase (NIK) has a key regulating role in activating the non-canonical NF- κ B pathway (Qing et al., 2005) through phosphorylation of IKK α (Xiao et al., 2001, Senftleben et al., 2001). Therefore, the effect of the NIK inhibitor (CW15407) was employed in the context of p100 phosphorylation induced by TNF α and IL-1 β to investigate whether NIK is involved in early activation of this pathway. The phosphorylation of p100 was induced by TNF α (Figure 4.28) or IL-1 β (Figure 4.29) in the manner anticipated. Over the low micromolar range CW15407 was ineffective; the compound did not cause any statistically significant change in the phosphorylation of p100. Only at a maximum concentration of 30 μ M was a statistically significant inhibition recorded.

A



...	30	0.3	1	3	10	30	CW15407 (μ M)
...	+	DMSO (0.15 %)
...	...	+	+	+	+	+	+	+	TNF α (5 ng/ml)

B

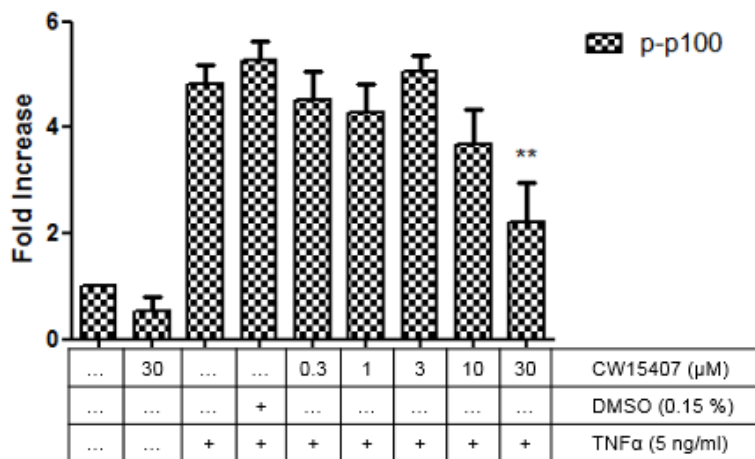
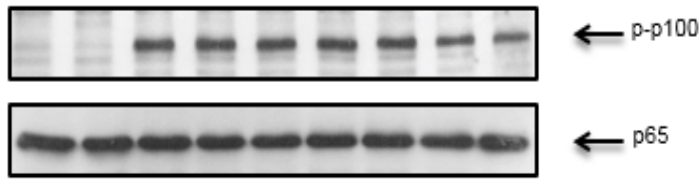


Figure 4.28: The effect of CW15407 on TNF α induced phosphorylation of p100 in U2OS cells. Cells were pre-treated with CW15407 for 1 h prior to stimulation with TNF α (5 ng/ml) for 15 min. Whole cell extracts were assessed for A) p-p100 (100 kDa) and total p65 (65 kDa) which was used as a loading control, as outlined in Section 2.5. Blots were semi-quantified by scanning densitometry and results expressed as fold increase relative to control for B) p100 phosphorylation. Each value represents the mean \pm SEM of three independent experiments. Data was analysed using a one-way ANOVA test, ** p <0.01 vs TNF α and DMSO as an agonist stimulated control.

A



...	30	0.3	1	3	10	30	CW15407 (μM)
...	+	DMSO (0.15 %)
...	...	+	+	+	+	+	+	+	IL-1 β (5 ng/ml)

B

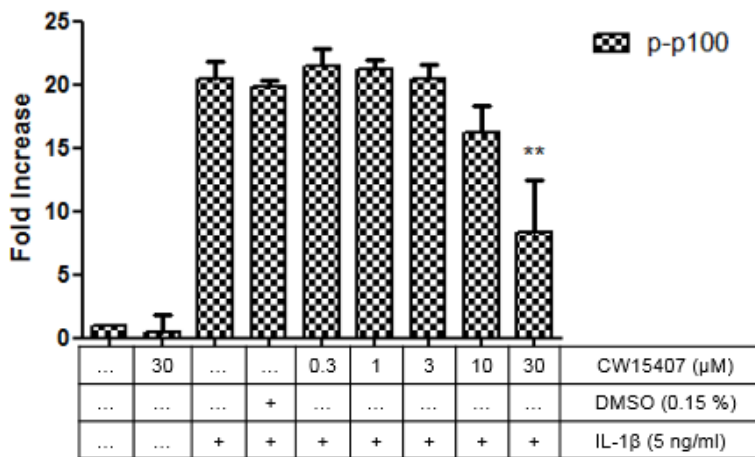
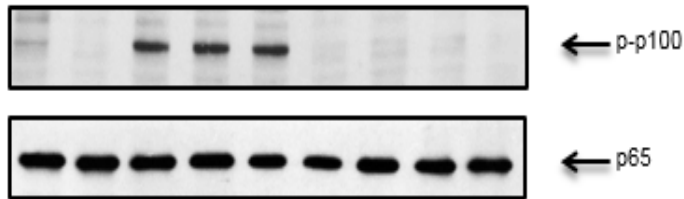


Figure 4.29: The effect of CW 15407 on IL-1 β induced phosphorylation of p100 in U2OS cells. Cells were pre-treated with CW15407 for 1 h prior to stimulation with IL-1 β (5 ng/ml) for 30 min. Whole cell extracts were assessed for A) p-p100 (100 kDa) and total p65 (65 kDa) which was used as a loading control, as outlined in Section 2.5. Blots were quantified by scanning densitometry and results expressed as fold increase relative to control for B) p100 phosphorylation. Each value represents the mean \pm SEM of three independent experiments. Data was analysed using a one-way ANOVA test, ** $p < 0.01$ vs IL-1 β and DMSO as an agonist stimulated control.

4.2.5 The effect of NIK inhibitor CW15407 upon $LT\alpha_1\beta_2$ -induced phosphorylation of p100 in U2OS cells

As with $TNF\alpha$ and $IL-1\beta$, the effect of CW15407 was investigated on $LT\alpha_1\beta_2$ -induced phosphorylation of p100 in U2OS cells (Figure 4.30). $LT\alpha_1\beta_2$ significantly induced phosphorylation of p100 resulting in an approximate three-fold increase (Fold increase = 2.99 ± 0.06 , $p < 0.001$). In contrast to the effects upon $TNF\alpha$ or $IL-1\beta$, CW15407 reduced $LT\alpha_1\beta_2$ -mediated phosphorylation of p100 with a significance reduction achieved between $1\mu M$ and $30\mu M$. The results demonstrated that NIK is implicated in the regulation of $LT\alpha_1\beta_2$ -induced p100 phosphorylation in U2OS cells.

A



...	30	0.3	1	3	10	30	CW15407 (μM)
...	+	DMSO (0.15 %)
...	...	+	+	+	+	+	+	+	LT $\alpha_1\beta_2$ (20 ng/ml)

B

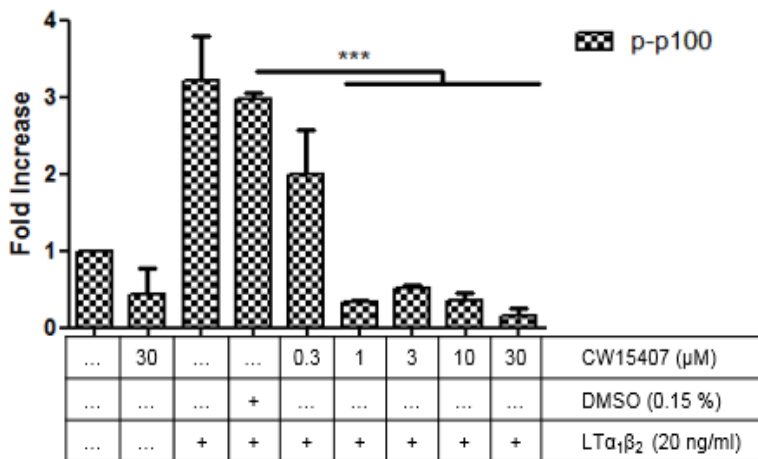
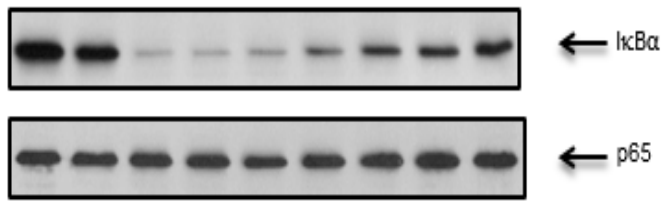


Figure 4.30: The effect CW15407 on LT $\alpha_1\beta_2$ induced phosphorylation of p100 in U2OS cells. Cells were pre-treated with CW15407 for 1 h prior to stimulation with LT $\alpha_1\beta_2$ (20 ng/ml) for 6 h. Whole cell extracts were assessed for A) p-p100 (100 kDa) and total p65 (65 kDa) which was used as a loading control, as outlined in Section 2.5. Blots were quantified by scanning densitometry and results expressed as fold increase relative to control for B) p100 phosphorylation. Each value represents the mean \pm SEM of three independent experiments. Data was analysed using a one-way ANOVA test, *** $p < 0.001$ vs LT $\alpha_1\beta_2$ and DMSO as an agonist stimulated control.

4.2.6 The effect of selective IKK β inhibitor IKK2 X1 upon TNF α -and IL-1 β - induced phosphorylation of p100 in U2OS cells

To further confirm that early p100 phosphorylation was IKK β independent the effect of the commercially available IKK β inhibitor (IKK2 X1) was investigated. Initially the effect of this inhibitor on cellular I κ B α loss as a marker of the canonical NF- κ B pathway signalling was examined and preliminary results confirmed that I κ B α loss induced by TNF α was significantly reversed in the presence of IKK2 X1 in a concentration-dependent manner over the low micromolar range (3-30 μ M) (Figure 4.31). Next, the effect of IKK2 X1 was tested upon p100 phosphorylation induced by TNF α or IL-1 β (Figures 4.32 and 4.33, respectively). Compared with unstimulated cells, both TNF α and IL-1 β mediated a significant increase in the phosphorylation of p100 (Fold increase = 5.20 ± 0.98 , Fold increase = 30.93 ± 2.89 , $p < 0.001$, respectively). However, either response was not altered significantly following treatment with IKK2 X1 up to a maximum concentration of 30 μ M.

A



...	30	0.3	1	3	10	30	IKK2 X1 (μM)
...	+	DMSO (0.15 %)
...	...	+	+	+	+	+	+	+	TNFα (5 ng/ml)

B

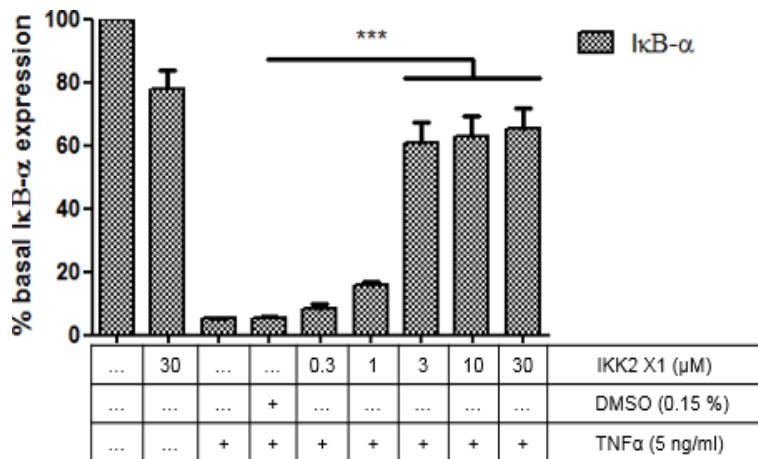
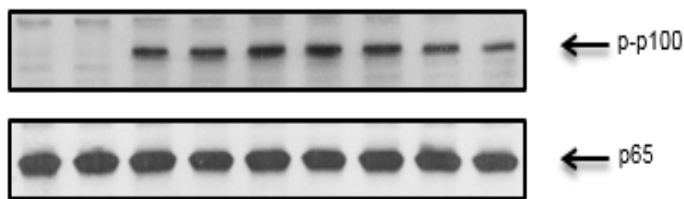


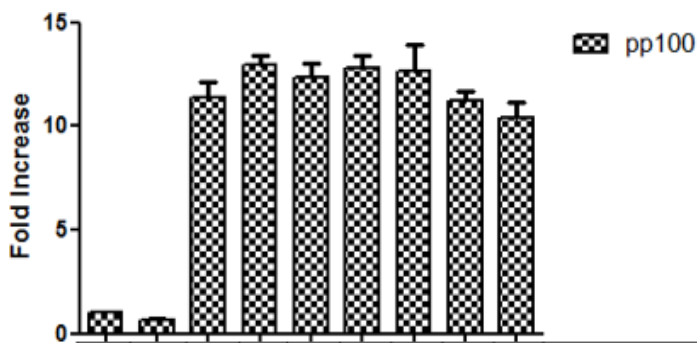
Figure 4.31: The effect IKK2 X1 on TNF α -mediated I κ B α degradation in U2OS cells. Cells were pre-treated with IKK2 X1 for 1 h prior to stimulation with TNF α (10 ng/ml) for 30 min. Whole cell extracts were assessed for I κ B α (37 kDa) and total p65 (65 kDa) which was used as a loading control, as outlined in Section 2.5. Blots were semi-quantified by scanning densitometry and results expressed as fold increase relative to control for B) I κ B α degradation. Each value represents the mean \pm SEM of three independent experiments. Data was analysed using a one-way ANOVA test, *** $p < 0.001$ vs TNF α and DMSO as an agonist stimulated control.

A



...	30	0.3	1	3	10	30	IKK2 X1 (μM)
...	+	DMSO (0.15 %)
...	...	+	+	+	+	+	+	+	TNF α (5 ng/ml)

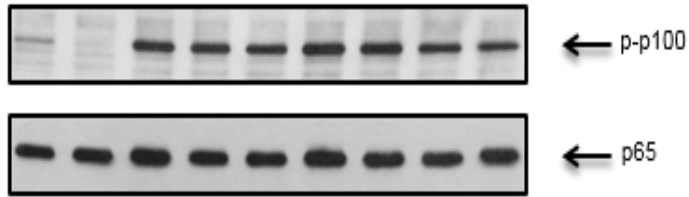
B



...	30	0.3	1	3	10	30	IKK2 X1 (μM)
...	+	DMSO (0.15 %)
...	...	+	+	+	+	+	+	+	TNF α (5 ng/ml)

Figure 4.32: The effect IKK2 X1 on TNF α induced phosphorylation of p100 in U2OS cells. Cells were pre-treated with IKK2 X1 for 1 h prior to stimulation with TNF α (5 ng/ml) for 15 min. Whole cell extracts were assessed for p-p100 (100 kDa) and total p65 (65 kDa) which was used as a loading control, as outlined in Section 2.5. Blots were semi-quantified by scanning densitometry and results expressed as fold increase relative to control for B) p100 phosphorylation. Each value represents the mean \pm SEM of three independent experiments. Data was analysed using a one-way ANOVA test.

A



...	30	0.3	1	3	10	30	IKK2 X1 (μM)
...	+	DMSO (0.15 %)
...	...	+	+	+	+	+	+	+	IL-1 β (5 ng/ml)

B

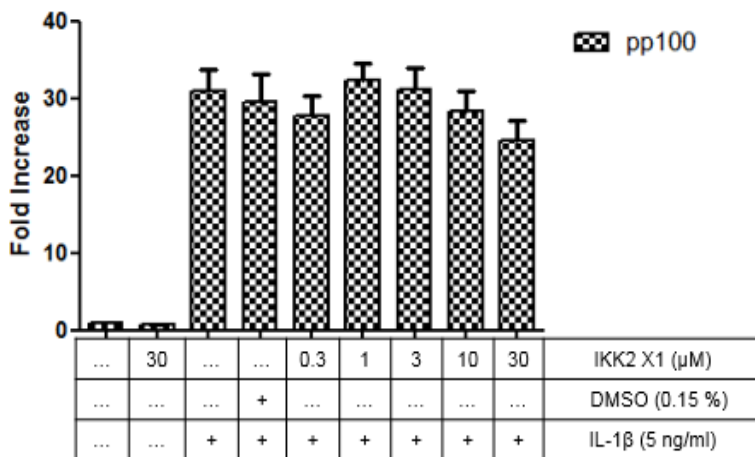


Figure 4.33: The effect IKK2 X1 on IL-1 β induced phosphorylation of p100 in U2OS cells. Cells were pre-treated with IKK2 X1 for 1 h prior to stimulation with IL-1 β (5 ng/ml) for 30 min. Whole cell extracts were assessed for p-p100 (100 kDa) and total p65 (65 kDa) which was used as a loading control, as outlined in Section 2.5. Blots were semi-quantified by scanning densitometry and results expressed as fold increase relative to control for B) p100 phosphorylation. Each value represents the mean \pm SEM of three independent experiments. Data was analysed using a one-way ANOVA test.

4.2.7 The role of IKK α in the regulation of CXCL12 expression in U2OS-CXCL12 cells

Our previous studies for both of IKK α knockdown and pharmacological intervention demonstrated that IKK α is involved in TNF α -and IL-1 β -induced non-canonical NF- κ B pathway in U2OS cells. Therefore, we sought to correlate these effects with the expression of likely IKK α dependent genes. Of those previously identified, CXCL12 is one which has the potential to be regulated by IKK α (Chapter 1 Sections 1.4.4.6 & 1.5.3). As described in Chapter 2 (Section 2.7.1), CXCL12 promoter construct (pPSDF1100LUC plasmid) was used to construct a CXCL12 reporter assay. CXCL12 expression was examined in two ways, firstly using a CXCL12 luciferase reporter cell line already developed in the laboratory designated as U2OS-CXCL12, and the second by examining endogenous CXCL12 mRNA using quantitative PCR.

4.2.7.1 LT $\alpha_1\beta_2$, TNF- α , and IL-1 β induced CXCL12 luciferase activity in U2OS- CXCL12 cells in concentration dependent manner

The initial aim was to identify the optimal concentration for agonist induced CXCL12 luciferase activity. In Figure 4.34, U2OS-CXCL12 cells were stimulated with increasing concentrations of LT $\alpha_1\beta_2$, TNF α and IL-1 β for 8 h. The response to LT $\alpha_1\beta_2$ was poor, the maximum concentration used only stimulated an approximate 1.5 fold increase in reporter activity (Fold induction for CXCL12 = 1.64 ± 0.05 , $p < 0.01$). By contrast, both TNF α and IL-1 β were able to stimulate CXCL12 to a maximal response at 5 ng/ml of TNF α and IL-1 β (TNF α Fold induction for CXCL12 = 2.95 ± 0.14 , $p < 0.001$, IL-1 β Fold induction for CXCL12 = 3.57 ± 0.19 , $p < 0.001$, respectively).

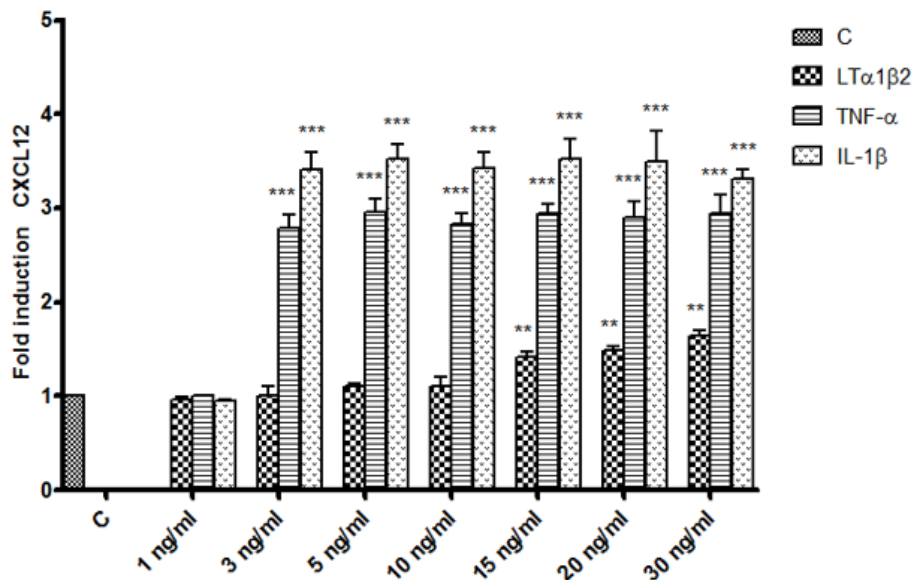


Figure 4.34: Concentration dependency of LT α 1 β 2, TNF α and IL-1 β -induced CXCL12 luciferase activity in U2OS-CXCL12 cells. Cells were stimulated with agonists at the indicated concentrations for 8 h. Whole cell extracts were then measured for luciferase assay as previously described in Section 2.7. Data shown is expressed as fold induction and each value represents the mean \pm SEM of three independent experiments. Data was analysed using a two-way ANOVA test, ** $p < 0.01$, *** $p < 0.001$ vs control.

4.2.7.2 LT α 1 β 2, TNF α and IL-1 β induce CXCL12 luciferase activity in U2OS-CXCL12 cells

Figure 4.35 illustrates a time course of LT α 1 β 2-TNF α -and IL-1 β -induced CXCL12 luciferase activity over 24 h. U2OS-CXCL12 cells were stimulated with LT α 1 β 2 (20 ng/ml), TNF α (5 ng/ml) and IL-1 β (5 ng/ml) for the indicated time points. Both TNF α and IL-1 β induced CXCL12 luciferase activity to a greater extent than LT α 1 β 2. Increased CXCL12 reporter activity was observed as early as 2 h and reached a maximum level by 8 h with no further increase up to 24 h, the longest time point examined (TNF α Fold induction for CXCL12 = 2.95 ± 0.14 , $p < 0.001$, IL-1 β Fold induction for CXCL12 = 3.57 ± 0.19 , $p < 0.001$). There was a delay in the response to LT α 1 β 2 before CXCL12 luciferase activity started to increase at 8 h which was the maximum response recorded (LT α 1 β 2 fold induction for CXCL12 = 2.06 ± 0.47 , $p < 0.05$).

Given that the responses to $LT\alpha_1\beta_2$ was very weak, the responses to $LT\alpha_1\beta_2$ in combination with either $TNF\alpha$ or $IL-\beta$ was examined as shown in Figure 4.36 $LT\alpha_1\beta_2$ (20 ng/ml) alone gave a modest increase CXCL12 luciferase activity (Fold induction = 1.52 ± 0.10) both $TNF\alpha$ or $IL-1\beta$ significantly increased CXCL12 as observed previously ($TNF\alpha$ Fold induction for CXCL12 = 2.83 ± 0.7 , $p < 0.001$; $IL-1\beta$ Fold induction for CXCL12 = 3.40 ± 0.02 , $p < 0.001$) compared to the control. Interestingly, the combination of either $TNF\alpha$ or $IL-1\beta$ with $LT\alpha_1\beta_2$ was largely additive with little evidence for synergy or marked potentiation ($LT\alpha_1\beta_2 + TNF\alpha$ Fold induction for CXCL12 = 2.93 ± 0.9 , $p < 0.001$, $LT\alpha_1\beta_2 + IL-1\beta$ Fold induction for CXCL12 = 3.67 ± 0.05 , $p < 0.001$).

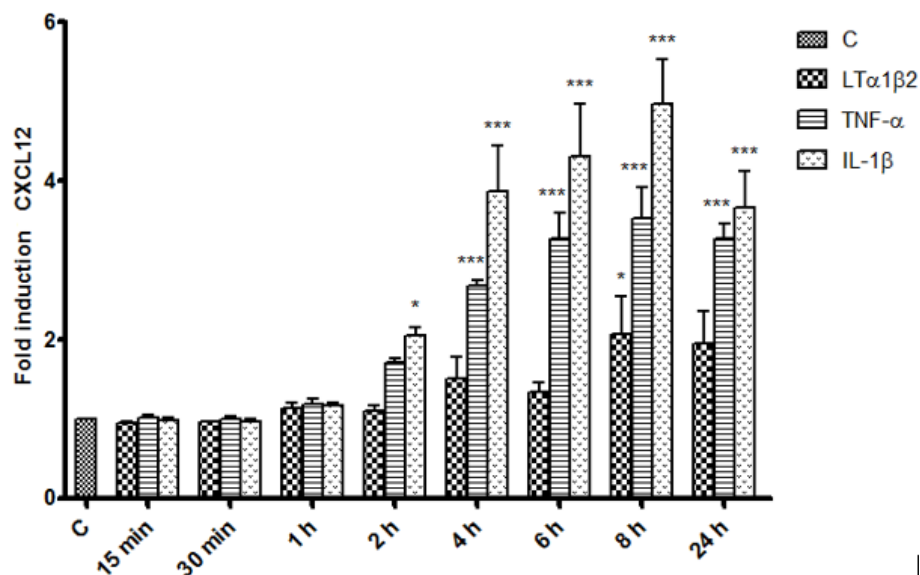


Figure 4.35: Time course of $LT\alpha_1\beta_2$, $TNF-\alpha$ and $IL-1\beta$ -mediated CXCL12 luciferase activity in U2OS-CXCL12 cells. Cells were stimulated with $LT\alpha_1\beta_2$ (20 ng/ml), $TNF\alpha$ (5 ng/ml) and $IL-1\beta$ (5 ng/ml) for the indicated time points. Whole cell extracts were then measured for luciferase assay as previously described in Section 2.7. Data shown is expressed as fold induction and each value represents the mean \pm SEM of three independent experiments. Data was analysed using a two-way ANOVA test, * $p < 0.05$, *** $p < 0.001$ vs control.

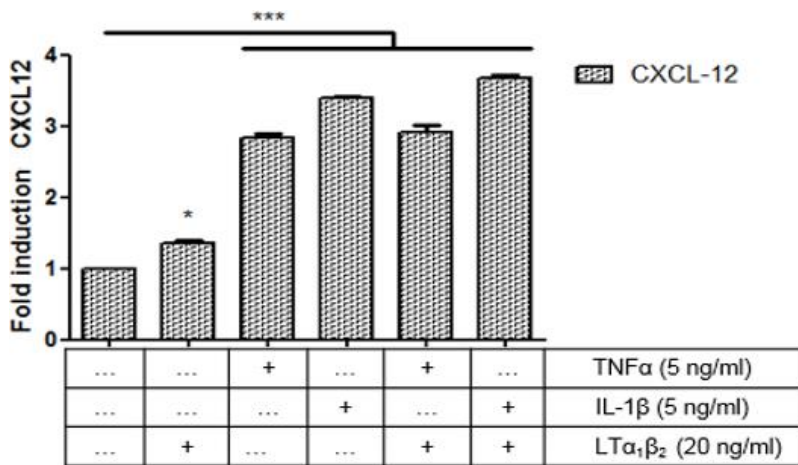


Figure 4.36: The effect of TNF- α and IL-1 β on LT $\alpha_1\beta_2$ -induced CXCL12 luciferase activity in U2OS-CXCL12 cells. Cells were either incubated with LT $\alpha_1\beta_2$ (20ng/ml), TNF- α (5ng/ml), and IL-1 β (5ng/ml) alone, or a combination of both cytokines (LT $\alpha_1\beta_2$ + TNF α) or (LT $\alpha_1\beta_2$ + IL-1 β) for 8 h. Whole cell extracts were then measured for luciferase activity as previously described in Section 2.7. Data shown is expressed as fold induction and each value represents the mean \pm SEM of three independent experiments. Data was analysed using a one-way ANOVA test, * $p < 0.05$, *** $p < 0.001$ vs control.

4.2.7.3 The effect of IKK α and IKK β siRNA silencing on LT $\alpha_1\beta_2$ -induced CXCL12 luciferase activity in U2OS-CXCL12 cells

Figure 4.37 shows the effect of IKK α and IKK β siRNA on LT $\alpha_1\beta_2$ induced-CXCL12 in U2OS-CXCL12 cells. The luciferase activity shows that LT $\alpha_1\beta_2$ alone modestly increased CXCL12 reporter activity compared to control (Fold induction = 2.17 ± 0.03 , $p < 0.001$). This response was not altered following transfection with either siRNA.

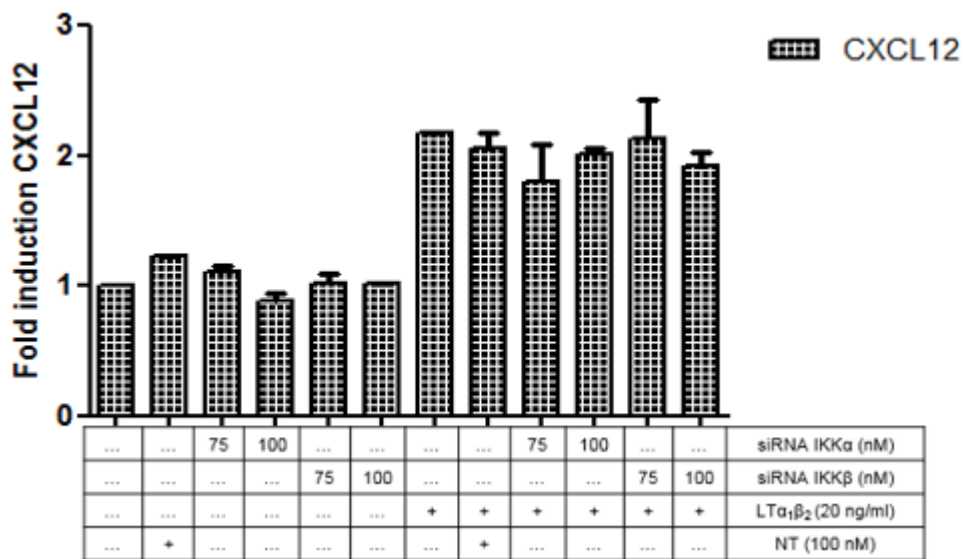


Figure 4.37: The effect of IKK α and IKK β siRNA on LT $\alpha_1\beta_2$ induced CXCL12 luciferase activity in U2OS-CXCL12 cells. Cells were transfected with 100nM of non-targeting (NT), IKK α and IKK β siRNA (75, 100 nM) for 96 h prior to stimulation with 20 ng/ml of LT $\alpha_1\beta_2$ for 8 h. Whole cell extracts were then measured for luciferase activity as previously described in Section 2.7. Data shown is expressed as fold induction and each value represents the mean \pm SEM of three independent experiments. Data was analysed using a one-way ANOVA test.

4.2.7.4 Characterisation of the role of IKK α and IKK β in the regulation of TNF α - induced CXCL12 luciferase activity in U2OS-CXCL12 cells

The effect of IKK knockdown on TNF α -stimulated CXCL12 reporter activity was explored in Figure 4.38, TNF α alone markedly increased CXCL12 luciferase activity compared to control (Fold induction = 2.97 ± 0.03 , $p < 0.001$). Transfecting cells with siRNA IKK α led to a significant, 30% reduction in TNF α -stimulated CXCL12 reporter activity compared to the non-target (NT) control (IKK α siRNA 75 nM: Fold induction = 2.31 ± 0.03 , IKK α siRNA 100 nM: Fold stim = 2.34 ± 0.03 $P < 0.01$). In contrast, transfecting cells with 75 or 100 nM of siRNA IKK β did not affect expression.

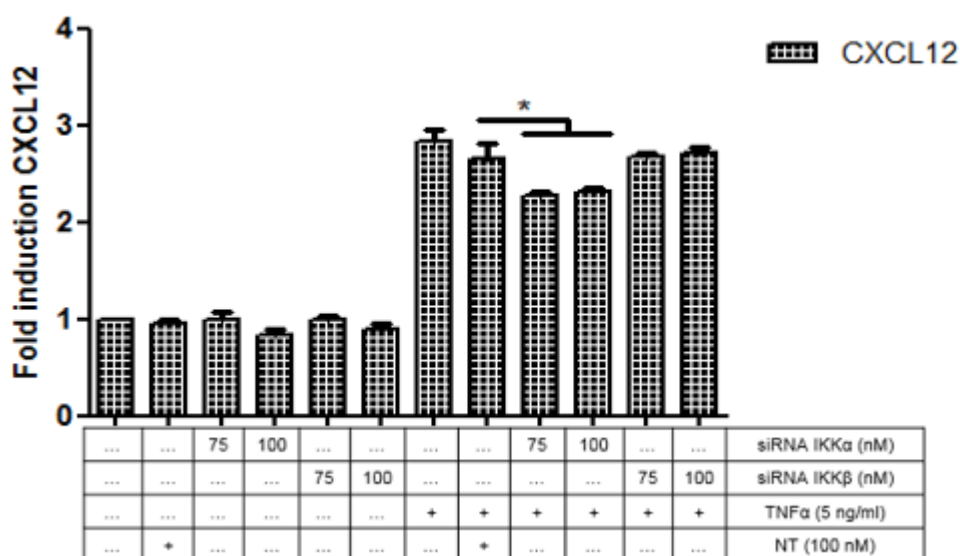


Figure 4.38: The effect of IKK α and IKK β siRNA on TNF α induced CXCL12 luciferase activity in U2OS-CXCL12 cells. Cells were transfected with 100 nM of non-targeting (NT), IKK α and IKK β siRNA (75 and 100 nM) for 96 h prior to stimulation with 5 ng/ml of TNF- α for 8 h. Whole cell extracts were then measured for luciferase activity as previously described in Section 2.7. Data shown is expressed as fold induction and each value represents the mean \pm SEM of three independent experiments. Data was analysed using a one-way ANOVA test, * $p < 0.05$ vs an agonist-stimulated control.

4.2.7.5 Characterisation of the role of IKK α and IKK β in the regulation of IL-1 β - induced CXCL12 luciferase activity in U2OS-CXCL12 cells

Figure 4.39 shows the effect of knockdown of IKK α and IKK β on IL-1 β -induced CXCL12 reporter activity in U2OS-CXCL12 cells. Transfecting U2OS cells with 75 and 100 nM siRNA IKK α led to a significant decline in CXCL12 luciferase activity from 4 fold to 3.46 fold. In contrast siRNA IKK β promoted a small but significant increase in CXCL12 luciferase activity (IKK β siRNA 75 nM: Fold induction = 4.48 ± 0.01 , IKK β siRNA 100 nM: Fold stim = 4.20 ± 0.08 , $p < 0.001$) compared to the non-target (NT) control.

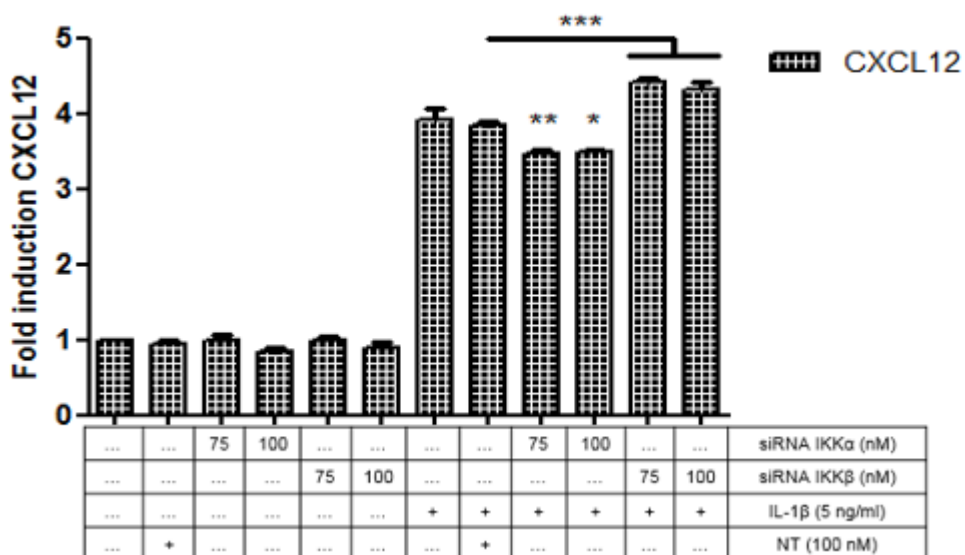


Figure 4.39: The effect of IKK α and IKK β siRNA on IL-1 β induced CXCL12 luciferase activity in U2OS-CXCL12 cells. Cells were transfected with 100 nM of non-targeting (NT), IKK α and IKK β siRNA (75 and 100 nM) for 96 h prior to stimulation with 5 ng/ml of IL-1 β for 8 h. Whole cell extracts were then measured for luciferase activity as previously described in section 2.7. Data shown is expressed as fold induction and each value represents the mean \pm SEM of three independent experiments. Data was analysed using a one-way ANOVA test, * $p < 0.05$, ** $p < 0.01$, *** $p < 0.001$ vs an agonist-stimulated control.

4.2.8 The effect of SU compounds on CXCL12 luciferase activity in U2OS-CXCL12 cells

4.2.8.1 The effect of SU compounds on $LT\alpha_1\beta_2$ induced CXCL12 luciferase activity in U2OS-CXCL12 cells

To further confirm a role for $IKK\alpha$ in CXCL12 luciferase activity, the SU compounds previously characterised were utilised. Figure 4.40 demonstrates the effect of SU1261 on $LT\alpha_1\beta_2$ induced CXCL12 luciferase activity in U2OS-CXCL12 cells. $LT\alpha_1\beta_2$ induced a modest increase in CXCL12 (Fold increase = 1.69 ± 0.06). This response was reduced by pre-treatment with increasing concentrations of SU1261, the inhibition being marked between 3-30 μM (3 μM : Fold increase = 0.78 ± 0.02 , 10 μM : 0.63 ± 0.03 , and 30 μM : 0.65 ± 0.06 $p < 0.001$). Similarly, SU1266 also significantly reduced CXCL12 luciferase activity in U2OS-CXCL12 cells in a concentration-dependent manner over the low micromolar range as shown in Figure 4.41 (3 μM : Fold increase = 1.01 ± 0.09 , 10 μM : 0.99 ± 0.05 , and 30 μM : 0.70 ± 0.01 , $p < 0.001$).

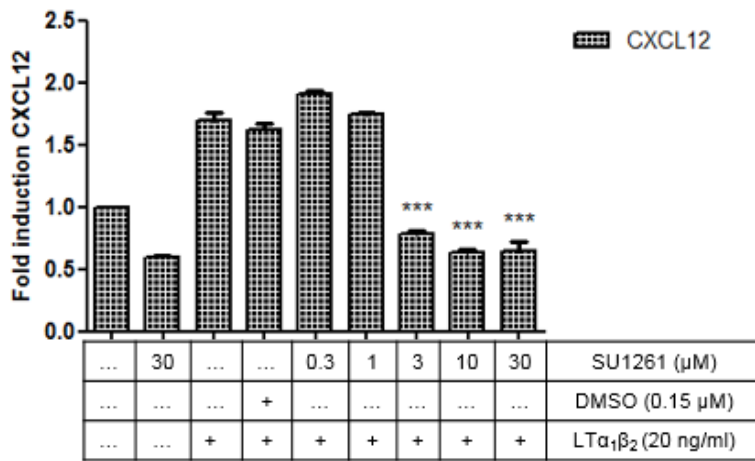


Figure 4.40: The effect of SU1261 upon LT $\alpha_1\beta_2$ -mediated CXCL12 luciferase activity in U2OS-CXCL12 cells. Cells were pre-treated with SU1261 for 1 h prior to stimulation with LT $\alpha_1\beta_2$ (20 ng/ml) for 8 h. Whole cell extracts were then measured for luciferase activity as previously described in Section 2.7. Data shown is expressed as fold induction and each value represents the mean \pm SEM of three independent experiments. Data was analysed using a one-way ANOVA test, *** p <0.001 vs an agonist-stimulated control.

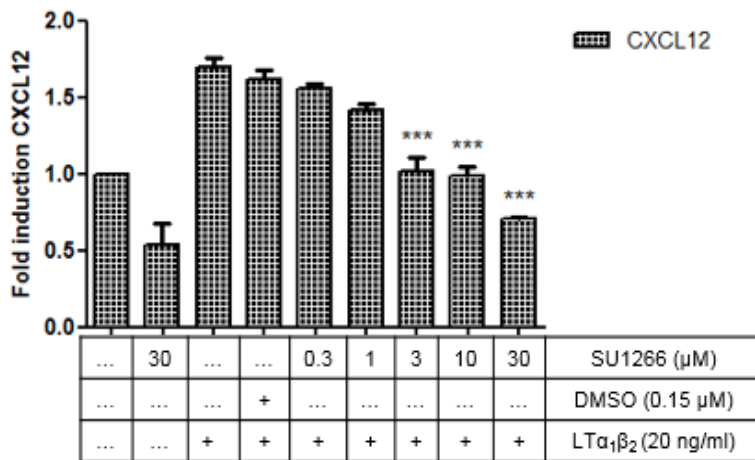


Figure 4.41: The effect of SU1266 upon LT $\alpha_1\beta_2$ -mediated CXCL12 luciferase activity in U2OS-CXCL12 cells. Cells were pre-treated with SU1266 for 1 h prior to stimulation with LT $\alpha_1\beta_2$ (20 ng/ml) for 8 h. Cell lysates were then measured for luciferase activity as previously described in Section 2.7. Data shown is expressed as fold induction and each value represents the mean \pm SEM of three independent experiments. Data was analysed using a one-way ANOVA test, *** p <0.001 vs an agonist-stimulated control.

4.2.8.2 The effect of SU compounds on TNF α -induced CXCL12 luciferase activity in U2OS-CXCL12 cells

Figure 4.42 shows the effect of SU1261 on TNF α -induced CXCL12 luciferase activity in U2OS-CXCL12 cells. TNF α was able to induce CXCL12 by 3.60 fold (\pm 0.11, $p < 0.001$). A concentration of 3 μ M SU1261 caused a significant inhibition in CXCL12 activity, approximately 70%, whereas a greater decrease was observed at 10 and 30 μ M. Likewise, CXCL12 reporter activity induced by TNF α was markedly decreased by pre-treatment with SU1266 over the low micromolar range (1-30 μ M) as shown in Figure 4.43. The highest concentration of SU1266 effectively abolished CXCL12 activity (SU1266 30 μ M: Fold increase = 0.22 ± 0.02 , $p < 0.001$).

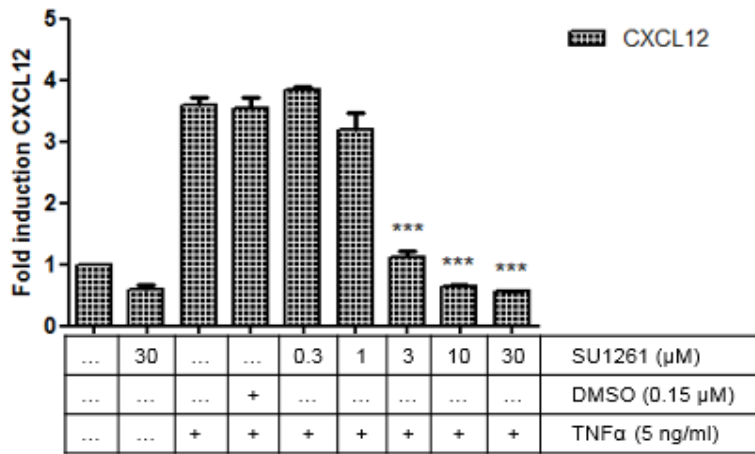


Figure 4.42: The effect of SU1261 upon TNF α -mediated CXCL12 luciferase activity in U2OS-CXCL12 cells. Cells were pre-treated with SU1261 for 1 h prior to stimulation with TNF α (5 ng/ml) for 8 h. Cell lysates were then measured for luciferase activity as previously described in Section 2.7. Data shown is expressed as fold induction and each value represents the mean \pm SEM of three independent experiments. Data was analysed using a one-way ANOVA test, *** p <0.001 vs an agonist-stimulated control.

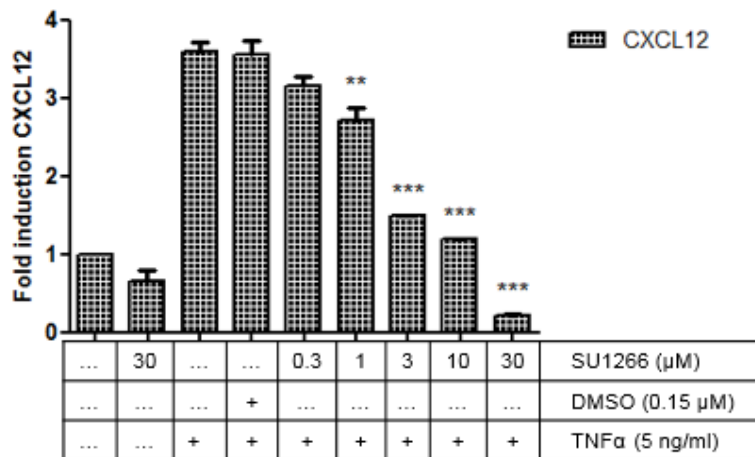


Figure 4.43: The effect of SU1266 upon TNF α -mediated CXCL12 luciferase activity in U2OS-CXCL12 cells. Cells were pre-treated with SU1266 for 1 h prior to stimulation with TNF α (5 ng/ml) for 8 h. Cell lysates were then measured for luciferase activity as previously described in Section 2.7. Data shown is expressed as fold induction and each value represents the mean \pm SEM of three independent experiments. Data was analysed using a one-way ANOVA test, ** p <0.01, *** p <0.001 vs an agonist-stimulated control.

4.2.8.3 The effect of SU compounds on IL-1 β -induced CXCL12 luciferase activity in U2OS-CXCL12 cells

Similar to their impact against TNF α , Figure 4.44 shows the effect of SU1261 against IL-1 β -induced CXCL12 luciferase activity in U2OS-CXCL12 cells. Stimulation with IL-1 β significantly increased CXCL12 reporter activity by more than four-fold (Fold increase = 4.34 ± 0.15 , $p < 0.001$). At micromolar concentrations of SU1261 (3-30 μ M), CXCL12 reporter activity was strongly inhibited by approximately 90% at the highest concentration. Similar to the effect SU1261, SU1266 (3-30 μ M) significantly reduced the reporter activity of CXCL12 induced by IL-1 β (Figure 4.45). Again, this response was inhibited by approximately 90% at 30 μ M.

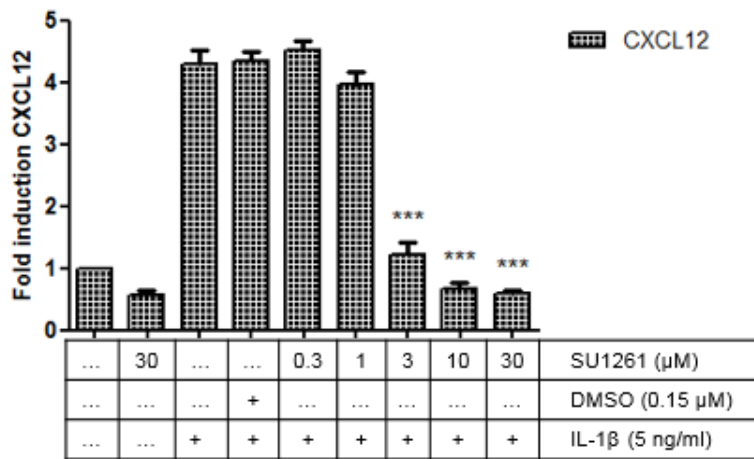


Figure 4.44: The effect of SU1261 upon IL-1 β -mediated CXCL12 luciferase activity in U2OS-CXCL12 cells. Cells were pre-treated with SU1261 for 1 h prior to stimulation with IL-1 β (5 ng/ml) for 8 h. Cell lysates were then measured for luciferase activity as previously described in Section 2.7. Data shown is expressed as fold induction and each value represents the mean \pm SEM of three independent experiments. Data was analysed using a one-way ANOVA test, *** p <0.001 vs an agonist-stimulated control.

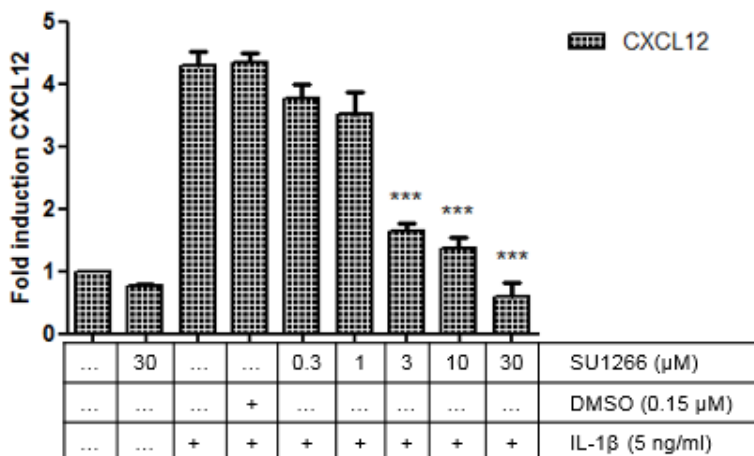


Figure 4.45: The effect of SU1266 upon IL-1 β -mediated CXCL12 luciferase activity in U2OS-CXCL12 cells. Cells were pre-treated with SU1266 for 1 h prior to stimulation with IL-1 β (5 ng/ml) for 8h. Cell lysates were then measured for luciferase activity as previously described in Section 2.7. Data shown is expressed as fold induction and each value represents the mean \pm SEM of three independent experiments. Data was analysed using a one-way ANOVA test, *** p <0.001 vs an agonist-stimulated control.

4.2.5.4 IC₅₀ values for CXCL12 luciferase activity by SU compounds in U2OS-CXCL12 cells

Next, IC₅₀ values for the SU compounds were calculated by analysis of the Western blotting results. The data were fitted in a sigmoidal concentration-response curve and the IC₅₀ values of SU1261 and SU1266 calculated using GraphPad Prism software (Figure 4.46). The IC₅₀ values for inhibition of CXCL12 luciferase activity by SU1261 and SU1266 were determined after stimulation with LT $\alpha_1\beta_2$ (20 ng/ml) (Panel A and B), TNF α (5 ng/ml) (Panel C and D) and IL-1 β (5 ng/ml) (panel E and F) for 8 h. A number of issues were identified, the concentration-response curves for SU1266 compound were shallow in comparison to SU1261 compound due to not enough points in the dynamic part of the curve for SU1266 compound, and therefore the range for this compound was not standard. However, SU1261 showed IC₅₀ against CXCL12 luciferase activity less than 1.74 μ M and it was more potent than SU1266.

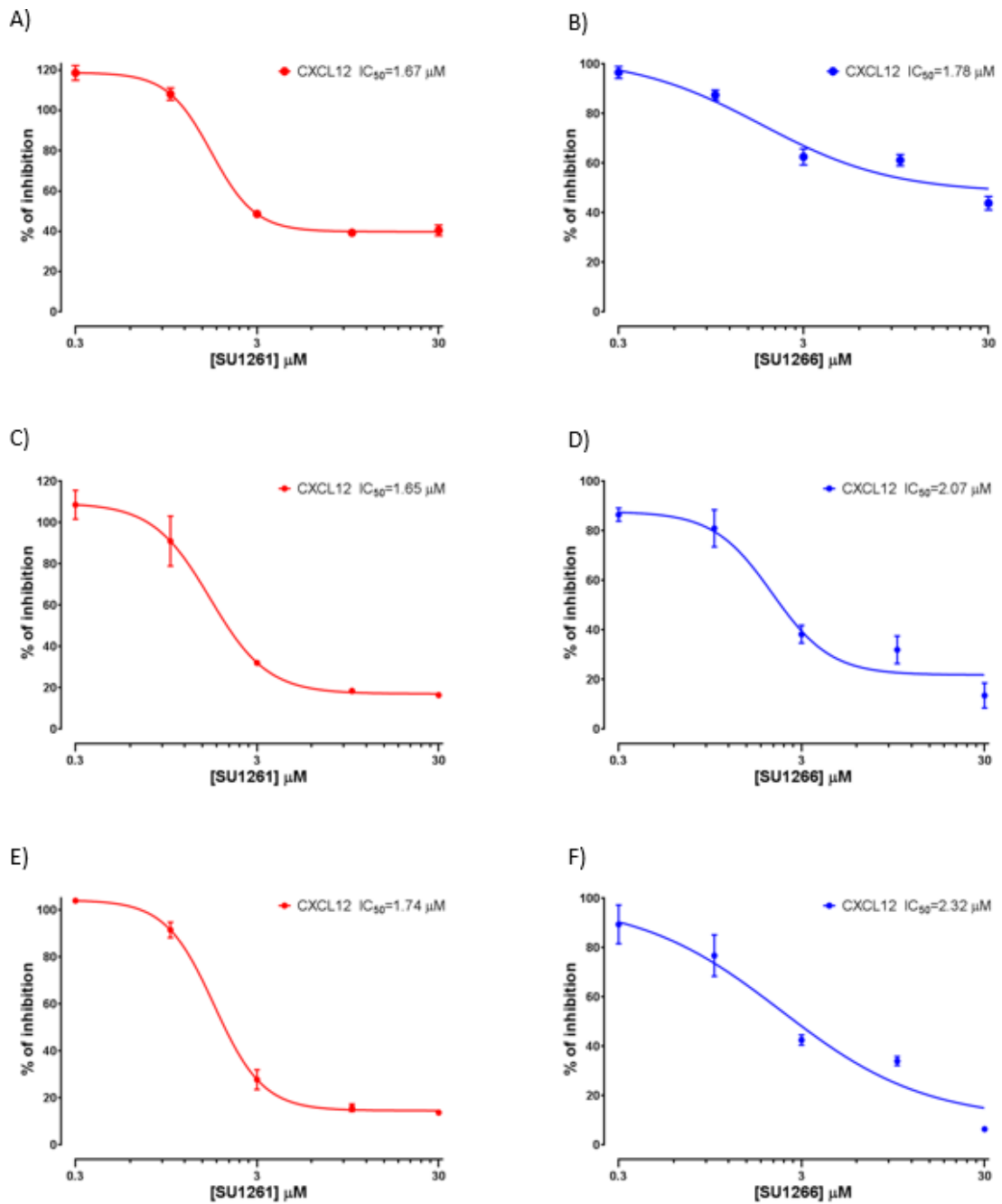


Figure 4.46: IC_{50} values for SU1261 and SU1266 against CXCL12 luciferase activity in U2OS-CXCL12 cells. Using GraphPad Prism software, version 7.0, the data obtained by Western blot analysis of SU1261 and SU1266 were fitted in a sigmoidal concentration-response curve for A) SU1261 following $\text{LT}\alpha_1\beta_2$ stimulation. B) SU1266 following $\text{LT}\alpha_1\beta_2$ stimulation C) SU1261 following $\text{TNF}\alpha$ stimulation. D) SU1266 following $\text{TNF}\alpha$ stimulation. E) SU1261 following $\text{IL-1}\beta$ stimulation. F) SU1266 following $\text{IL-1}\beta$ stimulation.

4.2.9 The role of IKK α in the regulation of CXCL12 expression using RT-qPCR in U2OS cells

The luciferase reporter activity data suggested differences in CXCL12 activity in response to the agonists used in this study and the role of IKK α in the regulation of this expression. Therefore, the role of IKK α in CXCL12 regulation was verified by endogenous expression using RT-qPCR.

Figure 4.47 shows a time course up to 24 h for LT $\alpha_1\beta_2$ for the induction of CXCL12 expression in U2OS cells. LT $\alpha_1\beta_2$ stimulation induced a minor increase in CXCL12 expression level at 8 h, which subsequently decreased at 24 h. In contrast, TNF α induced CXCL12 expression at 4 h, the maximum level of approximately three-fold was achieved at 8 h of stimulation and mRNA levels subsequently reduced at 24 h (Figure 4.48). IL-1 β induced the strongest CXCL12 response (Figure 4.49), expression significantly increased at 4 h ($p < 0.05$) with a maximum stimulation of 10 fold at 8 h (Fold increase = 10.76 ± 1.61 , $p < 0.001$). These findings demonstrated that TNF α and IL-1 β robustly up-regulates CXCL12 expression in U2OS cells in comparison to LT $\alpha_1\beta_2$, thus confirming the luciferase reporter data.

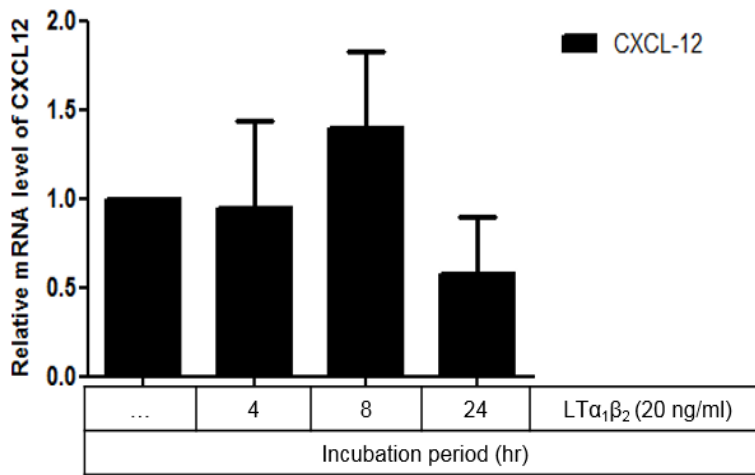


Figure 4.47: $LT\alpha_1\beta_2$ ligation induces non-canonical NF- κ B-dependent mRNA expression of CXCL12 in U2OS cells. Cells on 6-well plates were incubated with $LT\alpha_1\beta_2$ (20 ng/ml) for the indicated time points and RNA extraction as outlined in Section 2.8.1. Quantitative PCR analysis was performed as outlined in Section 2.8.4. Error bars represent the mean \pm SEM of triplicate determinations from three individual experiments. Data was analysed using a one-way ANOVA test.

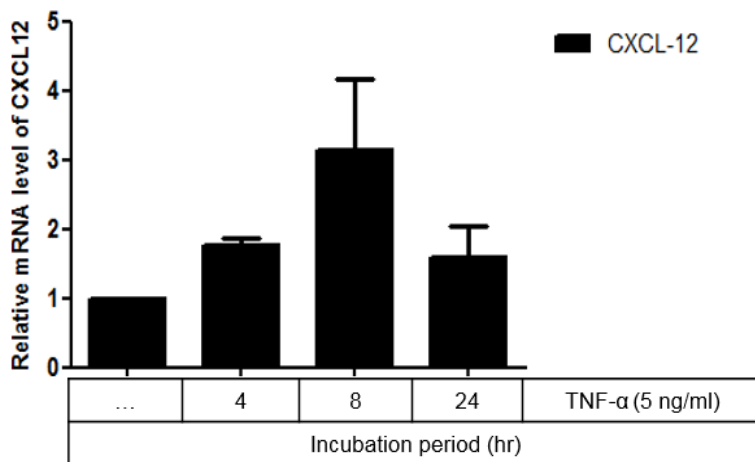


Figure 4.48: $TNF\alpha$ ligation induces non-canonical NF- κ B-dependent mRNA expression of CXCL12 in U2OS cells. Cells on 6-well plates were incubated with $TNF\alpha$ (5 ng/ml) for the indicated time points and RNA extraction as outlined in Section 2.8.1. Quantitative PCR analysis was performed as outlined in Section 2.8.4. Error bars represent the mean \pm SEM of triplicate determinations from three individual experiments. Data was analysed using a one-way ANOVA test.

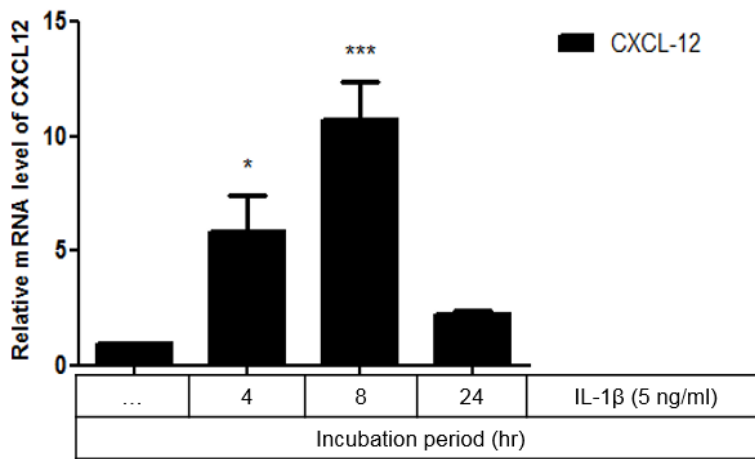


Figure 4.49: IL-1 β ligation induces non-canonical NF κ B-dependent mRNA expression of CXCL12 in U2OS cells. Cells on 6-well plates were incubated with IL-1 β (5 ng/ml) for the indicated time points and RNA extraction as outlined in Section 2.8.1. Quantitative PCR analysis was performed as outlined in Section 2.8.4. Error bars represent the mean \pm SEM of triplicate determinations from three individual experiments. Data was analysed using a one-way ANOVA test, * p <0.05, *** p <0.001 vs control.

4.2.9.1 The effect of SU1261 and IKK α siRNA silencing on IL-1 β -induced CXCL12 mRNA expression in U2OS cells

Next, the role of IKK α in the regulation of CXCL12 induction was explored by using SU1261 and IKK α siRNA (Figure 4.50). IL-1 β produced a robust 5.3-fold \pm 0.83 fold increase in CXCL12 mRNA expression in comparison to unstimulated cells (p < 0.001). Interestingly, it was found that SU1261 (10 μ M) markedly inhibited IL-1 β -induced CXCL12 mRNA expression by approximately 80% (SU1261 10 μ M: Fold increase = 1.61 \pm 0.53, p < 0.001). Furthermore, IKK α knockdown (100 nM) significantly reduced IL-1 β -induced CXCL12 expression by approximately 60% (siRNA IKK α 100nM Fold increase = 2.07 \pm 0.40, p < 0.05) compared to NT.

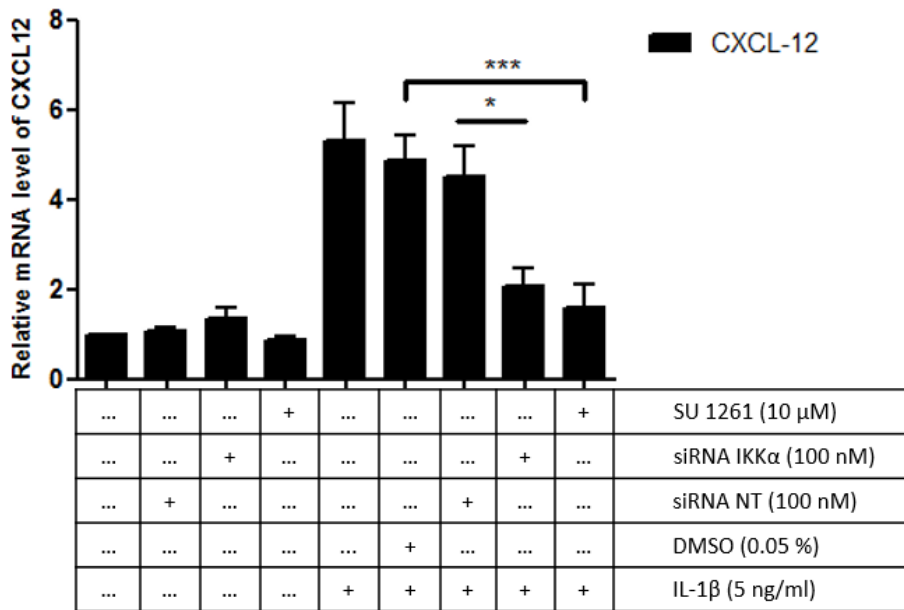


Figure 4.50: The effect of SU1261 and IKK α siRNA on IL-1 β induces non-canonical NF- κ B-dependent mRNA expression of CXCL12 in U2OS cells. Cells in 6-well culture plates and transfected with 100 nM of non-targeting (NT) and IKK α siRNA (100 nM) for 96 h, cells were also treated with 10 μ M SU1261 and 0.05% DMSO for 1 h. Cells were then stimulated with of IL-1 β (5 ng/ml) for 8 h. RNA extraction and qPCR was performed as outlined in sections 2.8.1 and 2.8.4. Error bars represent the mean \pm SEM of triplicate determinations from three individual experiments. Data was analysed using a one-way ANOVA test, * p < 0.05, *** p < 0.001 vs an agonist-stimulated control.

4.3 Discussion

Relatively little attention has focused on the role of the non-canonical NF- κ B pathway in the regulation of CXCL12, which is known to play a key role in a number of biological processes and cellular events related to tumour progression (Wharry et al., 2009). The aim of the chapter was to characterise the role of IKK α in the regulation of CXCL12 expression via the activation of non-canonical NF- κ B pathway in U2OS cells. Two approaches were employed to investigate the role of IKK α in this study, firstly the classical pharmacological inhibition strategy using SU compounds characterised in Chapter 3. Secondly, using small interference RNA (siRNA). These strategies have revealed an important role for IKK α in the regulation of CXCL12 expression via the non-canonical NF- κ B pathway activation in response to TNF α and IL-1 β , which were both found to activate this pathway in a manner different to the usual activation by LT α 1 β 2. Furthermore, luciferase reporter activity and RT-qPCR data revealed that IKK α could influence CXCL12 expression mediated by these agonists.

Initially, the kinetics of LT α 1 β 2 induced p100 phosphorylation and p100 processing was examined and compared to TNF α and IL-1 β ligands. Several studies showed that in various types of cells, the activation of non-canonical NF- κ B pathway in response to LT β R is slow (Ganef et al., 2011, Madge et al., 2008, Dejardin, 2006, Xiao et al., 2001, Matsushima et al., 2001) and consistent with the transcriptional responses which are thought to be delayed and longer-lasting (Sun, 2012, Werner et al., 2005). Our results agree with these studies; in U2OS cells LT α 1 β 2 stimulated a slow increase in p100 phosphorylation and nuclear translocation of NF- κ B isoforms, which in turn may be explained by the fact that NIK activation is a slow process involving TRAF3 mediated stabilisation NIK and *de novo* protein synthesis (Liao et al., 2004).

By contrast, TNF α and IL-1 β are well known stimuli for activating the canonical NF- κ B pathway (Plotnikov et al., 2011). Nonetheless, they were tested as activators of

the non-canonical NF- κ B pathway in U2OS cells in the expectation that they would stimulate p52 formation through increased p100 expression. Surprisingly, a far earlier kinetic profile for TNF α and IL-1 β was identified, the phosphorylation of p100 was rapid with onset as early as 15 min, while the activation of nuclear translocation of both p52-RelB was observed at 60 min (Figures 4.2, 4.5, 4.6 and 4.9). However, it should be noted that p52 levels did concomitantly increase with p100 expression, suggesting that newly synthesised p100 may dictate the levels of p52 irrespective whether or not *bona fide* processing is on-going. It is worth mentioning that the responses to TNF α or IL-1 β could not be replicated in other cells lines such as MCF7 or CAFs; this novel profile may therefore be restricted to certain cell types. According to recent studies, TNF α can activate the non-canonical NF- κ B pathway in specific cell types, but again this activation was found to be slow and long-lasting (Kim et al., 2011, Lotzer et al., 2010, Oeckinghaus and Ghosh, 2009). Our results have not been described previously, in which the most surprising aspect of the data is in the activation of non-canonical NF- κ B pathway at early times, suggesting differences in receptor coupling to intermediates of the non-canonical NF- κ B pathway.

The differences in activation of this pathway may be related to upstream modulation of the pathways by NIK, TRAF2 and TRAF3. The non-canonical NF- κ B pathway involves the activation of the NIK, stabilisation and accumulation occur through degradation of TRAF3 (Lich et al., 2007, Liao et al., 2004). In addition to TRAF3, TRAF2 is known to play a negative role in p100 to p52 processing (Grech et al., 2004), however, TRAF3 degradation is certainly a hallmark for non-canonical NF- κ B activation (Hacker and Karin, 2006). However, for so many of these studies conclusions are based on transfection experiments with often long stimulation times; the early action of the pathway in this study implies that sufficient NIK is already present or TRAF3 already degraded. A number of researchers have reported that

LT β R signalling requires NIK (Matsushima et al., 2001, Yin et al., 2001), the slow kinetics for this agonist found in U2OS cells is consistent with the general model described above. Again this would imply that in U2OS cells, the intermediates within the pathway are functioning normally.

Preliminary studies designed to assess events upstream in U2OS cells were not successful. As expected NIK levels were low in U2OS cells, compared with an adenoviral positive control and did not increase in response to LT $\alpha_1\beta_2$ nor IL-1 β (data not shown). One issue may be the quality of the antibodies used, non-specific binding was substantial and it was difficult to demonstrate clear binding to endogenous NIK. In contrast, whilst no changes were found in cellular TRAF2 levels in response to LT $\alpha_1\beta_2$, there was minor degradation of TRAF3. In addition, there was a partial degradation in both TRAF2 and TRAF3 in response to IL-1 β but again the quality of the antibodies were questionable (data not shown). This may however suggest that LT $\alpha_1\beta_2$ and IL-1 β have the potential to regulate the non-canonical NF- κ B pathway via the degradation of TRAF3 but further studies are required. The role of IKK α and NIK is however, not restricted to activation of the non-canonical NF- κ B pathway; there is compelling evidence showing that activation of IKK α induces its nuclear translocation and to independently regulates other factors that eventually lead to gene expression (Chapter 1 Figure 1.5) (Chariot, 2009).

In addition, there were a number of further inconsistencies which the data has revealed. In contrast to SU compounds, our results showed that phosphorylation of p100 and p52 formation induced by LT $\alpha_1\beta_2$ was not affected by siRNA IKK α but substantially inhibited by the selective inhibitors. This inconsistency may be due to the different inhibition strategies. Inhibition of a kinase as opposed to full protein deletion can give rise to different results (Weiss et al., 2007, Abeliovich et al., 2003). Given that IKK α operates in a complex with a number of other proteins then knock

down may result in a complex array of outcomes. In addition, it is possible that for the SU compounds there are off target effects and inhibition of other pathways which may affect regulation of the pathway particularly at later times. These possibilities await to be investigated. Interestingly, the canonical IKK signalling pathway can feed the non-canonical NF- κ B pathway through upregulation of p100, but the processing of p100 is solely dependent on its phosphorylation by IKK α which occurs by the activation of the NIK (Xiao et al., 2001, Senftleben et al., 2001).

The second part of this chapter linked IKK α knock down and pharmacological intervention to a downstream outcome. As mentioned in Chapter one, several studies identified CXCL12 as regulated by IKK α via the non-canonical NF- κ B pathway (Madge and May, 2010, Madge et al., 2008). This chemokine has been shown to be highly up-regulated in various types of human cancers, including bone sarcoma (Dewan et al., 2006, Perissinotto et al., 2005). A CXCL12 reporter assay and assessment of endogenous mRNA using RT-qPCR were used to define the role of IKK α in the regulation of CXCL12 induction. Initial time courses for both approaches demonstrated that the levels of CXCL12 induced by LT $\alpha_1\beta_2$ were lower than levels induced by TNF α or IL-1 β . This increase in CXCL2 expression is likely to be related to binding sites within the CXCL12 promoter for multiple regulatory elements and may suggest that activation of the non-canonical pathway alone is not sufficient for expression (Widmer et al., 1993). Moreover, this lower level of CXCL12 expression induced by LT $\alpha_1\beta_2$ may reflect the less robust p100 degradation and p52-ReI β nuclear translocation that was observed in response to LT $\alpha_1\beta_2$ compared to TNF α and IL-1 β . In terms of the pathways involved in regulation of CXCL12, results suggested a role for IKK α as defined by either siRNA or through the use of SU compounds. To date, work assessing the regulation of CXCL12 expression is restricted to very few papers, however analysis of the promoter region of the human CLCL12 gene revealed a

number of regulatory binding sites including Sp1, AP2, NFX3 and GR (Garcia-Moruja et al., 2005). Furthermore, a recent study has reported that hypoxia can regulate CXCL12 through two potential HIF-1 α binding sites, termed HBS1 and HBS2, in the promoter region of CXCL12 gene. In addition, it was found that HIF-1 α triggers CXCL12 synthesis through the HBS1 promoter region in endothelial cells (Ceradini et al., 2004).

However, specific IKK or p52 binding sites have not been identified. When examining the role of IKK α in CXCL12 regulation, it was found that IKK α siRNA was not effective against the small, LT α β β mediated response, whilst there was a small but significant inhibition of TNF α or IL-1 β -stimulated CXCL12 expression. In contrast, there was no effect of IKK β siRNA. The few other studies published support these results. Allen and colleagues found a role for non-canonical NF- κ B activation in increased CXCL12 mRNA expression in colon cancers (Allen et al., 2012). In endothelial cells, Madge and May demonstrated that siRNA knock down of IKK α inhibited CXCL12 mRNA whilst IKK β deletion enhanced CXCL12 production (Madge and May, 2010, Madge et al., 2008). This group further reported LT α β β induced CXCL12 expression via non-canonical NF- κ B activation, whereas TNF α regulated the level of p100 and RelB in endothelial cells via the canonical NF- κ B pathway, but did not activate the non-canonical pathway or induce the expression of CXCL12 (Madge et al., 2008). This partially supports the idea of IKK α driving CXCL12 expression but does imply that for U2OS cells activation of the canonical pathway either by TNF α or IL-1 β does not have a negative effect on CXCL12 expression. A recent study has shown that synergistic activation of both the canonical and non-canonical NF- κ B pathways resulted in a hyper induction of CXCL13 in mouse aorta smooth muscle cells (Lotzer et al., 2010). This may be the case in U2OS cells, further studies to address this were not carried out due to time constraints.

Other studies do however indicate a role for IKK α in the regulation of other genes which may be examined in the future. For example inhibition of NIK in mouse fibrosarcoma cells (BFS-1) reduced expression of CXCL2 stimulated in response to LT $\alpha_1\beta_2$ (Daller et al., 2011). Furthermore, IKK α regulates the production of other chemokines and cytokines such as IL-8/CXCL-8 and IL-6, kinase-dead NIK inhibits their production upon LT β R ligation (Smith et al., 2001). Other chemokines can be regulated by IKK α , including CXCL13, CCL21 and CCL19 (Wharry et al., 2009, Dejardin et al., 2002), suggesting that IKK α regulates chemokines via the non-canonical NF- κ B pathway. Therefore, one of the future strategies may be to conduct a chemokine/cytokine array and test IKK α sensitivity for each gene.

In summary, the findings in this chapter have identified for the first time a novel, rapid activation of the non-canonical NF- κ B pathway in U2OS cells by the cytokines TNF α and IL-1 β and suggest a mechanism of regulation distinct from the classical delayed response to LT $\alpha_1\beta_2$. Furthermore, this study establishes CXCL12 as a possible marker for IKK α dependent non-canonical NF- κ B activation in bone cancer. Furthermore, SU compounds could be a promising target for treating bone cancer and NF- κ B-associated diseases by virtue of CXCL12 inhibition.

Chapter Five

**Expression of CXCL12 and components of non-canonical
NF- κ B pathway in CAFs and NFs derived from clinical
specimens obtained from breast cancer patients**

5.1 Introduction

Having established in Chapter 4 that IKK α has the potential to regulate CXCL12 expression in U2OS cells, preliminary experiments were conducted in CAFs derived from breast cancer patients, which are known to express high levels of CXCL12. Thus, the potential for novel IKK α inhibitors to regulate CXCL12 production in a more pathologically relevant cancer model could be examined.

Cancer-associated fibroblasts (CAFs) have been described as the most abundant cellular component in the cancer stroma, and is one of the most important cell types in the tumour microenvironment (Kalluri, 2016, Lorusso and Ruegg, 2008). Haematological and solid tumour cells interact with CXCL12 within their microenvironment through its receptor, CXCR4. Orimo and co-workers demonstrated that CAFs within breast cancer promote tumour growth through the secretion of CXCL12 (Orimo et al., 2005). Another study reported that synergy between CXCL12 and TGF- β signalling in CAFs, derived from human breast cancer, leads to development of a tumour through promoting mammary stromal myofibroblasts (Kojima et al., 2010). As mentioned previously, IKK α -mediated non-canonical NF- κ B signalling in breast cancer (Hao et al., 2010, Cao et al., 2007, Cogswell et al., 2000), thus there is a potential link between IKK α , CXCL12 and cancer.

In this chapter, we focused on understanding the role of CAFs in breast cancer relative to activation of the non-canonical pathway and CXCL12 expression. The activation of non-canonical NF- κ B pathway was examined after exposure to LT $\alpha_1\beta_2$ and TNF α . Both siRNA and SU compounds were employed to prevent IKK α function and downstream effects on CXCL12 expression measured using RT-qPCR and ELISA assays.

5.2 Results

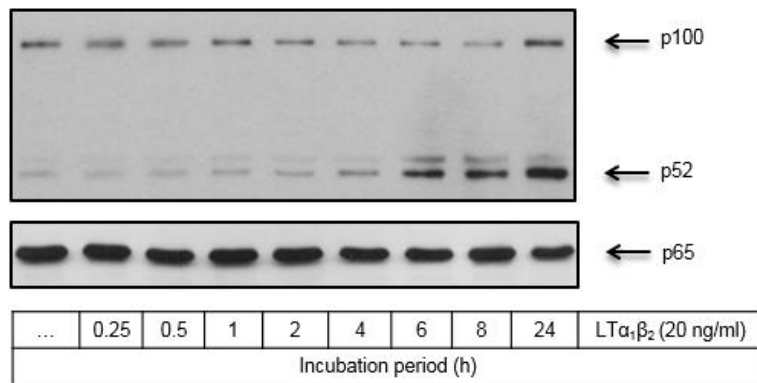
5.2.1 Activation of the non-canonical NF- κ B pathway in NFs and CAFs

Given that there is so little data on cellular signalling in CAFs a first step was to establish that induction of the non-canonical NF- κ B pathway could be observed in CAFs and NFs.

5.2.2 Activation of the non-canonical NF- κ B pathway in NFs

In preliminary experiments it was found that phosphorylation of p100 and p52 formation were not increased by TNF α (data not shown), while p100 processing was increased upon LT $\alpha_1\beta_2$ exposure. Figure 5.1 shows that in NFs exposed to LT $\alpha_1\beta_2$ (20 ng/ml), there was no discernible increase in the phosphorylation of p100 over a prolonged time course while p52 formation increased after a delay of 8 h and continued until the end of the time period. A significant response was achieved at 8 and 24 h compared to non-stimulated cells (Fold stim = 6.91 ± 0.89 , $p < 0.05$, Fold stim = 8.46 ± 2.39 , $p < 0.01$ respectively). Moreover, the expression of p100 decreased in response to LT $\alpha_1\beta_2$ to correspond with p52 accumulation.

A



B

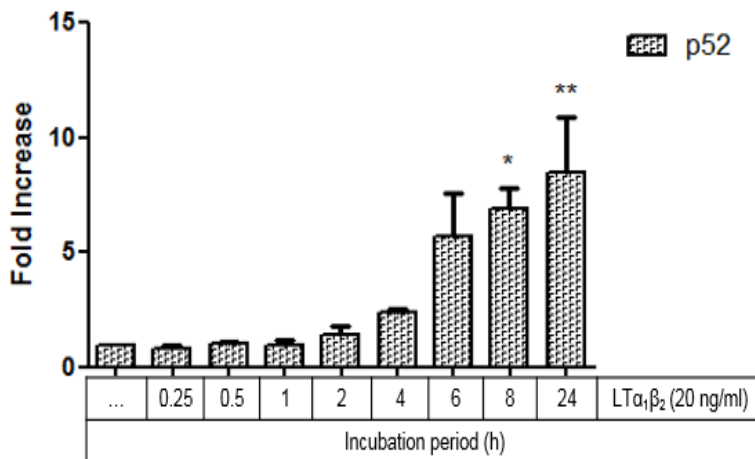


Figure 5.1: Time course of LT $\alpha_1\beta_2$ -mediated p100 processing in NFs. Cells were stimulated with LT $\alpha_1\beta_2$ (20 ng/ml) for a maximum 24 h time period. Whole cell extracts were assessed for A) p52 formation (52 kDa) and total p65 (65 kDa) which was used as a loading control, as outlined in Section 2.5. Blots were semi-quantified by scanning densitometry and results expressed as fold increase relative to control for B) p52 formation. Each value represents the mean \pm SEM of three independent experiments. Data was analysed using a one-way ANOVA test, * $p < 0.05$, ** $p < 0.01$ vs control.

5.2.2.1 TRAF2 and TRAF3 degradation in NFs

Given that little characterisation of the non-canonical NF- κ B pathway has been carried out it was essential to assess intermediates of the pathway under different conditions. In NFs cells, it was found that there was a partial degradation of TRAF2 between 8-24 h of exposure to $LT\alpha_1\beta_2$ as shown in Figure 5.2. Conversely, TRAF3 degradation was observed at 4 h with complete degradation achieved between 8 and 24 h of exposure to $LT\alpha_1\beta_2$. This suggests that $LT\alpha_1\beta_2$ can activate the non-canonical NF- κ B pathway in NFs cells via the degradation of TRAF2 and TRAF3.

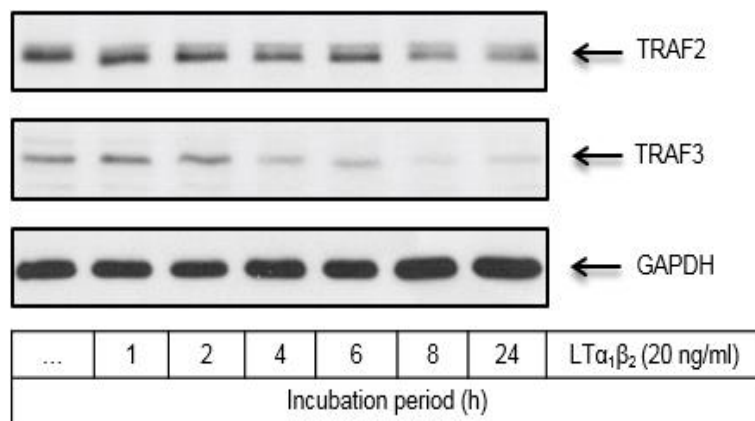


Figure 5.2: Time course of $LT\alpha_1\beta_2$ -mediated TRAF2 and TRAF3 degradation in NFs. Cells were exposed to $LT\alpha_1\beta_2$ (20 ng/ml) for various time periods. Whole cell extracts were assessed for expression of TRAF2 (53 kDa), TRAF3 (62 kDa) and GAPDH (37 kDa) which was used as a loading control, as outlined in Section 2.5. Each blot is representative of three independent experiments.

5.2.2.2 NIK expression in NFs

As mentioned in Chapter one, NIK is responsible for the processing of p100 to p52, in which IKK α is a preferential substrate for NIK, confirming its role in the non-canonical pathway (Xiao et al., 2001). Furthermore, it was found that NIK mediates stimulation through certain receptors, including LT β R (Akiba et al., 1998). Therefore, NFs were exposed to LT $\alpha_1\beta_2$ (20 ng/ml) and assessed for NIK expression. As shown in Figure 5.3, a slight increase in the levels of NIK was observed at two time points following exposure to LT $\alpha_1\beta_2$ for 1 and 4 h of stimulation, whilst it was clearer during other times of the time period compared to non-stimulated NFs.

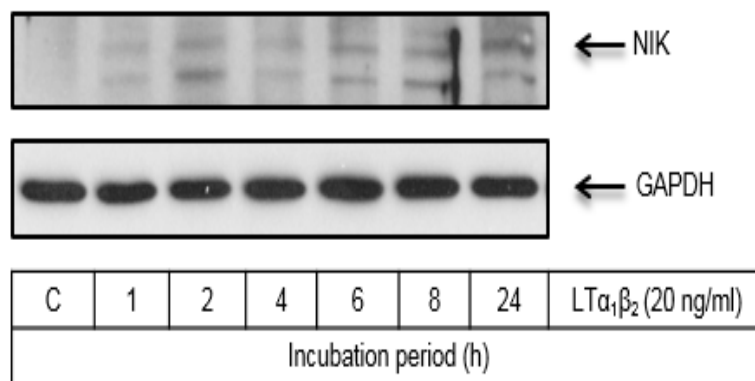
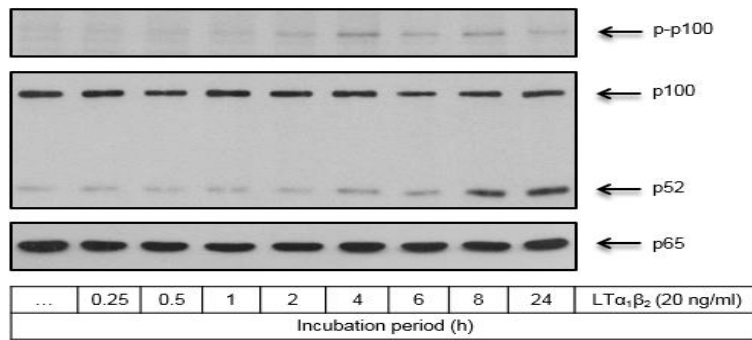


Figure 5.3: Time course of LT $\alpha_1\beta_2$ -mediated NIK expression in NFs. Cells were exposed to LT $\alpha_1\beta_2$ (20 ng/ml) for a maximum 24 h time period, whole cell extracts were assessed for NIK (120 kDa) and GAPDH (37 kDa) which was used as a loading control, as outlined in Section 2.5. Each blot is representative of three independent experiments.

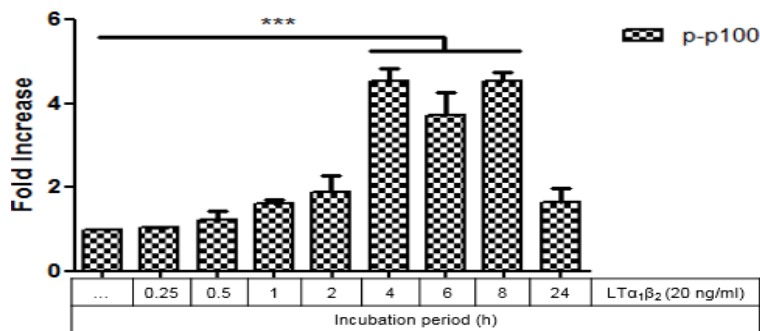
5.2.3 Activation of the non-canonical NF- κ B pathway in CAFs

Figure 5.4 shows that CAFs exposed to $LT\alpha_1\beta_2$ over a prolonged time course gave an increase in p100 phosphorylation. The response was moderate, initially observed at 4h and then increasing up to at 8 h giving a 4.5 fold increase in expression (± 0.19 , $p < 0.001$). In contrast, there was a clear increase in the formation of p52 at 8 h (Fold increase = 6.03 ± 0.75 , $p < 0.01$) with a further increase to around 7.5 fold after 24 h. Furthermore, this stimulation was accompanied by consistent levels of p100 protein.

A



B



C

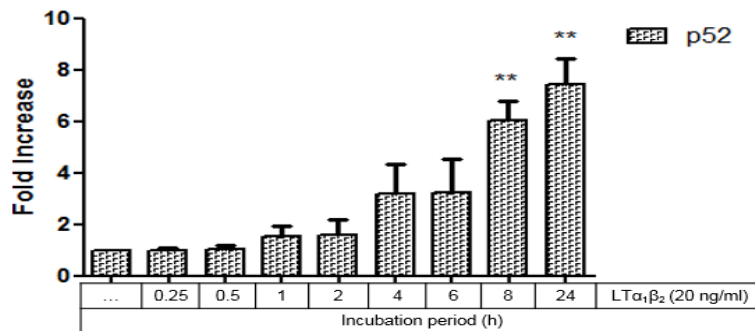


Figure 5.4: Time course of $LT\alpha_1\beta_2$ -mediated p100 phosphorylation and p100 processing in CAFs. Cells were stimulated with $LT\alpha_1\beta_2$ (20 ng/ml) for a maximum 24 h time period. Whole cell extracts were assessed for A) p100 phosphorylation (100 kDa), p52 formation (52 kDa) and total p65 (65 kDa) which was used as a loading control, as outlined in Section 2.5. Blots were semi-quantified by scanning densitometry and results expressed as fold increase relative to control for B) p-p100 and C) p52 formation. Each value represents the mean \pm SEM of three independent experiments. Data was analysed using a one-way ANOVA test, **p<0.01, ***p<0.001 vs control.

5.2.3.1 TRAF2 and TRAF3 degradation in CAFs

Figure 5.5 shows the kinetic profile of TRAF2 and 3 in CAFs. There was some degradation between 4 and 24 h following exposure to $LT\alpha_1\beta_2$ but this was not complete by the end of the time period. In contrast, TRAF3 levels were substantially reduced from 2 h up to the end of the experimental period. This suggests that $LT\alpha_1\beta_2$ does have the potential to regulate the non-canonical NF- κ B pathway in CAFs via the degradation of TRAF2 and TRAF3, and the results were consistent with the effects upon non-canonical NF- κ B pathway parameters.

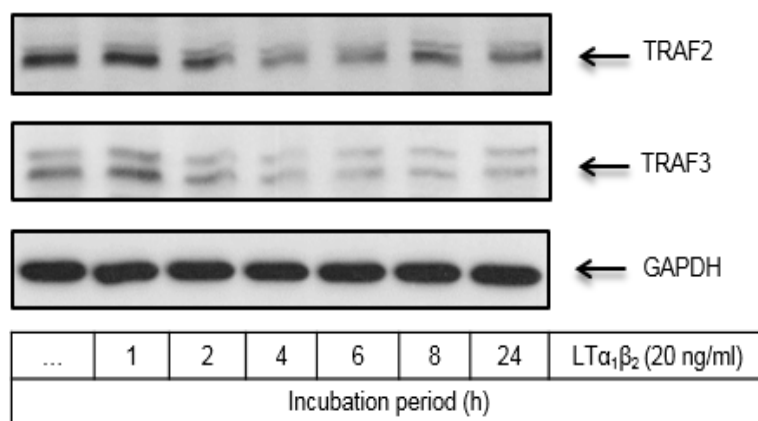


Figure 5.5: Time course of $LT\alpha_1\beta_2$ -mediated TRAF2 and TRAF3 degradation in CAFs. Cells were exposed to $LT\alpha_1\beta_2$ (20 ng/ml) for various time periods. Whole cell extracts were assessed for expression of TRAF2 (53 kDa), TRAF3 (62 kDa) and GAPDH (37 kDa) which was used as a loading control, as outlined in Section 2.5. Each blot is representative of three independent experiments.

5.2.3.2 NIK expression in CAFs

Figure 5.6 shows a time course of $LT\alpha_1\beta_2$ -mediated NIK expression in CAFs. Whilst the endogenous levels of NIK were absent in non-stimulating cells, there was accumulation of NIK expression over the 24 h post- $LT\alpha_1\beta_2$ stimulation time period.

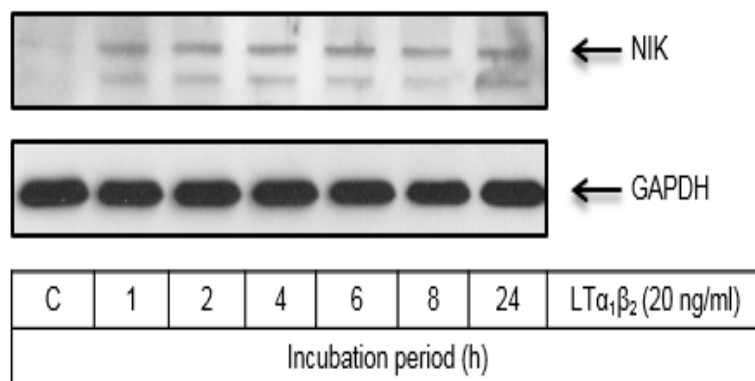


Figure 5.6: Time course of $LT\alpha_1\beta_2$ -mediated NIK expression in CAFs. Cells were exposed to $LT\alpha_1\beta_2$ (20 ng/ml) for a 24 h time period, whole cell extracts were assessed for NIK (120 kDa) and GAPDH (37 kDa) which was used as a loading control, as outlined in Section 2.5. Each blot is representative of three independent experiments.

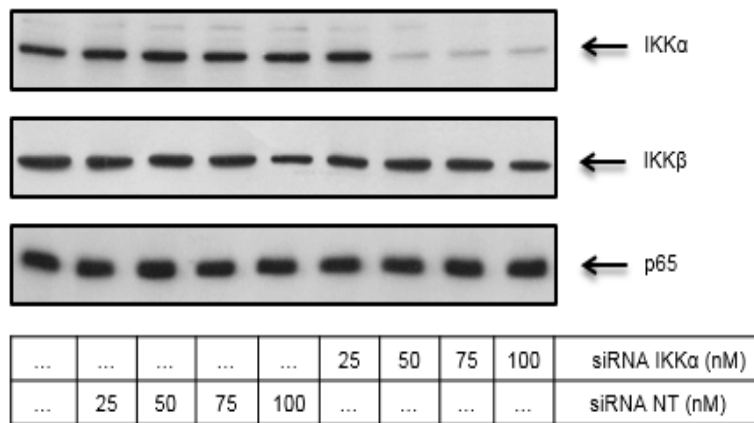
5.2.4 The effect of silencing cellular $IKK\alpha$ expression on the non-canonical NF- κ B pathway in primary CAFs and NFs

In order to block activation of the non-canonical NF- κ B signalling in response to $LT\alpha_1\beta_2$, the role of $IKK\alpha$ was explored in CAFs and NFs by reducing its expression or altering function using both siRNA as a molecular tool and SU compounds as pharmacological approach.

5.2.4.1 siRNA silencing of IKK α in NFs

To optimise the efficiency of the siRNA, 25-100 nM of siRNA IKK α or NT was transfected into NFs for 72 h which was found to be the optimal duration for silencing. Whilst the NT construct was without effect, expression of IKK α was greatly reduced after 72 h silencing at 50-100 nM as shown in Figure 5.7. Levels of IKK α were decreased to less than 10% compared to untreated cells for instance at 100 nM (% basal IKK α expression = 9.65 ± 0.18 , $p < 0.001$). Furthermore, treatment of cells with siRNA IKK α did not appear to have an effect against IKK β expression.

A



B

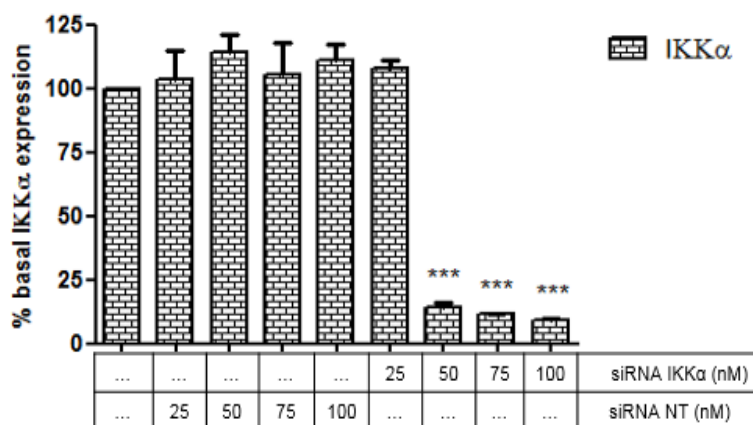
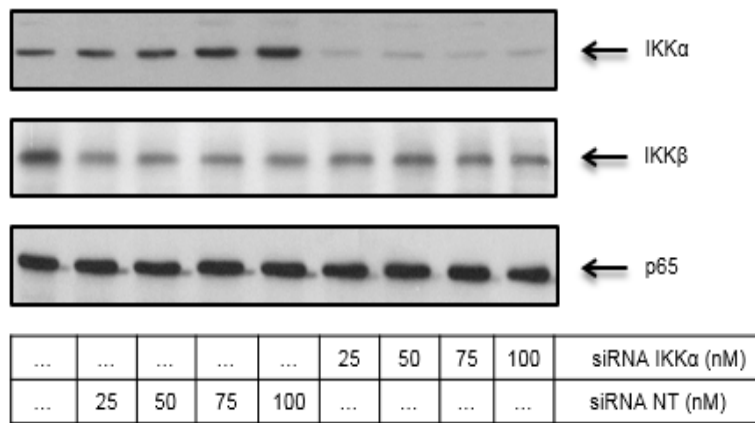


Figure 5.7: The effect of siRNA IKK α on IKK α expression in NFs. Cells transfected with siRNA IKK α or non-targeting (NT) up to a concentration of 100 nM for 72 h. Whole cell extracts were assessed for A) IKK α (84 kDa), IKK β and total p65 (65 kDa) which was used as a loading control, as outlined in Section 2.5. Blots were semi-quantified for percentage of basal IKK α expression by scanning densitometry and results expressed as a relative to untreated control for B) IKK α . Each value represents the mean percentage knockdown \pm S.E.M. of three independent experiments. Data was analysed using a one-way ANOVA test, *** p <0.001 vs control.

5.2.4.2 siRNA silencing of IKK α in CAFs

In CAFs, 25-100 nM of both siRNA IKK α and siRNA NT were transfected into cells for 72 h which was found to be the optimal duration for silencing. As shown in Figure 5.8, the impact of NT to increase of IKK α expression was observed at 75 and 100 nM. In contrast, siRNA IKK α effectively reduced expression of IKK α to approximately 90% at all concentrations tested for instance at 100 nM; % basal IKK α expression = 10.83 ± 0.93 ($p < 0.001$). Furthermore, IKK α siRNA was without effect against IKK β expression.

A



B

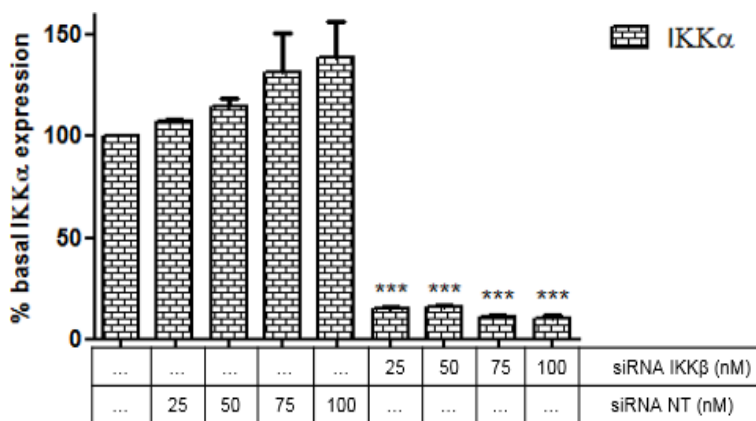


Figure 5.8: The effect of siRNA IKK α on IKK α expression in CAFs. Cells were transfected with siRNA IKK α or non-targeting (NT) up to a concentration of 100 nM for 72 h. Whole cell extracts were assessed for A) IKK α (84 kDa), IKK β and total p65 (65 kDa) which was used as a loading control, as outlined in Section 2.5. Blots were semi-quantified for percentage of basal IKK α expression by scanning densitometry and results expressed as a relative to untreated control for B) IKK α . Each value represents the mean percentage knockdown \pm S.E.M. of three independent experiments. Data was analysed using a one-way ANOVA test, *** $p < 0.001$ vs control.

5.2.4.3 The effect of siRNA IKK α silencing on LT $\alpha_1\beta_2$ induced p100 processing in NFs

Figure 5.9 illustrates the effect of IKK α siRNA on LT $\alpha_1\beta_2$ induced p100 processing in NFs. Cells were transfected with siRNA IKK α or siRNA NT (100 nM) for 72 h prior to exposure to LT $\alpha_1\beta_2$ for 8 h. Preliminary experiments indicated that LT $\alpha_1\beta_2$ alone caused a marked stimulation of p52 formation. Interestingly, p100 expression and p52 formation were substantially reduced by IKK α siRNA (100 nM) compared to the non-target (NT) control.

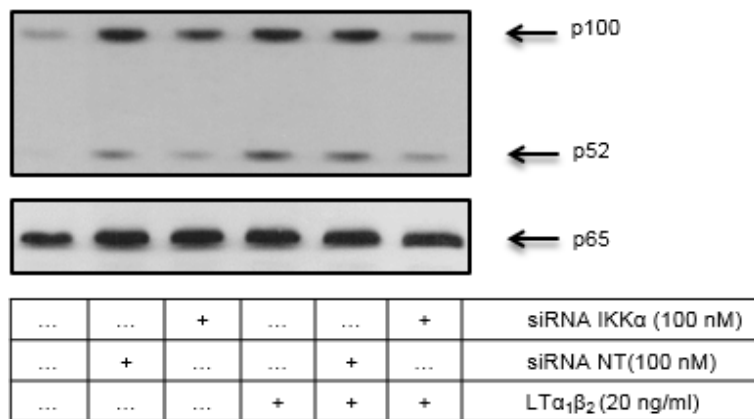


Figure 5.9: The effect of IKK α siRNA upon LT $\alpha_1\beta_2$ -mediated p52 formation in NFs. Cells were transfected with non-targeting siRNA (NT) (100 nM) and IKK α siRNA (100 nM) for 72 h prior stimulation with LT $\alpha_1\beta_2$ (20 ng/ml) for 8 h. Whole cell extracts were assessed for p52 formation (52 kDa) and total p65 (65 kDa) which was used as a loading control, as outlined in Section 2.5. Each blot is representative of two independent experiments.

5.2.4.4 The effect of siRNA IKK α silencing on LT $\alpha_1\beta_2$ induced p100 processing in CAFs

In a similar fashion, Figure 5.10 demonstrates the effect of siRNA IKK α on LT $\alpha_1\beta_2$ induced p100 processing in CAFs. Interestingly, as with NFs, preliminary experiments indicated that both p100 expression and p52 formation were markedly inhibited by IKK α siRNA (100 nM) compared to the non-target (NT) control.

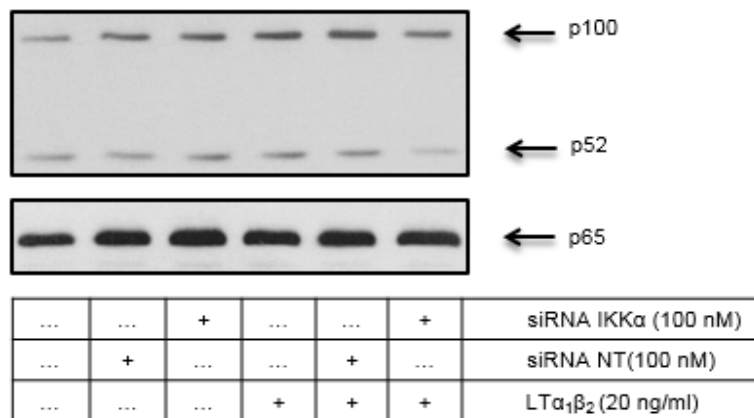


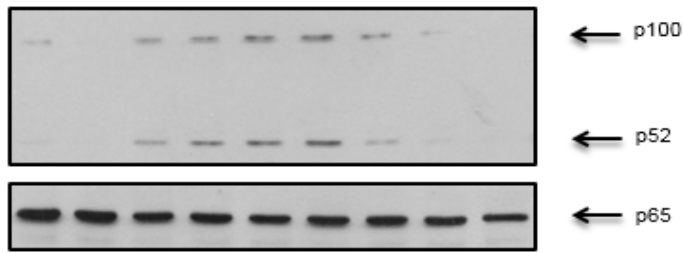
Figure 5.10: The effect of IKK α siRNA upon LT $\alpha_1\beta_2$ -mediated p52 formation in CAFs. Cells were transfected with non-targeting siRNA (NT) 100nM and IKK α siRNA (100 nM) for 72 h prior stimulation with LT $\alpha_1\beta_2$ (20 ng/ml) for 8 h. Whole cell extracts were assessed for p52 formation (52kDa) and total p65 (65 kDa) which was used as a loading control, as outlined in Section 2.5. Each blot is representative of two independent experiments.

5.2.5 The effect of SU compounds on non-canonical NF- κ B pathway in NFs and CAFs

5.2.5.1 The effect of SU compounds on LT $\alpha_1\beta_2$ induced p100 processing in NFs

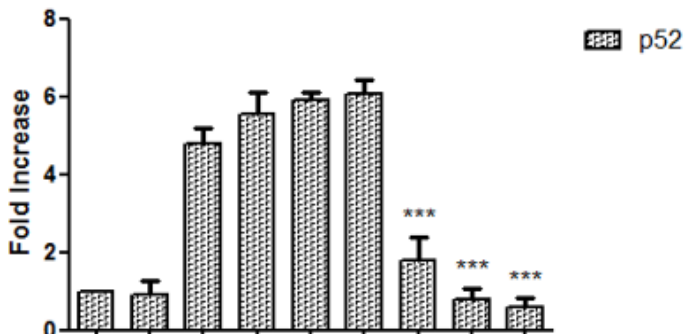
Figure 5.11 shows the effect of SU1349 compound on LT $\alpha_1\beta_2$ induced p52 formation in NFs. LT $\alpha_1\beta_2$ significantly stimulated p52 formation over 8 h with an approximate 5.5 fold increase (Fold increase = 5.56 ± 0.54 , $p < 0.001$). Pre-treatment of NFs with increasing concentrations of SU1349 significantly reduced p52 formation over the low micromolar range (1-10 μ M). The maximum inhibition was obtained at 10 μ M (Fold increase = 0.59 ± 0.24 , $p < 0.001$).

A



...	10	0.1	0.3	1	3	10	SU1349 (μM)
...	+	DMSO (0.05 %)
...	...	+	+	+	+	+	+	+	LT $\alpha_1\beta_2$ (20 ng/ml)

B



...	10	0.1	0.3	1	3	10	SU1349 (μM)
...	+	DMSO (0.05 %)
...	...	+	+	+	+	+	+	+	LT $\alpha_1\beta_2$ (20 ng/ml)

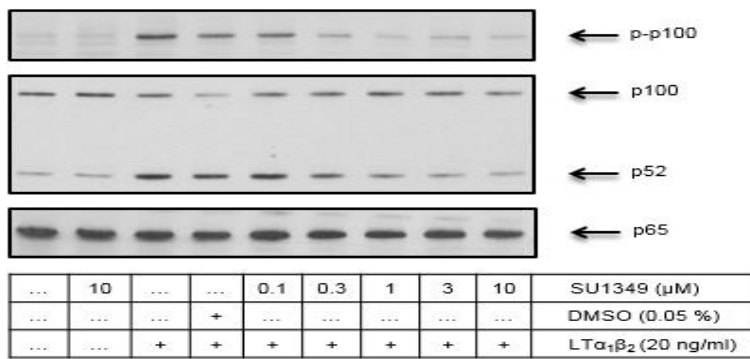
Figure 5.11: The effect of SU1349 upon LT $\alpha_1\beta_2$ -mediated p52 formation in NFs. Cells were pre-treated with SU1349 for 1 h prior to stimulation with LT $\alpha_1\beta_2$ (20 ng/ml) for 8 h. Whole cell extracts were assessed for A) p52 formation (p52 kDa) and total p65 (65 kDa) which was used as a loading control, as outlined in Section 2.5. Blots were semi-quantified by scanning densitometry and results expressed as fold increase relative to control for B) p52 formation. Each value represents the mean \pm SEM of three independent experiments. Data was analysed using a one-way ANOVA test, *** $p < 0.001$ vs LT $\alpha_1\beta_2$ and DMSO as an agonist stimulated control.

5.2.5.2 The effect of SU compounds on $LT\alpha_1\beta_2$ induced phosphorylation of p100 and p52 in CAFs

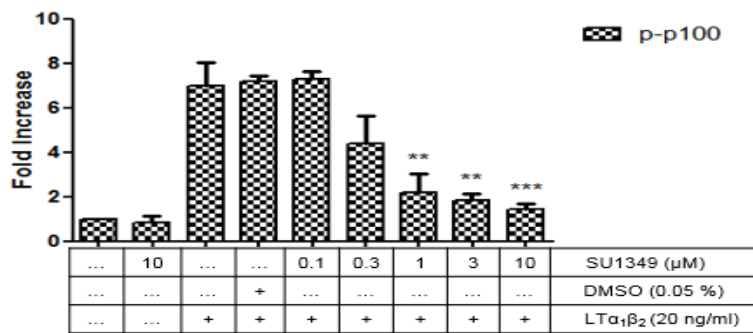
Figure 5.12 shows the effect of SU1349 on $LT\alpha_1\beta_2$ induced phosphorylation of p100 and p52 formation in CAFs. As expected, $LT\alpha_1\beta_2$ alone induced a significant increase in p100 phosphorylation and p52 formation (p-p100: Fold increase = 7.23 ± 0.22 , p52: Fold increase = 3.44 ± 0.29 , $p < 0.01$). With increasing concentrations of SU1349, both of p100 phosphorylation and p52 formation gradually decreased with significant inhibition achieved between 1 and 10 μM . The maximum concentration (10 μM) of SU1349 inhibited both p100 phosphorylation and p52 formation induced by $LT\alpha_1\beta_2$ by approximately 80% (pp100: Fold increase = 1.43 ± 0.24 , $p < 0.001$, p52: Fold increase = 0.62 ± 0.18 , $p < 0.001$).

Similarly, CAFs were treated with increasing concentrations of SU1433 prior exposure to $LT\alpha_1\beta_2$. As shown in Figure 5.13, concentrations of 3-10 μM SU1433 reduced phosphorylation of p100 and p52 formation by approximately 85% (p-p100: Fold increase = 0.46 ± 0.12 , p52: Fold increase = 0.45 ± 0.11 , $p < 0.001$).

A



B



C

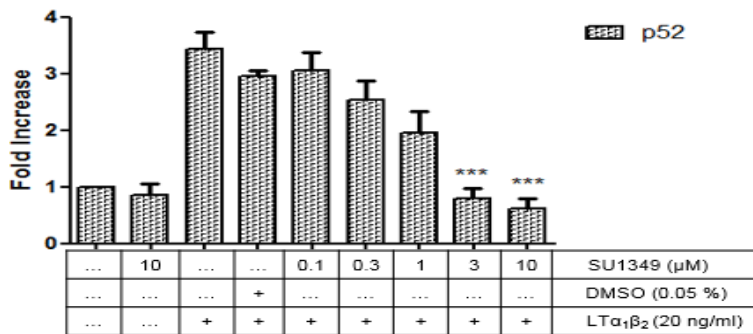


Figure 5.12: The effect of SU1349 upon LT $\alpha_1\beta_2$ -mediated p100 phosphorylation and p52 formation in CAFs. Cells were pre-treated with SU1349 for 1 h prior to stimulation with LT $\alpha_1\beta_2$ (20 ng/ml) for 8 h. Whole cell extracts were assessed for A) p100 phosphorylation (100 kDa), p52 formation (p52 kDa) and total p65 (65 kDa) which was used as a loading control, as outlined in Section 2.5. Blots were semi-quantified by scanning densitometry and results expressed as fold increase relative to control for B) p-p100 and C) p52. Each value represents the mean \pm SEM of three independent experiments. Data was analysed using a one-way ANOVA test, ** $p < 0.01$, *** $p < 0.001$ vs LT $\alpha_1\beta_2$ and DMSO as an agonist stimulated control.

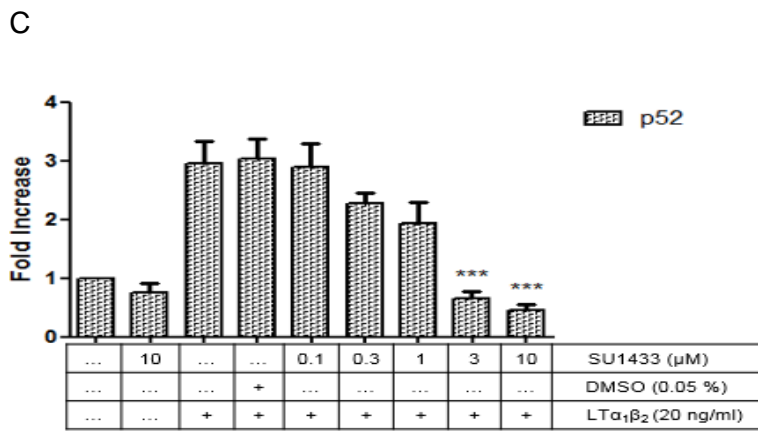
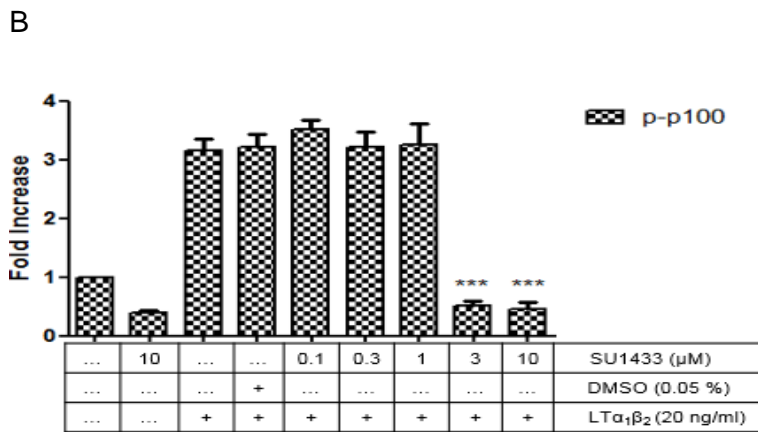
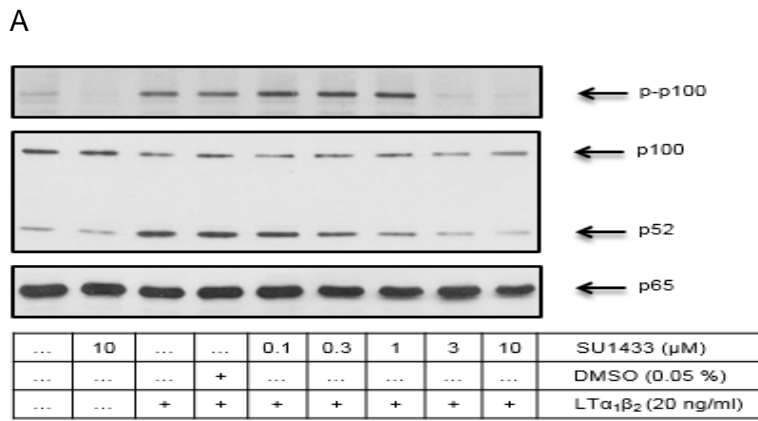


Figure 5.13: The effect of SU1433 upon LT $\alpha_1\beta_2$ -mediated p100 phosphorylation and p52 formation in CAFs. Cells were pre-treated with SU1433 for 1 h prior to stimulation with LT $\alpha_1\beta_2$ (20 ng/ml) for 8 h. Whole cell extracts were assessed for A) p100 phosphorylation (100 kDa), p52 formation (p52 kDa) and total p65 (65 kDa) which was used as a loading control, as outlined in Section 2.5. Blots were semi-quantified by scanning densitometry and results expressed as fold increase relative to control for B) pp100 and C) p52 formation. Each value represents the mean \pm SEM of three independent experiments. Data was analysed using a one-way ANOVA test, *** p <0.001 vs LT $\alpha_1\beta_2$ and DMSO as an agonist stimulated control.

5.2.6 The role of IKK α in CXCL12 expression in CAFs and NFs

As was demonstrated in Chapter 4, IKK α has been implicated as a possible regulator for CXCL12 in a bone cancer model. Therefore, quantitative real time PCR (RT-qPCR) was used to determine whether this kinase was implicated in the context of CXCL12 induction in CAFs and NFs. Figure 5.14 shows that exposure to LT $\alpha_1\beta_2$ failed to induce CXCL12 expression in CAFs, but significantly increased CXCL12 expression in NFs at 24 h (Fold increase = 1.96 ± 0.20 , $p < 0.01$). In contrast, IL-1 β failed to induce CXCL12 expression in both NFs and CAFs (Data not shown).

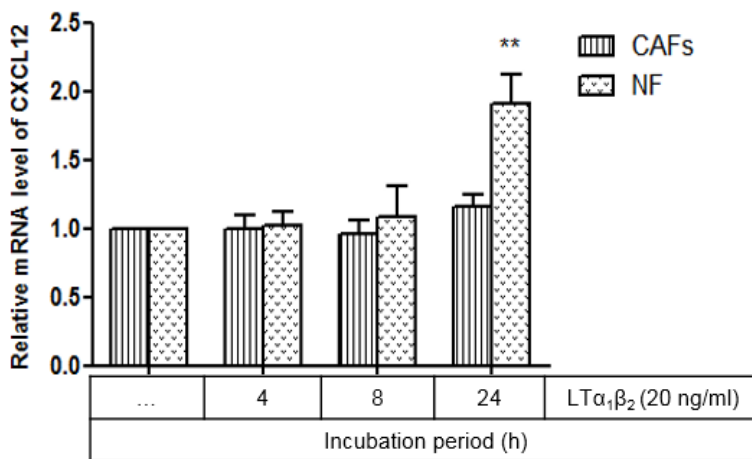


Figure 5.14: LT $\alpha_1\beta_2$ ligation induces non-canonical NF- κ B-dependent mRNA expression of CXCL12 in CAFs and NFs. Cells on 6-well plates were incubated with LT $\alpha_1\beta_2$ (20 ng/ml) for the indicated time points and assessed for CXCL12 as outlined in Section 2.8.4. Error bars represent the mean \pm SEM of triplicate determinations from three individual experiments. Data was analysed using a two-way ANOVA test, ** $p < 0.01$ vs control.

5.2.7 Detection of CXCL12 protein expression in CAFs and NF cells using ELISA

To investigate further the link between non-canonical NF- κ B signalling and CXCL12 expression, protein concentration was measured using an ELISA assay. As shown in Figure 5.15, there was no change in CXCL12 release in CAFs or NFs in response to LT $\alpha_1\beta_2$ stimulation. However, the results indicated elevated levels of CXCL12 protein in the conditioned media by the CAFs as compared with that by NFs.

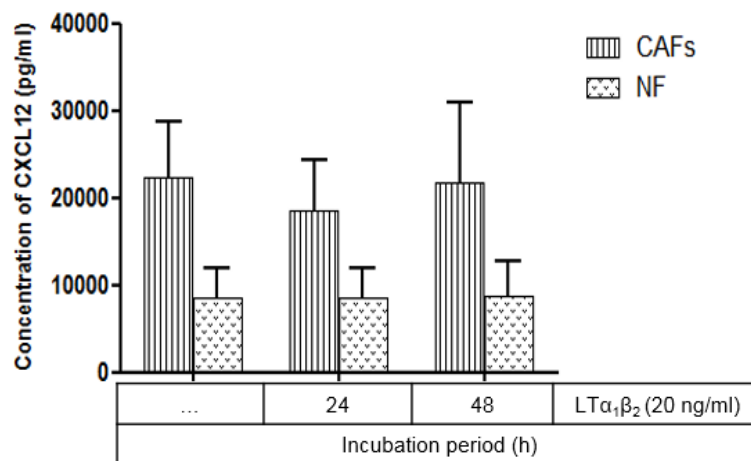


Figure 5.15: Expression level of CXCL12 protein in CAFs and NFs. Cells were seeded in 6-well culture plates and then stimulated with LT $\alpha_1\beta_2$ (20 ng/ml) for the indicated time points. Supernatants were collected and CXCL12 protein level assessed by ELISA assay as outlined in methods Section 2.9. Three independent experiments were performed in duplicate. Data are expressed as means \pm SEM. Data was analysed using a two-way ANOVA test.

5.2.7.1 The effect of SU1349 and IKK α siRNA silencing on CXCL12 protein expression in NFs and CAFs

As indicated in Figures 5.16 and 5.17, NFs and CAFs were treated with SU1349 (1 and 10 μ M) and IKK α siRNA (100 nM) for 24 h. Whilst siRNA IKK α was without effect, CXCL12 protein was slightly inhibited by SU1349 (1 μ M) in NFs, but this inhibition was not statistically significant (Figure 5.16). A similar outcome was observed in CAFs (Figure 5.17).

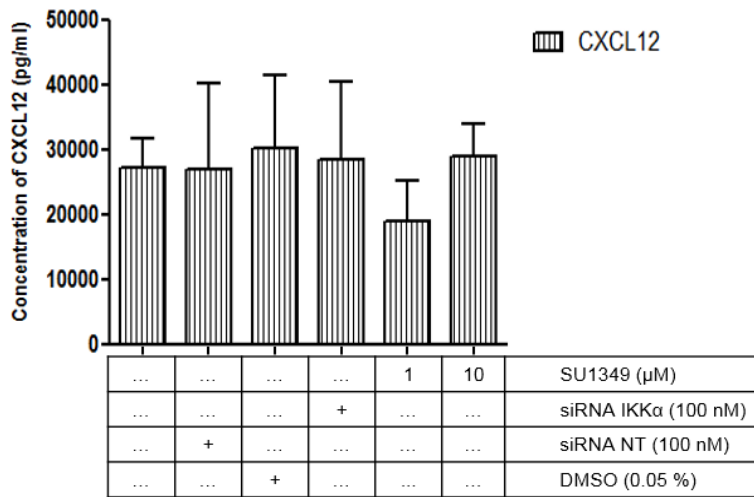


Figure 5.16: The effect of SU1349 and IKK α siRNA upon CXCL12 protein levels in NFs. Cells were seeded in 6-well culture plates and transfected with 100 nM of non-targeting (NT) and IKK α siRNA (100 nM) for 72 h, NFs were also treated with SU1349 (1 and 10 μM) and 0.05% DMSO for 24 h. Supernatants were collected and CXCL12 protein level assessed by ELISA assay as outlined in methods Section 2.9. Three independent experiments were performed in duplicate. Data are expressed as means \pm SEM. Data was analysed using a one-way ANOVA test.

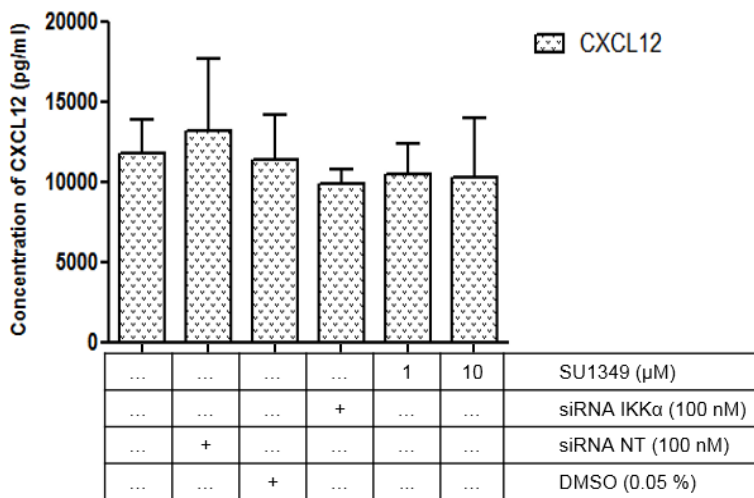


Figure 5.17: The effect of SU1349 and IKK α siRNA upon CXCL12 protein levels in CAFs. Cells were seeded in 6-well culture plates and transfected with 100 nM of non-targeting (NT) and IKK α siRNA (100 nM) for 72 h, CAFs were also treated with SU1349 (1 and 10 μM) and 0.05% DMSO for 24 h. Supernatants were collected and CXCL12 protein level assessed by ELISA assay as outlined in methods Section 2.9. Three independent experiments were performed in duplicate. Data are expressed as means \pm SEM. Data was analysed using a one-way ANOVA test.

5.3 Discussion

The tumour microenvironment has recently become a matter of interest in cancer research. Recent publications have revealed high levels of CXCL12 expressed by cancer cells and tumour-associated stromal cells of breast cancer cells, which directly stimulated the proliferation and invasiveness through both autocrine and paracrine mechanisms (Kojima et al., 2010, Burger and Kipps, 2006, Orimo et al., 2005). The major hurdle in treatment of breast cancer is its resistance to conventional therapies, which include surgery, radiotherapy, chemotherapy, and hormone therapy (Tang et al., 2016, Gonzalez-Angulo et al., 2007). Therefore, the disruption of the interaction of cancer cells with their microenvironment through targeting of CXCL12 could increase the efficacy of these therapies in tumours, including breast cancer.

Two primary fibroblast cells derived from clinical specimens of breast cancer patients were made available for this study, the Normal fibroblasts (NFs) and Cancer-associated fibroblasts (CAFs). These cells were obtained from the Beatson Institute for Cancer Research UK (BICR). Isolation of stromal fibroblasts from invasive cancer tissues of patients followed by low-passaged cultures *in vitro* is now a recognised approach to explore the biological characteristics of CAFs and their effects on tumour cells (Erez et al., 2010). Furthermore, other studies reported that CAFs at low passages cultured *in vitro* retained their original features in the absence of continuous interaction with carcinoma cells (Kalluri and Zeisberg, 2006, Orimo et al., 2005). CAFs or NFs ultimately turn into senescent cells after 10 to 15 passages, therefore, all of the primary cells in this study were at a maximum 10 passages, to maintain the closest phenotype to the primary tissues. CAFs isolated from cancer tissues, including breast cancer have high levels of CXCL12 (Yu et al., 2014, Kojima et al., 2010, Orimo et al., 2005). Another study also showed that CAFs could promote aggressive behaviour of

breast cancer cells and indeed, promoted migration and invasion of MDA-MB-231 cells in a CXCL12-dependent manner (Al-Ansari et al., 2013).

In this study, $LT\alpha_1\beta_2$ was found to activate the non-canonical NF- κ B pathway in NFs and CAFs. In contrast, this activation did not occur following exposure to TNF α in these cells. This is in agreement with other studies that have reported elevated levels of non-canonical NF- κ B pathway markers in response to $LT\alpha_1\beta_2$ in various cell types (Ganeff et al., 2011, Madge et al., 2008, Dejardin, 2006). The results of this study indicate that $LT\alpha_1\beta_2$ activates non-canonical NF- κ B pathway in CAFs in a manner different in comparison to NFs. In CAFs, phosphorylation of p100 was observed, and the formation of p52 was correlated with constant levels of p100, while in NFs, p100 phosphorylation was absent and loss of p100 correlated with p52 formation. It is possible that p52 formation may be partly a result of constitutive p100 degradation.

It should be noted that the activation of the non-canonical pathway in these cells is consistent with an increase in NIK expression and changes in TRAF2 and TRAF3. NIK expression was found to be detected in CAFs and NFs following exposure to $LT\alpha_1\beta_2$. It seems possible that these results are due to the degradation in TRAF3 which was found to be degraded prior to TRAF2, this suggests that TRAF3 degradation first disassembles the complex bound to NIK to relieve the suppression. These results agree with the findings of other studies discussed previously, which suggests that NIK is a key regulator of the alternative NF- κ B signalling which is absent or at minimal level in resting cells through a TRAF3, TRAF2, and cIAP1/2 complex that ubiquitinates NIK causing its proteasomal degradation (Vallabhapurapu et al., 2008). It was recently proposed that both $LT\beta$ R and NIK bind to the same site on TRAF2 and TRAF3, thus, following exposure to ligand, the receptor competes for the binding sites on TRAF3, consequently replacing NIK from the negative regulatory complex and relieving the degradation of NIK (Sanjo et al., 2010). Furthermore,

previous studies have reported that TRAF3 degradation precedes TRAF2 degradation by disassembling the complex bound to NIK (Vallabhapurapu et al., 2008, Zarnegar et al., 2008). Interestingly, whilst TNF α rapidly activate of the classical NF- κ B pathway in CAFs and NFs suggesting good receptor engagement (data not shown), there was no activation of the non-canonical NF- κ B pathway.

Again, RNA interference (siRNA) and SU compounds (IKK α inhibitors) were employed to confirm that IKK α mediated the activation of the non-canonical NF κ B pathway in CAFs and NFs, p100 processing was reduced to a great extent following IKK α silencing or by using SU compounds. In addition, ELISA and RT-qPCR assays were used to assess CXCL12 expression as a downstream marker of non-canonical pathway in CAFs and NFs. The results showed no difference was observed in levels of CXCL12 following activation of this pathway by LT $\alpha_1\beta_2$. The expression of CXCL12 was observed to be IKK α -dependent in U2OS cells (Chapter 4), but this has not been translated into this study, suggesting that this target is not selective for IKK α in these cells. Nevertheless, ELISA assay indicated that CXCL12 in the conditioned media from untreated CAFs was significantly higher than that from untreated NFs. This is in agreement with other studies that have reported elevated levels of CXCL12 in CAFs rather than NFs in breast cancer (Kojima et al., 2010, Huang et al., 2010, Orimo et al., 2005). The role of IKK α was examined in the constitutive production of CXCL12 by using both siRNA IKK α and SU1349. The findings by ELISA revealed there was no change in CXCL12 levels in CAFs, whereas there was a slight inhibition in NFs.

In conclusion, LT $\alpha_1\beta_2$ demonstrated a difference in the activation of non-canonical NF- κ B pathway in CAFs and NFs that were obtained from human breast cancer patients. Emerging evidence has suggested that CAFs show a critical role in the development of solid tumours, and is a potential target for breast cancer treatment.

CAFs can effect on tumour microenvironment through the expression of CXCL12 compared to NFs, which appears to be not affected by IKK α absence.

Chapter Six
General Discussion and Conclusion

6.1 General discussion and Future directions

Human osteosarcoma is the most frequent primary bone malignant tumour which affects children and adolescents, also middle ages and elderly persons and is considered the sixth most common type of cancer (Abarrategi et al., 2016, Mirabello et al., 2009, Niforou et al., 2008). Despite great progress in surgery and chemotherapy, the overall survival for patients with osteosarcoma is very poor and lung metastasis is the leading cause of death in 95% of patients with osteosarcoma (Basu-Roy et al., 2013, Banerjee et al., 2013, Perissinotto et al., 2005). Thus, inhibition of metastasis to the lung and other body organs is of critical importance in treating osteosarcoma. The second disease model used in this study employed cancer associated fibroblasts (CAFs) derived from breast cancer patients, one of the most important cell types in the tumour microenvironment (Kalluri, 2016). A large body of evidence indicates that CXCL12 and its receptor CXCR4 is involved in metastasis, tumorigenesis, angiogenesis and proliferation in various human cancers, including bone and breast cancer (Kojima et al., 2010, Lai et al., 2009, Perissinotto et al., 2005, Bachelder et al., 2002). A number of studies have shown that IKK α is involved in the regulation of CXCL12 via non-canonical NF- κ B pathway activation. However, no studies have examined the function of IKK α in relation to CXCL12 in U2OS cells and CAFs. Inhibition of IKK α may be a better strategy to improve treatment outcomes for bone and breast cancer patients. Therefore, the main objectives in this thesis were to firstly determine if IKK α could be activated in U2OS cells and CAFs. Secondly, to investigate the role of IKK α signalling in the regulation of CXCL12 expression and thirdly to determine whether this pathway could be inhibited using molecular and pharmacological approaches.

There are several hallmarks of cancer which contribute to uncontrolled cell growth including self-sustained proliferation and absence of apoptosis (Hanahan and

Weinberg, 2011). Since the discovery in 1986, NF- κ B is considered to be a major multi-component transcription factor pathway which plays a key role in normal physiology and disease (Tegowski and Baldwin, 2018, Hacker and Karin, 2006, Xiao and Ghosh, 2005), including arthritis, cancer and cardiovascular diseases. Thus, it has been an attractive target for scientists in oncology (Hoesel and Schmid, 2013). The NF- κ B has two major components; the canonical pathway and the non-canonical pathway. IKK β mediates the phosphorylation of I κ B α in the canonical pathway, which upon proteolytic degradation promotes the nuclear translocation of p65 and subsequent transcriptional regulation. Within the alternative pathway, NF- κ B inducing kinase (NIK) promotes the phosphorylation and activation of IKK α , which in turn drives the phosphorylation and degradation of a larger p100 and the subsequent nuclear translocation of p52 NF- κ B and RelB (Beinke and Ley, 2004). Each pathway leads to expression of a number of genes involved in immunity, inflammation, and cell survival in normal and cancerous cells (Oeckinghaus and Ghosh, 2009).

Over the past 15 years, the majority of studies have targeted the IKK β resulting in the development of a number of compounds such as ML120B from Millennium Pharmaceuticals, BMS-345541 from Bristol-Myers Squibb and SC-514 from Pfizer (Ivanenkov et al., 2011). However, IKK β inhibitors could not be clinically used due to adverse effects and significant toxicity that occurs due to severe reduction in anti-apoptotic protein expression in normal cells (Shukla et al., 2015, Gamble et al., 2012, Chariot, 2009).

A growing body of evidence now implicates a major role for IKK α in cancer progression and metastasis in a number of cancers including prostate, colorectal, pancreatic and breast cancer (Luo et al., 2007, Fernandez-Majada et al., 2007, Shiah et al., 2006, Park et al., 2005). However, selective IKK α inhibitors have not been identified to date. Initial results in Chapter three confirmed that the inhibition of the

non-canonical NF- κ B pathway via IKK α inhibitors can be used to further characterise the role of IKK α in cellular outcomes, in addition, it could be a good approach for the treatment in bone and breast cancer. A number of challenges were identified in the development of selective IKK α inhibitors. Firstly, in the absence of a crystal structure for IKK α to date, the high sequence-homology in the ATP-binding site of IKK α and IKK β , which share 52% overall sequence homology within N-terminal kinase domains (Gamble et al., 2012, DiDonato et al., 1997). Secondly, further enhancements in selectivity are required for these compounds to avoid the potential of off-target effects through improve their physiochemical properties including solubility and resistance to degradation and clearance. However, a novel class of IKK α inhibitors have been developed using standard SAR approaches using enzymatic kinases assays at the University of Strathclyde as part of a CRUK small molecule drug discovery programme, these compounds were provided for assessment in bone and breast cancer.

Initial experiments in this study demonstrated for the first time that our lead compounds were selective and effective in bone and breast cancer through inhibition of IKK α -mediated activation of the non-canonical NF- κ B pathway. Furthermore, data within our group also demonstrated the selectivity of these compounds for IKK α in different cancer cells. Furthermore, preliminary experiments showed another aspect in the clinical applicability of selective IKK α compounds; SU1349 combined with enzalutamide inhibited IKK α /SR signalling pathways in triple negative breast cancers patients TNBC (data not shown). Therefore, in future investigations, it might be possible to extend the findings in this thesis to other approaches cancer drug-discovery process, for example combination therapy or, depending on the off-target profile of the compound, multi-kinase inhibition. A number of kinase inhibitors have been documented to exhibit their anti-tumour activity through dual or multi-kinase

inhibition (Wada et al., 2014, Komarova and Boland, 2013, Schult et al., 2012). An important additional future strategy will be to investigate the potential effect of IKK α inhibitors using *in vivo* cancer models, in particular genetically engineered mouse models (GEMM) and primary xenografts.

Targeted therapies are dependent on adequate occupancy and target engagement to ensure clinical efficacy. Jafari and colleagues demonstrated that using the cellular thermostability assay CETSA could be useful for shortening the time required to select candidate drugs with higher likelihood of efficacy (Jafari et al., 2014). Although this study revealed a distinct melting curve for IKK α without drugs, the stability of IKK α was not affected by SU1261 so the interaction of the drug with the target protein could not be confirmed. If time had allowed it would be useful to increase the compound concentration and decrease the temperature in smaller increments to visualize possible small thermal shifts. In addition, the time used for incubation with the compounds that could alter the ability to engage the target protein, which in turn may affect the ability of antibodies to detect the target protein. Therefore to extend this work, it will be useful to use antibodies that do not distinguish between the various protein forms or using MS-based methods that detect either form. Alternatively, the gel electrophoresis method could be modified to separate different protein forms before Western blot-mediated quantification (Jafari et al., 2014).

The slow kinetics and dependence of *de novo* protein synthesis is the hallmark of the non-canonical NF- κ B activation (Liang et al., 2006, Claudio et al., 2002). The results in Chapter 4 indicated, for the first time, a novel rapid activation of this pathway in U2OS cells by TNF α and IL-1 β in comparison to classical delayed response to LT $\alpha_1\beta_2$, suggesting a new mechanism within the non-canonical NF- κ B pathway. In preliminary experiments to follow up this observations were unrevealing, however over-expression of Adv. wild type NIK resulted in an increase in p100 phosphorylation and

the formation of p52 in U2OS cells, in the absence of any change in p100 protein expression (Data not shown) suggesting the normal pathway is functional. Using the, the NIK inhibitor (CW 15407) showed conflicting effects but considerable off-target effects for this inhibitor are likely. Other kinases have been also identified as upstream IKK kinases acting in concert with NIK such as MEKK1 (Nakano et al., 1998) and TAK1 (Sakurai et al., 1998). Although IKK α can be activated by different signals, however only the NIK-dependent signals induce p100 processing (Xiao et al., 2004, Xiao et al., 2001) and given that rapid processing was absent this indicated a NIK independent pathway. Future research should therefore concentrate on molecular mechanisms underpinning this phenomenon.

A large body of evidence now implicates a major role for the CXCL12/CXCR4 axis in a number of physiological functions and pathophysiological conditions, particularly in cancer metastases, in addition to tumorigenicity, angiogenesis and proliferation (Greenbaum et al., 2013, Lewellis and Knaut, 2012, Kryczek et al., 2007, Dewan et al., 2006). However, to date, work assessing the regulation of CXCL12 expression is restricted to very few papers (Garcia-Moruja et al., 2005). The expression of CXCL12 has been proposed to be regulated by IKK α -mediated non-canonical NF- κ B pathway (Madge and May, 2010, Madge et al., 2008). One of the more significant findings to emerge from this study, for the first time, is that IKK α up-regulates CXCL12 expression through activation of the non-canonical NF- κ B pathway in U2OS cells (Chapter 4). Together, CXCL12 reporter activity and RT-qPCR data suggest that CXCL12 could be regulated by IKK α in bone cancer, moreover CXCL12 expression was inhibited by blocking IKK α by SU compounds and siRNA IKK α . The key strengths of this study are the possibility of targeting CXCL12 at the level of regulation, which is very important. Recently it has been demonstrated that CXCL12 is able to interact with another receptor CXCR7. Therefore this study suggests that a successful

approach would be to selectively target the kinase IKK α , therefore inhibiting CXCL12 as a downstream outcome. Hence, our study point a novel early kinetically distinct mode of regulation of non-canonical NF- κ B signalling regulated by IKK α in response to TNF α and IL-1 β compared to classical delayed response to LT $\alpha_1\beta_2$, which is significant in the induction of CXCL12. In addition to possibility of targeting CXCL12 expression through inhibiting of IKK α -mediated activation of the non-canonical NF- κ B pathway by SU compounds (Figure 6.1). The siRNA has been used widely to silence relevant target genes involved in a number of signalling pathways, however correlating this phenotypic impact with pharmacological small-molecule inhibition profiles is not always consistent (Weiss et al., 2007). Further investigation is needed using other RNA methods such as shRNA (small hairpin RNA) or using CRISPR (Clustered Regularly Interspaced Short Palindromic Repeats).

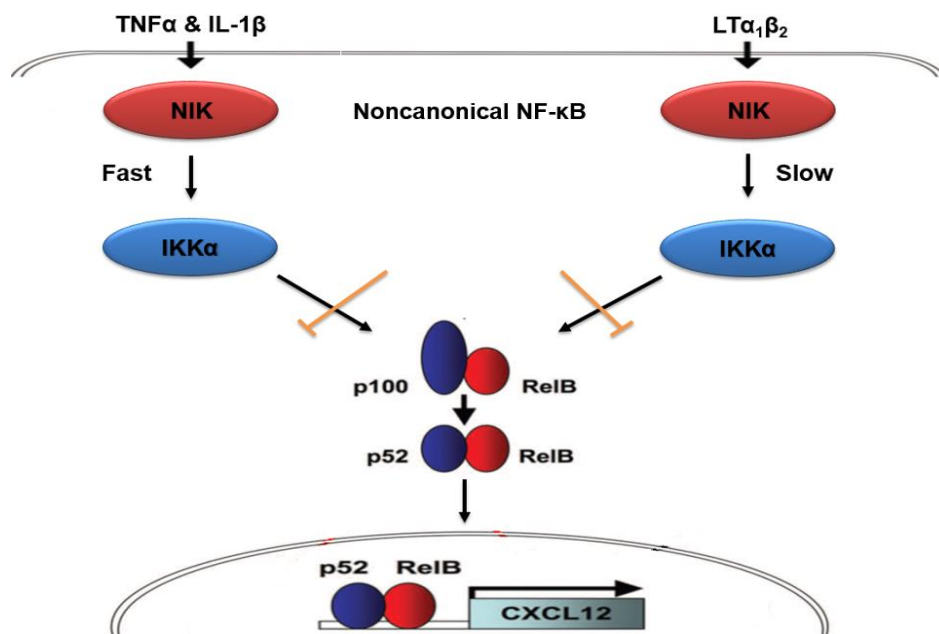


Figure 6.1: A schematic diagram shows the effect of SU compounds to inhibit CXCL12 expression induced by LT $\alpha_1\beta_2$, TNF α - and IL-1 β via the non-canonical NF- κ B pathway in U2OS cells. The non-canonical NF- κ B pathway involve the processing of p100 to generate p52 and the subsequent migration of RelB-p52 dimers into nucleus, as a consequence, activate the transcription process for CXCL12 expression.

Although the role of CXCL12/CXCR4 axis has been extensively studied in metastases in various types of carcinoma, including bone sarcoma, only a few studies mentioned this role in tumor growth and progression. CXCR4 inhibitors, such as AMD3100 and CTCE-9908, have been shown to be effective in inhibiting tumour cell metastasis by targeting interaction CXCL12/CXCR4 in U2OS and OS K7M2 cells (Huang et al., 2009, Kim et al., 2008). As regards tumour growth and progression in OS, Miura and co-workers demonstrated that the ability to form tumours in vivo positively correlated with the levels of CXCR4 expression in human HOS OS cells (Miura et al., 2005).

The results in Chapter 5 link to the expression of CXCL12 in CAFs and NFs derived from breast cancer patients. While a direct role for IKK α has not been reported in the regulation of CXCL12 expression in these cells, the findings were consistent with other research which found that CAFs have been identified as a major source of CXCL12 within the tumour microenvironment, which promotes tumour growth and angiogenesis (Kojima et al., 2010, Orimo et al., 2005). The SDF-1/CXCR4 axis can also induce the activation of NF- κ B, which plays an important role in tumour growth and breast cancer metastasis (Mukherjee and Zhao, 2013, Dewan et al., 2006). Several preclinical studies demonstrate used CXCR4 antagonists in solid tumours to sensitise tumour cells to chemotherapeutic therapies through disrupting CXCL12/CXCR4-dependent tumour-stroma interactions (Nervi et al., 2009, Zeng et al., 2009, Dillmann et al., 2009). Therefore, targeting of CXCL12 in tumour microenvironment may help to define novel strategies for more successful cancer treatment.

This work could be extended in a number of ways. For example, the effect of combined treatment of SU compounds and irradiation could be an attractive approach in breast cancer. Radiotherapy is a cancer therapy which uses radiation to kill cancer cells and is commonly used to treat different types of cancer including breast cancer

(Njeh et al., 2010). IKK α could promote resistance to radiation therapy in CAFs via the activation of the non-canonical NF- κ B pathway, which is highly expressed in CAFs biopsies, NF- κ B activation has been observed in cells treated with γ -radiation in breast cancer patients (Guo et al., 2004). Furthermore, several publications have reported that the inhibition of NF- κ B in combination with irradiation or chemotherapy induces a more favourable outcome (Nakanishi and Toi, 2005, Baldwin, 2001). Furthermore, preliminary studies in the Boyd laboratory (SIPBS) revealed an additive anti-tumour efficacy using a combination of SU1261 and radiation therapy in prostate cancer (PCa) cells, the results demonstrated a significant difference in survival fraction during combined treatment compared to cells treated with radiation therapy alone (Khalid personal communication). Further studies are needed to confirm whether disruption of the interaction of cancer cells with their microenvironment might fill the gap existing and can increase the efficacy of conventional therapies.

6.2 Conclusion

In conclusion, the findings of this thesis show SU compounds as novel first-in class IKK α inhibitors in bone and breast cancer. The novel findings obtained from this thesis highlight the significant role of IKK α in mediating the non-canonical NF- κ B pathway in the potential regulation of CXCL12 expression in bone cancer. Furthermore, our findings reveal for the first time novel, rapid activation of the non-canonical NF- κ B pathway. In addition, results presented using two primary cells of breast cancer patients, CAFs and NFs, suggest that IKK α is not required for the regulation of CXCL12, which appears to be a potential target for increasing the efficacy of conventional therapies in breast cancer. These findings from this study provide a novel foundation for a possible future translation via a wider study *in vivo* and then a clinical trial study.

References

- ABARRATEGI, A., TORNIN, J., MARTINEZ-CRUZADO, L., HAMILTON, A., MARTINEZ-CAMPOS, E., RODRIGO, J. P., GONZALEZ, M. V., BALDINI, N., GARCIA-CASTRO, J. & RODRIGUEZ, R. 2016. Osteosarcoma: Cells-of-Origin, Cancer Stem Cells, and Targeted Therapies. *Stem Cells Int*, 2016, 3631764.
- ABELIOVICH, H., ZHANG, C., DUNN, W. A., JR., SHOKAT, K. M. & KLIONSKY, D. J. 2003. Chemical genetic analysis of Apg1 reveals a non-kinase role in the induction of autophagy. *Mol Biol Cell*, 14, 477-90.
- ABU-AMER, Y. 2013. NF-kappaB signaling and bone resorption. *Osteoporos Int*, 24, 2377-86.
- AGARWAL, A., DAS, K., LERNER, N., SATHE, S., CICEK, M., CASEY, G. & SIZEMORE, N. 2005. The AKT/I kappa B kinase pathway promotes angiogenic/metastatic gene expression in colorectal cancer by activating nuclear factor-kappa B and beta-catenin. *Oncogene*, 24, 1021-31.
- AHMED, K. M. & LI, J. J. 2008. NF-kappa B-mediated adaptive resistance to ionizing radiation. *Free Radic Biol Med*, 44, 1-13.
- AIUTI, A., WEBB, I. J., BLEUL, C., SPRINGER, T. & GUTIERREZ-RAMOS, J. C. 1997. The chemokine SDF-1 is a chemoattractant for human CD34+ hematopoietic progenitor cells and provides a new mechanism to explain the mobilization of CD34+ progenitors to peripheral blood. *J Exp Med*, 185, 111-20.
- AKIBA, H., NAKANO, H., NISHINAKA, S., SHINDO, M., KOBATA, T., ATSUTA, M., MORIMOTO, C., WARE, C. F., MALININ, N. L., WALLACH, D., YAGITA, H. & OKUMURA, K. 1998. CD27, a member of the tumor necrosis factor receptor superfamily, activates NF-kappaB and stress-activated protein kinase/c-Jun N-terminal kinase via TRAF2, TRAF5, and NF-kappaB-inducing kinase. *J Biol Chem*, 273, 13353-8.
- AL-ANSARI, M. M., HENDRAYANI, S. F., SHEHATA, A. I. & ABOUSSEKHRA, A. 2013. p16(INK4A) represses the paracrine tumor-promoting effects of breast stromal fibroblasts. *Oncogene*, 32, 2356-64.
- ALLEN, I. C., WILSON, J. E., SCHNEIDER, M., LICH, J. D., ROBERTS, R. A., ARTHUR, J. C., WOODFORD, R. M., DAVIS, B. K., URONIS, J. M., HERFARTH, H. H., JOBIN, C., ROGERS, A. B. & TING, J. P. 2012. NLRP12 suppresses colon inflammation and tumorigenesis through the negative regulation of noncanonical NF-kappaB signaling. *Immunity*, 36, 742-54.
- AMIR, R. E., HAECKER, H., KARIN, M. & CIECHANOVER, A. 2004. Mechanism of processing of the NF-kappa B2 p100 precursor: identification of the specific polyubiquitin chain-anchoring lysine residue and analysis of the role of NEDD8-modification on the SCF(beta-TrCP) ubiquitin ligase. *Oncogene*, 23, 2540-7.
- AMMIRANTE, M., LUO, J. L., GRIVENNIKOV, S., NEDOSPASOV, S. & KARIN, M. 2010. B-cell-derived lymphotoxin promotes castration-resistant prostate cancer. *Nature*, 464, 302-5.
- ANNUNZIATA, C. M., DAVIS, R. E., DEMCHENKO, Y., BELLAMY, W., GABREA, A., ZHAN, F., LENZ, G., HANAMURA, I., WRIGHT, G., XIAO, W., DAVE, S., HURT, E. M., TAN, B., ZHAO, H., STEPHENS, O., SANTRA, M., WILLIAMS, D. R., DANG, L., BARLOGIE, B., SHAUGHNESSY, J. D., JR., KUEHL, W. M. & STAUDT, L. M. 2007. Frequent engagement of the classical and alternative NF-kappaB pathways by diverse genetic abnormalities in multiple myeloma. *Cancer Cell*, 12, 115-30.
- ANTHONY, N. G., BAIGET, J., BERRETTA, G., BOYD, M., BREEN, D., EDWARDS, J., GAMBLE, C., GRAY, A. I., HARVEY, A. L., HATZIEREMIA, S., HO, K. H., HUGGAN, J. K., LANG, S., LLONA-MINGUEZ, S., LUO, J. L., MCINTOSH,

- K., PAUL, A., PLEVIN, R. J., ROBERTSON, M. N., SCOTT, R., SUCKLING, C. J., SUTCLIFFE, O. B., YOUNG, L. C. & MACKAY, S. P. 2017. Inhibitory Kappa B Kinase alpha (IKKalpha) Inhibitors That Recapitulate Their Selectivity in Cells against Isoform-Related Biomarkers. *J Med Chem*, 60, 7043-7066.
- ASAMITSU, K., YAMAGUCHI, T., NAKATA, K., HIBI, Y., VICTORIANO, A. F., IMAI, K., ONOZAKI, K., KITADE, Y. & OKAMOTO, T. 2008. Inhibition of human immunodeficiency virus type 1 replication by blocking IkappaB kinase with noraristeromycin. *J Biochem*, 144, 581-9.
- BABIJ, P., ZHAO, W., SMALL, C., KHARODE, Y., YAWORSKY, P. J., BOUXSEIN, M. L., REDDY, P. S., BODINE, P. V., ROBINSON, J. A., BHAT, B., MARZOLF, J., MORAN, R. A. & BEX, F. 2003. High bone mass in mice expressing a mutant LRP5 gene. *J Bone Miner Res*, 18, 960-74.
- BACHELDER, R. E., WENDT, M. A. & MERCURIO, A. M. 2002. Vascular endothelial growth factor promotes breast carcinoma invasion in an autocrine manner by regulating the chemokine receptor CXCR4. *Cancer Res*, 62, 7203-6.
- BAEUERLE, P. A. & BALTIMORE, D. 1988. I kappa B: a specific inhibitor of the NF-kappa B transcription factor. *Science*, 242, 540-6.
- BAI, L., CHEN, J., MCEACHERN, D., LIU, L., ZHOU, H., AGUILAR, A. & WANG, S. 2014. BM-1197: a novel and specific Bcl-2/Bcl-xL inhibitor inducing complete and long-lasting tumor regression in vivo. *PLoS One*, 9, e99404.
- BAIN, J., MCLAUCHLAN, H., ELLIOTT, M. & COHEN, P. 2003. The specificities of protein kinase inhibitors: an update. *Biochem J*, 371, 199-204.
- BALABANIAN, K., LAGANE, B., INFANTINO, S., CHOW, K. Y., HARRIAGUE, J., MOEPPS, B., ARENZANA-SEISDEDOS, F., THELEN, M. & BACHELERIE, F. 2005. The chemokine SDF-1/CXCL12 binds to and signals through the orphan receptor RDC1 in T lymphocytes. *J Biol Chem*, 280, 35760-6.
- BALDWIN, A. S. 2001. Control of oncogenesis and cancer therapy resistance by the transcription factor NF-kappaB. *J Clin Invest*, 107, 241-6.
- BALKWILL, F. 2004. Cancer and the chemokine network. *Nat Rev Cancer*, 4, 540-50.
- BANDYOPADHYAY, A., AGYIN, J. K., WANG, L., TANG, Y., LEI, X., STORY, B. M., CORNELL, J. E., POLLOCK, B. H., MUNDY, G. R. & SUN, L. Z. 2006. Inhibition of pulmonary and skeletal metastasis by a transforming growth factor-beta type I receptor kinase inhibitor. *Cancer Res*, 66, 6714-21.
- BANERJEE, S., THAYANITHY, V., SANGWAN, V., MACKENZIE, T. N., SALUJA, A. K. & SUBRAMANIAN, S. 2013. Minnelide reduces tumor burden in preclinical models of osteosarcoma. *Cancer Lett*, 335, 412-20.
- BASU-ROY, U., BASILICO, C. & MANSUKHANI, A. 2013. Perspectives on cancer stem cells in osteosarcoma. *Cancer Lett*, 338, 158-67.
- BAUER, W., AUB, J. C. & ALBRIGHT, F. 1929. STUDIES OF CALCIUM AND PHOSPHORUS METABOLISM : V. A STUDY OF THE BONE TRABECULAE AS A READILY AVAILABLE RESERVE SUPPLY OF CALCIUM. *J Exp Med*, 49, 145-62.
- BAYANI, J., ZIELENSKA, M., PANDITA, A., AL-ROMAII, K., KARASKOVA, J., HARRISON, K., BRIDGE, J. A., SORENSEN, P., THORNER, P. & SQUIRE, J. A. 2003. Spectral karyotyping identifies recurrent complex rearrangements of chromosomes 8, 17, and 20 in osteosarcomas. *Genes Chromosomes Cancer*, 36, 7-16.
- BEEDERMAN, M., LAMPLLOT, J. D., NAN, G., WANG, J., LIU, X., YIN, L., LI, R., SHUI, W., ZHANG, H., KIM, S. H., ZHANG, W., ZHANG, J., KONG, Y., DENDULURI, S., ROGERS, M. R., PRATT, A., HAYDON, R. C., LUU, H. H., ANGELES, J., SHI, L. L. & HE, T. C. 2013. BMP signaling in mesenchymal stem cell differentiation and bone formation. *J Biomed Sci Eng*, 6, 32-52.

- BEG, A. A., RUBEN, S. M., SCHEINMAN, R. I., HASKILL, S., ROSEN, C. A. & BALDWIN, A. S., JR. 1992. I kappa B interacts with the nuclear localization sequences of the subunits of NF-kappa B: a mechanism for cytoplasmic retention. *Genes Dev*, 6, 1899-913.
- BEINKE, S. & LEY, S. C. 2004. Functions of NF-kappaB1 and NF-kappaB2 in immune cell biology. *Biochem J*, 382, 393-409.
- BEN-NERIAH, Y. & KARIN, M. 2011. Inflammation meets cancer, with NF-kappaB as the matchmaker. *Nat Immunol*, 12, 715-23.
- BENNETT, B. L., SASAKI, D. T., MURRAY, B. W., O'LEARY, E. C., SAKATA, S. T., XU, W., LEISTEN, J. C., MOTIWALA, A., PIERCE, S., SATOH, Y., BHAGWAT, S. S., MANNING, A. M. & ANDERSON, D. W. 2001. SP600125, an anthrapyrazolone inhibitor of Jun N-terminal kinase. *Proc Natl Acad Sci U S A*, 98, 13681-6.
- BENNETT, L., QUINN, J., MCCALL, P., MALLON, E. A., HORGAN, P. G., MCMILLAN, D. C., PAUL, A. & EDWARDS, J. 2017. High IKKalpha expression is associated with reduced time to recurrence and cancer specific survival in oestrogen receptor (ER)-positive breast cancer. *Int J Cancer*, 140, 1633-1644.
- BERENDSEN, A. D. & OLSEN, B. R. 2015. Bone development. *Bone*, 80, 14-18.
- BERGHUIS, D., SCHILHAM, M. W., SANTOS, S. J., SAVOLA, S., KNOWLES, H. J., DIRKSEN, U., SCHAEFER, K. L., VAKKILA, J., HOGENDOORN, P. C. & LANKESTER, A. C. 2012. The CXCR4-CXCL12 axis in Ewing sarcoma: promotion of tumor growth rather than metastatic disease. *Clin Sarcoma Res*, 2, 24.
- BIANCHI, K. & MEIER, P. 2009. A tangled web of ubiquitin chains: breaking news in TNF-R1 signaling. *Mol Cell*, 36, 736-42.
- BIRBACH, A., GOLD, P., BINDER, B. R., HOFER, E., DE MARTIN, R. & SCHMID, J. A. 2002. Signaling molecules of the NF-kappa B pathway shuttle constitutively between cytoplasm and nucleus. *J Biol Chem*, 277, 10842-51.
- BIRBRAIR, A., ZHANG, T., WANG, Z. M., MESSI, M. L., MINTZ, A. & DELBONO, O. 2015. Pericytes at the intersection between tissue regeneration and pathology. *Clin Sci (Lond)*, 128, 81-93.
- BLANK, V., KOURILSKY, P. & ISRAEL, A. 1992. NF-kappa B and related proteins: Rel/dorsal homologies meet ankyrin-like repeats. *Trends Biochem Sci*, 17, 135-40.
- BOEUF, S., BOVEE, J. V., LEHNER, B., HOGENDOORN, P. C. & RICHTER, W. 2010. Correlation of hypoxic signalling to histological grade and outcome in cartilage tumours. *Histopathology*, 56, 641-51.
- BONIG, H., PRIESTLEY, G. V., NILSSON, L. M., JIANG, Y. & PAPAYANNOPOULOU, T. 2004. PTX-sensitive signals in bone marrow homing of fetal and adult hematopoietic progenitor cells. *Blood*, 104, 2299-306.
- BONIZZI, G., BEBIEN, M., OTERO, D. C., JOHNSON-VROOM, K. E., CAO, Y., VU, D., JEGGA, A. G., ARONOW, B. J., GHOSH, G., RICKERT, R. C. & KARIN, M. 2004. Activation of IKKalpha target genes depends on recognition of specific kappaB binding sites by RelB:p52 dimers. *EMBO J*, 23, 4202-10.
- BONIZZI, G. & KARIN, M. 2004. The two NF-kappaB activation pathways and their role in innate and adaptive immunity. *Trends Immunol*, 25, 280-8.
- BOURS, V., FRANZOSO, G., AZARENKO, V., PARK, S., KANNO, T., BROWN, K. & SIEBENLIST, U. 1993. The oncoprotein Bcl-3 directly transactivates through kappa B motifs via association with DNA-binding p50B homodimers. *Cell*, 72, 729-39.

- BRAND, K., PAGE, S., ROGLER, G., BARTSCH, A., BRANDL, R., KNUECHEL, R., PAGE, M., KALTSCHMIDT, C., BAEUERLE, P. A. & NEUMEIER, D. 1996. Activated transcription factor nuclear factor-kappa B is present in the atherosclerotic lesion. *J Clin Invest*, 97, 1715-22.
- BRITANOVA, L. V., MAKEEV, V. J. & KUPRASH, D. V. 2008. In vitro selection of optimal RelB/p52 DNA-binding motifs. *Biochem Biophys Res Commun*, 365, 583-8.
- BROCKMAN, J. A., SCHERER, D. C., MCKINSEY, T. A., HALL, S. M., QI, X., LEE, W. Y. & BALLARD, D. W. 1995. Coupling of a signal response domain in I kappa B alpha to multiple pathways for NF-kappa B activation. *Mol Cell Biol*, 15, 2809-18.
- BROWN, A. M., LINHOFF, M. W., STEIN, B., WRIGHT, K. L., BALDWIN, A. S., JR., BASTA, P. V. & TING, J. P. 1994. Function of NF-kappa B/Rel binding sites in the major histocompatibility complex class II invariant chain promoter is dependent on cell-specific binding of different NF-kappa B/Rel subunits. *Mol Cell Biol*, 14, 2926-35.
- BROWNE, G., TAIPALEENMAKI, H., STEIN, G. S., STEIN, J. L. & LIAN, J. B. 2014. MicroRNAs in the control of metastatic bone disease. *Trends Endocrinol Metab*, 25, 320-7.
- BURGER, J. A. & KIPPS, T. J. 2006. CXCR4: a key receptor in the crosstalk between tumor cells and their microenvironment. *Blood*, 107, 1761-7.
- BURKE, J. R., PATTOLI, M. A., GREGOR, K. R., BRASSIL, P. J., MACMASTER, J. F., MCINTYRE, K. W., YANG, X., IOTZOVA, V. S., CLARKE, W., STRNAD, J., QIU, Y. & ZUSI, F. C. 2003. BMS-345541 is a highly selective inhibitor of I kappa B kinase that binds at an allosteric site of the enzyme and blocks NF-kappa B-dependent transcription in mice. *J Biol Chem*, 278, 1450-6.
- CAI, Y., CAI, T. & CHEN, Y. 2014. Wnt pathway in osteosarcoma, from oncogenic to therapeutic. *J Cell Biochem*, 115, 625-31.
- CAIROLI, R., BEGHINI, A., TURRINI, M., BERTANI, G., NADALI, G., RODEGHIRO, F., CASTAGNOLA, C., LAZZARONI, F., NICHELATTI, M., FERRARA, F., PIZZOLO, G., POGLIANI, E., ROSSI, G., MARTINELLI, G. & MORRA, E. 2013. Old and new prognostic factors in acute myeloid leukemia with deranged core-binding factor beta. *Am J Hematol*, 88, 594-600.
- CANCER_RESEARCH_UK. 2018. Available: <https://www.cancerresearchuk.org/about-cancer/bone-cancer/about> [Accessed 19/9/2018 2018].
- CAO, Y., LUO, J. L. & KARIN, M. 2007. I kappa B kinase alpha kinase activity is required for self-renewal of ErbB2/Her2-transformed mammary tumor-initiating cells. *Proc Natl Acad Sci U S A*, 104, 15852-7.
- CARAYOL, N. & WANG, C. Y. 2006. IKKalpha stabilizes cytosolic beta-catenin by inhibiting both canonical and non-canonical degradation pathways. *Cell Signal*, 18, 1941-6.
- CARREIRA, A. C., LOJUDICE, F. H., HALCSIK, E., NAVARRO, R. D., SOGAYAR, M. C. & GRANJEIRO, J. M. 2014. Bone morphogenetic proteins: facts, challenges, and future perspectives. *J Dent Res*, 93, 335-45.
- CASTRO, A. C., DANG, L. C., SOUCY, F., GRENIER, L., MAZDIYASNI, H., HOTTELET, M., PARENT, L., PIEN, C., PALOMBELLA, V. & ADAMS, J. 2003. Novel IKK inhibitors: beta-carbolines. *Bioorg Med Chem Lett*, 13, 2419-22.
- CATZ, S. D. & JOHNSON, J. L. 2001. Transcriptional regulation of bcl-2 by nuclear factor kappa B and its significance in prostate cancer. *Oncogene*, 20, 7342-51.

- CENTRELLA, M., MCCARTHY, T. L. & CANALIS, E. 1988. Skeletal tissue and transforming growth factor beta. *Faseb j*, 2, 3066-73.
- CERADINI, D. J., KULKARNI, A. R., CALLAGHAN, M. J., TEPPER, O. M., BASTIDAS, N., KLEINMAN, M. E., CAPLA, J. M., GALIANO, R. D., LEVINE, J. P. & GURTNER, G. C. 2004. Progenitor cell trafficking is regulated by hypoxic gradients through HIF-1 induction of SDF-1. *Nat Med*, 10, 858-64.
- CERVANTES, C. F., MARKWICK, P. R., SUE, S. C., MCCAMMON, J. A., DYSON, H. J. & KOMIVES, E. A. 2009. Functional dynamics of the folded ankyrin repeats of I kappa B alpha revealed by nuclear magnetic resonance. *Biochemistry*, 48, 8023-31.
- CHAISSON, M. L., BRANSTETTER, D. G., DERRY, J. M., ARMSTRONG, A. P., TOMETSKO, M. E., TAKEDA, K., AKIRA, S. & DOUGALL, W. C. 2004. Osteoclast differentiation is impaired in the absence of inhibitor of kappa B kinase alpha. *J Biol Chem*, 279, 54841-8.
- CHARALAMBOUS, M. P., MAIHOFNER, C., BHAMBRA, U., LIGHTFOOT, T. & GOODERHAM, N. J. 2003. Upregulation of cyclooxygenase-2 is accompanied by increased expression of nuclear factor-kappa B and I kappa B kinase-alpha in human colorectal cancer epithelial cells. *Br J Cancer*, 88, 1598-604.
- CHARIOT, A. 2009. The NF-kappaB-independent functions of IKK subunits in immunity and cancer. *Trends Cell Biol*, 19, 404-13.
- CHAUVIN, S., BENCSIK, M., BAMBINO, T. & NISSENSON, R. A. 2002. Parathyroid hormone receptor recycling: role of receptor dephosphorylation and beta-arrestin. *Mol Endocrinol*, 16, 2720-32.
- CHEN, F. E. & GHOSH, G. 1999. Regulation of DNA binding by Rel/NF-kappaB transcription factors: structural views. *Oncogene*, 18, 6845-52.
- CHEN, F. E., HUANG, D. B., CHEN, Y. Q. & GHOSH, G. 1998. Crystal structure of p50/p65 heterodimer of transcription factor NF-kappaB bound to DNA. *Nature*, 391, 410-3.
- CHEN, G., DENG, C. & LI, Y. P. 2012. TGF-beta and BMP signaling in osteoblast differentiation and bone formation. *Int J Biol Sci*, 8, 272-88.
- CHEN, Z. J., PARENT, L. & MANIATIS, T. 1996. Site-specific phosphorylation of I kappa B alpha by a novel ubiquitination-dependent protein kinase activity. *Cell*, 84, 853-62.
- CHU, T., TENG, J., JIANG, L., ZHONG, H. & HAN, B. 2014. Lung cancer-derived Dickkopf1 is associated with bone metastasis and the mechanism involves the inhibition of osteoblast differentiation. *Biochem Biophys Res Commun*, 443, 962-8.
- CILLONI, D., MESSA, F., ARRUGA, F., DEFILIPPI, I., MOROTTI, A., MESSA, E., CARTURAN, S., GIUGLIANO, E., PAUTASSO, M., BRACCO, E., ROSSO, V., SEN, A., MARTINELLI, G., BACCARANI, M. & SAGLIO, G. 2006. The NF-kappaB pathway blockade by the IKK inhibitor PS1145 can overcome imatinib resistance. *Leukemia*, 20, 61-7.
- CLARK, J. C., AKIYAMA, T., DASS, C. R. & CHOONG, P. F. 2010. New clinically relevant, orthotopic mouse models of human chondrosarcoma with spontaneous metastasis. *Cancer Cell Int*, 10, 20.
- CLAUDIO, E., BROWN, K., PARK, S., WANG, H. & SIEBENLIST, U. 2002. BAFF-induced NEMO-independent processing of NF-kappa B2 in maturing B cells. *Nat Immunol*, 3, 958-65.
- CLOHISY, J. C., YAMANAKA, Y., FACCIO, R. & ABU-AMER, Y. 2006. Inhibition of IKK activation, through sequestering NEMO, blocks PMMA-induced osteoclastogenesis and calvarial inflammatory osteolysis. *J Orthop Res*, 24, 1358-65.

- COGSWELL, P. C., GUTTRIDGE, D. C., FUNKHOUSER, W. K. & BALDWIN, A. S., JR. 2000. Selective activation of NF-kappa B subunits in human breast cancer: potential roles for NF-kappa B2/p52 and for Bcl-3. *Oncogene*, 19, 1123-31.
- COHEN, P. 1999. The development and therapeutic potential of protein kinase inhibitors. *Curr Opin Chem Biol*, 3, 459-65.
- COOPE, H. J., ATKINSON, P. G., HUHSE, B., BELICH, M., JANZEN, J., HOLMAN, M. J., KLAUS, G. G., JOHNSTON, L. H. & LEY, S. C. 2002. CD40 regulates the processing of NF-kappaB2 p100 to p52. *EMBO J*, 21, 5375-85.
- COSMAN, F. & LINDSAY, R. 2004. Therapeutic potential of parathyroid hormone. *Curr Osteoporos Rep*, 2, 5-11.
- CUENDA, A., ROUSE, J., DOZA, Y. N., MEIER, R., COHEN, P., GALLAGHER, T. F., YOUNG, P. R. & LEE, J. C. 1995. SB 203580 is a specific inhibitor of a MAP kinase homologue which is stimulated by cellular stresses and interleukin-1. *FEBS Lett*, 364, 229-33.
- DAI, X., MA, W., HE, X. & JHA, R. K. 2011. Review of therapeutic strategies for osteosarcoma, chondrosarcoma, and Ewing's sarcoma. *Med Sci Monit*, 17, Ra177-190.
- DALLER, B., MUSCH, W., ROHRL, J., TUMANOV, A. V., NEDOSPASOV, S. A., MANNEL, D. N., SCHNEIDER-BRACHER, W. & HEHLGANS, T. 2011. Lymphotoxin-beta receptor activation by lymphotoxin-alpha(1)beta(2) and LIGHT promotes tumor growth in an NFkappaB-dependent manner. *Int J Cancer*, 128, 1363-70.
- DATTA, N. S., PETTWAY, G. J., CHEN, C., KOH, A. J. & MCCAULEY, L. K. 2007. Cyclin D1 as a target for the proliferative effects of PTH and PTHrP in early osteoblastic cells. *J Bone Miner Res*, 22, 951-64.
- DAVIS, N., GHOSH, S., SIMMONS, D. L., TEMPST, P., LIOU, H. C., BALTIMORE, D. & BOSE, H. R., JR. 1991. Rel-associated pp40: an inhibitor of the rel family of transcription factors. *Science*, 253, 1268-71.
- DEJARDIN, E. 2006. The alternative NF-kappaB pathway from biochemistry to biology: pitfalls and promises for future drug development. *Biochem Pharmacol*, 72, 1161-79.
- DEJARDIN, E., DROIN, N. M., DELHASE, M., HAAS, E., CAO, Y., MAKRIS, C., LI, Z. W., KARIN, M., WARE, C. F. & GREEN, D. R. 2002. The lymphotoxin-beta receptor induces different patterns of gene expression via two NF-kappaB pathways. *Immunity*, 17, 525-35.
- DENK, A., GOEBELER, M., SCHMID, S., BERBERICH, I., RITZ, O., LINDEMANN, D., LUDWIG, S. & WIRTH, T. 2001. Activation of NF-kappa B via the Ikappa B kinase complex is both essential and sufficient for proinflammatory gene expression in primary endothelial cells. *J Biol Chem*, 276, 28451-8.
- DERYNCK, R. & AKHURST, R. J. 2007. Differentiation plasticity regulated by TGF-beta family proteins in development and disease. *Nat Cell Biol*, 9, 1000-4.
- DEVIN, A., LIN, Y., YAMAOKA, S., LI, Z., KARIN, M. & LIU, Z. 2001. The alpha and beta subunits of IkappaB kinase (IKK) mediate TRAF2-dependent IKK recruitment to tumor necrosis factor (TNF) receptor 1 in response to TNF. *Mol Cell Biol*, 21, 3986-94.
- DEWAN, M. Z., AHMED, S., IWASAKI, Y., OHBA, K., TOI, M. & YAMAMOTO, N. 2006. Stromal cell-derived factor-1 and CXCR4 receptor interaction in tumor growth and metastasis of breast cancer. *Biomed Pharmacother*, 60, 273-6.
- DIDONATO, J. A., HAYAKAWA, M., ROTHWARF, D. M., ZANDI, E. & KARIN, M. 1997. A cytokine-responsive IkappaB kinase that activates the transcription factor NF-kappaB. *Nature*, 388, 548-54.
- DIDONATO, J. A., MERCURIO, F. & KARIN, M. 2012. NF-kappaB and the link between inflammation and cancer. *Immunol Rev*, 246, 379-400.

- DILLMANN, F., VELDWIJK, M. R., LAUFS, S., SPERANDIO, M., CALANDRA, G., WENZ, F., ZELLER, J. & FRUEHAUF, S. 2009. Plerixafor inhibits chemotaxis toward SDF-1 and CXCR4-mediated stroma contact in a dose-dependent manner resulting in increased susceptibility of BCR-ABL+ cell to Imatinib and Nilotinib. *Leuk Lymphoma*, 50, 1676-86.
- DIMMELER, S., FLEMING, I., FISSLTHALER, B., HERMANN, C., BUSSE, R. & ZEIHNER, A. M. 1999. Activation of nitric oxide synthase in endothelial cells by Akt-dependent phosphorylation. *Nature*, 399, 601-5.
- DIPERSIO, J. F., MICALLEG, I. N., STIFF, P. J., BOLWELL, B. J., MAZIARZ, R. T., JACOBSEN, E., NADEMANEE, A., MCCARTY, J., BRIDGER, G. & CALANDRA, G. 2009. Phase III prospective randomized double-blind placebo-controlled trial of plerixafor plus granulocyte colony-stimulating factor compared with placebo plus granulocyte colony-stimulating factor for autologous stem-cell mobilization and transplantation for patients with non-Hodgkin's lymphoma. *J Clin Oncol*, 27, 4767-73.
- DOBRZANSKI, P., RYSECK, R. P. & BRAVO, R. 1993. Both N- and C-terminal domains of RelB are required for full transactivation: role of the N-terminal leucine zipper-like motif. *Mol Cell Biol*, 13, 1572-82.
- DOMANSKA, U. M., KRUIZINGA, R. C., NAGENGAST, W. B., TIMMER-BOSSCHA, H., HULS, G., DE VRIES, E. G. & WALENKAMP, A. M. 2013. A review on CXCR4/CXCL12 axis in oncology: no place to hide. *Eur J Cancer*, 49, 219-30.
- DOPPLER, H., LIOU, G. Y. & STORZ, P. 2013. Downregulation of TRAF2 mediates NIK-induced pancreatic cancer cell proliferation and tumorigenicity. *PLoS One*, 8, e53676.
- DU, R., LU, K. V., PETRITSCH, C., LIU, P., GANSS, R., PASSEGUE, E., SONG, H., VANDENBERG, S., JOHNSON, R. S., WERB, Z. & BERGERS, G. 2008. HIF1alpha induces the recruitment of bone marrow-derived vascular modulatory cells to regulate tumor angiogenesis and invasion. *Cancer Cell*, 13, 206-20.
- ELBASHIR, S. M., HARBORTH, J., LENDECKEL, W., YALCIN, A., WEBER, K. & TUSCHL, T. 2001. Duplexes of 21-nucleotide RNAs mediate RNA interference in cultured mammalian cells. *Nature*, 411, 494-8.
- ELISEEV, R. A., SCHWARZ, E. M., ZUSCIK, M. J., O'KEEFE, R. J., DRISSI, H. & ROSIER, R. N. 2006. Smad7 mediates inhibition of Saos2 osteosarcoma cell differentiation by NFkappaB. *Exp Cell Res*, 312, 40-50.
- ELL, B., MERCATALI, L., IBRAHIM, T., CAMPBELL, N., SCHWARZENBACH, H., PANTEL, K., AMADORI, D. & KANG, Y. 2013. Tumor-induced osteoclast miRNA changes as regulators and biomarkers of osteolytic bone metastasis. *Cancer Cell*, 24, 542-56.
- EREZ, N., TRUITT, M., OLSON, P., ARRON, S. T. & HANAHAN, D. 2010. Cancer-Associated Fibroblasts Are Activated in Incipient Neoplasia to Orchestrate Tumor-Promoting Inflammation in an NF-kappaB-Dependent Manner. *Cancer Cell*, 17, 135-47.
- FAROUK, S. S., RADER, D. J., REILLY, M. P. & MEHTA, N. N. 2010. CXCL12: a new player in coronary disease identified through human genetics. *Trends Cardiovasc Med*, 20, 204-9.
- FATA, J. E., KONG, Y. Y., LI, J., SASAKI, T., IRIE-SASAKI, J., MOOREHEAD, R. A., ELLIOTT, R., SCULLY, S., VOURA, E. B., LACEY, D. L., BOYLE, W. J., KHOKHA, R. & PENNINGER, J. M. 2000. The osteoclast differentiation factor osteoprotegerin-ligand is essential for mammary gland development. *Cell*, 103, 41-50.
- FENG, X. H. & DERYNCK, R. 2005. Specificity and versatility in tgf-beta signaling through Smads. *Annu Rev Cell Dev Biol*, 21, 659-93.

- FERLAY, J., SHIN, H. R., BRAY, F., FORMAN, D., MATHERS, C. & PARKIN, D. M. 2010. Estimates of worldwide burden of cancer in 2008: GLOBOCAN 2008. *Int J Cancer*, 127, 2893-917.
- FERNANDEZ-MAJADA, V., PUJADAS, J., VILARDELL, F., CAPELLA, G., MAYO, M. W., BIGAS, A. & ESPINOSA, L. 2007. Aberrant cytoplasmic localization of N-CoR in colorectal tumors. *Cell Cycle*, 6, 1748-52.
- FERREIRO, D. U. & KOMIVES, E. A. 2010. Molecular mechanisms of system control of NF-kappaB signaling by IkappaBalpha. *Biochemistry*, 49, 1560-7.
- FLORENCIO-SILVA, R., SASSO, G. R., SASSO-CERRI, E., SIMOES, M. J. & CERRI, P. S. 2015. Biology of Bone Tissue: Structure, Function, and Factors That Influence Bone Cells. *Biomed Res Int*, 2015, 421746.
- FRANTZ, B., KLATT, T., PANG, M., PARSONS, J., ROLANDO, A., WILLIAMS, H., TOCCI, M. J., O'KEEFE, S. J. & O'NEILL, E. A. 1998. The activation state of p38 mitogen-activated protein kinase determines the efficiency of ATP competition for pyridinylimidazole inhibitor binding. *Biochemistry*, 37, 13846-53.
- FRANZOSO, G., CARLSON, L., XING, L., POLJAK, L., SHORES, E. W., BROWN, K. D., LEONARDI, A., TRAN, T., BOYCE, B. F. & SIEBENLIST, U. 1997. Requirement for NF-kappaB in osteoclast and B-cell development. *Genes Dev*, 11, 3482-96.
- FUJITA, T., NOLAN, G. P., LIOU, H. C., SCOTT, M. L. & BALTIMORE, D. 1993. The candidate proto-oncogene bcl-3 encodes a transcriptional coactivator that activates through NF-kappa B p50 homodimers. *Genes Dev*, 7, 1354-63.
- FULDA, S. 2014. Molecular pathways: targeting inhibitor of apoptosis proteins in cancer--from molecular mechanism to therapeutic application. *Clin Cancer Res*, 20, 289-95.
- FUSELLA, F., SECLI, L., BUSO, E., KREPELOVA, A., MOISO, E., ROCCA, S., CONTI, L., ANNARATONE, L., RUBINETTO, C., MELLO-GRAND, M., SINGH, V., CHIORINO, G., SILENGO, L., ALTRUDA, F., TURCO, E., MOROTTI, A., OLIVIERO, S., CASTELLANO, I., CAVALLO, F., PROVERO, P., TARONE, G. & BRANCACCIO, M. 2017. The IKK/NF-kappaB signaling pathway requires Morgana to drive breast cancer metastasis. *Nat Commun*, 8, 1636.
- GAILLARD, P., JEANCLAUDE-ETTER, I., ARDISSONE, V., ARKINSTALL, S., CAMBET, Y., CAMPS, M., CHABERT, C., CHURCH, D., CIRILLO, R., GREENER, D., HALAZY, S., NICHOLS, A., SZYNDRALEWIEZ, C., VITTE, P. A. & GOTTELAND, J. P. 2005. Design and synthesis of the first generation of novel potent, selective, and in vivo active (benzothiazol-2-yl)acetonitrile inhibitors of the c-Jun N-terminal kinase. *J Med Chem*, 48, 4596-607.
- GAMBLE, C., MCINTOSH, K., SCOTT, R., HO, K. H., PLEVIN, R. & PAUL, A. 2012. Inhibitory kappa B Kinases as targets for pharmacological regulation. *Br J Pharmacol*, 165, 802-19.
- GANEFF, C., REMOUCHAMPS, C., BOUTAFFALA, L., BENEZECH, C., GALOPIN, G., VANDEPAER, S., BOUILLENNE, F., ORMENESE, S., CHARIOT, A., SCHNEIDER, P., CAAMANO, J., PIETTE, J. & DEJARDIN, E. 2011. Induction of the alternative NF-kappaB pathway by lymphotoxin alphabeta (LTalphabeta) relies on internalization of LTbeta receptor. *Mol Cell Biol*, 31, 4319-34.
- GARCIA-MORUJA, C., ALONSO-LOBO, J. M., RUEDA, P., TORRES, C., GONZALEZ, N., BERMEJO, M., LUQUE, F., ARENZANA-SEISDEDOS, F., ALCAMI, J. & CARUZ, A. 2005. Functional characterization of SDF-1 proximal promoter. *J Mol Biol*, 348, 43-62.

- GARDAM, S., TURNER, V. M., ANDERTON, H., LIMAYE, S., BASTEN, A., KOENTGEN, F., VAUX, D. L., SILKE, J. & BRINK, R. 2011. Deletion of cIAP1 and cIAP2 in murine B lymphocytes constitutively activates cell survival pathways and inactivates the germinal center response. *Blood*, 117, 4041-51.
- GASPARIAN, A. V., YAO, Y. J., KOWALCZYK, D., LYAKH, L. A., KARSELADZE, A., SLAGA, T. J. & BUDUNOVA, I. V. 2002. The role of IKK in constitutive activation of NF-kappaB transcription factor in prostate carcinoma cells. *J Cell Sci*, 115, 141-51.
- GELDERBLOM, H., HOGENDOORN, P. C., DIJKSTRA, S. D., VAN RIJSWIJK, C. S., KROL, A. D., TAMINIAU, A. H. & BOVEE, J. V. 2008. The clinical approach towards chondrosarcoma. *Oncologist*, 13, 320-9.
- GHOSH, S., MAY, M. J. & KOPP, E. B. 1998. NF-kappa B and Rel proteins: evolutionarily conserved mediators of immune responses. *Annu Rev Immunol*, 16, 225-60.
- GILL, J., AHLUWALIA, M. K., GELLER, D. & GORLICK, R. 2013. New targets and approaches in osteosarcoma. *Pharmacol Ther*, 137, 89-99.
- GLOIRE, G., HORION, J., EL MJIYAD, N., BEX, F., CHARIOT, A., DEJARDIN, E. & PIETTE, J. 2007. Promoter-dependent effect of IKKalpha on NF-kappaB/p65 DNA binding. *J Biol Chem*, 282, 21308-18.
- GOMPERTS, B. N., BELPERIO, J. A., RAO, P. N., RANDELL, S. H., FISHBEIN, M. C., BURDICK, M. D. & STRIETER, R. M. 2006. Circulating progenitor epithelial cells traffic via CXCR4/CXCL12 in response to airway injury. *J Immunol*, 176, 1916-27.
- GONZALEZ-ANGULO, A. M., MORALES-VASQUEZ, F. & HORTOBAGYI, G. N. 2007. Overview of resistance to systemic therapy in patients with breast cancer. *Adv Exp Med Biol*, 608, 1-22.
- GONZALO, J. A., LLOYD, C. M., PELED, A., DELANEY, T., COYLE, A. J. & GUTIERREZ-RAMOS, J. C. 2000. Critical involvement of the chemotactic axis CXCR4/stromal cell-derived factor-1 alpha in the inflammatory component of allergic airway disease. *J Immunol*, 165, 499-508.
- GRECH, A. P., AMESBURY, M., CHAN, T., GARDAM, S., BASTEN, A. & BRINK, R. 2004. TRAF2 differentially regulates the canonical and noncanonical pathways of NF-kappaB activation in mature B cells. *Immunity*, 21, 629-42.
- GREENBAUM, A., HSU, Y. M., DAY, R. B., SCHUETTPELZ, L. G., CHRISTOPHER, M. J., BORGERDING, J. N., NAGASAWA, T. & LINK, D. C. 2013. CXCL12 in early mesenchymal progenitors is required for haematopoietic stem-cell maintenance. *Nature*, 495, 227-30.
- GU, K., ZHANG, L., JIN, T. & RUTHERFORD, R. B. 2004. Identification of potential modifiers of Runx2/Cbfa1 activity in C2C12 cells in response to bone morphogenetic protein-7. *Cells Tissues Organs*, 176, 28-40.
- GUAN, H., HOU, S. & RICCIARDI, R. P. 2005. DNA binding of repressor nuclear factor-kappaB p50/p50 depends on phosphorylation of Ser337 by the protein kinase A catalytic subunit. *J Biol Chem*, 280, 9957-62.
- GUO, G., WANG, T., GAO, Q., TAMAE, D., WONG, P., CHEN, T., CHEN, W. C., SHIVELY, J. E., WONG, J. Y. & LI, J. J. 2004. Expression of ErbB2 enhances radiation-induced NF-kappaB activation. *Oncogene*, 23, 535-45.
- GUO, X. & WANG, X. F. 2009. Signaling cross-talk between TGF-beta/BMP and other pathways. *Cell Res*, 19, 71-88.
- GUYON, A. 2014. CXCL12 chemokine and its receptors as major players in the interactions between immune and nervous systems. *Front Cell Neurosci*, 8, 65.
- HACKER, H. & KARIN, M. 2006. Regulation and function of IKK and IKK-related kinases. *Sci STKE*, 2006, re13.

- HALL, J. M. & KORACH, K. S. 2003. Stromal cell-derived factor 1, a novel target of estrogen receptor action, mediates the mitogenic effects of estradiol in ovarian and breast cancer cells. *Mol Endocrinol*, 17, 792-803.
- HANAHAN, D. & WEINBERG, R. A. 2011. Hallmarks of cancer: the next generation. *Cell*, 144, 646-74.
- HAO, L., RIZZO, P., OSIPO, C., PANNUTI, A., WYATT, D., CHEUNG, L. W., SONENSHEIN, G., OSBORNE, B. A. & MIELE, L. 2010. Notch-1 activates estrogen receptor-alpha-dependent transcription via IKKalpha in breast cancer cells. *Oncogene*, 29, 201-13.
- HAUER, K., CALZADA-WACK, J., STEIGER, K., GRUNEWALD, T. G., BAUMHOER, D., PLEHM, S., BUCH, T., PRAZERES DA COSTA, O., ESPOSITO, I., BURDACH, S. & RICHTER, G. H. 2013. DKK2 mediates osteolysis, invasiveness, and metastatic spread in Ewing sarcoma. *Cancer Res*, 73, 967-77.
- HAYBAECK, J., ZELLER, N., WOLF, M. J., WEBER, A., WAGNER, U., KURRER, M. O., BREMER, J., IEZZI, G., GRAF, R., CLAVIEN, P. A., THIMME, R., BLUM, H., NEDOSPASOV, S. A., ZATLOUKAL, K., RAMZAN, M., CIESEK, S., PIETSCHMANN, T., MARCHE, P. N., KARIN, M., KOPF, M., BROWNING, J. L., AGUZZI, A. & HEIKENWALDER, M. 2009. A lymphotoxin-driven pathway to hepatocellular carcinoma. *Cancer Cell*, 16, 295-308.
- HAYDEN, M. S. & GHOSH, S. 2008. Shared principles in NF-kappaB signaling. *Cell*, 132, 344-62.
- HAYDEN, M. S. & GHOSH, S. 2012. NF-kappaB, the first quarter-century: remarkable progress and outstanding questions. *Genes Dev*, 26, 203-34.
- HEHLMANN, R., HOCHHAUS, A. & BACCARANI, M. 2007. Chronic myeloid leukaemia. *The Lancet*, 370, 342-350.
- HEMMATI, M., ABBASPOUR, A., ALIZADEH, A. M., KHANIKI, M., AMANZADEH, A., MOHAGHEGHI, M. A. & MOUSAVI, M. S. 2011. Rat xenograft chondrosarcoma development by human tissue fragment. *Exp Oncol*, 33, 52-4.
- HIDESHIMA, T., CHAUHAN, D., RICHARDSON, P., MITSIADES, C., MITSIADES, N., HAYASHI, T., MUNSHI, N., DANG, L., CASTRO, A., PALOMBELLA, V., ADAMS, J. & ANDERSON, K. C. 2002. NF-kappa B as a therapeutic target in multiple myeloma. *J Biol Chem*, 277, 16639-47.
- HINTON, C. V., AVRAHAM, S. & AVRAHAM, H. K. 2010. Role of the CXCR4/CXCL12 signaling axis in breast cancer metastasis to the brain. *Clin Exp Metastasis*, 27, 97-105.
- HINZ, M. & SCHEIDEREIT, C. 2014. The IkappaB kinase complex in NF-kappaB regulation and beyond. *EMBO Rep*, 15, 46-61.
- HIPPE, A., HOMEY, B. & MUELLER-HOMEY, A. 2010. Chemokines. *Recent Results Cancer Res*, 180, 35-50.
- HIRAGA, T., MYOUI, A., HASHIMOTO, N., SASAKI, A., HATA, K., MORITA, Y., YOSHIKAWA, H., ROSEN, C. J., MUNDY, G. R. & YONEDA, T. 2012. Bone-derived IGF mediates crosstalk between bone and breast cancer cells in bony metastases. *Cancer Res*, 72, 4238-49.
- HIRATA, Y., MAEDA, S., OHMAE, T., SHIBATA, W., YANAI, A., OGURA, K., YOSHIDA, H., KAWABE, T. & OMATA, M. 2006. Helicobacter pylori induces IkappaB kinase alpha nuclear translocation and chemokine production in gastric epithelial cells. *Infect Immun*, 74, 1452-61.
- HITCHON, C., WONG, K., MA, G., REED, J., LYTTLE, D. & EL-GABALAWY, H. 2002. Hypoxia-induced production of stromal cell-derived factor 1 (CXCL12) and vascular endothelial growth factor by synovial fibroblasts. *Arthritis Rheum*, 46, 2587-97.

- HJARNAA, P. J., JONSSON, E., LATINI, S., DHAR, S., LARSSON, R., BRAMM, E., SKOV, T. & BINDERUP, L. 1999. CHS 828, a novel pyridyl cyanoguanidine with potent antitumor activity in vitro and in vivo. *Cancer Res*, 59, 5751-7.
- HOESEL, B. & SCHMID, J. A. 2013. The complexity of NF-kappaB signaling in inflammation and cancer. *Mol Cancer*, 12, 86.
- HOSHINO, K., SUGIYAMA, T., MATSUMOTO, M., TANAKA, T., SAITO, M., HEMMI, H., OHARA, O., AKIRA, S. & KAISHO, T. 2006. IkappaB kinase-alpha is critical for interferon-alpha production induced by Toll-like receptors 7 and 9. *Nature*, 440, 949-53.
- HU, Y., BAUD, V., DELHASE, M., ZHANG, P., DEERINCK, T., ELLISMAN, M., JOHNSON, R. & KARIN, M. 1999. Abnormal morphogenesis but intact IKK activation in mice lacking the IKKalpha subunit of IkappaB kinase. *Science*, 284, 316-20.
- HUANG, C. Y., LEE, C. Y., CHEN, M. Y., YANG, W. H., CHEN, Y. H., CHANG, C. H., HSU, H. C., FONG, Y. C. & TANG, C. H. 2009. Stromal cell-derived factor-1/CXCR4 enhanced motility of human osteosarcoma cells involves MEK1/2, ERK and NF-kappaB-dependent pathways. *J Cell Physiol*, 221, 204-12.
- HUANG, M., LI, Y., ZHANG, H. & NAN, F. 2010. Breast cancer stromal fibroblasts promote the generation of CD44+CD24- cells through SDF-1/CXCR4 interaction. *J Exp Clin Cancer Res*, 29, 80.
- HUANG, S., ROBINSON, J. B., DEGUZMAN, A., BUCANA, C. D. & FIDLER, I. J. 2000. Blockade of nuclear factor-kappaB signaling inhibits angiogenesis and tumorigenicity of human ovarian cancer cells by suppressing expression of vascular endothelial growth factor and interleukin 8. *Cancer Res*, 60, 5334-9.
- HUANG, W. C., JU, T. K., HUNG, M. C. & CHEN, C. C. 2007. Phosphorylation of CBP by IKKalpha promotes cell growth by switching the binding preference of CBP from p53 to NF-kappaB. *Mol Cell*, 26, 75-87.
- HUXFORD, T. & GHOSH, G. 2009. A structural guide to proteins of the NF-kappaB signaling module. *Cold Spring Harb Perspect Biol*, 1, a000075.
- INOUE, J., KERR, L. D., KAKIZUKA, A. & VERMA, I. M. 1992. I kappa B gamma, a 70 kd protein identical to the C-terminal half of p110 NF-kappa B: a new member of the I kappa B family. *Cell*, 68, 1109-20.
- IOTSOVA, V., CAAMANO, J., LOY, J., YANG, Y., LEWIN, A. & BRAVO, R. 1997. Osteopetrosis in mice lacking NF-kappaB1 and NF-kappaB2. *Nat Med*, 3, 1285-9.
- IVANENKOV, Y. A., BALAKIN, K. V. & LAVROVSKY, Y. 2011. Small molecule inhibitors of NF-kB and JAK/STAT signal transduction pathways as promising anti-inflammatory therapeutics. *Mini Rev Med Chem*, 11, 55-78.
- JAFARI, R., ALMQVIST, H., AXELSSON, H., IGNATUSHCHENKO, M., LUNDBACK, T., NORDLUND, P. & MARTINEZ MOLINA, D. 2014. The cellular thermal shift assay for evaluating drug target interactions in cells. *Nat Protoc*, 9, 2100-22.
- JAFFRAY, E., WOOD, K. M. & HAY, R. T. 1995. Domain organization of I kappa B alpha and sites of interaction with NF-kappa B p65. *Mol Cell Biol*, 15, 2166-72.
- JAMIL, N., HOWIE, S. & SALTER, D. M. 2010. Therapeutic molecular targets in human chondrosarcoma. *Int J Exp Pathol*, 91, 387-93.
- JENNY, A. 2010. Planar cell polarity signaling in the Drosophila eye. *Curr Top Dev Biol*, 93, 189-227.
- JIMI, E., AOKI, K., SAITO, H., D'ACQUISTO, F., MAY, M. J., NAKAMURA, I., SUDO, T., KOJIMA, T., OKAMOTO, F., FUKUSHIMA, H., OKABE, K., OHYA, K. & GHOSH, S. 2004. Selective inhibition of NF-kappa B blocks osteoclastogenesis and prevents inflammatory bone destruction in vivo. *Nat Med*, 10, 617-24.

- JUNG, Y., WANG, J., SCHNEIDER, A., SUN, Y. X., KOH-PAIGE, A. J., OSMAN, N. I., MCCAULEY, L. K. & TAICHMAN, R. S. 2006. Regulation of SDF-1 (CXCL12) production by osteoblasts; a possible mechanism for stem cell homing. *Bone*, 38, 497-508.
- JUPPNER, H., ABOU-SAMRA, A. B., FREEMAN, M., KONG, X. F., SCHIPANI, E., RICHARDS, J., KOLAKOWSKI, L. F., JR., HOCK, J., POTTS, J. T., JR., KRONENBERG, H. M. & ET AL. 1991. A G protein-linked receptor for parathyroid hormone and parathyroid hormone-related peptide. *Science*, 254, 1024-6.
- KAILEH, M. & SEN, R. 2012. NF-kappaB function in B lymphocytes. *Immunol Rev*, 246, 254-71.
- KALLURI, R. 2016. The biology and function of fibroblasts in cancer. *Nature Reviews Cancer*, 16, 582.
- KALLURI, R. & ZEISBERG, M. 2006. Fibroblasts in cancer. *Nat Rev Cancer*, 6, 392-401.
- KANAYAMA, A., SETH, R. B., SUN, L., EA, C. K., HONG, M., SHAITO, A., CHIU, Y. H., DENG, L. & CHEN, Z. J. 2004. TAB2 and TAB3 activate the NF-kappaB pathway through binding to polyubiquitin chains. *Mol Cell*, 15, 535-48.
- KANG, Y., HE, W., TULLEY, S., GUPTA, G. P., SERGANOVA, I., CHEN, C. R., MANOVA-TODOROVA, K., BLASBERG, R., GERALD, W. L. & MASSAGUE, J. 2005. Breast cancer bone metastasis mediated by the Smad tumor suppressor pathway. *Proc Natl Acad Sci U S A*, 102, 13909-14.
- KARIN, M. 2006. Nuclear factor-kappaB in cancer development and progression. *Nature*, 441, 431-6.
- KARIN, M. & BEN-NERIAH, Y. 2000. Phosphorylation meets ubiquitination: the control of NF-[kappa]B activity. *Annu Rev Immunol*, 18, 621-63.
- KARIN, M., CAO, Y., GRETEN, F. R. & LI, Z. W. 2002. NF-kappaB in cancer: from innocent bystander to major culprit. *Nat Rev Cancer*, 2, 301-10.
- KARIN, M. & GRETEN, F. R. 2005. NF-kappaB: linking inflammation and immunity to cancer development and progression. *Nat Rev Immunol*, 5, 749-59.
- KATAYAMA, Y., BATTISTA, M., KAO, W. M., HIDALGO, A., PEIRED, A. J., THOMAS, S. A. & FRENETTE, P. S. 2006. Signals from the sympathetic nervous system regulate hematopoietic stem cell egress from bone marrow. *Cell*, 124, 407-21.
- KAYAGAKI, N., YAN, M., SESHASAYEE, D., WANG, H., LEE, W., FRENCH, D. M., GREWAL, I. S., COCHRAN, A. G., GORDON, N. C., YIN, J., STAROVASNIK, M. A. & DIXIT, V. M. 2002. BAFF/BLYS receptor 3 binds the B cell survival factor BAFF ligand through a discrete surface loop and promotes processing of NF-kappaB2. *Immunity*, 17, 515-24.
- KEATS, J. J., FONSECA, R., CHESI, M., SCHOP, R., BAKER, A., CHNG, W. J., VAN WIER, S., TIEDEMANN, R., SHI, C. X., SEBAG, M., BRAGGIO, E., HENRY, T., ZHU, Y. X., FOGLE, H., PRICE-TROSKA, T., AHMANN, G., MANCINI, C., BRENTS, L. A., KUMAR, S., GREIPP, P., DISPENZIERI, A., BRYANT, B., MULLIGAN, G., BRUHN, L., BARRETT, M., VALDEZ, R., TRENT, J., STEWART, A. K., CARPTEN, J. & BERGSAGEL, P. L. 2007. Promiscuous mutations activate the noncanonical NF-kappaB pathway in multiple myeloma. *Cancer Cell*, 12, 131-44.
- KIM, J. Y., MORGAN, M., KIM, D. G., LEE, J. Y., BAI, L., LIN, Y., LIU, Z. G. & KIM, Y. S. 2011. TNFalpha induced noncanonical NF-kappaB activation is attenuated by RIP1 through stabilization of TRAF2. *J Cell Sci*, 124, 647-56.
- KIM, S. Y., LEE, C. H., MIDURA, B. V., YEUNG, C., MENDOZA, A., HONG, S. H., REN, L., WONG, D., KORZ, W., MERZOUK, A., SALARI, H., ZHANG, H., HWANG, S. T., KHANNA, C. & HELMAN, L. J. 2008. Inhibition of the

- CXCR4/CXCL12 chemokine pathway reduces the development of murine pulmonary metastases. *Clin Exp Metastasis*, 25, 201-11.
- KINSEY, M., SMITH, R., IYER, A. K., MCCABE, E. R. & LESSNICK, S. L. 2009. EWS/FLI and its downstream target NR0B1 interact directly to modulate transcription and oncogenesis in Ewing's sarcoma. *Cancer Res*, 69, 9047-55.
- KISHIDA, S., SANJO, H., AKIRA, S., MATSUMOTO, K. & NINOMIYA-TSUJI, J. 2005. TAK1-binding protein 2 facilitates ubiquitination of TRAF6 and assembly of TRAF6 with IKK in the IL-1 signaling pathway. *Genes Cells*, 10, 447-54.
- KOCH, A. E., POLVERINI, P. J., KUNKEL, S. L., HARLOW, L. A., DIPIETRO, L. A., ELNER, V. M., ELNER, S. G. & STRIETER, R. M. 1992. Interleukin-8 as a macrophage-derived mediator of angiogenesis. *Science*, 258, 1798-801.
- KOCH, U. & RADTKE, F. 2007. Notch and cancer: a double-edged sword. *Cell Mol Life Sci*, 64, 2746-62.
- KOHN, A. D. & MOON, R. T. 2005. Wnt and calcium signaling: beta-catenin-independent pathways. *Cell Calcium*, 38, 439-46.
- KOJIMA, Y., ACAR, A., EATON, E. N., MELLODY, K. T., SCHEEL, C., BENPORATH, I., ONDER, T. T., WANG, Z. C., RICHARDSON, A. L., WEINBERG, R. A. & ORIMO, A. 2010. Autocrine TGF-beta and stromal cell-derived factor-1 (SDF-1) signaling drives the evolution of tumor-promoting mammary stromal myofibroblasts. *Proc Natl Acad Sci U S A*, 107, 20009-14.
- KOLLET, O., SHIVTIEL, S., CHEN, Y. Q., SURIAWINATA, J., THUNG, S. N., DABEVA, M. D., KAHN, J., SPIEGEL, A., DAR, A., SAMIRA, S., GOICHBURG, P., KALINKOVICH, A., ARENZANA-SEISDEDOS, F., NAGLER, A., HARDAN, I., REVEL, M., SHAFRITZ, D. A. & LAPIDOT, T. 2003. HGF, SDF-1, and MMP-9 are involved in stress-induced human CD34+ stem cell recruitment to the liver. *J Clin Invest*, 112, 160-9.
- KOMAROVA, N. L. & BOLAND, C. R. 2013. Cancer: calculated treatment. *Nature*, 499, 291-2.
- KOMINSKY, S. L., DOUCET, M., BRADY, K. & WEBER, K. L. 2007. TGF-beta promotes the establishment of renal cell carcinoma bone metastasis. *J Bone Miner Res*, 22, 37-44.
- KONG, Y. Y., FEIGE, U., SAROSI, I., BOLON, B., TAFURI, A., MORONY, S., CAPPARELLI, C., LI, J., ELLIOTT, R., MCCABE, S., WONG, T., CAMPAGNUOLO, G., MORAN, E., BOGOCH, E. R., VAN, G., NGUYEN, L. T., OHASHI, P. S., LACEY, D. L., FISH, E., BOYLE, W. J. & PENNINGER, J. M. 1999. Activated T cells regulate bone loss and joint destruction in adjuvant arthritis through osteoprotegerin ligand. *Nature*, 402, 304-9.
- KREIL, S., PFIRRMANN, M., HAFERLACH, C., WAGHORN, K., CHASE, A., HEHLMANN, R., REITER, A., HOCHHAUS, A. & CROSS, N. C. 2007. Heterogeneous prognostic impact of derivative chromosome 9 deletions in chronic myelogenous leukemia. *Blood*, 110, 1283-90.
- KRYCZEK, I., LANGE, A., MOTTRAM, P., ALVAREZ, X., CHENG, P., HOGAN, M., MOONS, L., WEI, S., ZOU, L., MACHELON, V., EMILIE, D., TERRASSA, M., LACKNER, A., CURIEL, T. J., CARMELIET, P. & ZOU, W. 2005. CXCL12 and vascular endothelial growth factor synergistically induce neoangiogenesis in human ovarian cancers. *Cancer Res*, 65, 465-72.
- KRYCZEK, I., WEI, S., KELLER, E., LIU, R. & ZOU, W. 2007. Stroma-derived factor (SDF-1/CXCL12) and human tumor pathogenesis. *Am J Physiol Cell Physiol*, 292, C987-95.
- KUCIA, M., RATAJCZAK, J., RECA, R., JANOWSKA-WIECZOREK, A. & RATAJCZAK, M. Z. 2004. Tissue-specific muscle, neural and liver stem/progenitor cells reside in the bone marrow, respond to an SDF-1 gradient

- and are mobilized into peripheral blood during stress and tissue injury. *Blood Cells Mol Dis*, 32, 52-7.
- KUCIA, M., RECA, R., MIEKUS, K., WANZECK, J., WOJAKOWSKI, W., JANOWSKA-WIECZOREK, A., RATAJCZAK, J. & RATAJCZAK, M. Z. 2005. Trafficking of normal stem cells and metastasis of cancer stem cells involve similar mechanisms: pivotal role of the SDF-1-CXCR4 axis. *Stem Cells*, 23, 879-94.
- KUWATA, H., MATSUMOTO, M., ATARASHI, K., MORISHITA, H., HIROTANI, T., KOGA, R. & TAKEDA, K. 2006. IkappaBNS inhibits induction of a subset of Toll-like receptor-dependent genes and limits inflammation. *Immunity*, 24, 41-51.
- KWAK, Y. T., LI, R., BECERRA, C. R., TRIPATHY, D., FRENKEL, E. P. & VERMA, U. N. 2005. IkappaB kinase alpha regulates subcellular distribution and turnover of cyclin D1 by phosphorylation. *J Biol Chem*, 280, 33945-52.
- LAGERSTROM, M. C. & SCHIOTH, H. B. 2008. Structural diversity of G protein-coupled receptors and significance for drug discovery. *Nat Rev Drug Discov*, 7, 339-57.
- LAI, T. H., FONG, Y. C., FU, W. M., YANG, R. S. & TANG, C. H. 2009. Stromal cell-derived factor-1 increase alphavbeta3 integrin expression and invasion in human chondrosarcoma cells. *J Cell Physiol*, 218, 334-42.
- LAM, L. T., DAVIS, R. E., PIERCE, J., HEPPELLE, M., XU, Y., HOTTELET, M., NONG, Y., WEN, D., ADAMS, J., DANG, L. & STAUDT, L. M. 2005. Small molecule inhibitors of IkappaB kinase are selectively toxic for subgroups of diffuse large B-cell lymphoma defined by gene expression profiling. *Clin Cancer Res*, 11, 28-40.
- LAWRENCE, T. & BEBIEN, M. 2007. IKKalpha in the regulation of inflammation and adaptive immunity. *Biochem Soc Trans*, 35, 270-2.
- LEE, D. F. & HUNG, M. C. 2008. Advances in targeting IKK and IKK-related kinases for cancer therapy. *Clin Cancer Res*, 14, 5656-62.
- LEE, D. F., KUO, H. P., CHEN, C. T., HSU, J. M., CHOU, C. K., WEI, Y., SUN, H. L., LI, L. Y., PING, B., HUANG, W. C., HE, X., HUNG, J. Y., LAI, C. C., DING, Q., SU, J. L., YANG, J. Y., SAHIN, A. A., HORTOBAGYI, G. N., TSAI, F. J., TSAI, C. H. & HUNG, M. C. 2007. IKK beta suppression of TSC1 links inflammation and tumor angiogenesis via the mTOR pathway. *Cell*, 130, 440-55.
- LEOPIZZI, M., COCCHIOLA, R., MILANETTI, E., RAIMONDO, D., POLITI, L., GIORDANO, C., SCANDURRA, R. & SCOTTO D'ABUSCO, A. 2017. IKKalpha inhibition by a glucosamine derivative enhances Maspin expression in osteosarcoma cell line. *Chem Biol Interact*, 262, 19-28.
- LEOW, P. C., BAHETY, P., BOON, C. P., LEE, C. Y., TAN, K. L., YANG, T. & EE, P. L. 2014. Functionalized curcumin analogs as potent modulators of the Wnt/beta-catenin signaling pathway. *Eur J Med Chem*, 71, 67-80.
- LESSNICK, S. L. & LADANYI, M. 2012. Molecular pathogenesis of Ewing sarcoma: new therapeutic and transcriptional targets. *Annu Rev Pathol*, 7, 145-59.
- LEVOYE, A., BALABANIAN, K., BALEUX, F., BACHELERIE, F. & LAGANE, B. 2009. CXCR7 heterodimerizes with CXCR4 and regulates CXCL12-mediated G protein signaling. *Blood*, 113, 6085-93.
- LEWELLIS, S. W. & KNAUT, H. 2012. Attractive guidance: how the chemokine SDF1/CXCL12 guides different cells to different locations. *Semin Cell Dev Biol*, 23, 333-40.
- LI, Q., LU, Q., HWANG, J. Y., BUSCHER, D., LEE, K. F., IZPISUA-BELMONTE, J. C. & VERMA, I. M. 1999a. IKK1-deficient mice exhibit abnormal development of skin and skeleton. *Genes Dev*, 13, 1322-8.

- LI, Q., VAN ANTWERP, D., MERCURIO, F., LEE, K. F. & VERMA, I. M. 1999b. Severe liver degeneration in mice lacking the I kappaB kinase 2 gene. *Science*, 284, 321-5.
- LI, Q. & VERMA, I. M. 2002. NF-kappaB regulation in the immune system. *Nat Rev Immunol*, 2, 725-34.
- LI, W. L., XIONG, L. X., SHI, X. Y., XIAO, L., QI, G. Y. & MENG, C. 2016. IKKbeta/NFkappaBp65 activated by interleukin-13 targets the autophagy-related genes LC3B and beclin 1 in fibroblasts co-cultured with breast cancer cells. *Exp Ther Med*, 11, 1259-1264.
- LI, Z. & NABEL, G. J. 1997. A new member of the I kappaB protein family, I kappaB epsilon, inhibits RelA (p65)-mediated NF-kappaB transcription. *Mol Cell Biol*, 17, 6184-90.
- LIANG, C., ZHANG, M. & SUN, S. C. 2006. beta-TrCP binding and processing of NF-kappaB2/p100 involve its phosphorylation at serines 866 and 870. *Cell Signal*, 18, 1309-17.
- LIAO, G., ZHANG, M., HARHAJ, E. W. & SUN, S. C. 2004. Regulation of the NF-kappaB-inducing kinase by tumor necrosis factor receptor-associated factor 3-induced degradation. *J Biol Chem*, 279, 26243-50.
- LIBERMAN, J., SARTELET, H., FLAHAUT, M., MUHLETHALER-MOTTET, A., COULON, A., NYALENDO, C., VASSAL, G., JOSEPH, J. M. & GROSS, N. 2012. Involvement of the CXCR7/CXCR4/CXCL12 axis in the malignant progression of human neuroblastoma. *PLoS One*, 7, e43665.
- LICH, J. D., WILLIAMS, K. L., MOORE, C. B., ARTHUR, J. C., DAVIS, B. K., TAXMAN, D. J. & TING, J. P. 2007. Monarch-1 suppresses non-canonical NF-kappaB activation and p52-dependent chemokine expression in monocytes. *J Immunol*, 178, 1256-60.
- LIEKENS, S., SCHOLS, D. & HATSE, S. 2010. CXCL12-CXCR4 axis in angiogenesis, metastasis and stem cell mobilization. *Curr Pharm Des*, 16, 3903-20.
- LIN, C. H., GUO, Y., GHAFAR, S., MCQUEEN, P., POURMORADY, J., CHRIST, A., ROONEY, K., JI, T., ESKANDER, R., ZI, X. & HOANG, B. H. 2013. Dkk-3, a secreted wnt antagonist, suppresses tumorigenic potential and pulmonary metastasis in osteosarcoma. *Sarcoma*, 2013, 147541.
- LINDSAY, R., ZHOU, H., COSMAN, F., NIEVES, J., DEMPSTER, D. W. & HODSMAN, A. B. 2007. Effects of a one-month treatment with PTH(1-34) on bone formation on cancellous, endocortical, and periosteal surfaces of the human ilium. *J Bone Miner Res*, 22, 495-502.
- LIU, G. Y., DOPPLER, H., NECELA, B., KRISHNA, M., CRAWFORD, H. C., RAIMONDO, M. & STORZ, P. 2013. Macrophage-secreted cytokines drive pancreatic acinar-to-ductal metaplasia through NF-kappaB and MMPs. *J Cell Biol*, 202, 563-77.
- LITTLE, R. D., CARULLI, J. P., DEL MASTRO, R. G., DUPUIS, J., OSBORNE, M., FOLZ, C., MANNING, S. P., SWAIN, P. M., ZHAO, S. C., EUSTACE, B., LAPPE, M. M., SPITZER, L., ZWEIER, S., BRAUNSCHWEIGER, K., BENCHEKROUN, Y., HU, X., ADAIR, R., CHEE, L., FITZGERALD, M. G., TULIG, C., CARUSO, A., TZELLAS, N., BAWA, A., FRANKLIN, B., MCGUIRE, S., NOGUES, X., GONG, G., ALLEN, K. M., ANISOWICZ, A., MORALES, A. J., LOMEDICO, P. T., RECKER, S. M., VAN EERDEWEGH, P., RECKER, R. R. & JOHNSON, M. L. 2002. A mutation in the LDL receptor-related protein 5 gene results in the autosomal dominant high-bone-mass trait. *Am J Hum Genet*, 70, 11-9.
- LIU, B., SUN, L., LIU, Q., GONG, C., YAO, Y., LV, X., LIN, L., YAO, H., SU, F., LI, D., ZENG, M. & SONG, E. 2015. A cytoplasmic NF-kappaB interacting long

- noncoding RNA blocks IkappaB phosphorylation and suppresses breast cancer metastasis. *Cancer Cell*, 27, 370-81.
- LIU, Y., BHAT, R. A., SEESTALLER-WEHR, L. M., FUKAYAMA, S., MANGINE, A., MORAN, R. A., KOMM, B. S., BODINE, P. V. & BILLIARD, J. 2007. The orphan receptor tyrosine kinase Ror2 promotes osteoblast differentiation and enhances ex vivo bone formation. *Mol Endocrinol*, 21, 376-87.
- LIU, Y., WANG, W., XU, J., LI, L., DONG, Q., SHI, Q., ZUO, G., ZHOU, L., WENG, Y., TANG, M., HE, T. & LUO, J. 2013. Dihydroartemisinin inhibits tumor growth of human osteosarcoma cells by suppressing Wnt/beta-catenin signaling. *Oncol Rep*, 30, 1723-30.
- LIVAK, K. J. & SCHMITTGEN, T. D. 2001. Analysis of relative gene expression data using real-time quantitative PCR and the 2(-Delta Delta C(T)) Method. *Methods*, 25, 402-8.
- LOETSCHER, P., MOSER, B. & BAGGIOLINI, M. 2000. Chemokines and their receptors in lymphocyte traffic and HIV infection. *Adv Immunol*, 74, 127-80.
- LOGAN, C. Y. & NUSSE, R. 2004. The Wnt signaling pathway in development and disease. *Annu Rev Cell Dev Biol*, 20, 781-810.
- LONG, F. & ORNITZ, D. M. 2013. Development of the endochondral skeleton. *Cold Spring Harb Perspect Biol*, 5, a008334.
- LORUSSO, G. & RUEGG, C. 2008. The tumor microenvironment and its contribution to tumor evolution toward metastasis. *Histochem Cell Biol*, 130, 1091-103.
- LOTZER, K., DOPPING, S., CONNERT, S., GRABNER, R., SPANBROEK, R., LEMSER, B., BEER, M., HILDNER, M., HEHLGANS, T., VAN DER WALL, M., MEBIUS, R. E., LOVAS, A., RANDOLPH, G. J., WEIH, F. & HABENICHT, A. J. 2010. Mouse aorta smooth muscle cells differentiate into lymphoid tissue organizer-like cells on combined tumor necrosis factor receptor-1/lymphotoxin beta-receptor NF-kappaB signaling. *Arterioscler Thromb Vasc Biol*, 30, 395-402.
- LU, T. & STARK, G. R. 2004. Cytokine overexpression and constitutive NFkappaB in cancer. *Cell Cycle*, 3, 1114-7.
- LUKASHEV, M., LEPAGE, D., WILSON, C., BAILLY, V., GARBER, E., LUKASHIN, A., NGAM-EK, A., ZENG, W., ALLAIRE, N., PERRIN, S., XU, X., SZELIGA, K., WORTHAM, K., KELLY, R., BOTTIGLIO, C., DING, J., GRIFFITH, L., HEANEY, G., SILVERIO, E., YANG, W., JARPE, M., FAWELL, S., REFF, M., CARMILLO, A., MIATKOWSKI, K., AMATUCCI, J., CROWELL, T., PRENTICE, H., MEIER, W., VIOLETTE, S. M., MACKAY, F., YANG, D., HOFFMAN, R. & BROWNING, J. L. 2006. Targeting the lymphotoxin-beta receptor with agonist antibodies as a potential cancer therapy. *Cancer Res*, 66, 9617-24.
- LUO, J. L., TAN, W., RICONO, J. M., KORCHYNSKYI, O., ZHANG, M., GONIAS, S. L., CHERESH, D. A. & KARIN, M. 2007. Nuclear cytokine-activated IKKalpha controls prostate cancer metastasis by repressing Maspin. *Nature*, 446, 690-4.
- MADGE, L. A., KLUGER, M. S., ORANGE, J. S. & MAY, M. J. 2008. Lymphotoxin-alpha 1 beta 2 and LIGHT induce classical and noncanonical NF-kappa B-dependent proinflammatory gene expression in vascular endothelial cells. *J Immunol*, 180, 3467-77.
- MADGE, L. A. & MAY, M. J. 2010. Classical NF-kappaB activation negatively regulates noncanonical NF-kappaB-dependent CXCL12 expression. *J Biol Chem*, 285, 38069-77.
- MALEK, S., HUXFORD, T. & GHOSH, G. 1998. Ikappa Balpha functions through direct contacts with the nuclear localization signals and the DNA binding sequences of NF-kappaB. *J Biol Chem*, 273, 25427-35.

- MANOLAGAS, S. C. 2000. Birth and death of bone cells: basic regulatory mechanisms and implications for the pathogenesis and treatment of osteoporosis. *Endocr Rev*, 21, 115-37.
- MANOLAGAS, S. C., BELLIDO, T. & JILKA, R. L. 1995. New insights into the cellular, biochemical, and molecular basis of postmenopausal and senile osteoporosis: roles of IL-6 and gp130. *Int J Immunopharmacol*, 17, 109-16.
- MARGALEF, P., FERNANDEZ-MAJADA, V., VILLANUEVA, A., GARCIA-CARBONELL, R., IGLESIAS, M., LOPEZ, L., MARTINEZ-INIESTA, M., VILLA-FREIXA, J., MULERO, M. C., ANDREU, M., TORRES, F., MAYO, M. W., BIGAS, A. & ESPINOSA, L. 2012. A truncated form of IKKalpha is responsible for specific nuclear IKK activity in colorectal cancer. *Cell Rep*, 2, 840-54.
- MARIENFELD, R., MAY, M. J., BERBERICH, I., SERFLING, E., GHOSH, S. & NEUMANN, M. 2003. RelB forms transcriptionally inactive complexes with RelA/p65. *J Biol Chem*, 278, 19852-60.
- MARTINEZ MOLINA, D., JAFARI, R., IGNATUSHCHENKO, M., SEKI, T., LARSSON, E. A., DAN, C., SREEKUMAR, L., CAO, Y. & NORDLUND, P. 2013. Monitoring drug target engagement in cells and tissues using the cellular thermal shift assay. *Science*, 341, 84-7.
- MASSAGUE, J., BLAIN, S. W. & LO, R. S. 2000. TGFbeta signaling in growth control, cancer, and heritable disorders. *Cell*, 103, 295-309.
- MATSUSHIMA, A., KAISHO, T., RENNERT, P. D., NAKANO, H., KUROSAWA, K., UCHIDA, D., TAKEDA, K., AKIRA, S. & MATSUMOTO, M. 2001. Essential role of nuclear factor (NF)-kappaB-inducing kinase and inhibitor of kappaB (IkappaB) kinase alpha in NF-kappaB activation through lymphotoxin beta receptor, but not through tumor necrosis factor receptor I. *J Exp Med*, 193, 631-6.
- MATSUSUE, R., KUBO, H., HISAMORI, S., OKOSHI, K., TAKAGI, H., HIDA, K., NAKANO, K., ITAMI, A., KAWADA, K., NAGAYAMA, S. & SAKAI, Y. 2009. Hepatic stellate cells promote liver metastasis of colon cancer cells by the action of SDF-1/CXCR4 axis. *Ann Surg Oncol*, 16, 2645-53.
- MATUSHANSKY, I. & MAKI, R. G. 2005. Mechanisms of sarcomagenesis. *Hematol Oncol Clin North Am*, 19, 427-49, v.
- MAY, M. J., MARIENFELD, R. B. & GHOSH, S. 2002. Characterization of the Ikappa B-kinase NEMO binding domain. *J Biol Chem*, 277, 45992-6000.
- MERCURIO, F., DIDONATO, J. A., ROSETTE, C. & KARIN, M. 1993. p105 and p98 precursor proteins play an active role in NF-kappa B-mediated signal transduction. *Genes Dev*, 7, 705-18.
- MERCURIO, F., ZHU, H., MURRAY, B. W., SHEVCHENKO, A., BENNETT, B. L., LI, J., YOUNG, D. B., BARBOSA, M., MANN, M., MANNING, A. & RAO, A. 1997. IKK-1 and IKK-2: cytokine-activated IkappaB kinases essential for NF-kappaB activation. *Science*, 278, 860-6.
- MICHEL, F., SOLER-LOPEZ, M., PETOSA, C., CRAMER, P., SIEBENLIST, U. & MULLER, C. W. 2001. Crystal structure of the ankyrin repeat domain of Bcl-3: a unique member of the IkappaB protein family. *EMBO J*, 20, 6180-90.
- MILLER, B. S. & ZANDI, E. 2001. Complete reconstitution of human IkappaB kinase (IKK) complex in yeast. Assessment of its stoichiometry and the role of IKKgamma on the complex activity in the absence of stimulation. *J Biol Chem*, 276, 36320-6.
- MIRABELLO, L., TROISI, R. J. & SAVAGE, S. A. 2009. International osteosarcoma incidence patterns in children and adolescents, middle ages and elderly persons. *Int J Cancer*, 125, 229-34.

- MIURA, K., UNIYAL, S., LEABU, M., ORAVECZ, T., CHAKRABARTI, S., MORRIS, V. L. & CHAN, B. M. 2005. Chemokine receptor CXCR4-beta1 integrin axis mediates tumorigenesis of osteosarcoma HOS cells. *Biochem Cell Biol*, 83, 36-48.
- MIYAZONO, K., MAEDA, S. & IMAMURA, T. 2005. BMP receptor signaling: transcriptional targets, regulation of signals, and signaling cross-talk. *Cytokine Growth Factor Rev*, 16, 251-63.
- MONTAGUT, C., TUSQUETS, I., FERRER, B., COROMINAS, J. M., BELLOSILLO, B., CAMPAS, C., SUAREZ, M., FABREGAT, X., CAMPO, E., GASCON, P., SERRANO, S., FERNANDEZ, P. L., ROVIRA, A. & ALBANELL, J. 2006. Activation of nuclear factor-kappa B is linked to resistance to neoadjuvant chemotherapy in breast cancer patients. *Endocr Relat Cancer*, 13, 607-16.
- MOUSTAKAS, A. & HELDIN, C. H. 2009. The regulation of TGFbeta signal transduction. *Development*, 136, 3699-714.
- MUKHERJEE, D. & ZHAO, J. 2013. The Role of chemokine receptor CXCR4 in breast cancer metastasis. *Am J Cancer Res*, 3, 46-57.
- MULLER, A., HOMEY, B., SOTO, H., GE, N., CATRON, D., BUCHANAN, M. E., MCCLANAHAN, T., MURPHY, E., YUAN, W., WAGNER, S. N., BARRERA, J. L., MOHAR, A., VERASTEGUI, E. & ZLOTNIK, A. 2001. Involvement of chemokine receptors in breast cancer metastasis. *Nature*, 410, 50-6.
- MURDOCH, C. 2000. CXCR4: chemokine receptor extraordinaire. *Immunol Rev*, 177, 175-84.
- MUTA, T. 2006. IkappaB-zeta: an inducible regulator of nuclear factor-kappaB. *Vitam Horm*, 74, 301-16.
- MUTSAERS, A. J. & WALKLEY, C. R. 2014. Cells of origin in osteosarcoma: mesenchymal stem cells or osteoblast committed cells? *Bone*, 62, 56-63.
- NADIMINTY, N., LOU, W., SUN, M., CHEN, J., YUE, J., KUNG, H. J., EVANS, C. P., ZHOU, Q. & GAO, A. C. 2010. Aberrant activation of the androgen receptor by NF-kappaB2/p52 in prostate cancer cells. *Cancer Res*, 70, 3309-19.
- NAGASAWA, T., HIROTA, S., TACHIBANA, K., TAKAKURA, N., NISHIKAWA, S., KITAMURA, Y., YOSHIDA, N., KIKUTANI, H. & KISHIMOTO, T. 1996. Defects of B-cell lymphopoiesis and bone-marrow myelopoiesis in mice lacking the CXC chemokine PBSF/SDF-1. *Nature*, 382, 635-8.
- NAKANISHI, C. & TOI, M. 2005. Nuclear factor-kappaB inhibitors as sensitizers to anticancer drugs. *Nat Rev Cancer*, 5, 297-309.
- NAKANO, H., SHINDO, M., SAKON, S., NISHINAKA, S., MIHARA, M., YAGITA, H. & OKUMURA, K. 1998. Differential regulation of IkappaB kinase alpha and beta by two upstream kinases, NF-kappaB-inducing kinase and mitogen-activated protein kinase/ERK kinase kinase-1. *Proc Natl Acad Sci U S A*, 95, 3537-42.
- NANKI, T., HAYASHIDA, K., EL-GABALAWY, H. S., SUSON, S., SHI, K., GIRSCHICK, H. J., YAVUZ, S. & LIPSKY, P. E. 2000. Stromal cell-derived factor-1-CXC chemokine receptor 4 interactions play a central role in CD4+ T cell accumulation in rheumatoid arthritis synovium. *J Immunol*, 165, 6590-8.
- NERVI, B., RAMIREZ, P., RETTIG, M. P., UY, G. L., HOLT, M. S., RITCHEY, J. K., PRIOR, J. L., PIWNICA-WORMS, D., BRIDGER, G., LEY, T. J. & DIPERSIO, J. F. 2009. Chemosensitization of acute myeloid leukemia (AML) following mobilization by the CXCR4 antagonist AMD3100. *Blood*, 113, 6206-14.
- NIFOROU, K. M., ANAGNOSTOPOULOS, A. K., VOUGAS, K., KITTAS, C., GORGOLIS, V. G. & TSANGARIS, G. T. 2008. The proteome profile of the human osteosarcoma U2OS cell line. *Cancer Genomics Proteomics*, 5, 63-78.

- NJEH, C. F., SAUNDERS, M. W. & LANGTON, C. M. 2010. Accelerated Partial Breast Irradiation (APBI): A review of available techniques. *Radiat Oncol*, 5, 90.
- NOEL, D., GAZIT, D., BOUQUET, C., APPARAILLY, F., BONY, C., PLENCE, P., MILLET, V., TURGEMAN, G., PERRICAUDET, M., SANY, J. & JORGENSEN, C. 2004. Short-term BMP-2 expression is sufficient for in vivo osteochondral differentiation of mesenchymal stem cells. *Stem Cells*, 22, 74-85.
- NOLAN, G. P., FUJITA, T., BHATIA, K., HUPPI, C., LIOU, H. C., SCOTT, M. L. & BALTIMORE, D. 1993. The bcl-3 proto-oncogene encodes a nuclear I kappa B-like molecule that preferentially interacts with NF-kappa B p50 and p52 in a phosphorylation-dependent manner. *Mol Cell Biol*, 13, 3557-66.
- NOVACK, D. V. 2011. Role of NF-kappaB in the skeleton. *Cell Res*, 21, 169-82.
- NOVACK, D. V., YIN, L., HAGEN-STAPLETON, A., SCHREIBER, R. D., GOEDEL, D. V., ROSS, F. P. & TEITELBAUM, S. L. 2003. The I kappa B function of NF-kappaB2 p100 controls stimulated osteoclastogenesis. *J Exp Med*, 198, 771-81.
- OECKINGHAUS, A. & GHOSH, S. 2009. The NF-kappaB family of transcription factors and its regulation. *Cold Spring Harb Perspect Biol*, 1, a000034.
- ORIMO, A., GUPTA, P. B., SGROI, D. C., ARENZANA-SEISDEDOS, F., DELAUNAY, T., NAEEM, R., CAREY, V. J., RICHARDSON, A. L. & WEINBERG, R. A. 2005. Stromal fibroblasts present in invasive human breast carcinomas promote tumor growth and angiogenesis through elevated SDF-1/CXCL12 secretion. *Cell*, 121, 335-48.
- PALANKI, M. S., GAYO-FUNG, L. M., SHEVLIN, G. I., ERDMAN, P., SATO, M., GOLDMAN, M., RANSONE, L. J. & SPOONER, C. 2002. Structure-activity relationship studies of ethyl 2-[(3-methyl-2,5-dioxo(3-pyrrolinyl)amino]-4-(trifluoromethyl)pyrimidine-5-carboxylate: an inhibitor of AP-1 and NF-kappaB mediated gene expression. *Bioorg Med Chem Lett*, 12, 2573-7.
- PAPACHRONI, K. K., KARATZAS, D. N., PAPAVALASSILIOU, K. A., BASDRA, E. K. & PAPAVALASSILIOU, A. G. 2009. Mechanotransduction in osteoblast regulation and bone disease. *Trends Mol Med*, 15, 208-16.
- PARGELLIS, C., TONG, L., CHURCHILL, L., CIRILLO, P. F., GILMORE, T., GRAHAM, A. G., GROB, P. M., HICKEY, E. R., MOSS, N., PAV, S. & REGAN, J. 2002. Inhibition of p38 MAP kinase by utilizing a novel allosteric binding site. *Nat Struct Biol*, 9, 268-72.
- PARK, K. J., KRISHNAN, V., O'MALLEY, B. W., YAMAMOTO, Y. & GAYNOR, R. B. 2005. Formation of an IKKalpha-dependent transcription complex is required for estrogen receptor-mediated gene activation. *Mol Cell*, 18, 71-82.
- PARK, Y., KIM, J. W., KIM, D. S., KIM, E. B., PARK, S. J., PARK, J. Y., CHOI, W. S., SONG, J. G., SEO, H. Y., OH, S. C., KIM, B. S., PARK, J. J., KIM, Y. H. & KIM, J. S. 2008. The Bone Morphogenesis Protein-2 (BMP-2) is associated with progression to metastatic disease in gastric cancer. *Cancer Res Treat*, 40, 127-32.
- PASCA DI MAGLIANO, M., BIANKIN, A. V., HEISER, P. W., CANO, D. A., GUTIERREZ, P. J., DERAMAUDT, T., SEGARA, D., DAWSON, A. C., KENCH, J. G., HENSHALL, S. M., SUTHERLAND, R. L., DLUGOSZ, A., RUSTGI, A. K. & HEBROK, M. 2007. Common activation of canonical Wnt signaling in pancreatic adenocarcinoma. *PLoS One*, 2, e1155.
- PASPARAKIS, M. 2009. Regulation of tissue homeostasis by NF-kappaB signalling: implications for inflammatory diseases. *Nat Rev Immunol*, 9, 778-88.
- PELED, A., PETIT, I., KOLLET, O., MAGID, M., PONOMARYOV, T., BYK, T., NAGLER, A., BEN-HUR, H., MANY, A., SHULTZ, L., LIDER, O., ALON, R., ZIPORI, D. & LAPIDOT, T. 1999. Dependence of human stem cell engraftment and repopulation of NOD/SCID mice on CXCR4. *Science*, 283, 845-8.

- PERISSINOTTO, E., CAVALLONI, G., LEONE, F., FONSAO, V., MITOLA, S., GRIGNANI, G., SURRENTI, N., SANGIOLO, D., BUSSOLINO, F., PIACIBELLO, W. & AGLIETTA, M. 2005. Involvement of chemokine receptor 4/stromal cell-derived factor 1 system during osteosarcoma tumor progression. *Clin Cancer Res*, 11, 490-7.
- PERKINS, N. D. 2007. Integrating cell-signalling pathways with NF-kappaB and IKK function. *Nat Rev Mol Cell Biol*, 8, 49-62.
- PETTIT, A. R., JI, H., VON STECHOW, D., MULLER, R., GOLDRING, S. R., CHOI, Y., BENOIST, C. & GRAVALLESE, E. M. 2001. TRANCE/RANKL knockout mice are protected from bone erosion in a serum transfer model of arthritis. *Am J Pathol*, 159, 1689-99.
- PICOT, J., COOPER, K., BRYANT, J. & CLEGG, A. J. 2011. The clinical effectiveness and cost-effectiveness of bortezomib and thalidomide in combination regimens with an alkylating agent and a corticosteroid for the first-line treatment of multiple myeloma: a systematic review and economic evaluation. *Health Technol Assess*, 15, 1-204.
- PLAKSIN, D., BAEUERLE, P. A. & EISENBACH, L. 1993. KBF1 (p50 NF-kappa B homodimer) acts as a repressor of H-2Kb gene expression in metastatic tumor cells. *J Exp Med*, 177, 1651-62.
- PLOTNIKOV, A., ZEHORAI, E., PROCACCIA, S. & SEGER, R. 2011. The MAPK cascades: signaling components, nuclear roles and mechanisms of nuclear translocation. *Biochim Biophys Acta*, 1813, 1619-33.
- PODOLIN, P. L., CALLAHAN, J. F., BOLOGNESE, B. J., LI, Y. H., CARLSON, K., DAVIS, T. G., MELLOR, G. W., EVANS, C. & ROSHAK, A. K. 2005. Attenuation of murine collagen-induced arthritis by a novel, potent, selective small molecule inhibitor of I kappa B Kinase 2, TPCA-1 (2-[(aminocarbonyl)amino]-5-(4-fluorophenyl)-3-thiophenecarboxamide), occurs via reduction of proinflammatory cytokines and antigen-induced T cell Proliferation. *J Pharmacol Exp Ther*, 312, 373-81.
- PONOMARYOV, T., PELED, A., PETIT, I., TAICHMAN, R. S., HABLER, L., SANDBANK, J., ARENZANA-SEISDEDOS, F., MAGERUS, A., CARUZ, A., FUJII, N., NAGLER, A., LAHAV, M., SZYPER-KRAVITZ, M., ZIPORI, D. & LAPIDOT, T. 2000. Induction of the chemokine stromal-derived factor-1 following DNA damage improves human stem cell function. *J Clin Invest*, 106, 1331-9.
- PRAJAPATI, S., TU, Z., YAMAMOTO, Y. & GAYNOR, R. B. 2006. IKKalpha regulates the mitotic phase of the cell cycle by modulating Aurora A phosphorylation. *Cell Cycle*, 5, 2371-80.
- PRIEUR, A., TIRODE, F., COHEN, P. & DELATTRE, O. 2004. EWS/FLI-1 silencing and gene profiling of Ewing cells reveal downstream oncogenic pathways and a crucial role for repression of insulin-like growth factor binding protein 3. *Mol Cell Biol*, 24, 7275-83.
- PUCHERT, M. & ENGELE, J. 2014. The peculiarities of the SDF-1/CXCL12 system: in some cells, CXCR4 and CXCR7 sing solos, in others, they sing duets. *Cell Tissue Res*, 355, 239-53.
- QIN, J. J., WANG, W., VORUGANTI, S., WANG, H., ZHANG, W. D. & ZHANG, R. 2015. Identification of a new class of natural product MDM2 inhibitor: In vitro and in vivo anti-breast cancer activities and target validation. *Oncotarget*, 6, 2623-40.
- QING, G., QU, Z. & XIAO, G. 2005. Stabilization of basally translated NF-kappaB-inducing kinase (NIK) protein functions as a molecular switch of processing of NF-kappaB2 p100. *J Biol Chem*, 280, 40578-82.

- QING, G., YAN, P., QU, Z., LIU, H. & XIAO, G. 2007. Hsp90 regulates processing of NF-kappa B2 p100 involving protection of NF-kappa B-inducing kinase (NIK) from autophagy-mediated degradation. *Cell Res*, 17, 520-30.
- QURESHI, A., AHMAD, Z., AZAM, M. & IDREES, R. 2010. Epidemiological data for common bone sarcomas. *Asian Pac J Cancer Prev*, 11, 393-5.
- RAAB, M. S., PODAR, K., BREITKREUTZ, I., RICHARDSON, P. G. & ANDERSON, K. C. 2009. Multiple myeloma. *Lancet*, 374, 324-39.
- RABBANI, S. A., ARAKELIAN, A. & FAROOKHI, R. 2013. LRP5 knockdown: effect on prostate cancer invasion growth and skeletal metastasis in vitro and in vivo. *Cancer Med*, 2, 625-35.
- RANDALL, R. M., SHAO, Y. Y., WANG, L. & BALLOCK, R. T. 2012. Activation of Wnt Planar Cell Polarity (PCP) signaling promotes growth plate column formation in vitro. *J Orthop Res*, 30, 1906-14.
- RATAJCZAK, M. Z., KUCIA, M., RECA, R., MAJKA, M., JANOWSKA-WIECZOREK, A. & RATAJCZAK, J. 2004. Stem cell plasticity revisited: CXCR4-positive cells expressing mRNA for early muscle, liver and neural cells 'hide out' in the bone marrow. *Leukemia*, 18, 29-40.
- RAWADI, G. & ROMAN-ROMAN, S. 2005. Wnt signalling pathway: a new target for the treatment of osteoporosis. *Expert Opin Ther Targets*, 9, 1063-77.
- RAY, P., ZHANG, D. H., ELIAS, J. A. & RAY, A. 1995. Cloning of a differentially expressed I kappa B-related protein. *J Biol Chem*, 270, 10680-5.
- RAZANI, B., ZARNEGAR, B., YTTERBERG, A. J., SHIBA, T., DEMPSEY, P. W., WARE, C. F., LOO, J. A. & CHENG, G. 2010. Negative feedback in noncanonical NF-kappaB signaling modulates NIK stability through IKKalpha-mediated phosphorylation. *Sci Signal*, 3, ra41.
- RICE, N. R., MACKICHAN, M. L. & ISRAEL, A. 1992. The precursor of NF-kappa B p50 has I kappa B-like functions. *Cell*, 71, 243-53.
- ROMIEU-MOUREZ, R., LANDESMAN-BOLLAG, E., SELDIN, D. C., TRAISH, A. M., MERCURIO, F. & SONENSHEIN, G. E. 2001. Roles of IKK kinases and protein kinase CK2 in activation of nuclear factor-kappaB in breast cancer. *Cancer Res*, 61, 3810-8.
- ROTHER, M., SARMA, V., DIXIT, V. M. & GOEDEL, D. V. 1995. TRAF2-mediated activation of NF-kappa B by TNF receptor 2 and CD40. *Science*, 269, 1424-7.
- ROTHWART, D. M., ZANDI, E., NATOLI, G. & KARIN, M. 1998. IKK-gamma is an essential regulatory subunit of the I kappa B kinase complex. *Nature*, 395, 297-300.
- RUOCCO, M. G., MAEDA, S., PARK, J. M., LAWRENCE, T., HSU, L. C., CAO, Y., SCHEIT, G., WAGNER, E. F. & KARIN, M. 2005. I{kappa}B kinase (IKK){beta}, but not IKK{alpha}, is a critical mediator of osteoclast survival and is required for inflammation-induced bone loss. *J Exp Med*, 201, 1677-87.
- RUSHE, M., SILVIAN, L., BIXLER, S., CHEN, L. L., CHEUNG, A., BOWES, S., CUERVO, H., BERKOWITZ, S., ZHENG, T., GUCKIAN, K., PELLEGRINI, M. & LUGOVSKOY, A. 2008. Structure of a NEMO/IKK-associating domain reveals architecture of the interaction site. *Structure*, 16, 798-808.
- RUSSELL, R. G. 2011. Bisphosphonates: the first 40 years. *Bone*, 49, 2-19.
- SAKURAI, H., SHIGEMORI, N., HASEGAWA, K. & SUGITA, T. 1998. TGF-beta-activated kinase 1 stimulates NF-kappa B activation by an NF-kappa B-inducing kinase-independent mechanism. *Biochem Biophys Res Commun*, 243, 545-9.
- SANJO, H., ZAJONC, D. M., BRADEN, R., NORRIS, P. S. & WARE, C. F. 2010. Allosteric regulation of the ubiquitin:NIK and ubiquitin:TRAF3 E3 ligases by the lymphotoxin-beta receptor. *J Biol Chem*, 285, 17148-55.

- SANTIAGO, B., CALONGE, E., DEL REY, M. J., GUTIERREZ-CANAS, I., IZQUIERDO, E., USATEGUI, A., GALINDO, M., ALCAMI, J. & PABLOS, J. L. 2011. CXCL12 gene expression is upregulated by hypoxia and growth arrest but not by inflammatory cytokines in rheumatoid synovial fibroblasts. *Cytokine*, 53, 184-90.
- SCHERER, D. C., BROCKMAN, J. A., CHEN, Z., MANIATIS, T. & BALLARD, D. W. 1995. Signal-induced degradation of I kappa B alpha requires site-specific ubiquitination. *Proc Natl Acad Sci U S A*, 92, 11259-63.
- SCHÖBER, A., KNARREN, S., LIETZ, M., LIN, E. A. & WEBER, C. 2003. Crucial role of stromal cell-derived factor-1alpha in neointima formation after vascular injury in apolipoprotein E-deficient mice. *Circulation*, 108, 2491-7.
- SCHULT, C., DAHLHAUS, M., GLASS, A., FISCHER, K., LANGE, S., FREUND, M. & JUNGHANSS, C. 2012. The dual kinase inhibitor NVP-BEZ235 in combination with cytotoxic drugs exerts anti-proliferative activity towards acute lymphoblastic leukemia cells. *Anticancer Res*, 32, 463-74.
- SCOTTO D'ABUSCO, A., POLITI, L., GIORDANO, C. & SCANDURRA, R. 2010. A peptidyl-glucosamine derivative affects IKKalpha kinase activity in human chondrocytes. *Arthritis Res Ther*, 12, R18.
- SEN, R. & BALTIMORE, D. 1986. Multiple nuclear factors interact with the immunoglobulin enhancer sequences. *Cell*, 46, 705-16.
- SENEGAS, A., GAUTHERON, J., MAURIN, A. G. & COURTOIS, G. 2015. IKK-related genetic diseases: probing NF-kappaB functions in humans and other matters. *Cell Mol Life Sci*, 72, 1275-87.
- SENFTLEBEN, U., CAO, Y., XIAO, G., GRETEN, F. R., KRAHN, G., BONIZZI, G., CHEN, Y., HU, Y., FONG, A., SUN, S. C. & KARIN, M. 2001. Activation by IKKalpha of a second, evolutionary conserved, NF-kappa B signaling pathway. *Science*, 293, 1495-9.
- SHEN, B., WEI, A., WHITTAKER, S., WILLIAMS, L. A., TAO, H., MA, D. D. & DIWAN, A. D. 2010. The role of BMP-7 in chondrogenic and osteogenic differentiation of human bone marrow multipotent mesenchymal stromal cells in vitro. *J Cell Biochem*, 109, 406-16.
- SHIAH, H. S., GAO, W., BAKER, D. C. & CHENG, Y. C. 2006. Inhibition of cell growth and nuclear factor-kappaB activity in pancreatic cancer cell lines by a tylophorine analogue, DCB-3503. *Mol Cancer Ther*, 5, 2484-93.
- SHOSTAK, K. & CHARIOT, A. 2015. EGFR and NF-kappaB: partners in cancer. *Trends Mol Med*, 21, 385-93.
- SHUKLA, S., KANWAL, R., SHANKAR, E., DATT, M., CHANCE, M. R., FU, P., MACLENNAN, G. T. & GUPTA, S. 2015. Apigenin blocks IKKalpha activation and suppresses prostate cancer progression. *Oncotarget*, 6, 31216-32.
- SIEBENLIST, U., FRANZOSO, G. & BROWN, K. 1994. Structure, regulation and function of NF-kappa B. *Annu Rev Cell Biol*, 10, 405-55.
- SIEGEL, P. M. & MASSAGUE, J. 2003. Cytostatic and apoptotic actions of TGF-beta in homeostasis and cancer. *Nat Rev Cancer*, 3, 807-21.
- SIEGEL, R., MA, J., ZOU, Z. & JEMAL, A. 2014. Cancer statistics, 2014. *CA Cancer J Clin*, 64, 9-29.
- SMITH, C., ANDREAKOS, E., CRAWLEY, J. B., BRENNAN, F. M., FELDMANN, M. & FOXWELL, B. M. 2001. NF-kappaB-inducing kinase is dispensable for activation of NF-kappaB in inflammatory settings but essential for lymphotoxin beta receptor activation of NF-kappaB in primary human fibroblasts. *J Immunol*, 167, 5895-903.
- SMITH, R., OWEN, L. A., TREM, D. J., WONG, J. S., WHANGBO, J. S., GOLUB, T. R. & LESSNICK, S. L. 2006. Expression profiling of EWS/FLI identifies NKX2.2 as a critical target gene in Ewing's sarcoma. *Cancer Cell*, 9, 405-16.

- SOLAN, N. J., MIYOSHI, H., CARMONA, E. M., BREN, G. D. & PAYA, C. V. 2002. RelB cellular regulation and transcriptional activity are regulated by p100. *J Biol Chem*, 277, 1405-18.
- SOLT, L. A., MADGE, L. A. & MAY, M. J. 2009. NEMO-binding domains of both IKKalpha and IKKbeta regulate IkappaB kinase complex assembly and classical NF-kappaB activation. *J Biol Chem*, 284, 27596-608.
- SOLTANOFF, C. S., YANG, S., CHEN, W. & LI, Y. P. 2009. Signaling networks that control the lineage commitment and differentiation of bone cells. *Crit Rev Eukaryot Gene Expr*, 19, 1-46.
- SONE, T., FUKUNAGA, M., ONO, S. & NISHIYAMA, T. 1995. A small dose of human parathyroid hormone(1-34) increased bone mass in the lumbar vertebrae in patients with senile osteoporosis. *Miner Electrolyte Metab*, 21, 232-5.
- SONG, L., DONG, W., GAO, M., LI, J., HU, M., GUO, N. & HUANG, C. 2010. A novel role of IKKalpha in the mediation of UVB-induced G0/G1 cell cycle arrest response by suppressing Cyclin D1 expression. *Biochim Biophys Acta*, 1803, 323-32.
- STEHLIK, C., DE MARTIN, R., KUMABASHIRI, I., SCHMID, J. A., BINDER, B. R. & LIPP, J. 1998. Nuclear factor (NF)-kappaB-regulated X-chromosome-linked iap gene expression protects endothelial cells from tumor necrosis factor alpha-induced apoptosis. *J Exp Med*, 188, 211-6.
- STORZ, P. 2013. Targeting the alternative NF-kappaB pathway in pancreatic cancer: a new direction for therapy? *Expert Rev Anticancer Ther*, 13, 501-4.
- SUN, L. 2004. Tumor-suppressive and promoting function of transforming growth factor beta. *Front Biosci*, 9, 1925-35.
- SUN, S. C. 2012. The noncanonical NF-kappaB pathway. *Immunol Rev*, 246, 125-40.
- SUN, X., CHENG, G., HAO, M., ZHENG, J., ZHOU, X., ZHANG, J., TAICHMAN, R. S., PIENTA, K. J. & WANG, J. 2010. CXCL12 / CXCR4 / CXCR7 chemokine axis and cancer progression. *Cancer Metastasis Rev*, 29, 709-22.
- SUVA, M. L., RIGGI, N., STEHLE, J. C., BAUMER, K., TERCIER, S., JOSEPH, J. M., SUVA, D., CLEMENT, V., PROVERO, P., CIRONI, L., OSTERHELD, M. C., GUILLOU, L. & STAMENKOVIC, I. 2009. Identification of cancer stem cells in Ewing's sarcoma. *Cancer Res*, 69, 1776-81.
- SWARTHOUT, J. T., D'ALONZO, R. C., SELVAMURUGAN, N. & PARTRIDGE, N. C. 2002. Parathyroid hormone-dependent signaling pathways regulating genes in bone cells. *Gene*, 282, 1-17.
- TAGLIAFERRI, P., ROSSI, M., DI MARTINO, M. T., AMODIO, N., LEONE, E., GULLA, A., NERI, A. & TASSONE, P. 2012. Promises and challenges of MicroRNA-based treatment of multiple myeloma. *Curr Cancer Drug Targets*, 12, 838-46.
- TAICHMAN, R. S., COOPER, C., KELLER, E. T., PIENTA, K. J., TAICHMAN, N. S. & MCCAULEY, L. K. 2002. Use of the stromal cell-derived factor-1/CXCR4 pathway in prostate cancer metastasis to bone. *Cancer Res*, 62, 1832-7.
- TAKAESU, G., KISHIDA, S., HIYAMA, A., YAMAGUCHI, K., SHIBUYA, H., IRIE, K., NINOMIYA-TSUJI, J. & MATSUMOTO, K. 2000. TAB2, a novel adaptor protein, mediates activation of TAK1 MAPKKK by linking TAK1 to TRAF6 in the IL-1 signal transduction pathway. *Mol Cell*, 5, 649-58.
- TAKAESU, G., SURABHI, R. M., PARK, K. J., NINOMIYA-TSUJI, J., MATSUMOTO, K. & GAYNOR, R. B. 2003. TAK1 is critical for IkappaB kinase-mediated activation of the NF-kappaB pathway. *J Mol Biol*, 326, 105-15.
- TAKESHITA, H., YOSHIZAKI, T., MILLER, W. E., SATO, H., FURUKAWA, M., PAGANO, J. S. & RAAB-TRAUB, N. 1999. Matrix metalloproteinase 9 expression is induced by Epstein-Barr virus latent membrane protein 1 C-terminal activation regions 1 and 2. *J Virol*, 73, 5548-55.

- TANG, Y., WANG, Y., KIANI, M. F. & WANG, B. 2016. Classification, Treatment Strategy, and Associated Drug Resistance in Breast Cancer. *Clin Breast Cancer*, 16, 335-343.
- TAWFEEK, H. A., QIAN, F. & ABOU-SAMRA, A. B. 2002. Phosphorylation of the receptor for PTH and PTHrP is required for internalization and regulates receptor signaling. *Mol Endocrinol*, 16, 1-13.
- TEGOWSKI, M. & BALDWIN, A. 2018. Noncanonical NF-kappaB in Cancer. *Biomedicines*, 6.
- TEICHER, B. A. & FRICKER, S. P. 2010. CXCL12 (SDF-1)/CXCR4 pathway in cancer. *Clin Cancer Res*, 16, 2927-31.
- TEITELBAUM, S. L. 2000. Bone resorption by osteoclasts. *Science*, 289, 1504-8.
- THOMPSON, J. E., PHILLIPS, R. J., ERDJUMENT-BROMAGE, H., TEMPST, P. & GHOSH, S. 1995. I kappa B-beta regulates the persistent response in a biphasic activation of NF-kappa B. *Cell*, 80, 573-82.
- TORRE, L. A., BRAY, F., SIEGEL, R. L., FERLAY, J., LORTET-TIEULENT, J. & JEMAL, A. 2015. Global cancer statistics, 2012. *CA Cancer J Clin*, 65, 87-108.
- TOWBIN, H., STAHELIN, T. & GORDON, J. 1979. Electrophoretic transfer of proteins from polyacrylamide gels to nitrocellulose sheets: procedure and some applications. *Proc Natl Acad Sci U S A*, 76, 4350-4.
- TZENG, Y. S., LI, H., KANG, Y. L., CHEN, W. C., CHENG, W. C. & LAI, D. M. 2011. Loss of Cxcl12/Sdf-1 in adult mice decreases the quiescent state of hematopoietic stem/progenitor cells and alters the pattern of hematopoietic regeneration after myelosuppression. *Blood*, 117, 429-39.
- URIST, M. R. 1997. Bone morphogenetic protein: the molecularization of skeletal system development. *J Bone Miner Res*, 12, 343-6.
- VAANANEN, H. K., ZHAO, H., MULARI, M. & HALLEEN, J. M. 2000. The cell biology of osteoclast function. *J Cell Sci*, 113 (Pt 3), 377-81.
- VAIRA, S., JOHNSON, T., HIRBE, A. C., ALHAWAGRI, M., ANWISYE, I., SAMMUT, B., O'NEAL, J., ZOU, W., WEILBAECHER, K. N., FACCIO, R. & NOVACK, D. V. 2008. RelB is the NF-kappaB subunit downstream of NIK responsible for osteoclast differentiation. *Proc Natl Acad Sci U S A*, 105, 3897-902.
- VALLABHAPURAPU, S., MATSUZAWA, A., ZHANG, W., TSENG, P. H., KEATS, J. J., WANG, H., VIGNALI, D. A., BERGSAGEL, P. L. & KARIN, M. 2008. Nonredundant and complementary functions of TRAF2 and TRAF3 in a ubiquitination cascade that activates NIK-dependent alternative NF-kappaB signaling. *Nat Immunol*, 9, 1364-70.
- VALLABHAPURAPU, S., PAGOLU, K. & VALLABHAPURAPU, S. 2013. Regulation of the alternative NF-kb pathway and its role in cancer. *J Cancer Sci Ther*, 5, 1-3.
- VAN OOSTERWIJK, J. G., ANNINGA, J. K., GELDERBLOM, H., CLETON-JANSEN, A. M. & BOVEE, J. V. 2013. Update on targets and novel treatment options for high-grade osteosarcoma and chondrosarcoma. *Hematol Oncol Clin North Am*, 27, 1021-48.
- VARFOLOMEEV, E., BLANKENSHIP, J. W., WAYSON, S. M., FEDOROVA, A. V., KAYAGAKI, N., GARG, P., ZOBEL, K., DYNEK, J. N., ELLIOTT, L. O., WALLWEBER, H. J., FLYGARE, J. A., FAIRBROTHER, W. J., DESHAYES, K., DIXIT, V. M. & VUCIC, D. 2007. IAP antagonists induce autoubiquitination of c-IAPs, NF-kappaB activation, and TNFalpha-dependent apoptosis. *Cell*, 131, 669-81.
- VEEMAN, M. T., AXELROD, J. D. & MOON, R. T. 2003. A second canon. Functions and mechanisms of beta-catenin-independent Wnt signaling. *Dev Cell*, 5, 367-77.

- VIENNOIS, E., CHEN, F. & MERLIN, D. 2013. NF-kappaB pathway in colitis-associated cancers. *Transl Gastrointest Cancer*, 2, 21-29.
- VINCE, J. E., WONG, W. W., KHAN, N., FELTHAM, R., CHAU, D., AHMED, A. U., BENETATOS, C. A., CHUNDURU, S. K., CONDON, S. M., MCKINLAY, M., BRINK, R., LEVERKUS, M., TERGAONKAR, V., SCHNEIDER, P., CALLUS, B. A., KOENTGEN, F., VAUX, D. L. & SILKE, J. 2007. IAP antagonists target cIAP1 to induce TNFalpha-dependent apoptosis. *Cell*, 131, 682-93.
- WADA, M., HORINAKA, M., YAMAZAKI, T., KATOH, N. & SAKAI, T. 2014. The dual RAF/MEK inhibitor CH5126766/RO5126766 may be a potential therapy for RAS-mutated tumor cells. *PLoS One*, 9, e113217.
- WAGNER, D. O., SIEBER, C., BHUSHAN, R., BORGERMANN, J. H., GRAF, D. & KNAUS, P. 2010. BMPs: from bone to body morphogenetic proteins. *Sci Signal*, 3, mr1.
- WAN, P. T., GARNETT, M. J., ROE, S. M., LEE, S., NICULESCU-DUVAZ, D., GOOD, V. M., JONES, C. M., MARSHALL, C. J., SPRINGER, C. J., BARFORD, D. & MARAIS, R. 2004. Mechanism of activation of the RAF-ERK signaling pathway by oncogenic mutations of B-RAF. *Cell*, 116, 855-67.
- WANG, B., SINHA, T., JIAO, K., SERRA, R. & WANG, J. 2011. Disruption of PCP signaling causes limb morphogenesis and skeletal defects and may underlie Robinow syndrome and brachydactyly type B. *Hum Mol Genet*, 20, 271-85.
- WANG, J., LOBERG, R. & TAICHMAN, R. S. 2006. The pivotal role of CXCL12 (SDF-1)/CXCR4 axis in bone metastasis. *Cancer Metastasis Rev*, 25, 573-87.
- WANG, W., MCLEOD, H. L. & CASSIDY, J. 2003. Disulfiram-mediated inhibition of NF-kappaB activity enhances cytotoxicity of 5-fluorouracil in human colorectal cancer cell lines. *Int J Cancer*, 104, 504-11.
- WEILBAECHER, K. N., GUISE, T. A. & MCCAULEY, L. K. 2011. Cancer to bone: a fatal attraction. *Nat Rev Cancer*, 11, 411-25.
- WEISS, W. A., TAYLOR, S. S. & SHOKAT, K. M. 2007. Recognizing and exploiting differences between RNAi and small-molecule inhibitors. *Nat Chem Biol*, 3, 739-44.
- WEN, D., NONG, Y., MORGAN, J. G., GANGURDE, P., BIELECKI, A., DASILVA, J., KEAVENEY, M., CHENG, H., FRASER, C., SCHOPF, L., HEPPELLE, M., HARRIMAN, G., JAFFEE, B. D., OCAIN, T. D. & XU, Y. 2006. A selective small molecule IkappaB Kinase beta inhibitor blocks nuclear factor kappaB-mediated inflammatory responses in human fibroblast-like synoviocytes, chondrocytes, and mast cells. *J Pharmacol Exp Ther*, 317, 989-1001.
- WERNER, S. L., BARKEN, D. & HOFFMANN, A. 2005. Stimulus specificity of gene expression programs determined by temporal control of IKK activity. *Science*, 309, 1857-61.
- WESTENDORF, J. J., KAHLER, R. A. & SCHROEDER, T. M. 2004. Wnt signaling in osteoblasts and bone diseases. *Gene*, 341, 19-39.
- WHARRY, C. E., HAINES, K. M., CARROLL, R. G. & MAY, M. J. 2009. Constitutive non-canonical NFkappaB signaling in pancreatic cancer cells. *Cancer Biol Ther*, 8, 1567-76.
- WIDMER, U., MANOGUE, K. R., CERAMI, A. & SHERRY, B. 1993. Genomic cloning and promoter analysis of macrophage inflammatory protein (MIP)-2, MIP-1 alpha, and MIP-1 beta, members of the chemokine superfamily of proinflammatory cytokines. *J Immunol*, 150, 4996-5012.
- WITTE, F., CHAN, D., ECONOMIDES, A. N., MUNDLOS, S. & STRICKER, S. 2010. Receptor tyrosine kinase-like orphan receptor 2 (ROR2) and Indian hedgehog regulate digit outgrowth mediated by the phalanx-forming region. *Proc Natl Acad Sci U S A*, 107, 14211-6.

- XIAO, C. & GHOSH, S. 2005. NF-kappaB, an evolutionarily conserved mediator of immune and inflammatory responses. *Adv Exp Med Biol*, 560, 41-5.
- XIAO, G., FONG, A. & SUN, S. C. 2004. Induction of p100 processing by NF-kappaB-inducing kinase involves docking IkkappaB kinase alpha (IKKalpha) to p100 and IKKalpha-mediated phosphorylation. *J Biol Chem*, 279, 30099-105.
- XIAO, G. & FU, J. 2011. NF-kappaB and cancer: a paradigm of Yin-Yang. *Am J Cancer Res*, 1, 192-221.
- XIAO, G., HARHAJ, E. W. & SUN, S. C. 2001. NF-kappaB-inducing kinase regulates the processing of NF-kappaB2 p100. *Mol Cell*, 7, 401-9.
- XIAO, G., RABSON, A. B., YOUNG, W., QING, G. & QU, Z. 2006. Alternative pathways of NF-kappaB activation: a double-edged sword in health and disease. *Cytokine Growth Factor Rev*, 17, 281-93.
- XIAO, M., INAL, C. E., PAREKH, V. I., LI, X. H. & WHITNALL, M. H. 2009. Role of NF-kappaB in hematopoietic niche function of osteoblasts after radiation injury. *Exp Hematol*, 37, 52-64.
- YAMAMOTO, Y., VERMA, U. N., PRAJAPATI, S., KWAK, Y. T. & GAYNOR, R. B. 2003. Histone H3 phosphorylation by IKK-alpha is critical for cytokine-induced gene expression. *Nature*, 423, 655-9.
- YAMAOKA, S., COURTOIS, G., BESSIA, C., WHITESIDE, S. T., WEIL, R., AGOU, F., KIRK, H. E., KAY, R. J. & ISRAEL, A. 1998. Complementation cloning of NEMO, a component of the IkkappaB kinase complex essential for NF-kappaB activation. *Cell*, 93, 1231-40.
- YANG, D., UD DIN, N., BROWNING, D. D., ABRAMS, S. I. & LIU, K. 2007. Targeting lymphotoxin beta receptor with tumor-specific T lymphocytes for tumor regression. *Clin Cancer Res*, 13, 5202-10.
- YANG, J., SPLITTGERBER, R., YULL, F. E., KANTROW, S., AYERS, G. D., KARIN, M. & RICHMOND, A. 2010. Conditional ablation of Ikkb inhibits melanoma tumor development in mice. *J Clin Invest*, 120, 2563-74.
- YANG, S. R., VALVO, S., YAO, H., KODE, A., RAJENDRASOZHAN, S., EDIRISINGHE, I., CAITO, S., ADENUGA, D., HENRY, R., FROMM, G., MAGGIRWAR, S., LI, J. D., BULGER, M. & RAHMAN, I. 2008. IKK alpha causes chromatin modification on pro-inflammatory genes by cigarette smoke in mouse lung. *Am J Respir Cell Mol Biol*, 38, 689-98.
- YASUI, T., KADONO, Y., NAKAMURA, M., OSHIMA, Y., MATSUMOTO, T., MASUDA, H., HIROSE, J., OMATA, Y., YASUDA, H., IMAMURA, T., NAKAMURA, K. & TANAKA, S. 2011. Regulation of RANKL-induced osteoclastogenesis by TGF-beta through molecular interaction between Smad3 and Traf6. *J Bone Miner Res*, 26, 1447-56.
- YEMELYANOV, A., GASPARIAN, A., LINDHOLM, P., DANG, L., PIERCE, J. W., KISSELJOV, F., KARSELADZE, A. & BUDUNOVA, I. 2006. Effects of IKK inhibitor PS1145 on NF-kappaB function, proliferation, apoptosis and invasion activity in prostate carcinoma cells. *Oncogene*, 25, 387-98.
- YI, J. J., BARNES, A. P., HAND, R., POLLEUX, F. & EHLERS, M. D. 2010. TGF-beta signaling specifies axons during brain development. *Cell*, 142, 144-57.
- YIN, L., WU, L., WESCHE, H., ARTHUR, C. D., WHITE, J. M., GOEDEL, D. V. & SCHREIBER, R. D. 2001. Defective lymphotoxin-beta receptor-induced NF-kappaB transcriptional activity in NIK-deficient mice. *Science*, 291, 2162-5.
- YU, L., CECIL, J., PENG, S. B., SCHREMENTI, J., KOVACEVIC, S., PAUL, D., SU, E. W. & WANG, J. 2006. Identification and expression of novel isoforms of human stromal cell-derived factor 1. *Gene*, 374, 174-9.
- YU, Y., XIAO, C. H., TAN, L. D., WANG, Q. S., LI, X. Q. & FENG, Y. M. 2014. Cancer-associated fibroblasts induce epithelial-mesenchymal transition of breast cancer cells through paracrine TGF-beta signalling. *Br J Cancer*, 110, 724-32.

- ZABEL, U. & BAEUERLE, P. A. 1990. Purified human I kappa B can rapidly dissociate the complex of the NF-kappa B transcription factor with its cognate DNA. *Cell*, 61, 255-65.
- ZAHEER, S., LEBOFF, M. & LEWIECKI, E. M. 2015. Denosumab for the treatment of osteoporosis. *Expert Opin Drug Metab Toxicol*, 11, 461-70.
- ZARNEGAR, B. J., WANG, Y., MAHONEY, D. J., DEMPSEY, P. W., CHEUNG, H. H., HE, J., SHIBA, T., YANG, X., YE, W. C., MAK, T. W., KORNELUK, R. G. & CHENG, G. 2008. Noncanonical NF-kappaB activation requires coordinated assembly of a regulatory complex of the adaptors cIAP1, cIAP2, TRAF2 and TRAF3 and the kinase NIK. *Nat Immunol*, 9, 1371-8.
- ZENG, G., GERMINARO, M., MICSENYI, A., MONGA, N. K., BELL, A., SOOD, A., MALHOTRA, V., SOOD, N., MIDDA, V., MONGA, D. K., KOKKINAKIS, D. M. & MONGA, S. P. 2006. Aberrant Wnt/beta-catenin signaling in pancreatic adenocarcinoma. *Neoplasia*, 8, 279-89.
- ZENG, Z., SHI, Y. X., SAMUDIO, I. J., WANG, R. Y., LING, X., FROLOVA, O., LEVINS, M., RUBIN, J. B., NEGRIN, R. R., ESTEY, E. H., KONOPLEV, S., ANDREEFF, M. & KONOPLEVA, M. 2009. Targeting the leukemia microenvironment by CXCR4 inhibition overcomes resistance to kinase inhibitors and chemotherapy in AML. *Blood*, 113, 6215-24.
- ZERNECKE, A., SCHÖBER, A., BOT, I., VON HUNDELSHAUSEN, P., LIEHN, E. A., MOPPS, B., MERICKS, M., GIERSCHIK, P., BIESSEN, E. A. & WEBER, C. 2005. SDF-1alpha/CXCR4 axis is instrumental in neointimal hyperplasia and recruitment of smooth muscle progenitor cells. *Circ Res*, 96, 784-91.
- ZHANG, T., INESTA-VAQUERA, F., NIEPEL, M., ZHANG, J., FICARRO, S. B., MACHLEIDT, T., XIE, T., MARTO, J. A., KIM, N., SIM, T., LAUGHLIN, J. D., PARK, H., LOGRASSO, P. V., PATRICELLI, M., NOMANBHOY, T. K., SORGER, P. K., ALESSI, D. R. & GRAY, N. S. 2012. Discovery of potent and selective covalent inhibitors of JNK. *Chem Biol*, 19, 140-54.
- ZHENG, B., ZHOU, R., GONG, Y., YANG, X. & SHAN, Q. 2012. Proteasome inhibitor bortezomib overcomes P-gp-mediated multidrug resistance in resistant leukemic cell lines. *Int J Lab Hematol*, 34, 237-47.
- ZLOTNIK, A. & YOSHIE, O. 2000. Chemokines: a new classification system and their role in immunity. *Immunity*, 12, 121-7.
- ZOU, W., MACHELON, V., COULOMB-L'HERMIN, A., BORVAK, J., NOME, F., ISAEVA, T., WEI, S., KRZYSIEK, R., DURAND-GASSELIN, I., GORDON, A., PUSTILNIK, T., CURIEL, D. T., GALANAUD, P., CAPRON, F., EMILIE, D. & CURIEL, T. J. 2001. Stromal-derived factor-1 in human tumors recruits and alters the function of plasmacytoid precursor dendritic cells. *Nat Med*, 7, 1339-46.